UNIVERSITY OF SOUTHAMPTON

FACULTY OF PHYSICAL SCIENCES AND ENGINEERING

School of Physics and Astronomy

The flavour puzzle in grand unification and cosmology

by

Fredrik Björkeroth

Thesis for the degree of Doctor of Philosophy

October 2017

UNIVERSITY OF SOUTHAMPTON

ABSTRACT

FACULTY OF PHYSICAL SCIENCES AND ENGINEERING
School of Physics and Astronomy

Doctor of Philosophy

THE FLAVOUR PUZZLE IN GRAND UNIFICATION AND COSMOLOGY

by Fredrik Björkeroth

The discovery of neutrino masses and large lepton mixing may be an indication for an underlying non-Abelian family symmetry in nature, although the measurement of a relatively large reactor angle effectively ruled out the simplest models of flavour, such as those predicting tri-bimaximal mixing. However, more sophisticated realisations are still viable, such as those based on constrained sequential dominance (CSD) with a type-I seesaw mechanism. We study the CSD(n) class of models, showing how special vacuum alignments of Standard Model singlet flavons may give rise to highly constrained lepton mass matrices. A dedicated numerical fit based on χ^2 minimisation gives predictions for lepton mixing parameters, and excellent agreement with experimental data is found for $n = 3$.

The CSD(3) alignments are implemented in several supersymmetric grand unified theories (GUTs) of flavour with discrete family symmetries. We propose fairly complete models based on $A_4 \times SU(5)$, $\Delta(27) \times SO(10)$, and $S_4 \times SO(10)$, which are spontaneously broken to the minimal supersymmetric Standard Model. Each model leads to predictive mass matrix structures for both quarks and leptons; in particular, those based on $SO(10)$ lead naturally to near-universal matrices as sums over low-rank matrices, so-called universal sequential dominance, giving a natural explanation for fermion mass hierarchies. Theoretical predictions are underpinned by dedicated χ^2 fits, and in the $S_4 \times SO(10)$ model, estimates of the errors using Monte Carlo methods. We show that thermal leptogenesis from decays of the lightest right-handed neutrino can produce the observed baryon asymmetry of the Universe in CSD(n), and in the $A_4 \times SU(5)$ and $\Delta(27) \times SO(10)$ models. GUT breaking, proton decay, doublet-triplet splitting and the μ problem are also addressed.

Contents

List of Figures

List of Tables

Declaration of Authorship

I, Fredrik Björkeroth, declare that the thesis entitled *The flavour puzzle in grand unification and cosmology* and the work presented in the thesis are both my own, and have been generated by me as the result of my own original research. I confirm that:

- this work was done wholly or mainly while in candidature for a research degree at this University;
- where any part of this thesis has previously been submitted for a degree or any other qualification at this University or any other institution, this has been clearly stated;
- where I have consulted the published work of others, this is always clearly attributed;
- where I have quoted from the work of others, the source is always given. With the exception of such quotations, this thesis is entirely my own work;
- I have acknowledged all main sources of help;
- where the thesis is based on work done by myself jointly with others, I have made clear exactly what was done by others and what I have contributed myself;
- parts of this work have been published as: [1], [2], [3], [4], [5] and [6].

Signed:.....

Date:.....

Acknowledgements

I am fortunate to have a wonderful group of friends, colleagues and loved ones, to whom I owe the completion of this thesis. First and foremost, I want to thank my supervisor, Steve King. Under your guidance I have managed to produce something of which I am very proud. You have consistently offered your expertise and practical advice, but most importantly your time and attention, on both professional and personal matters. My thanks also to Ivo, for your mentorship.

My gratitude extends to the first of my two work families, the theorists, not least for allowing me my frequent wanders into your offices for a chat or a conundrum whenever I needed a break from work. In particular, thank you Declan, for your help tackling stress, and your unique renditions of hit songs, Juri and Miguel for helping me grapple with the strange world of academia, and Pete and Zoë for reminding me about the world outside it. I couldn't have asked for a better crew to start PhD life with.

To my adoptive family, the astronomers: thank you for allowing me into your home, i.e. the Astro library, for the honorary astronomer status which I treasure, and for many Friday morning breakfasts and evening pubs. My appreciation extends to all, but none more so than Aarran, my flatmate and best friend, for your sage wisdom and evenings watching Suits and sampling from your gin collection. To Rob, for the hours well spent playing GeoGuessr and your always-underappreciated puns, to Georgios, for the stories and your eternal generosity, to Andy, Becca, CFro, James, Keira, Sam, Sadie, and to those not mentioned but not forgotten, thank you. I also wish to acknowledge the work by Elena, and the Women's Physics Network, to promote women in physics.

I would not be where I am today without my parents, Nelda and Claes, and my sister Teresa. You knew how valuable and rewarding an education can be, and encouraged me to always challenge myself. You have offered advice when asked, support when needed, and love always. Thank you to Jesper, my oldest and closest friend, and my nona Dragica and nono Đenio, on whom I've always been able to rely.

Finally, to Juliana, my partner and my love. You have made the difficult times bearable and the good times wonderful, and I cannot imagine my time here in Southampton without you. Thank you for your infinite patience and support; you are my rock.

Nomenclature

SM	Standard Model
LHC	Large Hadron Collider
BSM	Beyond the Standard Model
EW	Electroweak
QCD	Quantum chromodynamics
VEV	Vacuum expectation values
CKM	Cabibbo-Kobayashi-Maskawa
PMNS	Pontecorvo-Maki–Nakagawa–Sakata
CMB	Cosmic microwave background
CP	Charge-parity
SUSY	Supersymmetry
MSSM	Minimal supersymmetric Standard Model
LSP	Lightest supersymmetric particle
WIMP	Weakly interacting massive particle
GUT	Grand unified theory
TB	Tri-bimaximal
BAU	Baryon asymmetry of the Universe
SD	Sequential dominance
CSD	Constrained sequential dominance
MP	Missing partner
CG	Clebsch-Gordan
DW	Dimopoulos-Wilczek

Chapter 1

Introduction

1.1 The Standard Model

The Standard Model (SM) is a remarkably successful theory of quarks and leptons which has withstood almost every experimental test over the course of decades. Most recently, the last missing piece, the Higgs boson, was discovered by the ATLAS [7] and CMS [8] collaborations at the Large Hadron Collider (LHC). The exception to this success was the discovery of neutrino oscillations [9, 10], which proved experimentally that neutrinos are massive and undergo flavour mixing. In further departure from the Standard Model, mixing in the lepton sector appears fundamentally different to that of quarks, stimulating research into understanding the origin of quark and lepton flavour. Somewhat frustratingly, no other clear signals of new physics beyond the Standard Model (BSM) have been detected, although widespread efforts have been made to develop interesting extended models and identify channels for detecting new physics at the LHC and future experiments. Conversely, the experimental evidence for the Standard Model is steadily increasing. It is worth noting that most avenues of investigation for BSM physics are motivated by theory rather than experimental discrepancies. For instance, one of the strongest motivations for seeking new physics at TeV scale is the electroweak (EW) hierarchy problem: what protects the Higgs boson mass from arbitrarily large corrections from physics at high scale? Furthermore, the scale evolution of the Standard Model gauge couplings and the apparent quantisation of electric charge point to unification of the fundamental forces of nature at a scale around 10^{16} GeV. We will return to these topics and other theoretical motivations for BSM physics in due course.

1.1.1 Symmetries and fields

Let us first, however, present the Standard Model. It is chiefly defined by two parts: a set of symmetries, either gauged or global, and a set of fields. The gauge symmetry is

$SU(3)_C \times SU(2)_L \times U(1)_Y$, where $SU(3)_C$ is the gauge group of quantum chromodynamics (QCD) [11–13], while $SU(2)_L \times U(1)_Y$ is the electroweak gauge group [14–17]. The subscript L refers to the fact that $SU(2)_L$ acts only on left-handed particles. The $SU(2)_L$ quantum number is weak isospin, while Y refers to weak hypercharge. The electroweak group breaks to the $U(1)$ of electromagnetism, i.e.

$$SU(3)_C \times SU(2)_L \times U(1)_Y \to SU(3)_C \times U(1)_{\text{em}}. \tag{1.1}$$

Field	Representation		
	$SU(3)_C$	$SU(2)_L$	$U(1)_Y$
Q_{Li}	3	2	1/6
u_{Ri}	3	1	2/3
d_{Ri}	3	1	-1/3
L_{Li}	1	2	-1/2
e_{Ri}	1	1	-1
ν_{Ri}	1	1	0
G^a	8	1	0
W^a	1	3	0
B	1	1	0
H	1	2	1/2

Table 1.1: Standard Model field content.

The field content of the Standard Model is given in Table 1.1, showing their representations under the gauge group. It contains three types of fields: fermions, gauge bosons and the Higgs field. The fermions are the constituent parts of atoms, and make up the matter content of the Universe. As such, they are frequently referred to as "matter". Subscripts L and R denote left- and right-handedness, respectively. The subscript i is a family (or generation) index. $Q_{Li} = (u_{Li}, d_{Li})$ denote the doublets containing left-handed up and down ($i = 1$), charm and strange ($i = 2$), and top and bottom ($i = 3$) quarks, while u_{Ri} and d_{Ri} are the respective right-handed states. An additional colour $SU(3)$ index is suppressed for clarity. Similarly, $L_{Li} = (\nu_{Li}, e_{Li})$ denote the doublets of a left-handed charged lepton and its corresponding neutrino (for the electron, muon and tau), and e_{Ri} denote the right-handed charged leptons. Noting that each quark has three colour degrees of freedom, there are in total 15 chiral states in each family (or 16 if ν_R is included). Gauge bosons comprise the gluons G of the unbroken $SU(3)_C$, and the W and B bosons of the electroweak $SU(2)_L$ and $U(1)_Y$, respectively. Finally, we have the Higgs field H which, in addition to breaking electroweak symmetry, gives masses to fermions via Yukawa interactions.

In Table 1.1 we have added three right-handed neutrinos ν_{Ri}, which are not part of the original Standard Model. However, the observation of neutrino oscillations requires neutrinos to have mass. Adding a companion right-handed neutrino to each generation of

the lepton doublet allows us to write a Yukawa coupling for neutrinos, as done for charged fermions; this is the minimal extension to the Standard Model that can accommodate massive neutrinos. Neutrino mass will be discussed in more detail in Section 1.2 and, alongside understanding the nature and origin of Yukawa interactions, are a central theme of this work.

Given the above symmetries and fields we write down the Standard Model Lagrangian as the sum of three parts,

$$\mathcal{L} = \mathcal{L}_{\text{kinetic}} + \mathcal{L}_{\text{Yukawa}} + \mathcal{L}_{\text{Higgs}}. \tag{1.2}$$

$\mathcal{L}_{\text{kinetic}}$ contains the kinetic terms for gauge fields and fermions,

$$\mathcal{L}_{\text{kinetic}} = \sum_{\psi} i\bar{\psi}\sigma^{\mu}D_{\mu}\psi - \frac{1}{4}G^{a}_{\mu\nu}G^{a\mu\nu} - \frac{1}{4}W^{a}_{\mu\nu}W^{a\mu\nu} - \frac{1}{4}B_{\mu\nu}B^{\mu\nu}, \tag{1.3}$$

with ψ running over all fermions. D_μ are covariant derivatives, containing a derivative part ∂_μ and one or several gauge coupling parts, depending on the representation of ψ under the Standard Model group. Colour singlets such as leptons will not couple to gluons, for instance, while right-handed fermions do not couple to W fields. The quark doublet is a non-singlet under all groups, such that

$$D_{\mu}Q_L = \left(\partial_{\mu} - ig_3G^{a}_{\mu}\mathrm{T}^{a}_{SU(3)} - igW^{a}_{\mu}\mathrm{T}^{a}_{SU(2)} - ig'B_{\mu}Y\right)Q_L, \tag{1.4}$$

where $\mathrm{T}_{\mathcal{G}}$ are the generators of the group $\mathcal{G}$, Y is hypercharge, and g_3, g and g' are the gauge coupling constants for $SU(3)$, $SU(2)$ and $U(1)$, respectively. The gauge field strengths are given in terms of structure constants f^{abc} and ϵ^{abc} by

$$\begin{aligned} G^{a}_{\mu\nu} &= \partial_{\mu}G^{a}_{\nu} - \partial_{\nu}G^{a}_{\mu} - g_3\, f^{abc}G^{b}_{\mu}G^{c}_{\nu}, \\ W^{a}_{\mu\nu} &= \partial_{\mu}W^{a}_{\nu} - \partial_{\nu}W^{a}_{\mu} - g\,\epsilon^{abc}W^{b}_{\mu}W^{c}_{\nu}, \\ B_{\mu\nu} &= \partial_{\mu}B_{\nu} - \partial_{\nu}B_{\mu}. \end{aligned} \tag{1.5}$$

The Higgs Lagrangian is given by

$$\mathcal{L}_{\text{Higgs}} = (D_{\mu}H)^{\dagger}(D^{\mu}H) - \mu^2H^{\dagger}H - \lambda(H^{\dagger}H)^2, \tag{1.6}$$

where $D_\mu H = (\partial_\mu - igW^a_\mu \mathrm{T}^a_{SU(2)} - \frac{1}{2}ig'B_\mu)H$. Its potential has a minimum with non-zero field values corresponding to a vacuum expectation value (VEV) $v = \sqrt{-\mu^2/(2\lambda)} \approx 174$ GeV, which breaks $SU(2)_L \times U(1)_Y \to U(1)_{\text{em}}$. The generator Q of $U(1)_{\text{em}}$, corresponding to electric charge, is given by a sum of electroweak generators

$$Q = T^3_{SU(2)} + Y. \tag{1.7}$$

Higgs couplings to $SU(2)$ gauge fields via the covariant derivative gives the the latter masses on the order of v, while self-couplings give also the Higgs boson a mass. This is the essence of the Higgs mechanism [18–21]. Moreover, the neutral gauge components B_μ and W^3_μ mix, leading to the physical bosons Z^0, which becomes massive, and the photon A_μ, which remains massless and corresponds to the unbroken $U(1)_{\rm em}$. This shift between (B_μ, W^3_μ) and (A_μ, Z^0_μ) bases is characterised by the weak mixing angle θ_W, with $\sin^2\theta_W = 0.2223(21)$ [22]. It is related to the electroweak gauge couplings g, g' by

$$\cos\theta_W = \frac{g}{\sqrt{g^2 + g'^2}}, \tag{1.8}$$

and the weak boson masses by $\cos\theta_W = m_W/m_Z$. The Higgs field also has the correct quantum numbers to allow it to couple to left- and right-handed fermion fields, giving an immediate explanation also for fermion masses. This is encoded in the Yukawa Lagrangian $\mathcal{L}_{\rm Yukawa}$.

1.1.2 Quark mixing

The quark Yukawa couplings are given by

$$\mathcal{L}_{\rm Yukawa,Q} = -Y^d_{ij}\overline{Q_L}_i H d_{Rj} - Y^u_{ij}\overline{Q_L}_i \varepsilon H^* u_{Rj} + \text{h.c.}, \tag{1.9}$$

in the weak flavour-eigenstate basis, where $i, j = 1, 2, 3$ are family indices and ε is the 2×2 antisymmetric tensor. There is a mismatch between the flavour and mass eigenstates, which are related by unitary matrices. More precisely, the up-type quark mass eigenstates may be obtained by diagonalising Y^u by two unitary matrices $V^u_{L,R}$ such that

$$Y^{u,\rm diag} = V^u_L Y^u (V^u_R)^\dagger. \tag{1.10}$$

Similarly, Y^d may be diagonalised by matrices $V^d_{L,R}$ such that

$$Y^{d,\rm diag} = V^d_L Y^d (V^d_R)^\dagger. \tag{1.11}$$

Without loss of generality we may move to the basis where the up-type quark flavour and mass eigenstates coincide, by performing the transformations $Q_{Li} \to (V^u_L)^*_{ik} Q_{Lk}$ and $u_{Rj} \to (V^u_R)^\dagger_{jl} u_{Rl}$. However, as the quark doublet Q_L is shared among up- and down-type quarks, we cannot simultaneously diagonalise the down-type quark Yukawa matrix. The misalignment between bases and resultant mixing between quark flavour states is encoded in a single unitary matrix known as the Cabibbo-Kobayashi-Maskawa (CKM) matrix,

$$V_{\rm CKM} = V^u_L V^{d\dagger}_L. \tag{1.12}$$

The CKM matrix can be parametrised in terms of three Euler angles θ_{ij}^q and one complex phase δ^q. With $c_{ij} = \cos\theta_{ij}^q$ and $s_{ij} = \sin\theta_{ij}^q$,

$$V_{\text{CKM}} = \begin{pmatrix} 1 & 0 & 0 \\ 0 & c_{23} & s_{23} \\ 0 & -s_{23} & c_{23} \end{pmatrix} \begin{pmatrix} c_{13} & 0 & s_{13}e^{-i\delta^q} \\ 0 & 1 & 0 \\ -s_{13}e^{i\delta^q} & 0 & c_{13} \end{pmatrix} \begin{pmatrix} c_{12} & s_{12} & 0 \\ -s_{12} & c_{12} & 0 \\ 0 & 0 & 1 \end{pmatrix}. \tag{1.13}$$

This is the parametrisation employed by the Particle Data Group (PDG) [23]. Their Standard Model values are given in Table 1.2, taken from the UTFit collaboration [24]. We also present the quark masses, extracted from the latest PDG review. As free quarks have never been observed due to QCD confinement, there is some variability in how quark masses are defined. For more details, we refer the reader to the PDG review.[1] These values are presented for only completeness, and are not used directly in the model fits presented within this thesis. The reason for this is that mass and mixing parameters can change considerably with scale; this "running" is governed by renormalisation group equations and encoded in so-called β functions. The parameters depend also on features of the model itself, including the presence (or not) of supersymmetry. In future chapters we present the relevant data, run up to high scale and taking into supersymmetric corrections, to which we can directly compare our models.

Parameter	Value	
	Degrees	Radians
θ_{12}^q	12.91 ±0.04	0.2254 ±0.0007
θ_{13}^q	0.209 ±0.007	0.00364 ±0.00013
θ_{23}^q	2.410 ±0.037	0.04207 ±0.00064
δ^q	69.21 ±3.09	1.208 ±0.054

(a) CKM parameters.

Parameter	Mass
m_u /MeV	$2.2\ ^{+0.6}_{-0.4}$
m_c /GeV	1.28 ±0.03
m_t /GeV	173.5 ±1.1
m_d /MeV	$4.7\ ^{+0.5}_{-0.4}$
m_s /GeV	$96\ ^{+8}_{-4}$
m_b /GeV	$4.18\ ^{+0.04}_{-0.03}$

(b) Quark masses.

Table 1.2: Standard Model experimental quark masses and CKM mixing parameters, from. CKM parameters are obtained from [24]. Quark masses are obtained from [23], and are given in the $\overline{\text{MS}}$ scheme, with $\mu \approx 2$ GeV for the light quarks.

1.2 Neutrino mass, mixing and the seesaw mechanism

Charged leptons acquire masses analogously to quarks, via Yukawa couplings to the Higgs. Meanwhile, in the original formulation of the Standard Model, neutrinos were massless and therefore no lepton mixing was allowed. The minimal extension which

[1] We note that the values in Table 1.2 are given in the $\overline{\text{MS}}$ scheme, with $\mu \approx 2$ GeV for the light quarks.

permits neutrino masses is by introducing right-handed neutrinos ν_R, which are gauge singlets. They couple to the Higgs field in a Yukawa term $Y^\nu_{ij}\overline{L_{Li}}\varepsilon H^*\nu_{Rj}$, which generates neutrino Dirac masses when the Higgs acquires a VEV v, in complete analogy with charged fermions. Phenomenologically, this would be sufficient to explain observations, but implies neutrino Yukawa couplings no larger than $\mathcal{O}(10^{-11})$, many orders of magnitude below the smallest known coupling (the electron Yukawa), of $\mathcal{O}(10^{-6})$.

However, a key feature of right-handed neutrinos that distinguishes the neutrino mass generation mechanism is that they are Majorana particles, i.e. their own antiparticle. We may write a mass term directly for the right-handed neutrinos like $(M_R)_{ij}\overline{\nu^c_{Ri}}\nu_{Rj}$, where M_R is an $n\times n$ matrix (for n neutrinos), and the charge conjugate ν^c_R transforms as a left-handed field.[2] As this mass term is not constrained by any gauge symmetry, right-handed neutrinos can be arbitrarily heavy, i.e. $M_R \gg vY^\nu$. Under these conditions, left-handed neutrinos can acquire small Majorana masses via the type-I seesaw mechanism, first proposed in [25–28] (see also [29, 30]). Variations of the seesaw mechanism have also been constructed involving $SU(2)$ Higgs triplets (type-II) [31–33] or lepton triplets (type-III) [34, 35].

The lepton Yukawa Lagrangian is thus given by

$$\mathcal{L}_{\text{Yukawa},L} = -Y^e_{ij}\overline{L_{Li}}He_{Rj} - Y^\nu_{ij}\overline{L_{Li}}\varepsilon H^*\nu_{Rj} - \tfrac{1}{2}(M_R)_{ij}\overline{\nu^c_{Ri}}\nu_{Rj} + \text{h.c.}. \tag{1.14}$$

The mass matrix for the $3+n$ neutrinos can be written as[3]

$$M_\nu = \begin{pmatrix} 0 & vY^\nu \\ v(Y^\nu)^\intercal & M_R \end{pmatrix}. \tag{1.15}$$

A mass term like $m\overline{\nu^c_L}\nu_L$ is forbidden at the renormalisable level by gauge invariance. It is instead generated at the effective level when right-handed neutrinos are integrated out of the theory, equivalent to diagonalising M_ν. The texture zero in M_ν becomes populated by effective couplings that are naturally suppressed by the scale of right-handed neutrinos which, if these are large, provides a natural explanation for the smallness of neutrino mass. The light effective neutrino mass matrix m^ν, defined in the convention

$$\mathcal{L} = -\tfrac{1}{2}m^\nu_{ij}\overline{\nu^c_{Li}}\nu_{Lj} + \text{h.c.}, \tag{1.16}$$

[2] A note on notation: subscripts L and R on the Weyl spinors listed in Table 1.1 refer to the action under $SU(2)_L$, i.e. fermions ψ_R do not couple to W bosons. Under conjugation, denoted by superscript c, the chirality of the field changes but the action under $SU(2)_L$ does not, e.g. ψ^c_R transforms as a left-handed field but remains an $SU(2)_L$ singlet. At the level of four-component Dirac spinors, conjugation is defined by $\psi^c = C\overline{\psi}^\intercal$, where C is a 4×4 matrix satisfying the relation $C^{-1}\gamma^\mu C = -\gamma^{\mu\intercal}$. Occasionally in the literature L and R refer instead to the components of the Dirac spinor, obtained via the projection operators $P_{R/L} = \frac{1}{2}(1\pm\gamma^5)$, e.g. $(\psi^c)_R = P_R\psi^c$ is the right-handed component of the Dirac spinor ψ^c. The two pictures are related by noting that $\psi^c_R = (P_R\psi)^c = P_L\psi^c = (\psi^c)_L$.

[3] Assuming the seesaw mechanism is a true description of physics, we require $n \geq 2$ in order to explain neutrino oscillation data that indicates at least two physical neutrinos are massive.

is given by

$$m^\nu = -v^2 Y^\nu M_R^{-1} (Y^\nu)^\intercal. \tag{1.17}$$

To demonstrate the interplay between scales, let us consider a toy model with only one generation of neutrinos. M_ν in Eq. 1.15 is now a 2×2 matrix, giving a single light neutrino with mass $m^\nu = v^2 y^2 / M$, where y is a representative Yukawa coupling and M is the right-handed neutrino mass. The charged fermion Yukawa couplings range from $\mathcal{O}(10^{-6})$ to $\mathcal{O}(1)$, with the upper end of that scale typically considered the most "natural". For definiteness, let us set $y = 0.1$. Neutrino oscillation experiments indicate that at least one neutrino has mass around 50 meV. In this approximation, let us set $m^\nu = 100$ meV. Recalling that $v \approx 174$ GeV, we arrive at an estimate for the right-handed neutrino mass

$$M \sim \frac{v^2 y^2}{m^\nu} \sim 3 \times 10^{12}\,\text{GeV}. \tag{1.18}$$

The seesaw scale is naturally very high, implying direct detection of right-handed neutrinos is impossible.

Flavour mixing in the lepton sector is encoded in the Pontecorvo-Maki-Nakagawa-Sakata (PMNS) matrix. It differs slightly in form from the CKM matrix due to the fact that neutrinos may be Majorana particles. The charged lepton Yukawa matrix may be diagonalised by unitary matrices U_L^e and U_R^e, such that

$$Y^{e,\text{diag}} = U_L^e Y^e (U_R^e)^\dagger. \tag{1.19}$$

The light neutrino mass matrix m^ν is symmetric, and diagonalised by an orthogonal matrix U_L^ν, giving

$$m^{\nu,\text{diag}} = U_L^\nu m^\nu (U_L^\nu)^\intercal. \tag{1.20}$$

Both matrices cannot be diagonalised simultaneously by a basis transformation, leading to flavour mixing described by the PMNS matrix

$$U_\text{PMNS} = U_L^e (U_L^\nu)^\dagger. \tag{1.21}$$

Although this is often referred to as neutrino mixing, contributions to U_PMNS may originate from either or both lepton matrices. In the basis where charged leptons are diagonal, the PMNS matrix relates the neutrino flavour eigenstates $|\nu_\alpha\rangle$ ($\alpha = e, \mu, \tau$) to mass eigenstates $|\nu_i\rangle$ ($i = 1, 2, 3$) by

$$|\nu_\alpha\rangle = \sum_i (U_\text{PMNS})_{\alpha i} \, |\nu_i\rangle \,. \tag{1.22}$$

In the PDG parametrisation, U_{PMNS} is described by three mixing angles θ_{ij}^{ℓ} and three phases δ^{ℓ}, α_{21} and α_{31}. With $c_{ij} = \cos\theta_{ij}^{\ell}$ and $s_{ij} = \sin\theta_{ij}^{\ell}$,

$$U_{\text{PMNS}} = \begin{pmatrix} 1 & 0 & 0 \\ 0 & c_{23} & s_{23} \\ 0 & -s_{23} & c_{23} \end{pmatrix} \begin{pmatrix} c_{13} & 0 & s_{13}e^{-i\delta^{\ell}} \\ 0 & 1 & 0 \\ -s_{13}e^{i\delta^{\ell}} & 0 & c_{13} \end{pmatrix} \begin{pmatrix} c_{12} & s_{12} & 0 \\ -s_{12} & c_{12} & 0 \\ 0 & 0 & 1 \end{pmatrix} \times \text{diag}(1, e^{i\alpha_{21}/2}, e^{i\alpha_{31}/2}). \tag{1.23}$$

If neutrinos are Dirac particles, the phases α_{21} and α_{31} become unphysical, and the PMNS matrix is exactly analogous to the CKM matrix. In shorthand, we may write the above as $U_{\text{PMNS}} = R_{23}^{\ell} U_{13}^{\ell} R_{12}^{\ell} P$.

Neutrino oscillation experiments do not measure the neutrino masses directly, and can only constrain the mass squared differences $\Delta m_{ij}^2 = m_i^2 - m_j^2$. The absolute scale of neutrino mass, characterised by the lightest neutrino mass m_1, is not known. Moreover, the ordering of neutrino masses is not yet fixed. While it is known that the first and second neutrinos obey $m_1 < m_2$ (equivalent to $\Delta m_{21}^2 > 0$), at current experimental precision it is not known whether the third neutrino with mass m_3 is the heaviest, so-called normal ordering (NO), or the lightest, dubbed inverted ordering (IO). In other words, the sign of Δm_{31}^2 is undetermined, although global fits to data show a mild preference for normal ordering [36]. For normal ordering, the strongest hierarchy occurs when m_1 is small: for $m_1 \lesssim 5$ meV, $m_2/m_3 \sim 0.2$. Meanwhile an inverted ordering requires the first and second neutrinos to be similar, i.e. $m_1 \lesssim m_2$, while the third neutrino is lighter. Observations of the cosmic microwave background (CMB) puts an upper bound on the sum of neutrino masses $\sum m_i < 0.23$ eV [37]. Bounds on the neutrino masses are also given by searches for neutrinoless double beta ($0\nu2\beta$) decay. Specifically, the $0\nu2\beta$ decay rate is proportional to the square of the effective Majorana mass $|m_{\beta\beta}| = |\sum_i U_{ei}^2 m_i|$. Future experiments may be able to place upper bounds on $|m_{\beta\beta}|$ which is in tension with oscillation data for an inverted hierarchy (or alternatively, confirm it).

In Table 1.3 we present the current best fit values for normal ordering to the three lepton mixing angles θ_{ij}^{ℓ}, Dirac charge-parity (CP) phase δ^{ℓ} and neutrino mass-squared differences Δm_{ij}^2, taken from the NuFit collaboration [36], as well as the measured masses of the electron, muon and tau [23].

1.3 The flavour puzzle

The flavour puzzle can be approached in a number of equivalent ways. For instance, we may ask:

Parameter	Value	
	Best fit $\pm 1\sigma$	3σ range
$\sin^2\theta_{12}^\ell$	0.306 ± 0.012	$0.271 \to 0.345$
$\theta_{12}^\ell/^\circ$	$33.56\ ^{+0.77}_{-0.75}$	$31.58 \to 35.99$
$\sin^2\theta_{23}^\ell$	$0.441\ ^{+0.027}_{-0.021}$	$0.385 \to 0.635$
$\theta_{23}^\ell/^\circ$	$41.6\ ^{+1.5}_{-1.2}$	$38.4 \to 52.8$
$\sin^2\theta_{13}^\ell$	0.02166 ± 0.00075	$0.01934 \to 0.02392$
$\theta_{13}^\ell/^\circ$	8.46 ± 0.15	$7.99 \to 8.90$
$\delta^\ell/^\circ$	$261\ ^{+51}_{-59}$	$0 \to 360$
$\Delta m_{21}^2\ /10^{-5}\ \text{eV}^2$	$7.50\ ^{+0.19}_{-0.17}$	$7.03 \to 8.09$
$\Delta m_{31}^2\ /10^{-3}\ \text{eV}^2$	$2.524\ ^{+0.039}_{-0.040}$	$2.407 \to 2.643$
m_e /MeV	0.5109989461 (31)	
m_μ /MeV	105.6583745 (24)	
m_τ /GeV	1.77686 (12)	

Table 1.3: Standard Model experimental lepton masses and PMNS mixing parameters, from [23, 36].

- Why are there three families (or generations) of each Standard Model fermion field, in the same representation of the gauge group, differing only by their mass?
- Why is there such a large hierarchy among fermion masses, ranging from the lightest neutrino, on the order of meV, to the top quark, with $m_t \approx 173$ GeV?
- Why is flavour mixing in the quark sector, characterised by the CKM matrix, rather small while lepton mixing, characterised by the PMNS matrix, is large?
- A majority of the free parameters in the Standard Model originate in the Yukawa couplings of fermions to the Higgs field; do they have a common origin?

The first question can be understood by looking at Table 1.2. For instance, the down, strange and bottom quarks behave identically under the Standard Model gauge group, but have respective masses of order 10^{-3}, 10^{-1} and 1 GeV, respectively. The particles can be made distinct by taking into account their different charges under additional flavour quantum numbers, e.g. strangeness S and bottomness B', but these quantum numbers are anyway broken by weak interactions and not particularly illuminating. Moreover, this does not explain the apparent need for three families, rather than one or two, and does not forbid a fourth family of quarks, for which there is no experimental evidence [23].

A compelling hint towards explaining the number three lies in CP violation: it was observed by Kobayashi and Maskawa [38] that in a theory with three weakly interacting families, the mixing matrix (now referred to as the CKM matrix) allows a single complex

phase which is not present in a two-family system, leading to interactions which violate CP. To date, this is the only confirmed source of CP violation in the Standard Model, although current experimental hints in the lepton sector [36] indicate that also the analogous CP-violating phase in the lepton mixing matrix is non-zero. From a physical perspective, CP violation is necessary to explain the baryon-antibaryon asymmetry of the Universe, which would motivate the existence of three families, although this observation is complicated by the fact that the observed CP violation in the Standard Model in any case is not nearly sufficient to explain the observed baryon asymmetry. We return to this point in the discussion on baryo- and leptogenesis, below.

In addition to understanding the fact of three families, we are tasked with understanding why the fermions, both across families and within a single family, have wildly different masses. As seen in Table 1.2, quark masses range from a few MeV to over 100 GeV, five orders of magnitude. In addition, the hierarchies in each sector of charged fermions – up-type quarks, down-type quarks and charged leptons – are not the same, e.g. the ratio of up and down quark masses $m_u/m_d \lesssim 1$ differs from that of charm and strange quarks ($m_c/m_s \sim 10$), or top and bottom quarks ($m_t/m_b \sim 50$).[4] Finally, we must explain why neutrinos, whose masses are no larger than $\mathcal{O}(100)$ meV, are many orders of magnitude lighter than charged fermions. Between the lightest charged fermion (the electron, with mass $m_e \sim 0.5$ MeV) and the neutrinos lies seven orders of magnitude. One compelling solution has already been presented, in the seesaw mechanism.

Turning to the third question above, we wish to understand why quark mixing, which is dominated by the Cabibbo angle $\theta_{12}^q \approx 13^\circ$, is much smaller than lepton mixing, where all mixing angles are sizeable. This may be tied to the previous question about mass hierarchies, and can be reformulated as the question why the hierarchy in neutrino masses appears much milder than those for charged fermions. Moreover it is still not known with certainty whether the neutrino mass ordering is normal or inverted.

Finally, we note that all the above questions ultimately derive from our lack of understanding about the nature of the Yukawa couplings of Standard Model fermions to the Higgs, from which most masses are thought to derive. The Yukawa sector contains most of the free parameters of the Standard Model, such that each fermion mass is essentially an input parameter of the theory. It is certainly possible that the distribution of free parameters is random, however this is unlikely given the indications of structure in the distribution of masses across families. In any given theory, there are many factors which may influence the Yukawa couplings to the Higgs. In this work, we have relied on two guiding principles which show promise for resolving the flavour puzzle: family symmetry, and grand unification.

[4] The ratios change depending on the scale at which they are evaluated, due to renormalisation group running of the fermion masses. These numbers are merely indicative.

1.4 Supersymmetry

Supersymmetry (SUSY) [39–43] has been at the centre of extensive research into physics beyond the Standard Model for several decades, and remains one of the most compelling possibilities for new physics, both on theoretical and phenomenological grounds. In this section, we limit ourselves to summarising the necessary nomenclature, consistent with that of [44], as well as describing the hierarchy problem and introducing the minimal supersymmetric Standard Model (MSSM). This constitutes neither a review of the theory of supersymmetry (which can extend to aspects of gravity, string theory, and extra dimensions), nor of the current experimental status of supersymmetry searches at colliders; both of these topics have a large associated literature.

1.4.1 A symmetry of fermions and bosons

Supersymmetry is an extension of the Poincaré symmetry of spacetime which relates fermions and bosons. In other words, a supersymmetry transformation turns a fermionic state f into a bosonic one b and *vice versa*, via some operators Q and $Q^\dagger$ such that $Q\,|f\rangle = |b\rangle$ and $Q\,|b\rangle = |f\rangle$. These operators carry spin angular momentum, and satisfy certain commutation and anticommutation relations (the supersymmetry algebra), which are detailed in [44].

As the ultimate goal is to embed the Standard Model in a supersymmetric framework, we must incorporate all (fermion) matter fields, (vector) gauge fields and the (scalar) Higgs. The irreducible representations of the supersymmetry algebra – supermultiplets – contain both fermionic and bosonic states. More precisely, each supermultiplet contains equal numbers of fermionic and bosonic degrees of freedom. The combination of a Weyl fermion and complex scalar field is referred to as a chiral supermultiplet; these will house the Standard Model fermions, along with their scalar counterparts, referred to as sfermions (e.g. stop, sbottom, stau). Meanwhile, the vector gauge fields live within gauge supermultiplets, along with a spin-1/2 gaugino superpartner (e.g. wino, bino). Finally, a scalar spin-0 field such as the Higgs can be accommodated in a chiral multiplet, together with a spin-1/2 superpartner (in the case of the Higgs, a Higgsino).

In the limit where supersymmetry is preserved, the elements of a supermultiplet share many properties. They have equal masses, and reside in the same representation of the gauge group. As the supersymmetry generators commute with those of gauge transformations, in the context of the Standard Model group this implies all fields within a supermultiplet have the same weak hypercharge, weak isospin, and colour charge; consequently they also have the same electric charge.

The requirement that a supermultiplet contains equal number of fermionic and bosonic degrees of freedom fails when particles are off-shell, i.e. the supersymmetry algebra

only closes when the classical equations of motions are satisfied. In order to consistently define a chiral supermultiplet also off-shell, an auxiliary component field F is introduced. It is a complex scalar field, but does not have a kinetic term, and its equation of motion is simply $F = F^* = 0$. A similar term D is added to gauge supermultiplets. In short, a chiral supermultiplet is made up of a Weyl fermion ψ, complex scalar ϕ and auxiliary field F, while a gauge supermultiplet contains a gauge field A_μ, gaugino λ and auxiliary field D. In theories of flavour, we will see that enforcing vanishing F terms of new fields known as driving fields can constrain the vacuum alignments of family symmetry-breaking fields, leading to predictive mass structures. This mechanism is called F-term alignment.

In a theory with several chiral supermultiplets ψ_i, the interacting (i.e. non-gauge) part of a Lagrangian invariant under supersymmetry may be written as

$$\mathcal{L} = -\frac{1}{2}W^{ij}\psi_i\psi_j + W^i F_i + \text{h.c.}, \tag{1.24}$$

in terms of a single function W known as the superpotential, which is holomorphic over the scalar fields. W^i and W^{ij} are given by functional derivatives,

$$W^i = \frac{\delta W}{\delta \phi_i}, \qquad W^{ij} = \frac{\delta^2 W}{\delta\phi_i \delta\phi_j}. \tag{1.25}$$

It can also be shown that the equations of motion of the auxiliary fields F_i and their conjugates are $F_i = -W_i^*$ and $F^{*i} = -W^i$. The free part of the Lagrangian contains terms $F_i F^{*i} = |F_i|^2$. The auxiliary fields may then be eliminated, giving $F_i F^{*i} = W^i W_i^* = |W_i|^2$, which is the form of a scalar potential $V(\phi, \phi^*)$. The complete scalar potential includes also contributions from D terms and is given by $V = |F_i|^2 + |D_i|^2$. As this thesis concerns the flavour sector of the Standard Model and its extensions, which is encoded in the superpotential, D terms will not be considered further here.

A more elegant description of supersymmetry promotes the supermultiplet to an object known as a superfield. It is defined on a manifold called superspace, which extends the usual four-component spacetime coordinates by anticommuting spinor coordinates θ and $\theta^\dagger$. Theories defined in terms of superfields are manifestly invariant under supersymmetry transformations. Now consider a single chiral superfield $\hat{\Phi}$ which describes the supermultiplet (ψ, ϕ, F). In appropriately chosen spacetime coordinates x_μ, $\hat{\Phi}$ may be written as

$$\hat{\Phi} = \phi(x) + \sqrt{2}\theta\psi(x) + \theta\theta F(x). \tag{1.26}$$

The superpotential defined above and its derivatives are identically described in terms of $\hat{\Phi}$ rather than ϕ.

1.4.2 The hierarchy problem

Having established some of the key components of a supersymmetric theory, we turn to arguably the greatest motivation for seeking low-scale supersymmetry: the hierarchy problem. Recall that the Higgs, just like fermions, acquires a mass when electroweak symmetry is broken. This suggests that the natural scale of the Higgs mass is the electroweak scale $\Lambda_{\text{EW}} \sim 100$ GeV, corroborated by the measurement of $m_H \approx 125$ GeV. Unfortunately, the Higgs mass is not stable against corrections coming from new physics at higher scales. For instance, the Higgs propagator is subject to corrections from loops containing fermions. The loop integral may be regulated by imposing a momentum cutoff Λ, on the scale of new physics; corrections to the Higgs mass are quadratic in this scale, i.e. $\Delta m_H^2 \propto \Lambda^2$. Even if no new physics and no new scale is inserted by hand, gravity effects are expected to come into effect at the Planck scale $M_P \sim 10^{19}$ GeV, implying a tuning of up to 17 orders of magnitude between tree- and loop-level contributions to m_H^2, which would need to be performed at every order in perturbation theory.

In supersymmetry, however, the postulated scalar partners of each Standard Model fermion give rise to additional loop contributions to the Higgs mass that exactly cancel the quadratic contribution from the fermion loop. This is due to the fact that the couplings to the Higgs of scalar and fermion components (λ_S and λ_f, respectively) of a given supermultiplet are related, namely $\lambda_S = |\lambda_f|^2$. By the non-renormalisation theorem [45] of supersymmetry, this cancellation occurs to all orders. This is promising, but immediately raises a concern: supersymmetry cannot remain unbroken at the electroweak scale, or these superpartners would already have been discovered. However, the relationship between couplings that yields the successful cancellation of quadratic corrections is dependent on how supersymmetry is broken. It was understood that the breaking must be mediated by terms with positive mass dimension, so-called soft supersymmetry breaking.[5]

The presence of soft breaking terms runs the risk of reintroducing the very problem it was intended to resolve, as they induce corrections to the Higgs mass proportional to the scale soft supersymmetry breaking m_{soft}, i.e. $\Delta m_H^2 \sim m_{\text{soft}}^2$. If $m_{\text{soft}} \gg m_H$, a fine-tuning reappears. m_{soft} should therefore not far exceed the electroweak scale. However, experimental searches at the LHC have failed to find any evidence of supersymmetry, up to scales of approximately 2 TeV, suggesting naively that a tuning of at least one in ten is required. This has put a dent in the paradigm of "natural" supersymmetry, but has not broken it entirely.

[5] The expectation is that supersymmetry, if it exists, is an exact symmetry which is broken spontaneously, analogous to electroweak symmetry breaking. In this context, the soft parameters are a parametrisation of our ignorance of how this breaking occurs.

1.4.3 The minimal supersymmetric Standard Model

Name	Particle		Superpartner	
	Field	Spin	Field	Spin
(s)quarks	Q_i	1/2	$\widetilde{Q}_i$	0
	u_i^c	1/2	$\widetilde{u}_i^c$	0
	d_i^c	1/2	$\widetilde{d}_i^c$	0
(s)leptons	L_i	1/2	$\widetilde{L}_i$	0
	e_i^c	1/2	$\widetilde{e}_i^c$	0
Gluon/gluino	G	1	$\widetilde{G}$	1/2
W boson/wino	W	1	$\widetilde{W}$	1/2
B boson/bino	B	1	$\widetilde{B}$	1/2
Higgs(ino)	H_u	0	$\widetilde{H}_u$	1/2
	H_d	0	$\widetilde{H}_d$	1/2

Table 1.4: MSSM field content.

We complete this section by writing down the superpotential of the MSSM, to which the models presented in subsequent chapters reduce in the low-scale limit. The field content is given in Table 1.4. Without right-handed neutrinos, the superpotential is

$$W_{\text{MSSM}} = Y^u_{ij}\hat{Q}_i\hat{u^c_j}\hat{H}_u + Y^d_{ij}\hat{Q}_i\hat{d^c_j}\hat{H}_d + Y^e_{ij}\hat{L}_i\hat{e^c_j}\hat{H}_d + \mu\hat{H}_u\hat{H}_d. \tag{1.27}$$

All superfields $\hat{Q}, \hat{u^c}, \hat{d^c}, \hat{L}, \hat{e^c}, \hat{H}_u$ and $\hat{H}_d$ are defined as left-chiral; the $\hat{d^c}$ and $\hat{u^c}$ are therefore equivalent to right-handed (s)quark states, while $\hat{e^c}$ corresponds to the right-handed (s)electron.[6] For simplicity, we suppress colour and weak isospin indices, but we keep family indices. As the superpotential is holomorphic, it is not possible to couple up-type quarks to the complex conjugate of a single Higgs as done in the Standard Model (see Eqs. 1.9 and 1.14). One must instead introduce a second Higgs doublet H_u with opposite hypercharge to H_d which can couple to up-type fermions.[7]

The final term in Eq. 1.27 is the μ term, and generates masses for the Higgs fields. As noted above, the Higgs also receives corrections from soft supersymmetry-breaking terms. In order to avoid tuning problems, neither ought to be much larger than the electroweak scale. A value $\mu \lesssim 1$ TeV may be considered natural, but as it is not protected by any symmetry it can ostensibly take any value, up to M_P. Explaining its closeness to the electroweak scale is known as the μ problem. The (neutral components of) Higgs fields within H_u and H_d acquire VEVs, which consequently break electroweak symmetry. The VEVs are written v_u and v_d, respectively, and satisfy

$$v_u^2 + v_d^2 = v^2 \simeq 174 \text{ GeV}, \tag{1.28}$$

[6] The hats (ˆ) indicating superfields will be dropped henceforth.
[7] A second Higgs doublet is also required in the MSSM in order to cancel all gauge anomalies.

where v is the Standard Model electroweak VEV. We may also define the ratio

$$\tan\beta = \frac{v_u}{v_d}, \tag{1.29}$$

as a free parameter in the MSSM.

Theories of supersymmetry generally possess an additional symmetry known as R symmetry, which transforms the supercharges into each other, typically given by a global $U(1)$ symmetry or a discrete $\mathbb{Z}_N$. It is often broken to a $\mathbb{Z}_2$ subgroup, so called R or matter parity. The MSSM (and many extensions) thereby contains massive particles which are R-parity odd. The lightest supersymmetric particle (LSP) is therefore stable and, if electrically neutral, forms an excellent dark matter candidate, in the category of "weakly interacting massive particles" (WIMP).

1.5 Grand unification

Grand unification was first proposed in [46, 47], and a grand unified theory (GUT) of quarks and leptons has remained a compelling candidate for BSM physics. Although the earliest and simplest GUTs, which were non-supersymmetric, have since been ruled out, more advanced realisations including SUSY GUTs remain viable. In this section we review the motivations for grand unification, how the Standard Model may be embedded into the $SU(5)$ and $SO(10)$ groups, and discuss briefly the phenomenological consequences.

1.5.1 Motivation for a unified gauge group

The principle of grand unification is that the Standard Model gauge group $SU(3) \times SU(2) \times U(1)$ is embedded in a higher-rank group, which is spontaneously broken at some scale Λ, at which the Standard Model gauge couplings must be equal. Λ is therefore obviously not the electroweak scale, where the couplings are very different. However, they change with scale according to their renormalisation group equations, suggesting they may converge at some higher scale. Remarkably, it was found that the Standard Model gauge couplings (very nearly) acquired the same value at $\Lambda = M_{\text{GUT}} \sim 10^{15-16}$ GeV, consequently dubbed the GUT scale.

As the errors on the couplings were reduced, it became evident that exact unification in the simplest models was not possible. However, the situation could be improved with the inclusion of supersymmetry. In the MSSM it can be seen that the couplings meet at a single point at $\Lambda \sim 10^{16}$ GeV, to very good precision. This provides a strong motivation not only for a GUT, but a SUSY GUT. In Figure 1.1 we see how the gauge couplings,

reparametrised in terms of α_i^{-1}, where $\alpha_i = g_i^2/4\pi$,[8] change with renormalisation scale Q in both the Standard Model and the MSSM.

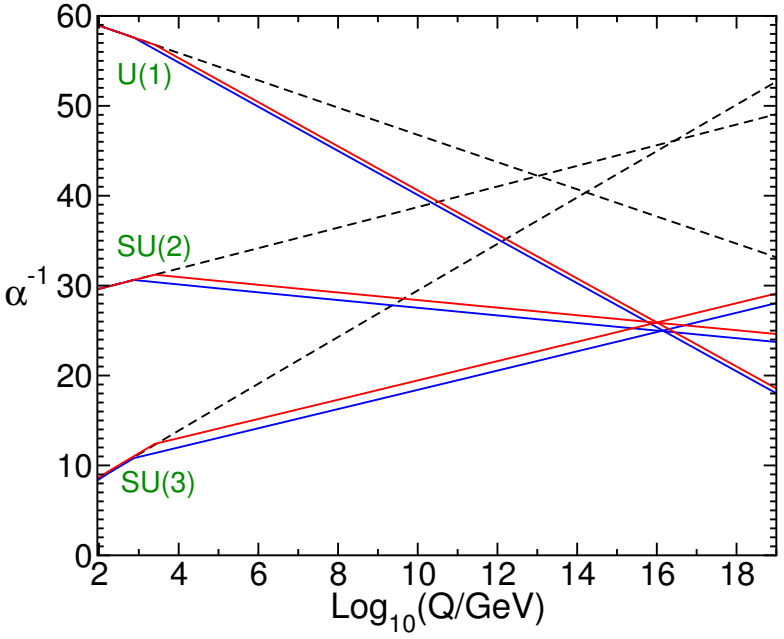

Figure 1.1: Renormalisation group evolution of inverse gauge couplings α_i^{-1} with scale Q for the Standard Model (dashed lines) and MSSM (solid lines). Figure from [44].

An additional feature of the Standard Model that provides strong motivation for gauge unification is charge quantisation, namely why quarks have electric charges that are integer multiples of $e/3$, where e is the electron charge. While free quarks have not been observed, all composite particles, whether two-component mesons such as the pion or three-component baryons such as the proton, are observed to have integer total charge (in units of e), from which we conclude that all quarks have charges $-e/3$ if they are down-type and $+2e/3$ if they are up-type. The question may also be phrased as one of why the smallest observed electric charge unit is $e/3$.

1.5.2 Embedding the Standard Model

Several options exist for the choice of group into which the Standard Model should be embedded. As the Standard Model group has total rank four, any embedding group must also be of rank four or greater. A candidate can consist of a single gauge group, such as $SU(5)$ [46] or $SO(10)$ [48, 49], or a product of groups as the Pati-Salam group $SU(4)_C \times SU(2)_L \times SU(2)_R$ [47]. While the Pati-Salam group arguably does not constitute true grand unification, as there are still three distinct gauge couplings, it was the first to propose a unification of quarks and leptons into a single representation, interpreting lepton number as the "fourth colour", and explains electric charge quantisation.

[8] In this normalisation, $g_2 = g$ and $g_1 = \sqrt{5/3}g'$.

Moreover it is a subgroup of $SO(10)$. It is possible to construct viable models based on larger $SU(N)$ groups or the exceptional group E_6, but these will not be discussed further here.

As the only rank-4 group that fulfils the above requirements, $SU(5)$ may be thought of as "minimal" unification. The Standard Model gauge fields (gluons and electroweak bosons) are unified in a single adjoint **24**,

$$A_\mu = \sum_{a=1}^{24} A_\mu^a \mathrm{T}^a, \tag{1.30}$$

where T^a are the generators of $SU(5)$ and may be written as 5×5 matrices. Eight of these reduce to the generators of $SU(3)$ which give the gluon degrees of freedom while three reduce to the $SU(2)$ generators which, together with the hypercharge generator, give the electroweak degrees of freedom. This accounts for half the degrees of freedom in A_μ. The remaining 12 are the X and Y gauge bosons, with masses naturally of order the scale where $SU(5)$ is broken, and which carry both colour and electroweak charges, allowing for new couplings between quarks and leptons. Moreover, above the unification scale, all gauge fields A_μ^a have a single associated coupling, i.e.

$$g_5 = g_3 = g = \sqrt{\frac{5}{3}} g'. \tag{1.31}$$

$SU(5)$ is broken by the VEV of a new Higgs field Φ at high scale, analogous to electroweak symmetry breaking. As rank is preserved, this Higgs is necessarily in the adjoint **24** representation, and acquires a VEV $\langle \Phi \rangle \propto \mathrm{diag}(2, 2, 2, -3, -3)$.

$SU(5)$ accommodates the Standard Model fermions of a single family in two representations, namely a $\bar{\mathbf{5}}$ and **10**.[9] They may be organised as

$$\bar{\mathbf{5}} = \begin{pmatrix} d_1^c \\ d_2^c \\ d_3^c \\ e \\ -\nu_e \end{pmatrix}, \qquad \mathbf{10} = \begin{pmatrix} 0 & u_3^c & -u_2^c & -u_1 & -d_1 \\ -u_3^c & 0 & u_1^c & -u_2 & -d_2 \\ u_2^c & -u_1^c & 0 & -u_3 & -d_3 \\ u_1 & u_2 & u_3 & 0 & -e^c \\ d_1 & d_2 & d_3 & e^c & 0 \end{pmatrix}, \tag{1.32}$$

where the subscripts on u and d fields are colour indices, and the GUT multiplets are defined as left-chiral. Furthermore, the Higgs field, which is an $SU(2)$ doublet, is minimally contained in a **5** of $SU(5)$. In other words, we simply extend the Standard Model fundamental doublet to a complete multiplet of the GUT, i.e. the fundamental **5** of $SU(5)$.[10] This however leads to an issue known as the doublet-triplet splitting problem.

[9] The bar in the $\bar{\mathbf{5}}$ refers to a conjugate or anti-fundamental representation.
[10] The two Higgs doublets of the MSSM are contained in a $\mathbf{5} + \bar{\mathbf{5}}$ pair.

When the GUT group is broken to the Standard Model, the Higgs **5** is decomposed into two parts: the electroweak Higgs doublet, and an $SU(3)$ triplet. As discussed shortly, the scale Λ, which is directly related to the mass of the Higgs triplet, is necessarily very high, close to M_{GUT}. The natural expectation is for fields arising from the same GUT multiplet to have equal-scale masses, which in the case of the Higgs either suggests electroweak-scale triplets (giving very rapid proton decay) or GUT-scale doublets, neither of which is acceptable. This problem is not unique to $SU(5)$; in appendices we demonstrate how doublet-triplet splitting may be achieved in specific models based on $SU(5)$ and $SO(10)$, respectively.

Electric charge is defined in Eq. 1.7 by $Q = T^3 + Y$ in terms of the electroweak generators, which have natural analogues in $SU(5)$. As these generators are traceless, the sum of all charges in the fermion $\bar{\mathbf{5}} = (d_1^c, d_2^c, d_3^c, e, \nu)$ must equal zero. More precisely, we get $Q = \mathrm{diag}(1/3, 1/3, 1/3, -1, 0)$, which correspond to the known electric charges of the down antiquark, electron and neutrino and enforces the electron charge to be exactly three times larger than the down quark charge. Finally, it is worth noting that $SU(5)$ does not naturally predict right-handed neutrinos, as all observed fermions are adequately accommodated in the $\bar{\mathbf{5}} + \mathbf{10}$, but they can be added by hand as pure singlet **1**s. In the absence of a flavour symmetry which unifies families of fermions, the Standard Model when embedded in $SU(5)$ consists of at least six matter fields: three each of a $\bar{\mathbf{5}}$ and **10**, plus another two or three singlets if right-handed neutrinos are desired.

The degree of unification can be improved if one goes to $SO(10)$, where all fermions of a single family can be united in a spinorial **16**, which mandates a particle with quantum numbers of a right-handed neutrino. The vector bosons are in the adjoint **45** representation. The electroweak Higgs doublets can again reside within a fundamental representation of the group – a **10** – as the $SO(10)$ product $\mathbf{10} \cdot \mathbf{16} \cdot \mathbf{16}$ contains a singlet, such that we may write down a Yukawa term. If only a single **10** Higgs is present, this is the only allowed Yukawa term, implying all particles within a family have the same mass, which is phenomenologically unacceptable. To construct a theory with viable Yukawa structures one must add additional Higgs fields; at least one must anyway be added which spontaneously breaks $SO(10)$. The desirable properties of gauge coupling unification and charge quantisation in $SU(5)$ are present also for $SO(10)$, as is the problem of doublet-triplet splitting. Unlike $SU(5)$, which is necessarily broken by an adjoint Higgs VEV, $SO(10)$ allows more than one path to the Standard Model. It contains the maximal subgroups $SU(5) \times U(1)$ and $SU(4) \times SU(2) \times SU(2)$ (the Pati-Salam group). The breaking pattern to either group or to a lower-rank subgroup depends on the representation of the Higgs field that acquires the VEV. For an overview of possible breaking schemes, see e.g. [50], where also group theory of $SO(10)$ is discussed.

1.5.3 Phenomenology

In the Standard Model, the stability of the proton is ensured by conservation of baryon number B. As has been noted above, a generic prediction of GUTs is new particles which can mediate interactions that violate B (and lepton number L), such as the X and Y gauge bosons and Higgs triplets T. Both can couple either to two quarks (generically labelled q, either Q_i, u_i^c or d_i^c) or one quark and one lepton (labelled ℓ, either L_i or e_i^c). This leads to annihilation processes like $qq \to X, Y, T \to q\ell$, and effective four-fermion interactions $qqq\ell/\Lambda^2$,[11] where Λ is closely related to the mass of the mediating particle. Consequently the proton is unstable and decays, with an associated lifetime inversely proportional to its decay rate. As the proton lifetime is strongly constrained by experiment to be larger than 10^{31-33} years (depending on the decay mode) [23], the above B-violating interactions must be strongly suppressed.This implies either Λ is very large, or the dangerous effective terms (including all relevant higher-order terms) are forbidden by some symmetry.

For the X and Y bosons, the $qqq\ell$ interactions are naturally suppressed by $\Lambda \sim M_{\mathrm{GUT}}$, as X, Y are expected to acquire masses from the (super)field that breaks the GUT. There is ambiguity in the natural expectation for the mass of Higgs triplets, due to the doublet-triplet splitting problem. However from a phenomenological standpoint they too must have masses near M_{GUT}.

There is a second consideration when establishing the masses of new particles: gauge coupling unification must not be spoiled. If the particles are gauge non-singlets, they will enter as loop corrections to the running of the relevant couplings, primarily at energy scales equivalent to their mass. The remarkable unification in the MSSM seen in Figure 1.1 relies on the assumption that there is no additional field content between the supersymmetry scale, which is typically taken to be $\mathcal{O}(\mathrm{TeV})$, and the GUT scale M_{GUT}. Additional fields at an intermediary scale could affect the running of the gauge couplings and spoil the impressive confluence exhibited in the minimal model. Conversely, in a non-SUSY GUT, the presence of new physics at an intermediary scale may induce the necessary corrections to achieve unification.

1.6 Family symmetry

The Standard Model has, in the absence of mass terms, a large accidental global symmetry $[U(3)]^5$, i.e. it is the maximal symmetry that preserves the kinetic terms. Each $U(3)$ can be understood to arise from the freedom to redefine the three families of a given type of fermion f, where $f = Q_L, u_R, d_R, L_L, e_R$. In its minimal extension with (also massless) right-handed neutrinos ν_R, this symmetry is extended to $[U(3)]^6$. While

[11] In supersymmetry, the corresponding superpotential term is $qqq\ell/\Lambda$.

these symmetries are necessarily broken by the observed fermion masses, it is interesting to consider a scenario where some global symmetry is made manifest at high scale, and broken spontaneously by the VEV of some scalar field. Such fields, called flavons, are typically gauge singlets, and often denoted ϕ. Fermions ψ couple to these flavon fields (and the Higgs H), which subsequently acquire VEVs, giving effective Yukawa terms. In other words, the Standard Model Yukawa parameters are given a dynamical origin. Schematically,

$$\mathcal{L} \sim \frac{1}{\Lambda}\phi H\bar{\psi}\psi \to \frac{\langle\phi\rangle}{\Lambda}H\bar{\psi}\psi \to yH\bar{\psi}\psi. \tag{1.33}$$

The manner in which this symmetry is broken, and how fermions couple to flavons, dictate the structure of Yukawa and mass matrices. This can give a powerful insight into the flavour puzzle.

Models have been constructed based on continuous family symmetries such as a global $SU(3)$ [51, 52]. However the state of the art is to use non-Abelian discrete symmetries (for reviews, see e.g. [53–56]), which can lead to sharp predictions for mixing parameters, and do not lead to massless Goldstone modes as in a spontaneously broken continuous symmetry.[12] Whether continuous or discrete, choosing a non-Abelian symmetry has the immediate consequence that Standard Model fermions are collected in non-trivial representation of the group: family unification. It is particularly relevant to consider groups which admit triplet representations, providing an *a posteriori* justification for the observation of three families of fermions. The smallest such group is A_4, which describes the symmetries of a tetrahedron. Other popular choices are S_4 (describing the permutation of four elements) and $\Delta(27)$. A_4 and S_4 are subgroups of $SO(3)$, while the $\Delta(27)$ is a subgroup of $SU(3)$ and allows both triplet and antitriplet representations; all three have been implemented in realistic GUT models described in Chapters 3, 4 and 5. Their representations and product rules are given in Appendix A.

Before moving on to discuss model building with non-Abelian symmetries, we remark on a very popular alternative based on Abelian symmetry: the Froggatt-Nielsen mechanism [58]. The idea is to assume a single global $U(1)$ (or $\mathbb{Z}_N$ if a discrete symmetry is preferred), and a scalar flavon field ξ. Fermions are given charges under this $U(1)$ which dictate their coupling to the ξ field. In the effective theory below the $U(1)$-breaking scale Λ, the Yukawa couplings Y_{ij} are replaced by effective couplings involving various powers of ξ/Λ. If ξ now acquires a VEV somewhat below Λ (say, an order of magnitude), the resultant Yukawa matrices are naturally hierarchical, with their structures determined solely by the $U(1)$ charge assignments. The Froggatt-Nielsen mechanism remains a top candidate for explaining the existence of mass hierarchies. A complete realisation of this mechanism requires adding additional field content to make the theory renormalisable.

[12] Discrete symmetries also permit in principle a mechanism to escape the gravity problem of global symmetries, namely the common understanding that gravitational interactions at the Planck scale do not respect global symmetries, as discussed in [57]. This may be circumvented in the case of a discrete symmetry if one assumes it to be the remnant subgroup of a spontaneously broken gauge symmetry, on the condition that all discrete anomalies cancel within the model.

For example, each effective term like $\xi^n \bar{\psi}\psi H/\Lambda^n$ can be understood as the result of integrating out n heavy vector-like fermion pairs. A discrete version of this mechanism is implemented in a model based on $A_4 \times SU(5)$ in Chapter 3, giving the up-type quark Yukawa matrix (which also controls most quark mixing). It demonstrates also that Abelian and non-Abelian symmetries are not exclusive, and may be used in harmony to explain flavour structures.

In models with discrete non-Abelian symmetries, flavour structure is dictated by the alignments of the flavon VEVs which couple to fermions, and which break the original symmetry, either down to a subgroup, or to nothing. The exact form of the couplings of these flavons to fermions will inform the structures of the Yukawa and mass matrices. The first option, where a residual symmetry remains after flavour breaking, leads to so-called "direct" models of flavour, while the latter, where no part of the original symmetry is present at low scale, corresponds to "indirect" models.

Direct models are motivated by the presence of accidental symmetries in the lepton sector, namely a $\mathbb{Z}_2 \times \mathbb{Z}_2$ Klein symmetry in the neutrino mass matrix and a $\mathbb{Z}_3$ in the charged lepton matrix. A flavour model postulates a family symmetry G_F which is broken in a way that preserves these symmetries. For small groups, only a small set of alignments can do this, which gives sharp predictions for lepton mixing parameters that are in conflict with experiment. Perhaps the most popular realisation (prior to the measurement of a non-zero reactor angle) of the direct approach was to use A_4 or S_4 to produce so-called tri-bimaximal (TB) mixing [59, 60], which respects the accidental symmetries of the mass matrices, and wherein the columns of $U_{\rm PMNS}$ are proportional to, respectively, $(-2, 1, 1)$, $(1, 1, 1)$ and $(0, 1, -1)$. It predicts $\sin\theta_{23} = 1/\sqrt{2}$, $\sin\theta_{12} = 1/\sqrt{3}$, $\theta_{13} = 0$ and no CP violation. The good agreement with data at the time fueled the interest in flavour models with non-Abelian discrete symmetry. In light of the most recent data, this approach requires $\Delta(6n^2)$ for large values of n [61–65].[13]

In the indirect approach, there is no requirement for a subgroup of the original symmetry to remain, i.e. the accidental symmetries of the mass matrices are not identified with any part of G_F. This allows flavons to acquire a much wider range of alignments, with the possibility of constructing phenomenologically more successful flavour models, even with small discrete groups. The price to pay for this freedom is that specifying the vacuum alignments becomes model-dependent: the precise field content and allowed couplings will dictate the flavon alignments. The models in Chapters 2, 3 and 4 are all indirect, while that in Chapter 5 is semi-direct: only part of the accidental symmetry can be identified with a generator of the family symmetry.

[13] An analogous approach based on $\Delta(6n^2)$ has also been considered in the quark sector [66–68].

1.7 Leptogenesis

In this section we describe the open question of the baryon asymmetry of the Universe, and its potential resolution via the leptogenesis mechanism. We also calculate the baryon asymmetry in a toy model of thermal N_1 leptogenesis.

1.7.1 The baryon asymmetry of the Universe

The current "standard model" of cosmology is the ΛCDM model [69], where Λ refers to the (positive) cosmological constant responsible for the acceleration of the Universe [70], and CDM stands for "cold dark matter". It is a hot Big Bang model, which postulates an initially very dense, hot Universe that subsequently expands. It is widely believed that this is preceded by a period of superluminal expansion known as inflation [71–73]. As the Universe cools, hadrons and then light nuclei (hydrogen, helium, lithium) form in what is known as Big Bang nucleosynthesis (BBN), which then combine with electrons to form atoms, and eventually larger structures. The ΛCDM model successfully explains most cosmological observables, including the existence and anisotropies of the CMB, the accelerating expansion of the Universe, large scale galaxy structure, and the abundances of the light elements.

However, it fails to explain why we have only observed primordial matter but not antimatter, i.e. the baryon asymmetry of the Universe (BAU). Assuming an inflationary period, any pre-existing asymmetry would be washed out by the rapid expansion; it must therefore be generated after inflation and before BBN. The conditions for generating a BAU are understood, and several mechanisms have been proposed that necessarily extend beyond the Standard Models of both particle physics and cosmology. The ultimate goal is to understand a single parameter: the number density of baryons in the Universe. We are concerned with the difference in baryon and antibaryon densities $n_B - n_{\overline{B}}$. However, given that primordial antimatter has not been observed, $n_B \gg n_{\overline{B}}$ (barring some exotic model). One typically considers the baryon-to-photon ratio

$$\eta_B = \frac{n_B - n_{\overline{B}}}{n_\gamma} = (6.10 \pm 0.04) \times 10^{-10}. \tag{1.34}$$

Alternatively, the asymmetry may be normalised by the entropy density, giving

$$Y_B = (0.87 \pm 0.01) \times 10^{-10}. \tag{1.35}$$

See [74, 75] for reviews and [37] for a recent determination of the error.

It was discovered by Sakharov [76] that in a particle physics theory, three conditions need to be satisfied in order to produce a baryon asymmetry. The first condition is baryon number (B) violation; clearly, all interactions of the theory cannot preserve the

net number of baryons. The second condition is charge (C) and charge-parity (CP) violation. To demonstrate this, let us consider the decay of a particle X into a baryon q and some other particle p. If C is conserved, the production rates of baryons and antibaryons are equal, i.e. $\Gamma(X \to pq) = \Gamma(\overline{X} \to \bar{p}\bar{q})$, and no net asymmetry is formed. Next, consider decays of X into pairs of either left- or right-handed baryons. While $\Gamma(X \to q_L q_L) \neq \Gamma(\overline{X} \to \bar{q}_L \bar{q}_L)$ in general, CP conservation dictates $\Gamma(X \to q_L q_L) = \Gamma(\overline{X} \to \bar{q}_R \bar{q}_R)$ and $\Gamma(X \to q_R q_R) = \Gamma(\overline{X} \to \bar{q}_L \bar{q}_L)$. The total decay rates of X and $\overline{X}$ into baryons and antibaryons, respectively, are again equal:

$$\Gamma(X \to q_L q_L) + \Gamma(X \to q_R q_R) = \Gamma(\overline{X} \to \bar{q}_R \bar{q}_R) + \Gamma(\overline{X} \to \bar{q}_L \bar{q}_L). \tag{1.36}$$

The third condition is that some of the interactions capable of producing a baryon asymmetry must occur outside of thermal equilibrium. If all relevant processes remain in equilibrium, any baryon production is washed out by the inverse process, i.e. $\Gamma(X \to pq) = \Gamma(pq \to X)$.

In fact all these conditions may be satisfied within the Standard Model itself (without right-handed neutrinos). However, the size of the BAU generated by the Standard Model is insufficient to explain the observed η_B. In particular, it was found that CP violation in the quark sector was too small [77]. An explanation must therefore come from new physics, including new sources of CP violation. One potential solution exists within GUTs such as $SU(5)$, where the asymmetry is generated from decays of heavy gauge bosons. This is now disfavoured, as the generated asymmetry is expected to be washed out by nonperturbative $(B + L)$-violating processes known as sphalerons. A more promising candidate, first proposed by Fukugita and Yanagida [78], is that the asymmetry is first generated in the lepton sector and subsequently transformed into a baryon asymmetry by these same sphalerons; this is leptogenesis.

1.7.2 The leptogenesis mechanism

In its original and simplest formulation, leptogenesis postulates two or more heavy right-handed neutrinos, which decay into lepton-Higgs (or antilepton-Higgs) pairs via the Yukawa coupling. Although the tree-level matrix element is automatically CP-conserving and thus decays equally to leptons and antileptons, interference effects at one loop can lead to CP violation and a net lepton asymmetry. This relies on a non-zero PMNS phase δ^ℓ, which is currently favoured by global fits to experiment (indeed, a near-maximal phase $\delta^\ell \sim -\pi/2$ seems preferred) [36]. It can also be understood that at least some of these interactions will take place out of thermal equilibrium, when the temperature of the Universe falls below the energy scale of the decaying neutrinos.

Some fraction of this lepton asymmetry must then be converted into a baryon asymmetry. The mechanism for this is embedded within the Standard Model, in the form of

sphalerons. They are non-perturbative solutions to the classical field equations which break B (thus fulfilling the last of Sakharov's conditions) and L, while conserving $B-L$. Above the electroweak breaking scale, such sphaleron interactions are in thermal equilibrium and efficient. Therefore, a net asymmetry in either leptons or baryons will get mixed into the other. What constitutes a problem for GUT baryogenesis, as sphalerons wash out the net baryon asymmetry, is in leptogenesis a desirable feature.

Any theory with right-handed neutrinos contains the necessary ingredients for leptogenesis to proceed. Whether or not the correct BAU can be achieved is a *quantitative* statement, taking into account not only the size of the produced asymmetry but also washout effects due to inverse decays or scattering. It turns out leptogenesis is highly compatible with the type-I seesaw mechanism, as the required right-handed neutrino masses are of similar order in both cases. Let us sketch the mechanism in a toy model of thermal leptogenesis. We limit ourselves here to the non-SUSY case; the mechanism works very similarly in supersymmetry, up to various numerical coefficients, as we will see in later chapters.

Thermal leptogenesis refers to the scenario where the right-handed neutrinos N_i are produced in the thermal bath at high temperatures, i.e. the neutrino abundances N_{N_i} are initially zero. Let us simplify the discussion by assuming the neutrino masses are very hierarchical, and the dominant contribution to leptogenesis comes from the lightest neutrino N_1. The evolution of the neutrino abundance is given by the Boltzmann equation

$$\frac{dN_{N_1}}{dz} = -D\left(N_{N_1} - N_{N_1}^{\mathrm{eq}}\right). \tag{1.37}$$

$N_{N_1}^{\mathrm{eq}}$ is the abundance at thermal equilibrium, and $z \equiv M_1/T$. D is a decay factor, which relates the total decay rate Γ_D and the Hubble expansion rate H, and depends on z. For a detailed study of what comprises D, see e.g. [79]. We also need to determine the lepton asymmetry. It is often convenient to consider the $B-L$ asymmetry N_{B-L}, whose evolution is described by

$$\frac{dN_{B-L}}{dz} = -\varepsilon_1 D\left(N_{N_1} - N_{N_1}^{\mathrm{eq}}\right) - W N_{B-L}. \tag{1.38}$$

The first term on the right-hand side is a source term for the $B-L$ asymmetry, given in terms of the CP (or decay) asymmetry ε_1. The second term describes washout, governed by the factor W which contains information about inverse decays and scattering effects. Again we refer to [79] for details. Eqs. 1.37 and 1.38 form a set of coupled differential equations, which may be solved for thermal initial conditions at $z = 0$ to give the final asymmetry N_{B-L}^{f} at $z \gg 1$. The solution may be parametrised in terms of ε_1 and a parameter κ_1 known as the efficiency factor, by $N_{B-L}^{\mathrm{f}} = \varepsilon_1 \kappa_1$. The quantity of interest, the baryon-to-photon ratio η_B, is then given simply by

$$\eta_B = a_{\mathrm{sph}} \frac{N_{B-L}^{\mathrm{f}}}{N_\gamma^{\mathrm{rec}}} \simeq 0.96 \times 10^{-2} \varepsilon_1 \kappa_1, \tag{1.39}$$

in the Standard Model, where $N_\gamma^{\rm rec} \approx 37$ accounts for the production of photons after leptogenesis until recombination[14] and $a_{\rm sph} = 28/79 \approx 1/3$ is the fraction of the lepton asymmetry converted into a baryon asymmetry by sphalerons.

In summary, to calculate the BAU one needs to evaluate the CP asymmetry ε_1 as well as the decay and washout factors D and W. These depend on the model under consideration and assumptions made. We leave the discussion on D and W here, but let us say a few additional words about the CP asymmetry ε_1, as it is closely related to the neutrino Yukawa matrix, which features prominently in the flavour models within this thesis. It is defined by

$$\varepsilon_1 = \frac{\Gamma_1 - \bar{\Gamma}_1}{\Gamma_1 + \bar{\Gamma}_1}, \tag{1.40}$$

where Γ_1 and $\bar{\Gamma}_1$ are the decay rates of N_1 neutrinos decaying, respectively, into ℓH_u lepton-Higgs or $\bar{\ell} H_u^\dagger$ antilepton-Higgs pairs. It is determined by calculating the interference between the tree-level diagram and one-loop self-energy and vertex diagrams, shown in Figure 1.2,[15] and given by

$$\varepsilon_1 = \frac{1}{8\pi} \sum_{j=2,3} \frac{\mathrm{Im}\left[\left((\lambda^\dagger\lambda)^2\right)_{1j}\right]}{(\lambda^\dagger\lambda)_{11}} g^{\rm SM}\left(\frac{M_j^2}{M_1^2}\right), \tag{1.41}$$

where λ is the neutrino Yukawa matrix and $g^{\rm SM}(x)$ a loop function given by

$$g^{\rm SM}(x) = \sqrt{x}\left((1+x)\ln\left(\frac{1+x}{x}\right) - \frac{2-x}{1-x}\right). \tag{1.42}$$

In the hierarchical limit $x = (M_j/M_1)^2 \gg 1$, this simplifies to $g^{\rm SM}(x) \approx -3/(2\sqrt{x})$.

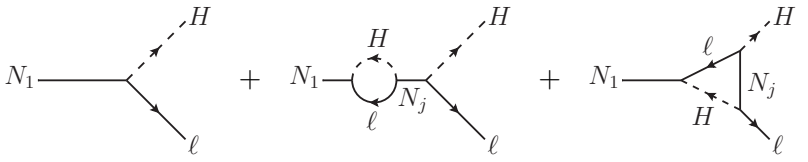

Figure 1.2: Diagrams contributing to CP asymmetry in neutrino decays.

[14] Recombination, referring to when nuclei and electrons combined to form atoms, occurred approximately 3×10^5 years after the Big Bang, corresponding to $T \sim 0.3$ eV.

[15] These and all future interaction diagrams were drawn with `JaxoDraw` [80].

Chapter 2

Constrained sequential dominance

In this chapter we introduce the framework of sequential dominance for understanding the nature of neutrino mass and mixing, showing how predictive mass structures may arise from vacuum alignment of triplet flavons. The contents of this chapter are derived primarily from work published in [1], where a dedicated numerical analysis is performed for a class of models known as CSD(n), and [3], which discusses leptogenesis in these models. As a point of notation, we refer in this chapter to the PMNS parameters as θ_{ij} and $\delta_{\rm CP}$, consistent with the notation in [1, 3]. In other chapters they are denoted θ^{ℓ}_{ij} and δ^{ℓ}.

2.1 The sequential dominance framework

As discussed in the Introduction, one of the most attractive possibilities for generating small neutrino masses is the type-I seesaw mechanism involving two or three right-handed neutrinos. The effective Majorana mass matrix for the light neutrinos[1] is given by the seesaw formula,

$$m^{\nu} = -m^{D} M_R^{-1} (m^{D})^{\intercal}, \tag{2.1}$$

where m^D and M_R are the Dirac and right-handed Majorana mass matrices, respectively. A natural way to obtain large lepton mixing and normal neutrino hierarchy within type-I seesaw is to assume the sequential dominance (SD) of right-handed neutrinos [81–83]. The idea behind SD is that there are three right-handed neutrinos $\nu_R^{\rm atm}$, $\nu_R^{\rm sol}$ and $\nu_R^{\rm dec}$, where $\nu_R^{\rm dec}$, usually the heaviest one with mass $M_{\rm dec}$, is almost decoupled from the seesaw mechanism, and is responsible for the lightest physical neutrino mass m_1. Of the remaining two, $\nu_R^{\rm atm}$, with mass $M_{\rm atm}$, gives the dominant seesaw contribution and is mainly responsible for the (heaviest) atmospheric neutrino mass m_3 and mixing θ_{23}, while $\nu_R^{\rm atm}$, with mass $M_{\rm sol}$, gives a subdominant contribution, responsible

[1] m^{ν} is occasionally referred to as the physical mass matrix.

for the (second-heaviest) solar neutrino mass m_2 and mixing θ_{12}. SD therefore immediately predicts a normal neutrino mass hierarchy $m_1 \ll m_2 \ll m_3$. The magnitude of atmospheric and solar mixing is determined by ratios of Yukawa couplings, which can easily be large, while reactor mixing is typically $U_{e3}^{\rm PMNS} \lesssim \mathcal{O}(m_2/m_3) \approx 0.17$, as shown in [84]. This successful prediction was made over a decade before the reactor angle θ_{13} was measured [85–87].

This argument can be made more precise when we define the neutrino mass matrices that enter the seesaw formula. In the basis where the right-handed neutrino mass matrix is diagonal, i.e. $M_R = \mathrm{diag}(M_{\rm atm}, M_{\rm sol}, M_{\rm dec})$, we construct the neutrino Dirac mass matrix m^D from three columns as $m^D = (m^D_{\rm atm}, m^D_{\rm sol}, m^D_{\rm dec})$. Applying the seesaw formula gives

$$m^\nu = \frac{m^D_{\rm atm}(m^D_{\rm atm})^\intercal}{M_{\rm atm}} + \frac{m^D_{\rm sol}(m^D_{\rm sol})^\intercal}{M_{\rm sol}} + \frac{m^D_{\rm dec}(m^D_{\rm dec})^\intercal}{M_{\rm dec}}, \tag{2.2}$$

where

$$\frac{(m^D_{\rm atm})^\dagger m^D_{\rm atm}}{M_{\rm atm}} \gg \frac{(m^D_{\rm sol})^\dagger m^D_{\rm sol}}{M_{\rm sol}} \gg \frac{(m^D_{\rm dec})^\dagger m^D_{\rm dec}}{M_{\rm dec}}, \tag{2.3}$$

To obtain precise predictions for mixing one can go further and impose constraints on the Yukawa couplings, dubbed constrained sequential dominance (CSD) [88]. The observed pattern of lepton mixing angles can be understood in the above SD framework as follows. We work in the basis where the charged lepton and right-handed neutrino mass matrices are diagonal, known as the flavour basis, such that all mixing originates in the Dirac matrix m^D. If the dominant neutrino $\nu_R^{\rm atm}$ has couplings $m^D_{\rm atm} = (0, a_1, a_2)$ to $(\nu_e, \nu_\mu, \nu_\tau)$, then this implies $\tan\theta_{23} \sim a_1/a_2$ [81, 82] and a bound $\theta_{13} \lesssim m_2/m_3$ [84, 89]. The subdominant neutrino $\nu_R^{\rm sol}$ has couplings $m^D_{\rm sol} = (b_1, b_2, b_3)$ to $(\nu_e, \nu_\mu, \nu_\tau)$ which further yield $\tan\theta_{12} \sim \sqrt{2}b_1/(b_2 - b_3)$ [83]. However, in practice these estimates are subject to large corrections beyond the SD approximation, and as the analysis presented in this chapter will show, the atmospheric and reactor angles in particular depend sensitively on a choice of phase. By the SD assumption, the mixing angles are of course largely insensitive to the decoupled neutrino $\nu_R^{\rm dec}$.

In order to obtain sharp predictions for lepton mixing angles, the relevant Yukawa coupling ratios need to be fixed, for example using vacuum alignment of family symmetry-breaking flavons. Flavons, their alignments, and how to integrate them into models of flavour will be discussed more in the next section. The first attempts to use vacuum alignment within an $SU(3)$ family symmetry to predict maximal atmospheric mixing ($\tan\theta_{23} \sim 1$) from equal $\nu_R^{\rm atm}$ couplings $m^D_{\rm atm} = (0, a, a)$ were discussed in [51, 52]. Subsequently, constrained sequential dominance (CSD) [88] was proposed to explain tri-bimaximal (TB) mixing with a zero reactor angle by using vacuum alignment to fix the $\nu_R^{\rm sol}$ couplings to also be equal up to a sign, namely $m^D_{\rm sol} = (b, b, -b)$.[2]

[2] Note that $(0, a, a) \cdot (b, b, -b) = 0$. This orthogonality is related to the fact that CSD(1) respects form dominance, since columns of the Dirac mass matrix in the flavour basis are proportional to the columns of the unitary PMNS matrix [90, 91].

Following the measurement of the reactor angle, various types of CSD have been proposed, which preserves the atmospheric couplings and hence an approximate maximal atmospheric angle $\tan\theta_{23} \sim a_1/a_2 \sim 1$, while proposing alternative solar couplings as follows:

- CSD(2): $m^D_{\rm sol} = (b, 2b, 0)$ [92],
- CSD(3): $m^D_{\rm sol} = (b, 3b, b)$ [93],
- CSD(4): $m^D_{\rm sol} = (b, 4b, 2b)$ [94].

All these examples maintain an approximate trimaximal value for the solar leptonic angle $\tan\theta_{12} \sim \sqrt{2}b_1/(b_2 - b_3) \sim 1/\sqrt{2}$, while switching on the reactor angle.[3] Since experiment indicates that the bound $\theta_{13} \lesssim m_2/m_3$ is almost saturated, these schemes also require certain phase choices $\arg[b/a]$ in order to achieve the desired reactor angle, leading to predictions for the CP-violating phase $\delta_{\rm CP}$. The purpose of [1] was to generalise and then systematically study such patterns of couplings. One may consider the class of models wherein the dominant (atmospheric) and the subdominant (solar) right-handed neutrinos have couplings to $(\nu_e, \nu_\mu, \nu_\tau)$ given respectively by

$$m^D_{\rm atm} = (0, a, a), \qquad m^D_{\rm sol} = (b, nb, (n-2)b), \tag{2.4}$$

where n is any positive integer; we refer to this as CSD(n). Before proceeding with the numerical analysis, we shall justify such a pattern of couplings and show how it may arise from a more fundamental theory based on a non-Abelian family symmetry.

2.2 Vacuum alignment

2.2.1 Vacuum expectation values of flavons

In the Standard Model, the fermion mass and Yukawa matrices are simply numerical 3×3 matrices which collect the various couplings to the Higgs. The basic idea behind vacuum alignment is to postulate a non-Abelian family symmetry G_F along with one or several flavon fields ϕ (or superfields in a supersymmetric context), which are singlets under the Standard Model gauge group. Flavons couple to fermions, giving rise to terms which resemble $\phi H\overline{\psi}\psi$. The symmetry is broken spontaneously at some flavour-breaking scale Λ. By analogy with the Higgs mechanism, the flavons acquire vacuum expectation values, resulting in effective Yukawa terms. The scale Λ is not fixed by any

[3] More recently, CSD(3) with only two right-handed neutrinos has been studied under the moniker Littlest Seesaw [95–97]. CSD(4), when implemented in unified models with $Y^u = Y^\nu$, with the second column proportional to $(1, 4, 2)$, predicts a Cabibbo angle $\theta_C \approx 1/4$ in the diagonal $Y^d \sim Y^e$ basis. Pati-Salam models have been constructed along these lines [98, 99].

experimental evidence, but is often predicted by the model. In GUT models considered in future chapters, we will see that G_F is naturally broken at the GUT scale, i.e. $\Lambda \sim M_{\rm GUT} \sim 10^{16}$ GeV. The family symmetry cannot be present at low scales, as this would imply fermions unified under G_F have identical couplings to the Higgs. Because fermions are in non-trivial representations of G_F, the vacuum structure of the theory will inform the fermion flavour structure.

In all models studied in this thesis, G_F admits triplet representations, along with any number of other representations including at least one singlet. Flavons ϕ_i are then triplets under G_F, as are at least one set of Standard Model fermions. As an example, assume the three lepton $SU(2)$ doublets L_i are united in a single triplet representation L of G_F, while the right-handed leptons ℓ_i are singlets. The Lagrangian will then contain terms resembling $(\overline{L} \cdot \phi_i)\ell_i H/\Lambda$, where the parentheses $(\ \cdot\ )$ denote a triplet contraction into a singlet and the index i runs over the three generations. This example therefore involves three different flavons which couple exclusively to one family of right-handed leptons. When the ϕ_i acquire VEVs, these terms will populate each column of the lepton Yukawa matrices with values proportional to the alignment of a given flavon VEV. For instance, the first column of the charged lepton Yukawa matrix Y^e comes from a term $(L \cdot \phi_e)\ell_e H$. If ϕ_e acquires a VEV in a particular direction, say $\phi_e = v_e(1,0,0)$, the (1,1) element of Y^e is populated while the (2,1) and (3,1) elements are zero.

The above argument is intended only as a simple illustration of how vacuum alignment can lead to particular Yukawa and mass structures; a more complete example will be presented shortly in a supersymmetric context, and explicit vacuum alignment sectors are given for the models in Chapters 3 and 4. However the connection to the discussion on CSD(n) can now be made more transparent: the arbitrarily chosen couplings $(0, a, a)$ and $(b, nb, (n-2)b)$ of leptons to, respectively, right-handed neutrinos $\nu_R^{\rm atm}$ and $\nu_R^{\rm sol}$ can be explained if they arise from couplings to flavons that acquire VEVs proportional to $(0,1,1)$ and $(1, n, n-2)$.

How can alignments be obtained in a model? In supersymmetry, a consistent prescription is that of F-term alignment. One postulates a set of superfields A_i and O_i called driving fields, which are characterised by having R charge 2, do not acquire VEVs, and do not couple directly to fermions. They do, however couple to flavons, described by a driving superpotential $W_{\rm driving}$, which is dependent on the symmetries and precise field content of the model. Their F term conditions $F_{A_i} = 0$ and $F_{O_i} = 0$ enforce relations between components of the triplet flavons ϕ, giving rise to particular allowed alignments in the vacuum.

2.2.2 Example: CSD(n) from A_4

Here we show how a sequence of symmetry and orthogonality conditions can produce the CSD(n) alignments in a simple MSSM-like model with an A_4 family symmetry. The family symmetry is broken by triplet flavons ϕ_i. The relevant superpotential terms that produce the correct Yukawa structure in the neutrino sector are

$$\frac{1}{\Lambda}H_u(L\cdot\phi_{\rm atm})\nu^c_{\rm atm}+\frac{1}{\Lambda}H_u(L\cdot\phi_{\rm sol})\nu^c_{\rm sol}+\frac{1}{\Lambda}H_u(L\cdot\phi_{\rm dec})\nu^c_{\rm dec}, \tag{2.5}$$

where L is the SU(2) lepton doublet, transforming as a triplet under A_4, while $\nu^c_{\rm atm}$, $\nu^c_{\rm sol}$, $\nu^c_{\rm dec}$ are CP conjugates of the right-handed neutrinos and H_u is the up-type Higgs field. The right-handed neutrinos are A_4 singlets but distinguished by some additional quantum numbers. In the charged-lepton sector,

$$\frac{1}{\Lambda}H_d(L\cdot\phi_e)e^c+\frac{1}{\Lambda}H_d(L\cdot\phi_\mu)\mu^c+\frac{1}{\Lambda}H_d(L\cdot\phi_\tau)\tau^c, \tag{2.6}$$

where e^c,μ^c,τ^c contain the right-handed electron, muon and tau respectively. The right-handed neutrino Majorana superpotential is chosen to give a diagonal mass matrix,

$$M_R=\mathrm{diag}(M_{\rm atm},M_{\rm sol},M_{\rm dec}). \tag{2.7}$$

Details of the construction of this superpotential (e.g. in terms of flavons), the relative values of $M_{\rm atm}$, $M_{\rm sol}$, $M_{\rm dec}$ as well as the inclusion of any off-diagonal terms in M_R will all depend on additional specifications of the model but are not important for this discussion.

The CSD(n) vacuum alignments arise from effective operators involving three triplet flavon fields $\phi_{\rm atm}$, $\phi_{\rm sol}$, and $\phi_{\rm dec}$. The subscripts are chosen by noting that $\phi_{\rm atm}$ correlates with the atmospheric neutrino mass m_3, $\phi_{\rm sol}$ with the solar neutrino mass m_2, and $\phi_{\rm dec}$ with the lightest neutrino mass m_1, which in CSD is light enough that the associated third right-handed neutrino can, to good approximation, be thought of as decoupled from the theory [81]. CSD(n) is defined to be the choice of vacuum alignments

$$\langle\phi_{\rm atm}\rangle\propto\begin{pmatrix}0\\1\\1\end{pmatrix},\quad \langle\phi_{\rm sol}\rangle\propto\begin{pmatrix}1\\n\\n-2\end{pmatrix},\quad \langle\phi_{\rm dec}\rangle\propto\begin{pmatrix}0\\0\\1\end{pmatrix}, \tag{2.8}$$

where n is a positive integer, and the only phases allowed are in the overall proportionality constants.[4] Such vacuum alignments arise from symmetry-preserving alignments together with orthogonality conditions [93, 94].

[4] In general also the elements of flavon VEVs can have relative signs as in the last alignment in Eq. 2.9. However, for a given choice of such alignment, orthogonality fixes the relative signs of the elements of subsequent alignments, with only the overall complex proportionality factor remaining.

The starting point for understanding the alignments in Eq. 2.8 are the symmetry-preserving vacuum alignments of A_4, namely

$$\begin{pmatrix}1\\0\\0\end{pmatrix}, \quad \begin{pmatrix}0\\1\\0\end{pmatrix}, \quad \begin{pmatrix}0\\0\\1\end{pmatrix}, \quad \begin{pmatrix}\pm 1\\\pm 1\\\pm 1\end{pmatrix}, \tag{2.9}$$

which each preserve some subgroup of A_4 in a basis where the 12 group elements in the triplet representation are real, i.e. each alignment in Eq. 2.9 is an eigenvector of at least one non-trivial group element with eigenvalue $+1$. In a flavour model the above alignments would also arise from the VEVs of triplet flavons, which however do not couple to fermions. As such, their immediate role beyond producing the CSD(n) alignments is unclear, though they may have an impact on early Universe physics, for example in flavon inflation [100].

The above alignments can be fixed by coupling flavons ϕ_i to driving fields A_i that are triplets under the family symmetry, by writing down renormalisable terms like $A_i\phi_i\phi_i$. Since each A_i has three components, it leads to three separate F term conditions $F_{A_i^1} = F_{A_i^2} = F_{A_i^3} = 0$, which can only be satisfied if all components of ϕ_i are equal or two are zero.

The first (atm) alignment in Eq. 2.8, which completely breaks the A_4 symmetry, arises from the orthogonality conditions

$$\begin{pmatrix}0\\1\\1\end{pmatrix} \perp \begin{pmatrix}1\\1\\-1\end{pmatrix}, \begin{pmatrix}1\\0\\0\end{pmatrix}, \tag{2.10}$$

involving two symmetry-preserving alignments selected from Eq. 2.9. Next, the alignment $(2, -1, 1)$ may be obtained by noting that it is orthogonal to the alignment in Eq. 2.10 and one of the symmetry-preserving alignments,

$$\begin{pmatrix}2\\-1\\1\end{pmatrix} \perp \begin{pmatrix}1\\1\\-1\end{pmatrix}, \begin{pmatrix}0\\1\\1\end{pmatrix}. \tag{2.11}$$

The CSD(n) (or sol) alignment in Eq. 2.8 is in turn orthogonal to the above alignment, i.e.

$$\begin{pmatrix}1\\n\\n-2\end{pmatrix} \perp \begin{pmatrix}2\\-1\\1\end{pmatrix}, \tag{2.12}$$

where the orthogonality in Eq. 2.12 is maintained for any value of n (not necessarily integer). To pin down the value of n and show that it is a particular integer requires a

further orthogonality condition.[5]

For example, for $n = 3$, the desired alignment is obtained from the two orthogonality conditions,

$$\begin{pmatrix}1\\3\\1\end{pmatrix} \perp \begin{pmatrix}2\\-1\\1\end{pmatrix}, \begin{pmatrix}1\\0\\-1\end{pmatrix}, \tag{2.13}$$

where the first condition above is a particular case of Eq. 2.12 and the second condition involves a new alignment, obtained from two of the symmetry-preserving alignments in Eq. 2.9, namely

$$\begin{pmatrix}1\\0\\-1\end{pmatrix} \perp \begin{pmatrix}1\\1\\1\end{pmatrix}, \begin{pmatrix}0\\1\\0\end{pmatrix}. \tag{2.14}$$

Using Eq. 2.5, the vacuum alignments in Eq. 2.8 make up the columns of the neutrino Yukawa matrix, consistent with Eq. 2.4 where $m^D = (m^D_{\rm atm}, m^D_{\rm sol}, m^D_{\rm dec})$. The charged-lepton Yukawa matrix is chosen to be diagonal, corresponding to the three flavons ϕ_e, ϕ_μ and ϕ_τ acquiring VEVs with alignments

$$\langle\phi_e\rangle \propto \begin{pmatrix}1\\0\\0\end{pmatrix}, \quad \langle\phi_\mu\rangle \propto \begin{pmatrix}0\\1\\0\end{pmatrix}, \quad \langle\phi_\tau\rangle \propto \begin{pmatrix}0\\0\\1\end{pmatrix}. \tag{2.15}$$

2.3 Numerical analysis of CSD(n)

We turn now to a dedicated numerical analysis of the general class of CSD(n) models in the framework described above but independent of a specific model, allowing the positive integer n to take any integer value. The results of this analysis were first published in [1].

2.3.1 Key features

CSD(n) is a generalisation of examples studied in the literature so far for $n = 2, 3, 4$, including the original CSD (TB mixing) identified here as CSD(1). As we will see shortly, after the seesaw mechanism has been implemented, with just two right-handed neutrinos, the light effective Majorana neutrino mass matrix depends on just two mass parameters m_a and m_b and a relative phase η. For each value of n we perform a fit to five observed neutrino parameters: three mixing angles and two mass-squared differences.

[5] We could simply use the alignment in Eq. 2.12, where n is a real number to be fitted. However, we prefer to fix n to be a small positive integer to increase predictivity.

It is worth mentioning several features of the analysis, and some key results. Firstly, we find good fits for the CSD(3) and CSD(4) alignments, with favoured values of η near $2\pi/3$ and $4\pi/5$, respectively. This is consistent with previous works where η is associated with spontaneous CP violation of an Abelian $\mathbb{Z}_{3N}$ [93] or $\mathbb{Z}_{5N}$ [94] symmetry. Unlike these earlier studies, however, here we perform a systematic fit leading to more robust results which allow the input phase to be determined from the data on the mixing angles. Indeed it is reassuring to see the simple rational values of the input phase $2\pi/3$ or $4\pi/5$ emerge from the fit.

The value of the CP phase $\delta_{\rm CP}$ emerges as a genuine prediction. Moreover, in CSD(n) with just two right-handed neutrinos, there is a direct link between the oscillation phase $\delta_{\rm CP}$ and the leptogenesis phase, since there is only one phase η which is responsible for both. The more general case with a third approximately decoupled right-handed neutrino provides a close approximation to this situation. Therefore in both cases, observation of leptonic CP violation in low energy neutrino oscillation experiments is directly linked to cosmological CP violation, which both vanish in the same limit.

We consider the effect of a third right-handed neutrino giving $m^D_{\rm dec} \propto (0,0,1)$, which introduces a further mass parameter m_c and relative phase ξ, in order to gauge the effect of having a non-zero lightest neutrino mass m_1. For low values of m_c, this provides a perturbation to the two-neutrino results, leading to an upper limit on the lightest physical neutrino mass $m_1 \lesssim 1$ meV for the viable cases.

Though the analysis here is independent of a specific model (such as a GUT), it is to be understood that the CSD alignments are discussed with a mind to integration within a more complete model that ideally can explain all fermionic mass and mixing. The remaining chapters in this thesis are aimed at fulfilling exactly this goal. As such, numerical results presented here give an important foundational step in an approach to solving the flavour puzzle.

2.3.2 Mass matrices

Recall from Eq. 1.14 that the charged lepton Yukawa matrix Y^e and neutrino Yukawa matrix Y^ν are defined in a left-right convention by[6]

$$\mathcal{L}^{LR} = -H_d Y^e_{ij} \overline{L_{Li}} e_{Rj} - H_u Y^\nu_{ij} \overline{L_{Li}} \nu_{Rj} + \text{h.c.}. \tag{2.16}$$

where $i,j = 1,2,3$ label the three families of lepton doublets L_{Li}, right-handed charged leptons e_{Rj} and right-handed neutrinos ν_{Rj}. The physical effective neutrino Majorana mass matrix m^ν is determined from the columns of Y^ν via the seesaw mechanism,

[6] This left-right convention for the Yukawa matrix differs by an Hermitian conjugation compared to that used in the MPT package [101] due to the right-left (RL) convention used there. Subsequently, the neutrino mass matrix after seesaw m^ν also differs by Hermitian conjugation.

$m^\nu = -v_u^2 Y^\nu M_R^{-1} (Y^\nu)^\intercal$, where m^ν is defined by

$$\mathcal{L}_\nu^L = -\tfrac{1}{2} m_{ij}^\nu \overline{\nu_L^c}_i \nu_{Lj} + \text{h.c.}, \tag{2.17}$$

while the right-handed neutrino Majorana mass matrix M_R is defined by

$$\mathcal{L}_\nu^R = -\tfrac{1}{2} (M_R)_{ij} \overline{\nu_R^c}_i \nu_{Rj} + \text{h.c.}. \tag{2.18}$$

In these conventions, the CSD(n) mass matrices $m^D = v_u Y^\nu$ and M_R are given by

$$m^D = v_u Y^\nu = \begin{pmatrix} 0 & b & 0 \\ a & nb & 0 \\ a & (n-2)b & c \end{pmatrix}, \quad M_R = \begin{pmatrix} M_{\text{atm}} & 0 & 0 \\ 0 & M_{\text{sol}} & 0 \\ 0 & 0 & M_{\text{dec}} \end{pmatrix}, \tag{2.19}$$

where a, b and c are generally complex. The seesaw formula yields

$$m_{(n)}^\nu = m_a e^{i\alpha} \begin{pmatrix} 0 & 0 & 0 \\ 0 & 1 & 1 \\ 0 & 1 & 1 \end{pmatrix} + m_b e^{i\beta} \begin{pmatrix} 1 & n & n-2 \\ n & n^2 & n(n-2) \\ n-2 & n(n-2) & (n-2)^2 \end{pmatrix} + m_c e^{i\gamma} \begin{pmatrix} 0 & 0 & 0 \\ 0 & 0 & 0 \\ 0 & 0 & 1 \end{pmatrix}, \tag{2.20}$$

where $m_a = |a|^2/M_{\text{atm}}$, $m_b = |b|^2/M_{\text{sol}}$ and $m_c = |c|^2/M_{\text{dec}}$ are real and positive, with the phases displayed explicitly as $\alpha = \arg[a^2]$, $\beta = \arg[b^2]$ and $\gamma = \arg[c^2]$. One overall phase multiplying the entire matrix is unphysical. Choosing this to be α, it may be factored out and then dropped in order to make the term proportional to m_a real. This results in two physical phases, defined by $\eta = \beta - \alpha$ and $\xi = \gamma - \alpha$. Hence $\eta = \arg[b^2/a^2]$ and $\xi = \arg[c^2/a^2]$.

We use the PDG parametrisation of the PMNS matrix defined in Eq. 1.23, where $U_{\text{PMNS}} = R_{23}^l U_{13}^l R_{12}^l P$, expressed in terms of three mixing angles θ_{ij}, a Dirac phase δ_{CP} (residing in U_{13}) and two Majorana phases α_{21}, α_{31} contained in P. If Y^e is diagonal, U_{PMNS} is simply the matrix that diagonalises the neutrino mass matrix (up to charged lepton phase rotations).

2.3.3 Fitting method

Here we describe the method used for finding the best fit of the CSD(n) matrices to data. We must first clarify that we do not use raw experimental data. Rather, the "data" corresponds to the predictions of physical observables μ_i (masses, mixing angles) and associated uncertainties as obtained by a global fit to true experimental data, where

$$\mu_i \in \{\sin^2\theta_{12}, \sin^2\theta_{13}, \sin^2\theta_{23}, \Delta m_{21}^2, \Delta m_{31}^2\}. \tag{2.21}$$

As such we have not performed a global fit to the data, but instead fit the model parameters, which are collected into a vector x, to the existing results of a global fit. For a given input vector x one obtains a set of predicted values $P_i(x)$ which may be compared to the corresponding values μ_i. In this analysis, $x = (m_a, m_b, m_c, \eta, \xi)$, or a subset thereof. We use a standard χ^2 test statistic to compare predictions for different x; optimum x, yielding the best fit, was found by minimising the χ^2 function. The test statistic χ^2 is defined by[7]

$$\chi^2 = \sum_{i=1}^{N} \left(\frac{P_i(x) - \mu_i}{\sigma_i} \right)^2 , \tag{2.22}$$

where $N = 5$ is the number of input parameters in this analysis, μ_i are the current global best fit values to experimental data, and σ_i are the associated 1σ errors, while P_i are the model predictions for physical observables, i.e. the (squared sines of) three lepton mixing angles θ_{ij} and two mass-squared differences Δm^2_{21} and Δm^2_{31}.

For definiteness, all "data" μ_i is taken from just one of the global fits, namely that of the NuFit collaboration. The most up-to-date values at the time of publication of [1], on which much of this chapter is based, were NuFit 2.0 [105], which are given in Table 2.1. The following discussion is based on those results, which differ slightly from the current best fit values, which were presented in Chapter 1 and are used in Chapter 5. In NuFit 2.0, the CP-violating phase $\delta_{\rm CP}$ is constrained at 1σ, but is completely undetermined at 3σ, and so is left as a pure prediction in this analysis, as are the two Majorana phases.

Parameter	Value	
	Best fit $\pm 1\sigma$	3σ range
$\sin^2\theta^\ell_{12}$	$0.304\ ^{+0.13}_{-0.12}$	$0.270 \to 0.344$
$\theta^\ell_{12}/^\circ$	$33.48\ ^{+0.78}_{-0.75}$	$31.29 \to 35.91$
$\sin^2\theta^\ell_{23}$	$0.451\ ^{+0.052}_{-0.028}$	$0.382 \to 0.643$
$\theta^\ell_{23}/^\circ$	$42.3\ ^{+3.0}_{-1.6}$	$38.2 \to 53.3$
$\sin^2\theta^\ell_{13}$	0.0218 ± 0.0010	$0.0186 \to 0.0250$
$\theta^\ell_{13}/^\circ$	$8.50\ ^{+0.20}_{-0.21}$	$7.85 \to 9.10$
$\delta^\ell/^\circ$	$306\ ^{+39}_{-70}$	$0 \to 360$
$\Delta m^2_{21}\,/10^{-5}$ eV^2	$7.50\ ^{+0.19}_{-0.17}$	$7.02 \to 8.09$
$\Delta m^2_{31}\,/10^{-3}$ eV^2	2.457 ± 0.047	$2.317 \to 2.607$

Table 2.1: Standard Model experimental neutrino mass-squared differences and PMNS mixing parameters from NuFit 2.0 [105].

The error σ_i is equivalent to the standard deviation of the global best fit values if the global fit distribution of the observable is Gaussian. This is essentially the case for most fitted observables, with the notable exception of the atmospheric angle θ_{23}. As seen in

[7] This is the standard definition; the implementation used here of χ^2-minimisation for finding best fits of models to data is analogous to that in [102], and more recently in [103, 104].

[105], the $\Delta\chi^2$ distribution for θ_{23} has two minima on either side of 45°, with a slight preference for $\theta_{23} < 45°$ for normal ordering, and a best fit value $\theta_{23} = 42.3°$. This is reflected in the asymmetric error $^{+3.0°}_{-1.6°}$ which in terms of $\sin^2\theta_{23}$ is $^{+0.052}_{-0.028}$. So as to not overstate the error (and consequently underestimate χ^2), we assume the distribution to be Gaussian about the best fit point, setting $\sigma_{\theta_{23}} = 1.6$, or equivalently $\sigma_{\sin^2\theta_{23}} = 0.028$. For best fit values larger than 42.3° this will overestimate the χ^2, so we are being conservative in presenting our results when the data is not Gaussian.

It is generically true that additional input parameters can improve a model fit. One may thus be tempted to calculate a reduced chi-squared χ^2_{red}, i.e. the χ^2 per degree of freedom (d.o.f.), where the number of d.o.f. is naively given by the number of observables minus the number of input parameters. In the conventional picture, a good fit has $\chi^2_{\text{red}} \simeq 1$. However, as discussed in [106] this interpretation is only valid for linear models; the PMNS matrix which diagonalises the CSD(n) matrix is certainly not linearly dependent on the parameters. While χ^2 is a valid tool for comparing models to each other, since it is not possible to establish an exact number of d.o.f., we cannot reliably define χ^2_{red}.

Initially, a coarse Monte-Carlo was used to examine the five-dimensional parameter space. A random vector $x = (m_a, m_b, m_c, \eta, \xi)$ is chosen, all PMNS parameters are calculated numerically using the Mixing Parameter Tools (`MPT`) package for Mathematica [101], and χ^2 is evaluated. A large-N search of this type reveals the existence of two distinct regions of low χ^2. These regions in parameter space are characterised by having the same approximate values of m_a and m_b, while m_c and ξ are allowed to take a broad range of values (in fact ξ can take any value at all in $[-\pi, \pi]$). Meanwhile η is constrained only up to a sign: the two minima then correspond to equal and opposite values of η. Refining the input parameter space by allowing only $\eta \in (0, \pi)$ leaves a single global minimum region. This minimum is well-defined and generally stable, meaning our χ^2 statistic is a good test for goodness-of-fit over this space; this is true for all CSD(n).

To demonstrate this, see Figure 2.1, which plots the results of the random search Monte Carlo for the representative cases CSD(3) and CSD(4), which as we will see are the most physically interesting cases. Specifically, it plots the lower envelope of χ^2 as a function of a given input parameter, evaluated for 10^6 points in the parameter space spanned by (m_a, m_b, m_c, η). Other CSD(n) alignments observe similar behaviours. The shape of the curves for m_a, m_b, and η show clearly defined minima, while the range of low-χ^2 values is comparatively wider and includes $m_c = 0$. Nevertheless, although m_c may take a large range of values and produce reasonably good χ^2 fits, it appears to have a single minimum region. The value of the phase ξ does not have a significant effect on the position and nature of the minimum and is fixed to either of two values, η and 0, for convenience. These phase choices are discussed below.

Figure 2.2 shows the best fit χ^2 with respect to the two input masses m_a and m_b for a two-neutrino model with CSD(3) and CSD(4). It is clear from the contours that both

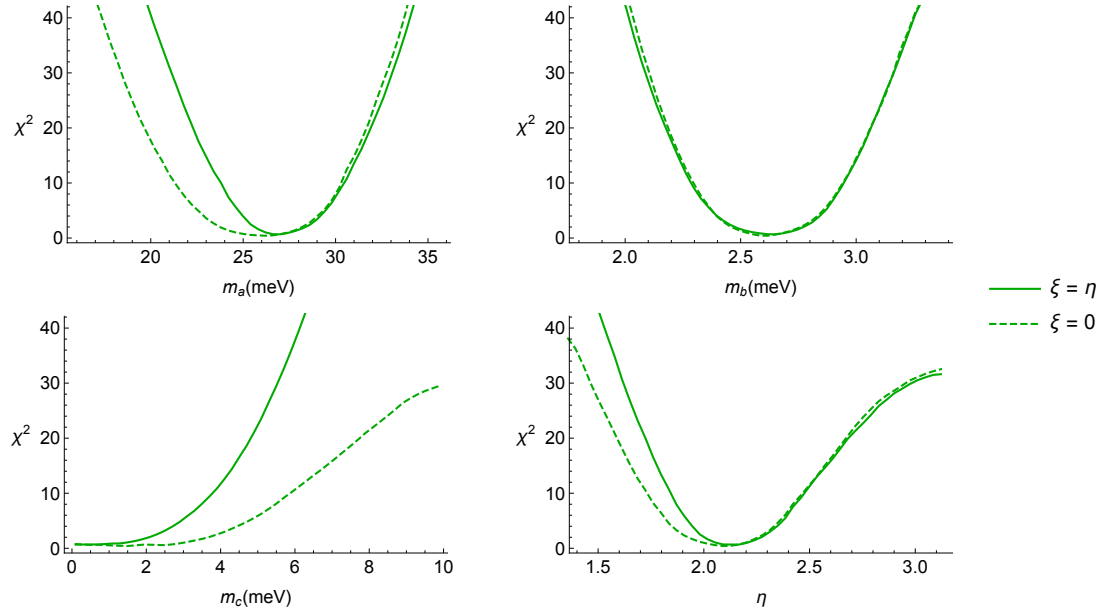

(a) CSD(3)

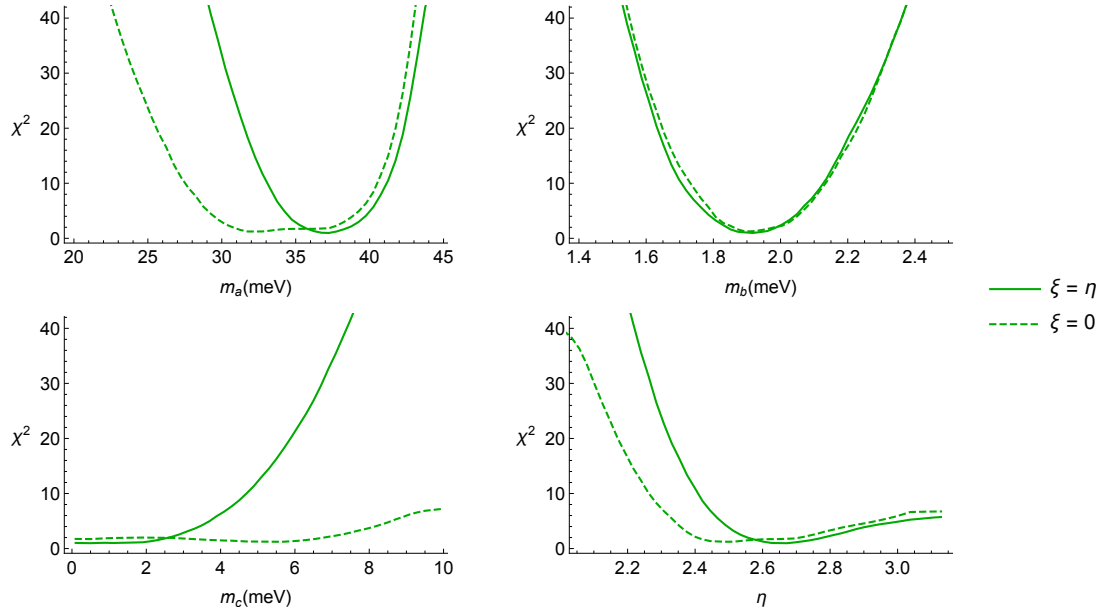

(b) CSD(4)

Figure 2.1: Lower envelope of best fit χ^2 in the neighbourhood of the global best fit of input parameters $m_{a,b,c}$, η for CSD(3) and CSD(4), with fixed ξ.

input masses are quite tightly constrained. Any fit that gives $\chi^2 < 50$ will correspond to a deviation from the best fit value of no more than 10-15%. It is also confirmed that the addition of a third right-handed neutrino does not significantly alter the best fit or the spread of m_a and m_b, since m_c is small (as required by CSD). This lends validity to our assertion that the two physical neutrino masses $m_{2,3}$ are largely derived from the input masses $m_{a,b}$, leaving (in the two-neutrino case) only a single phase η which

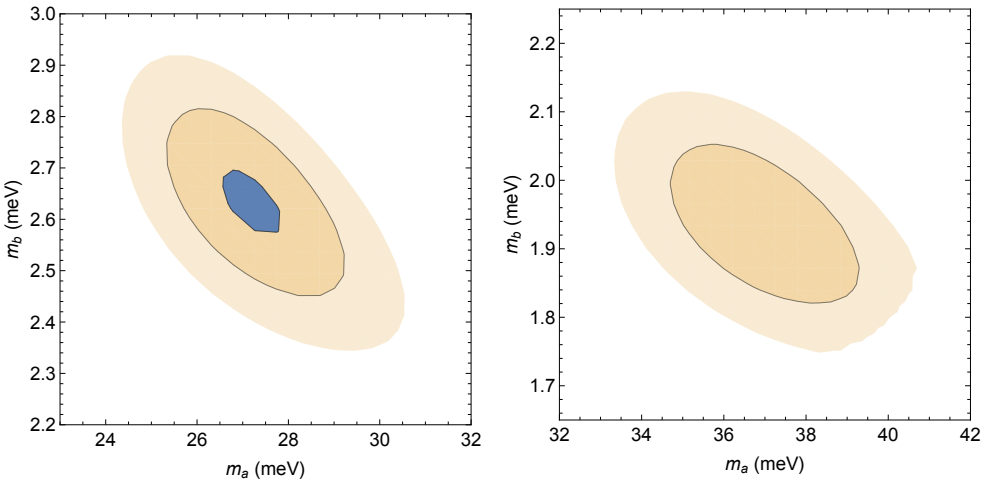

(a) CSD(3) (b) CSD(4)

Figure 2.2: Variation of χ^2 with input masses m_a and m_b for CSD(3) and CSD(4). The dark blue region corresponds to $\chi^2 \leq 5$, while the surrounding regions correspond to $\chi^2 \leq 20$ and $\chi^2 \leq 50$.

controls the detailed prediction of the PMNS matrix. Once the single global minimum is confirmed, numerical minimisation is performed in Mathematica, which preferentially uses the method of differential evolution to find local minima. Heuristically, it works by maintaining a population of candidate solutions. This is moved around in parameter space by choosing new points based on the current population, which are added to the set if they correspond to a better fit (in this case, a lower χ^2), otherwise discarded.

2.3.4 Results for two right-handed neutrinos

Here we present results of the fit to data of CSD(n) with two right-handed neutrinos. In all subsequent plots, a thick solid gridline corresponds to a best fit value of a mixing angle or neutrino mass, while thin solid gridlines show the 1σ limits, and thin dashed gridlines show the 3σ range.

Models with only two right-handed neutrinos are compelling as they are typically highly predictive. Here, the neutrino mass matrix in Eq. 2.20 simplifies to

$$m^{\nu}_{(n)} = m_a \begin{pmatrix} 0 & 0 & 0 \\ 0 & 1 & 1 \\ 0 & 1 & 1 \end{pmatrix} + m_b e^{i\eta} \begin{pmatrix} 1 & n & n-2 \\ n & n^2 & n(n-2) \\ n-2 & n(n-2) & (n-2)^2 \end{pmatrix}, \tag{2.23}$$

with $\eta = \beta - \alpha$ after removing an overall unphysical phase α. As this matrix has rank 2, it immediately predicts the lightest physical neutrino mass to be zero, $m_1 = 0$. Moreover, since $m_1 = 0$ in this case $m_2 = \sqrt{\Delta m^2_{21}}$ and $m_3 = \sqrt{\Delta m^2_{31}}$. For a given choice of alignment n, there are three real input parameters m_a, m_b and η from which two light physical neutrino masses m_2, m_3, three lepton mixing angles, the CP-violating

phase $\delta_{\rm CP}$ and two Majorana phases are derived; a total of nine physical parameters from three input parameters, i.e. six predictions for each value of n. As the Majorana phases are not known and $\delta_{\rm CP}$ is only tentatively constrained by experiment, this leaves five presently well-measured observables, namely the two neutrino mass squared differences and the three lepton mixing angles, from only three input parameters.

n	m_a (meV)	m_b (meV)	η (rad)	θ_{12} (°)	θ_{13} (°)	θ_{23} (°)	$\lvert\delta_{\rm CP}\rvert$ (°)	m_2 (meV)	m_3 (meV)	χ^2
1	24.8	2.89	3.14	35.3	0	45.0	0	8.66	49.6	485
2	19.7	3.66	0	34.5	7.65	56.0	0	8.85	48.8	95.1
3	27.3	2.62	2.17	34.4	8.39	44.5	92.2	8.69	49.5	3.98
4	36.6	1.95	2.63	34.3	8.72	38.4	120	8.61	49.8	8.82
5	45.9	1.55	2.88	34.2	9.03	34.4	142	8.53	50.0	33.8
6	55.0	1.29	3.13	34.2	9.30	31.6	179	8.46	50.2	65.2
7	63.0	1.12	3.14	34.1	9.68	31.0	180	8.35	50.6	100
8	71.0	0.984	3.14	34.0	9.96	30.6	180	8.25	50.8	135
9	79.0	0.880	3.14	33.9	10.2	30.3	180	8.17	51.0	168

Table 2.2: Best fit parameters for CSD(n) with two right-handed neutrinos. Additionally, we predict one massless neutrino with $m_1 = 0$ and one zero Majorana phase.

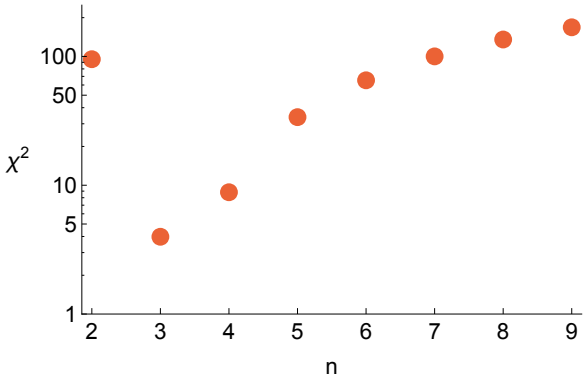

Figure 2.3: Best fit χ^2 with respect to n, for CSD(n) with two right-handed neutrinos.

Table 2.2 shows all best fit parameters with respect to n, while Figure 2.3 plots the corresponding best fit χ^2. In Table 2.2, the fitted three input parameters m_a, m_b and η yield nine physical predictions, but only six physical outputs are shown. The undisplayed outputs are $m_1 = 0$ in each case and two Majorana phases, one of which is zero. Both CSD(3) and CSD(4) have $\chi^2 < 10$, while all others have significantly higher values, generally increasing with n. We view the fit for $n = 3$ as a good fit, particularly in light of the fact that it can naturally predict a CP phase $\delta_{\rm CP}$ close to the current experimental preferred value of $\sim -\pi/2$. Similarly the fit for CSD(4) shows promise for

model building, with a prediction $|\delta_{\rm CP}| = 120°$. For $n \geq 4$, the largest contribution to χ^2 is typically θ_{23}, while for $n = 3$ there is no dominant contribution.

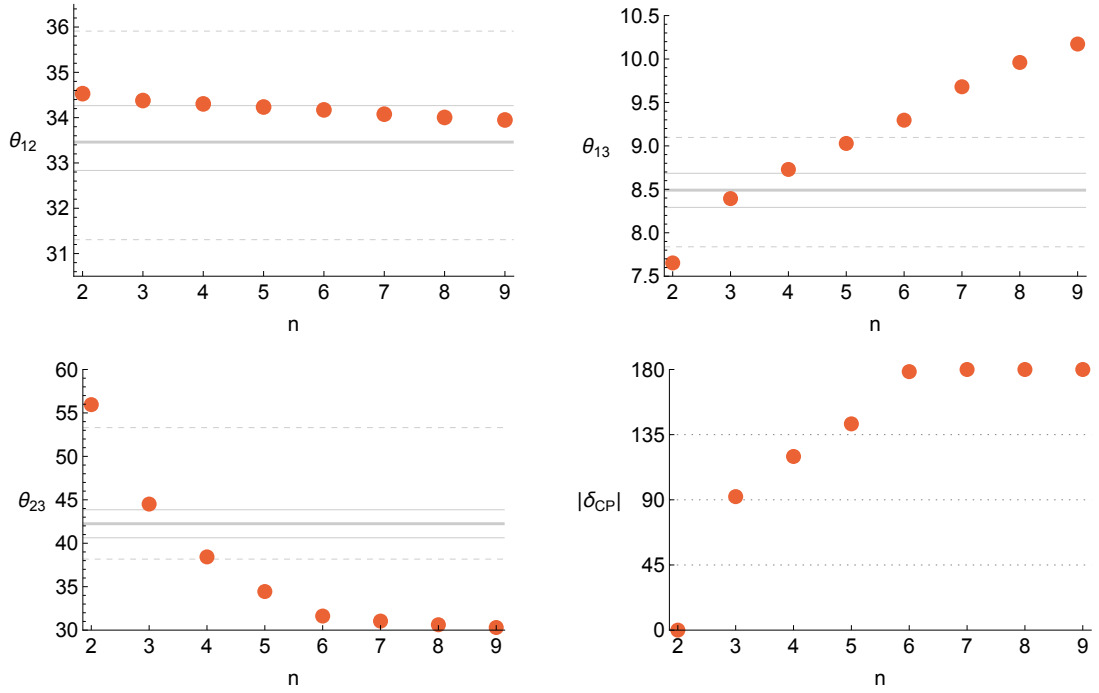

Figure 2.4: Best fit lepton mixing angles and CP-violating phase with respect to n, for CSD(n) with two right-handed neutrinos.

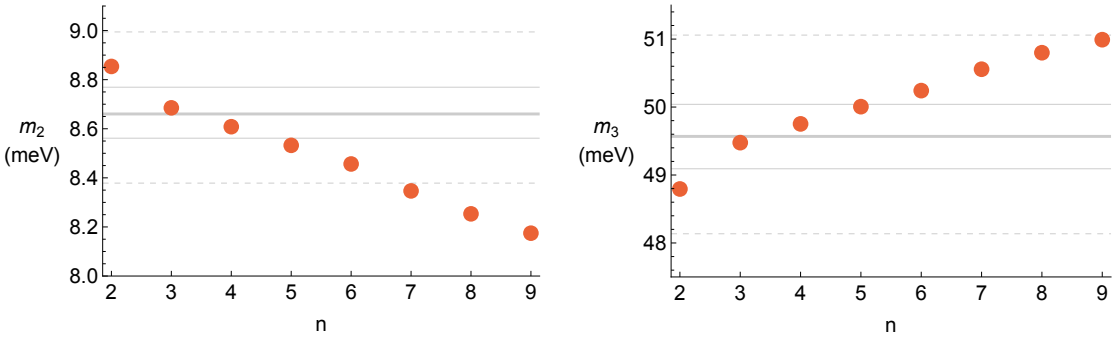

Figure 2.5: Best fit light neutrino masses with respect to n, for CSD(n) with two right-handed neutrinos.

Figures 2.4 and 2.5 show the variation of physical masses and neutrino mixing angles with respect to n. Note that, in the conventions defined earlier, a positive value of η, namely $\eta \in (0, \pi)$, yields a negative CP-violating angle, i.e. $\delta_{\rm CP} \in (0, -\pi)$, while the mirror global minimum for $\eta \in (-\pi, 0)$ corresponds uniquely to $\delta_{\rm CP} \in (\pi, 0)$. As η is unconstrained (unless some model explicitly restricts its domain), only the absolute value of $\delta_{\rm CP}$ can be predicted in this framework. In Table 2.2 we only show positive η values, for which $\delta_{\rm CP}$ is negative. It is also worth noting that both CSD(3) and CSD(4) yield predictions within the preferred range $|\delta_{\rm CP}| \sim 90° \pm 45°$ but may be distinguished by their differing predictions for the atmospheric angle $\theta_{23} \approx 45°$ and $\theta_{23} \approx 38°$, respectively.

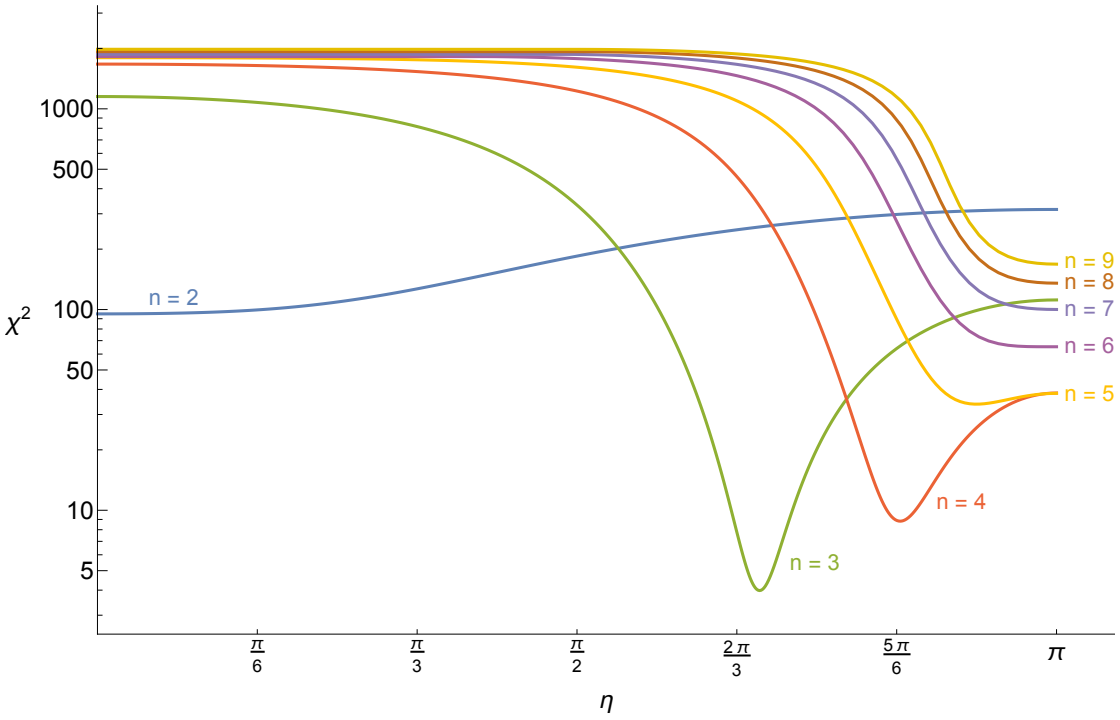

Figure 2.6: Variation of χ^2 with phase η, for CSD(n) with two right-handed neutrinos.

The two input masses m_a and m_b are essentially fitted to the two light neutrino masses m_2, m_3 after which the entire PMNS matrix is determined from only one parameter, namely the phase η. *A priori*, CSD(n) need not lead to low χ^2 values for any choice of n, due to the sensitivity of the predictions to the phase η, yet in fact the results show that it gives very good fits to the leptonic mixing angles for $n = 3, 4$, for special values of η, yielding a value of $|\delta_{\rm CP}|$ as a genuine prediction, along with preferred values for the lepton angles. This is illustrated in Figure 2.6 which shows the variation of χ^2 with η, for $1 \leq n \leq 9$. It is clear that η is quite strongly constrained, even for CSD(3) and CSD(4); with CSD(3), the values (in radians) of η that give $\chi^2 < 10$ are $2.08 \lesssim \eta \lesssim 2.27$, which is a range of approximately 11°. This range includes the value $2\pi/3$. Such a value could be produced in a model with a discrete symmetry such as $\mathbb{Z}_{3N}$. As hinted by the earlier Monte Carlo scan, the neutrino masses are also tightly constrained, for all CSD(n).

To make the link between χ^2 minimisation and physical prediction more concrete, let us examine the variation in the three mixing angles with η, as plotted in Figure 2.7, for the physically most interesting cases of CSD(n) with $n = 3, 4, 5$. We see that although θ_{12} is largely insensitive to η, there is a complicated dependence of the other two mixing angles on η, which is different for different n. These plots demonstrate what the χ^2 value suggests: for some small set of values η, the predicted mixing angles converge on the experimental best fit values for CSD(3) and CSD(4). Meanwhile for CSD(5) we begin to see tension between the fits to θ_{13} and θ_{23}; this tension grows with large n.

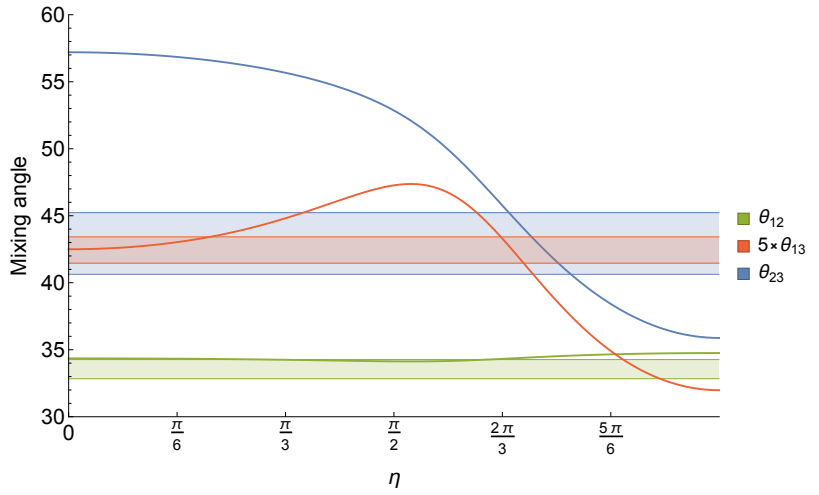

(a) CSD(3)

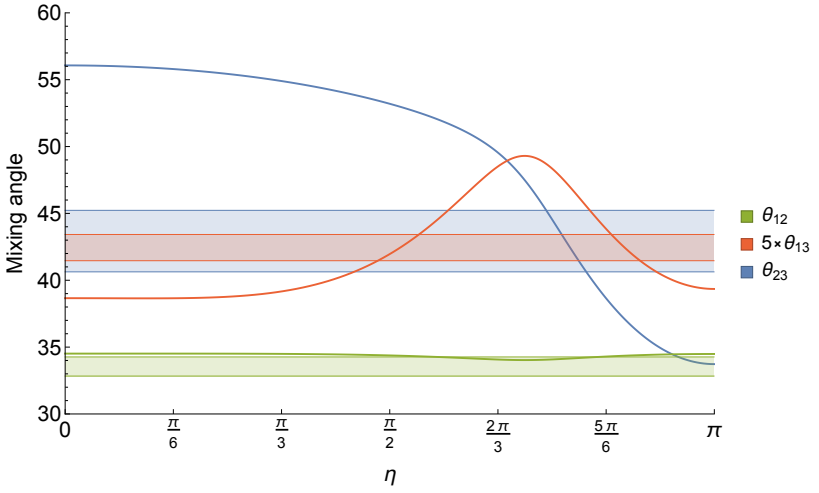

(b) CSD(4)

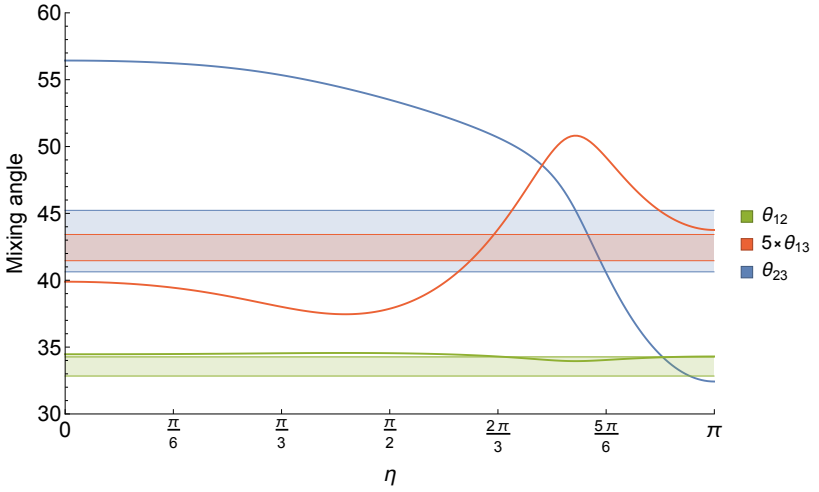

(c) CSD(5)

Figure 2.7: Variation of the lepton mixing angles θ_{ij} with phase η, for CSD(n) with two right-handed neutrinos. Shaded regions represent the $\pm 1\sigma$ range for θ_{ij} (in colours corresponding to the drawn curve). The reactor angle θ_{13} has been multiplied by a factor 5 for the sake of visual ease.

2.3.5 Results for three right-handed neutrinos

We turn now to the results of the fit for CSD(n) with three right-handed neutrinos. As in previous figures, a thick solid gridline corresponds to a best fit value of a mixing angle or neutrino mass, while thin solid gridlines show the 1σ limits, and thin dashed gridlines show the 3σ range.

We now extend the analysis to the case of three right-handed neutrinos. Removing the unphysical overall phase α from Eq. 2.20 gives

$$m^{\nu}_{(n)} = m_a \begin{pmatrix} 0 & 0 & 0 \\ 0 & 1 & 1 \\ 0 & 1 & 1 \end{pmatrix} + m_b e^{i\eta} \begin{pmatrix} 1 & n & n-2 \\ n & n^2 & n(n-2) \\ n-2 & n(n-2) & (n-2)^2 \end{pmatrix} + m_c e^{i\xi} \begin{pmatrix} 0 & 0 & 0 \\ 0 & 0 & 0 \\ 0 & 0 & 1 \end{pmatrix}. \tag{2.24}$$

The immediate effect of including a third right-handed neutrino is to switch on a non-zero value for the lightest physical neutrino mass m_1, where previously for the case of two right-handed neutrinos we had $m_1 = 0$.

Since the contribution from the third right-handed neutrino is assumed to be a perturbation to the case of two right-handed neutrinos considered in the previous subsection, the detailed structure of the third matrix is irrelevant, and it is sufficient to only keep the most important term in the third matrix. This analysis assumes it to be in the (3,3) entry, since in unified models where $Y^u \sim Y^\nu$ this entry is responsible for the top quark Yukawa coupling (see e.g. [4, 6, 98, 99]). The third term brings in a further undetermined relative phase ξ which complicates the analysis somewhat. As indicated by the Monte Carlo scan, the results are comparatively less sensitive to this phase ξ, particularly for the physically interesting cases of $n = 3, 4$. By considering only the cases where $\xi = 0$ (phase aligned with dominant mass matrix) or $\xi = \eta$ (phase aligned with subdominant mass matrix), we can illustrate the sensitivity of the results to this phase without over-complicating the analysis. Such a constraint on the value of ξ, corresponding to the phase of either of the other matrices that make up m^ν (proportional to m_a or m_b) may also arise directly from a model, such as in [98, 99].

Tables 2.3 and 2.4 show the results for the best fit physical parameters (masses, mixing angles and $\delta_{\rm CP}$) and input parameters, respectively, for the case $\xi = 0$. Similarly, Tables 2.5 and 2.6 show the best fit physical and input parameters for the case $\xi = \eta$. As in the two right-handed neutrino case, only CSD(3) and CSD(4) can achieve $\chi^2 < 10$. More generally for each CSD(n), the associated χ^2 values are slight improvements over the two-neutrino case, which is expected as there is an additional free parameter m_c. However, by the SD assumption, the third right-handed neutrino is nearly decoupled from the theory, constraining m_c to be small. As noted previously, evaluating the number of excess degrees of freedom is non-trivial. One may cautiously regard χ^2 values between unity and, say, up to 10 as encouraging, bearing in mind also that $\delta_{\rm CP}$ is not

n	θ_{12} (°)	θ_{13} (°)	θ_{23} (°)	$\lvert\delta_{\rm CP}\rvert$ (°)	m_1 (meV)	m_2 (meV)	m_3 (meV)	χ^2
1	33.5	0.293	41.4	245	0.874	8.71	49.6	474
2	34.5	7.65	56.0	0	0	8.85	48.8	95.1
3	33.6	8.37	44.6	81.3	0.278	8.69	49.5	2.59
4	33.0	8.70	38.8	89.1	0.692	8.64	49.7	6.51
5	32.4	8.92	35.6	89.2	0.964	8.62	49.9	25.1
6	31.8	9.04	33.6	88.6	1.12	8.61	50.0	43.1
7	31.3	9.12	32.3	87.9	1.22	8.61	50.1	58.1
8	31.0	9.29	32.0	87.5	1.23	8.57	50.1	70.9
9	30.7	9.44	32.1	86.9	1.22	8.54	50.2	82.4

Table 2.3: Best fit physical parameters for CSD(n) with $\xi = 0$.

n	m_a (meV)	m_b (meV)	m_c (meV)	η (rad)
1	23.3	2.81	5.77	1.62
2	19.7	3.66	0	0
3	26.0	2.60	1.77	2.1
4	32.3	1.94	4.75	2.48
5	38.3	1.52	7.10	2.65
6	44.5	1.25	9.81	2.74
7	50.7	1.06	10	2.81
8	57.3	0.92	10	2.85
9	64.0	0.82	10	2.88

Table 2.4: Best fit input parameters for CSD(n) with $\xi = 0$.

n	θ_{12} (°)	θ_{13} (°)	θ_{23} (°)	$\lvert\delta_{\rm CP}\rvert$ (°)	m_1 (meV)	m_2 (meV)	m_3 (meV)	χ^2
1	33.3	0.069	44.2	180	0.197	8.66	49.6	477
2	34.5	7.65	56.0	0	0	8.85	48.8	95.1
3	33.7	8.37	44.8	92.7	0.092	8.69	49.5	3.14
4	33.0	8.67	39.0	123	0.215	8.62	49.7	5.53
5	32.5	8.93	35.2	149	0.307	8.55	50.0	27.6
6	32.1	9.27	33.1	180	0.356	8.46	50.2	56.8
7	32.0	9.66	32.6	180	0.364	8.34	50.6	92.4
8	32.0	9.95	32.1	180	0.358	8.24	50.9	129
9	32.0	10.2	31.7	180	0.341	8.15	51.1	163

Table 2.5: Best fit physical parameters for CSD(n) with $\xi = \eta$.

n	m_a (meV)	m_b (meV)	m_c (meV)	η (rad)
1	24.5	2.75	1.26	0
2	19.7	3.66	0	0
3	27.3	2.61	0.558	2.16
4	36.8	1.93	1.30	2.63
5	46.5	1.52	1.85	2.91
6	55.4	1.27	2.15	3.14
7	63.4	1.10	2.2	3.14
8	71.4	0.97	2.16	3.14
9	79.3	0.87	2.05	3.14

Table 2.6: Best fit input parameters for CSD(n) with $\xi = \eta$.

included in the fit, and also that the error on the atmospheric angle θ_{23} is asymmetric. In the light of all of the above, there is some variability in the χ^2 values, and they should be interpreted with care.

As n increases, the fit prefers a stronger hierarchy of input neutrino masses m_a and m_b, while the contribution from m_c becomes stronger. The input mass parameters m_a, m_b and m_c are allowed to be free apart from an upper limit imposed on $m_c < 10$ meV in order not to violate the SD condition. In the case of $\xi = 0$, m_c reaches the soft upper bound of 10 meV for CSD($n \geq 7$). Note that a fit that requires a large m_c is not CSD. A proper analysis of such a non-CSD model necessarily includes contributions from elements of the third matrix (proportional to $m_c e^{i\xi}$) other than the largest (3,3) element, which have been neglected thus far. This would destroy the predictivity of the scheme which makes CSD(n) so appealing. This justifies imposing the chosen upper bound on m_c. However for the successful cases CSD(3) and CSD(4), the best fit values of m_c are comfortably below 10 meV, so these cases naturally prefer a quite decoupled third right-handed neutrino for which the upper limit of m_c is irrelevant. Consequently, restricting our analysis to only examine two values of ξ appears justified for small n. For larger n, the overall contribution from the third matrix is larger, yet nevertheless fails to significantly improve the (poor) fit to data.

Among physical parameters, of particular note in Tables 2.3 and 2.5 is the CP-violating phase $\delta_{\rm CP}$, which is close to $\pm 90^\circ$ for CSD(3), for both choices of ξ. Furthermore, the alignment of ξ with the dominant or subdominant mass matrix appears to greatly affect the prediction for $\delta_{\rm CP}$ for other n, suggesting a relationship between η, ξ and $\delta_{\rm CP}$. Notice that when $\xi = \eta$, the best fit of both is 180° for $n \geq 6$. An analytic treatment would be required for a deeper understanding of their connection, which we did not perform, but note that this behaviour only appears for CSD($n \geq 6$) with poor fits which are of less physical relevance.

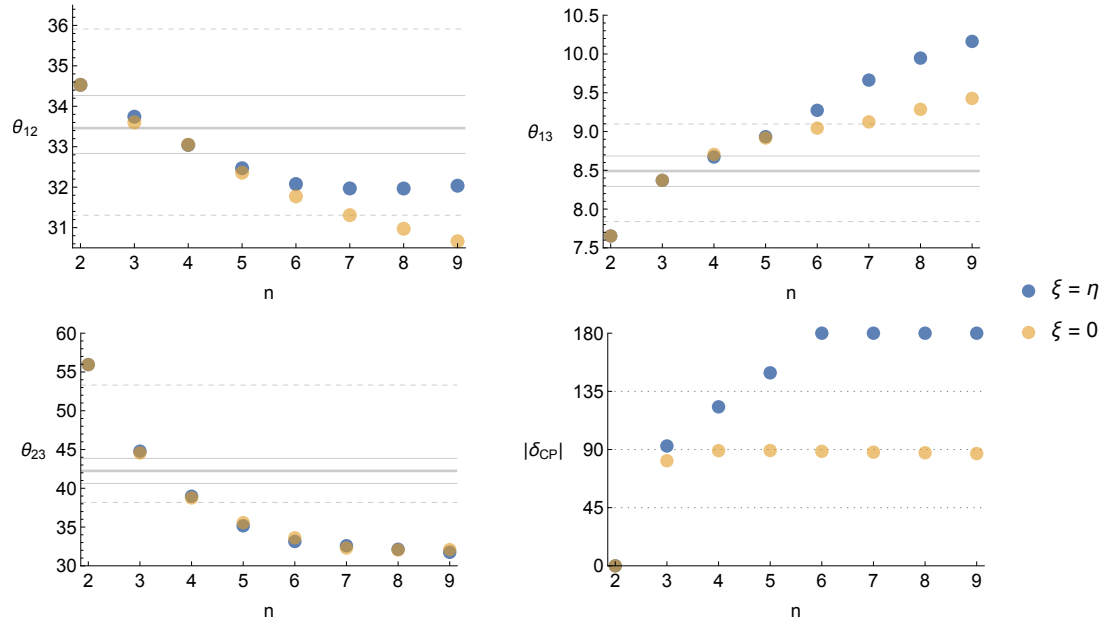

Figure 2.8: Best fit lepton mixing angles and CP-violating phase with respect to n, for CSD(n) with three right-handed neutrinos. The cases $\xi = 0$ ($\xi = \eta$) correspond to yellow (blue) dots.

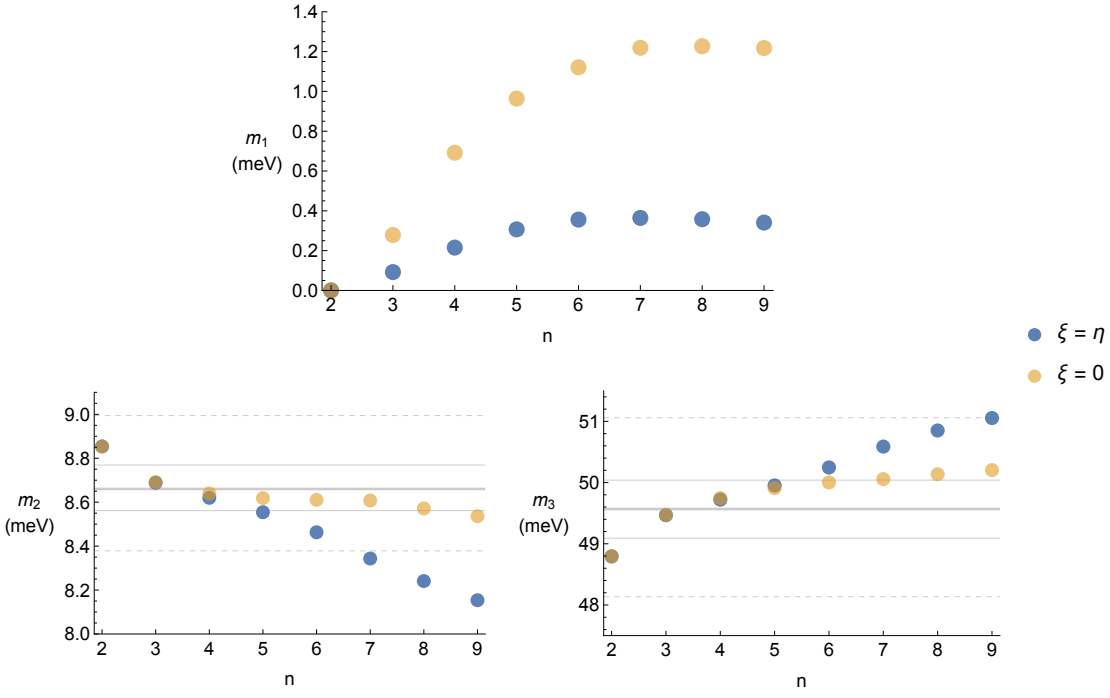

Figure 2.9: Best fit light neutrino masses with respect to n, for CSD(n) with three right-handed neutrinos. The horizontal lines drawn assume m_1 is negligible, such that $m_2 \simeq \sqrt{\Delta m^2_{21}}$ and $m_3 \simeq \sqrt{\Delta m^2_{31}}$. The cases $\xi = 0$ ($\xi = \eta$) correspond to yellow (blue) dots.

Figures 2.8 and 2.9 show the variation of the best fit physical parameters as a function of n. In Figure 2.8 we see that the reactor angle increases with n while the atmospheric and solar angles decrease. Examining the 3σ ranges (dashed lines) we also see that θ_{23} is typically worst fit (only CSD(3) lies within the 1σ bounds), and is also least sensitive to the choice of phase ξ, which can otherwise improve the fit of θ_{12} or θ_{13} at large n.

Note the similarities between the predictions in Figures 2.8 and 2.9 and the corresponding figures for models with two neutrinos (Figures 2.4 and 2.5). The primary difference when a third neutrino is introduced is that θ_{12} is pushed to a lower value. The two-neutrino case has been studied in depth more recently in [95], where they provide exact mixing angle sum rules. In particular, they find that $\tan\theta_{12} = [(1 - 3\sin^2\theta_{13})/2]^{1/2}$ for any n. As θ_{13} is relatively small, $\theta_{12} \simeq 1/\sqrt{2}$ to good approximation, in agreement with the result in Figure 2.4. However, no such analytical results are available for the three-neutrino scenario; the addition of one complex free parameter, coupled with the fact that all matrix elements are sizeable, allows for non-trivial modifications to the mixing angles. In the absence of analytical results, which may or may not be attainable, and are anyway beyond the scope of the numerical analysis presented here, it is not immediately clear why θ_{12} is dominantly affected when a third neutrino is introduced. The best fit values of m_1 in Figure 2.9 indicates that it can vary greatly with n for some phase choices. It is however unlikely that this can be used to constrain models in the near future, as the mass scale is well below current experimental bounds of $\sum m_\nu < 0.23$ eV [37].[8]

The variation of χ^2 with respect to the phase η and the third input neutrino mass m_c is shown in Figure 2.10, for CSD(n) with $3 \leq n \leq 5$. As in the case with two neutrinos, η is quite tightly constrained. Meanwhile, m_c typically has a rather large range of acceptable values, particularly when $\xi = 0$, and does not appear strongly correlated with η. Similarly, the best fit values of the physical lightest neutrino mass m_1 lie in rather shallow minima of χ^2, as shown in Figure 2.11 where the dashed line refers to the $\xi = 0$ case, while the solid line refers to the $\xi = \eta$ case.

Figures 2.13 and 2.14 show the dependence on the lightest neutrino mass m_1 of the predicted mixing angles and neutrino masses, respectively, while Figure 2.12 shows the variation of best fit input parameters with m_1. We see in Figure 2.12 that m_c and m_1 are closely correlated, while best fit $m_{a,b}$ are not strongly affected by the introduction of a third neutrino. Meanwhile in Figure 2.13, the variation is primarily in θ_{12} when m_1 is small. Again in these plots the dashed line refers to the $\xi = 0$ case, while the solid line refers to the $\xi = \eta$ case.

We observe that the choice of phase ξ has a small effect on the χ^2 value of the global minimum, but can noticeably shift its location in parameter space. Naturally the largest

[8] At time of publication of [1], the most current Planck results were [107], which give approximately the same bound.

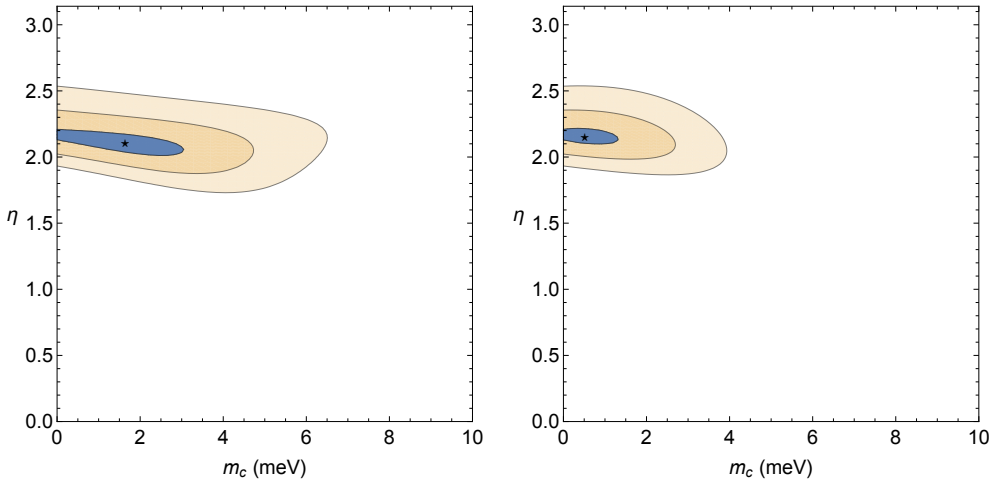

(a) CSD(3), $\xi = 0$

(b) CSD(3), $\xi = \eta$

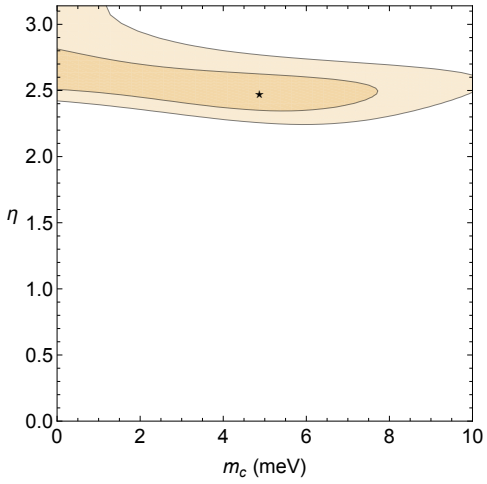

(c) CSD(4), $\xi = 0$

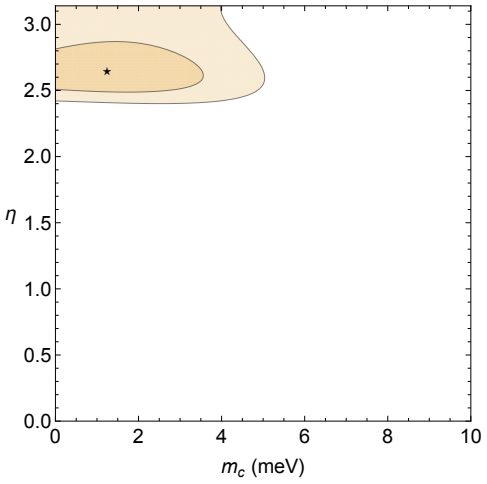

(d) CSD(4), $\xi = \eta$

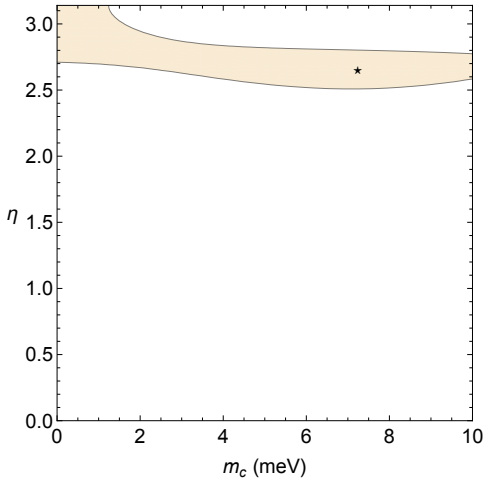

(e) CSD(5), $\xi = 0$

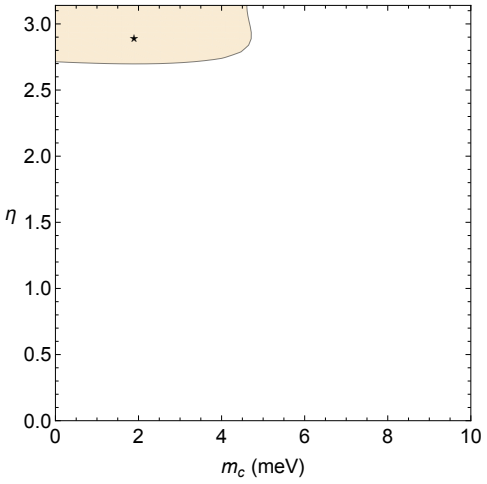

(f) CSD(5), $\xi = \eta$

Figure 2.10: Best fit χ^2 with respect to the phase η and third input neutrino mass m_c. The dark blue region corresponds to $\chi^2 \leq 5$, while surrounding regions correspond to $\chi^2 \leq 20$ and $\chi^2 \leq 50$. The best fit points are indicated by stars.

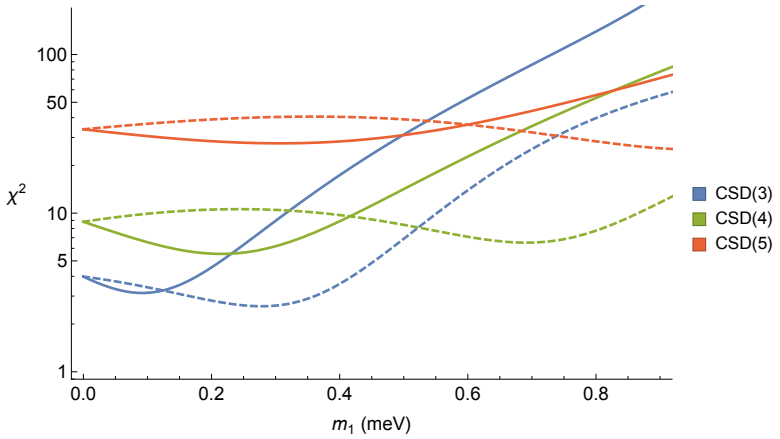

Figure 2.11: Variation of χ^2 with the lightest neutrino mass m_1. Dashed and solid lines refer, respectively, to $\xi = 0$ and $\xi = \eta$.

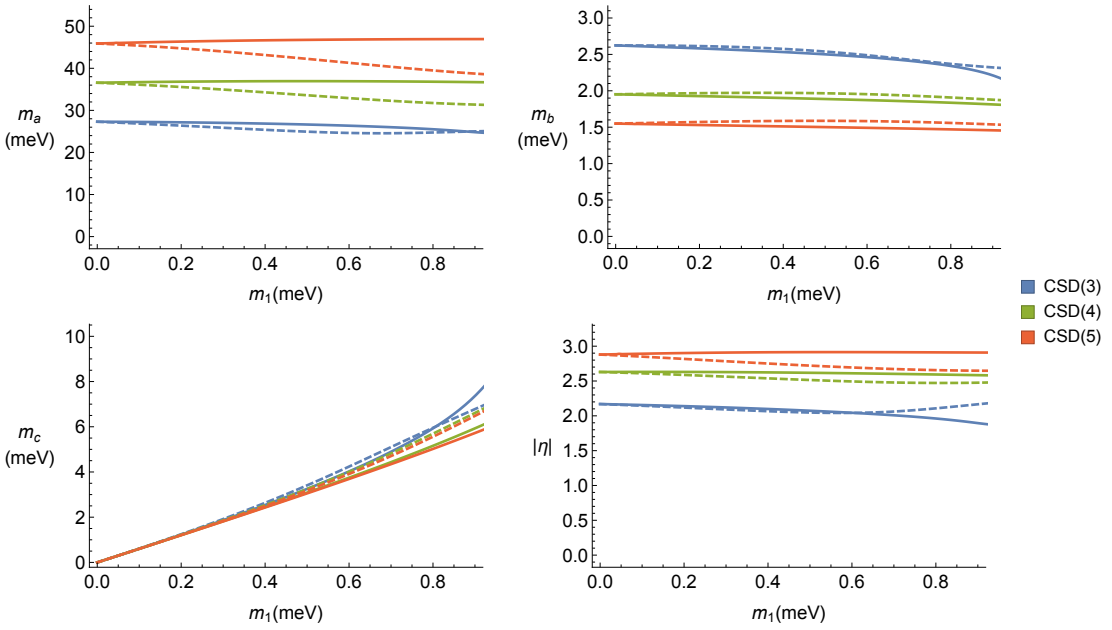

Figure 2.12: Variation of the best fit input parameters with m_1. Dashed and solid lines refer, respectively, to $\xi = 0$ and $\xi = \eta$.

effect is on the best fit value and range of validity of m_c, but it also contributes to interference between the three mass matrices in Eq. 2.24. The practical effect is that each of the three vacuum alignments contribute in varying amounts to each of the three PMNS mixing angles depending on the relative phase between the matrices, which can be seen particularly in Figure 2.13, where the choice of ξ alters the shape of the variation of the mixing angles. As noted earlier, the addition of a third neutrino appears to most dramatically affect the solar angle θ_{12}, in contrast to the two-neutrino model, where it is essentially constant. The physical neutrino masses in Figure 2.14 are comparatively far less sensitive to changes in ξ.

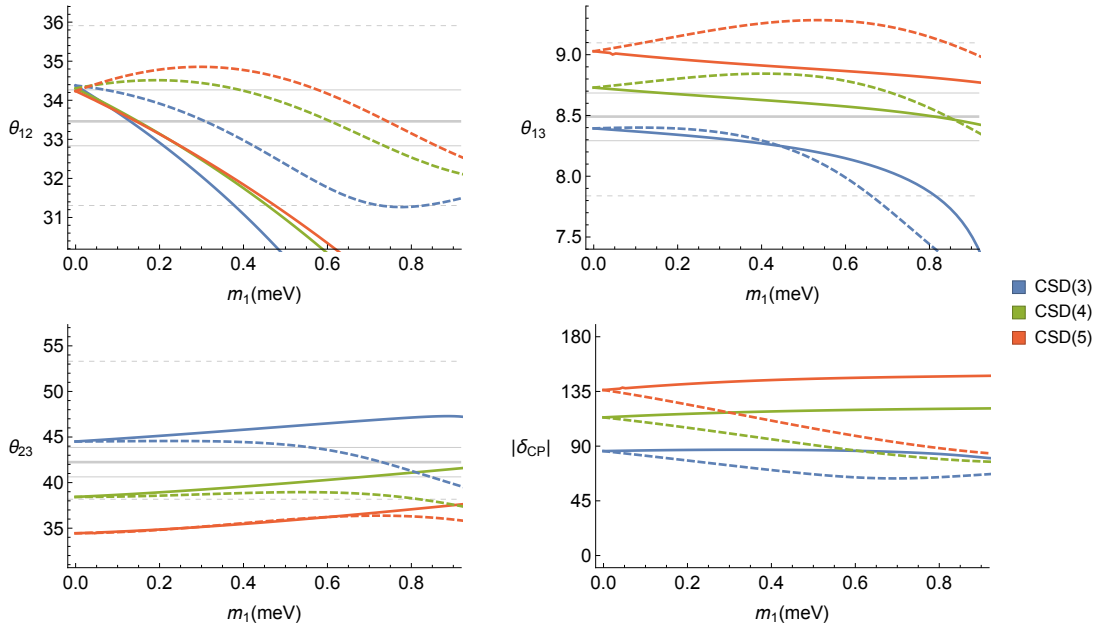

Figure 2.13: Variation of the best fit PMNS parameters with m_1. Dashed and solid lines refer, respectively, to $\xi = 0$ and $\xi = \eta$.

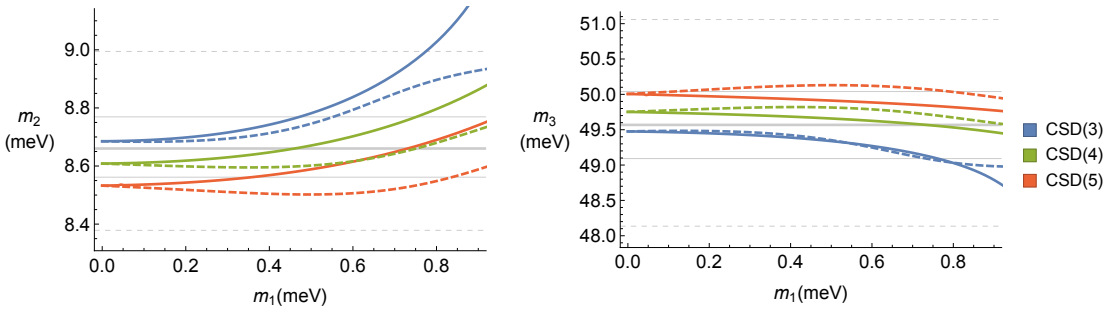

Figure 2.14: Variation of the best fit neutrino masses m_2 and m_3 with respect to m_1. Horizontal gridlines assume m_1 is negligible, such that $m_2 \simeq \sqrt{\Delta m^2_{21}}$ and $m_3 \simeq \sqrt{\Delta m^2_{31}}$. Dashed and solid lines refer, respectively, to $\xi = 0$ and $\xi = \eta$.

2.3.6 Special cases: CSD(3) and CSD(4) with fixed phases

It is interesting that the optimal fit for the CSD(3), with $\chi^2 = 2.59(3.14)$, corresponds to a choice of input phase $|\eta| = 2.10(2.16) = 0.669\pi(0.682\pi)$, for the $\xi = 0$ ($\xi = \eta$) cases, respectively. Its closeness to the value $2\pi/3$, independently of ξ, is a compelling quality in favour of flavour models that predict additional $\mathbb{Z}_{3N}$ symmetries, which tend to predict quantised phases as multiples of $\pi/3$. This motivates a χ^2 analysis with a fixed value of $\eta = 2\pi/3$, for a reduced input vector $x = (m_a, m_b, m_c)$. The resulting input and output parameters for fixed $\eta = 2\pi/3$ are given in Table 2.7. The best fits give $\chi^2 = 2.59(5.25)$, for the $\xi = 0$ ($\xi = \eta$) cases, respectively, marginally worse than in the case of unconstrained η fits which gave $\chi^2 = 2.59(3.14)$.

Parameter	Best fit value $\xi = 0$	$\xi = \eta$
m_a /meV	25.9	26.7
m_b /meV	2.60	2.64
m_c /meV	1.80	0.88
m_1 /meV	0.29	0.14
m_2 /meV	8.71	8.63
m_3 /meV	48.2	49.7
θ_{12} /°	32.1	33.3
θ_{13} /°	8.74	8.54
θ_{23} /°	46.2	45.8
$\lvert\delta_{\rm CP}\rvert$ /°	90.2	89.1

Table 2.7: Best fit input and output values for CSD(3) with fixed input phase $\eta = 2\pi/3$.

Turning to the other promising candidate, CSD(4), we see that, for $\xi = 0$ ($\xi = \eta$), we have $\chi^2 = 6.51(5.53)$ for $|\eta| = 2.48(2.63) = 0.79\pi(0.84\pi)$, which is close to $4\pi/5$. It is meaningful to examine the parameter space for a fixed phase $\eta = \pm\frac{4\pi}{5}$ and $\xi = 0$ (as in [98]) or $\xi = \eta$ (as in [99]), although in such realistic models charged lepton corrections also play a role. The fit yields $\chi^2 = 7.20(14.7)$ with corresponding input and output parameters given in Table 2.8.

Parameter	Best fit value $\xi = 0$	$\xi = \eta$
m_a /meV	33.0	35.4
m_b /meV	1.94	1.99
m_c /meV	4.42	1.60
m_1 /meV	0.66	0.26
m_2 /meV	8.65	8.49
m_3 /meV	49.7	50.2
θ_{12} /°	33.5	32.7
θ_{13} /°	8.68	9.05
θ_{23} /°	38.2	41.3
$\lvert\delta_{\rm CP}\rvert$ /°	93.6	112

Table 2.8: Best fit input and output values for CSD(4) with fixed input phase $\eta = 4\pi/5$.

2.4 Leptogenesis in CSD(n) models

In this section we show how successful N_1 leptogenesis may be realised in CSD(n) models, based on the work in [3]. In [3] we also applied the results to an $A_4 \times SU(5)$ SUSY GUT

which realises the CSD(3) vacuum alignment. This model and its leptogenesis predictions will be discussed in Chapter 3. Recall that the leptogenesis mechanism involves at least two right-handed neutrinos, whose CP-violating decays give rise to a lepton asymmetry, which is subsequently converted into a baryon asymmetry by sphalerons. By the SD assumption, the third right-handed neutrino is almost decoupled from the theory. As demonstrated in the above numerical analysis, it has only minor effect on predictions for low-scale neutrino parameters. Its contribution to leptogenesis will also be negligible, so here we consider the class of models involving only two right-handed neutrinos. We begin by establishing the link between the phase η in the light neutrino mass matrix m^ν, as defined in Eq. 2.23, and the leptogenesis phase. Next, the baryon asymmetry of the Universe (BAU) from thermal N_1 leptogenesis is calculated in the CSD(n) framework, and numerical results are presented for the most viable cases, namely $3 \leq n \leq 5$. The leptogenesis calculation primarily follows the method described in [108], which builds on previous efforts in [109–111] towards understanding the importance of flavour in thermal leptogenesis.

2.4.1 Link between the CP and leptogenesis phases

In the original form of CSD, i.e. TB mixing or CSD(1), the columns of the neutrino Dirac mass matrix m^D in the flavour basis were orthogonal to each other and consequently the CP asymmetries for cosmological leptogenesis vanished [108, 112]. Following the subsequent observation that leptogenesis also vanished for a range of other family symmetry models [113–115], this undesirable feature was eventually understood [116] to be a general consequence of seesaw models with form dominance [90, 91], i.e. in which the columns of m^D in the flavour basis are proportional to the columns of the PMNS matrix.

For general CSD(n), leptogenesis does not vanish since the columns of m^D are not orthogonal. To be precise, $m^D_{\rm atm} = (0, a, a)$ and $m^D_{\rm sol} = (b, nb, (n-2)b)$ from Eq. 2.4 are not orthogonal for $n > 1$. The original CSD($n = 1$) case satisfies form dominance since $(0, a, a) \cdot (b, b, -b) = 0$, and leptogenesis vanishes in this case. CSD(1) is anyway excluded due to observed reactor angle and confirmed by our analysis, which gives $\chi^2 \sim 500$. Interestingly, since the seesaw mechanism in CSD(n) with two right-handed neutrinos only involves a single phase η, both the leptogenesis asymmetries and the neutrino oscillation phase $\delta_{\rm CP}$ must necessarily originate from η, providing a direct link between the two CP-violating phenomena in this class of models.

Before delving into a detailed analysis, let us sketch this dependence to understand its significance. The produced baryon asymmetry Y_B from leptogenesis in CSD(n) models with two right-handed neutrinos satisfies, following the arguments in [108],

$$Y_B \propto \pm \sin \eta, \tag{2.25}$$

where the "+" sign applies to the case $M_{\rm atm} \ll M_{\rm sol}$ and the "−" sign holds for the case $M_{\rm sol} \ll M_{\rm atm}$. Since the observed baryon asymmetry Y_B is positive, it follows that for $M_{\rm atm} \ll M_{\rm sol}$ $\sin\eta$ must be positive, while for $M_{\rm sol} \ll M_{\rm atm}$ $\sin\eta$ must be negative. We have seen that, for CSD(n), positive η is associated with negative $\delta_{\rm CP}$ and *vice versa*. Although the global fits do not distinguish the sign of η, the present hint that $\delta_{\rm CP} \sim -\pi/2$ would require positive η. Then in order to achieve positive Y_B we require $M_{\rm atm} \ll M_{\rm sol}$. Leptogenesis with two right-handed neutrinos with this relation was considered in [117], however those results are geared towards preserving TB mixing. Leptogenesis was has also been studied for CSD(2) [92], which involves two texture zeroes. Here we find a link for CSD(n), even with only one texture zero, due to the appearance of only a single phase η in the seesaw mechanism.

The above conclusions remain approximately true when the nearly-decoupled third right-handed neutrino is introduced. As discussed in [108], the relative size of the additional contribution to the CP asymmetry when a third neutrino is present[9] is $\mathcal{O}(m_c/m_b) \sim 0.1$.

2.4.2 Calculating the baryon asymmetry

A sketch of the N_1 leptogenesis mechanism was presented in the Introduction for the minimally extended Standard Model (by three right-handed neutrinos). Since all models considered in subsequent chapters are supersymmetric, and indeed the vacuum alignment mechanism discussed earlier is based on solutions to F-term equations of various superfields, it is prudent to consider also leptogenesis in a supersymmetric context. This will involve additional contributions from sneutrino decays, which in practice primarily results in modifications to several constants in the calculation. We must also take into account flavour effects, where we distinguish between the flavour indices (e, μ, τ) of the leptons produced by neutrino decays.

A note on notation: as discussed in the Introduction, the final BAU can be parametrised in terms of a CP asymmetry part and an efficiency part. Commonly in the literature the symbols ε and κ are used, respectively. In flavour-dependent scenarios the BAU is given by the sum over contributions in each flavour, i.e. $\eta_B \propto Y_B \propto \sum_\alpha \varepsilon_\alpha \kappa_\alpha$. Here we instead write the CP asymmetries and efficiency factors as $\varepsilon_{1,\alpha}$ and $\eta_{1,\alpha}$, respectively, consistent with notation in [3], which builds on work in [108]. The subscript "1" refers to the fact that we are considering only the contribution from N_1 decays.

At the theory level, the inputs that determine the size of the lepton asymmetry due to right-handed neutrino decays are the neutrino Yukawa matrix λ_ν and the right-handed

[9] A third right-handed neutrino is necessary in the realistic Pati-Salam models based on CSD(4) in [98, 99]. In these models the new phase is either given by $\xi = 0$ or $\xi = \eta$, so no new leptogenesis phase appears. However the mechanism for leptogenesis is necessarily quite different in these models, since the lightest right-handed neutrino of mass $M_{\rm atm}$ is too light to generate successful leptogenesis in its decays. Instead one must rely on the decays of the second lightest right-handed neutrino of mass $M_{\rm sol}$ [118].

neutrino Majorana mass matrix M^c. In the basis where charged leptons are diagonal, the relevant terms are defined by the superpotential

$$W_\nu = y^i_{\rm atm} H L_i N^c_{\rm atm} + y^i_{\rm sol} H L_i N^c_{\rm sol} + M_{\rm atm} N^c_{\rm atm} N^c_{\rm atm} + M_{\rm sol} N^c_{\rm sol} N^c_{\rm sol}, \tag{2.26}$$

where L_i are three families of lepton doublets, and the right-handed neutrinos $N^c_{\rm atm}$ and $N^c_{\rm sol}$ (with real positive masses $M_{\rm atm}$ and $M_{\rm sol}$, respectively) do not mix. The couplings $y^i_{\rm atm}$ and $y^i_{\rm sol}$ make up the first and second column, respectively, of λ_ν. Assuming the CSD(n) relations in Eq. 2.4, the Yukawa matrix and (conjugated) right-handed mass matrix in this basis are

$$\lambda_\nu = \begin{pmatrix} 0 & b \\ a & nb \\ a & (n-2)b \end{pmatrix}, \qquad M^c = \begin{pmatrix} M_1 & 0 \\ 0 & M_2 \end{pmatrix}, \tag{2.27}$$

where we have written $M_1 = M_{\rm atm}$ and $M_2 = M_{\rm sol}$, with $M_1 < M_2$, in anticipation of the result that the lighter right-handed neutrino is the dominant (atm) one.[10]

The above superpotential specifies the basis used for the leptogenesis calculations. This basis choice (the leptogenesis or SUSY basis) differs from that used in the earlier numerical analysis (the seesaw basis), by complex conjugation. This must be taken into account when comparing to numerical results for neutrino parameters at low scale. The two bases and the dictionary between them will be discussed below, but for the calculation that follows it is sufficient to consider a, b, $M_{1,2}$ as free parameters (with a, b complex).

The degree to which flavour effects play a role in determining the BAU depends on which Yukawa interactions are in thermal equilibrium at temperatures $T \sim M_1$. Generically, at high temperatures the interaction rate of a given charged lepton, which is proportional to the square of the Yukawa coupling [119], is smaller than the expansion rate of the Universe, characterised by the Hubble parameter. When the temperature drops, charged lepton interactions become efficient and successively come into thermal equilibrium, first the tau (which has the largest coupling), followed by the muon and eventually the electron. In leptogenesis this can be translated into a statement about the right-handed neutrino mass, such that three distinct regimes must be considered, which are summarised in [108]. The flavour-independent regime, i.e. where all charged lepton flavours are out of equilibrium, corresponds in the MSSM to

$$M_1 > (1 + \tan^2\beta) \times 10^{12}\ \text{GeV}. \tag{2.28}$$

[10] Since M^c is diagonal, there is no distinction between the parameters $N^c_{\rm atm,sol}$ and mass eigenstates $M_{1,2}$. This will not be the case when we consider leptogenesis in a $\Delta(27) \times SO(10)$ SUSY GUT in Chapter 4. It is therefore valuable to introduce a more general notation here.

The two-flavour regime, where the tau is treated separately but the electron and muon are indistinguishable, corresponds to

$$(1+\tan^2\beta)\times 10^9\,\text{GeV} \lesssim M_1 \lesssim (1+\tan^2\beta)\times 10^{12}\ \text{GeV}. \tag{2.29}$$

Finally, the regime where all flavours are to be treated separately corresponds to

$$(1+\tan^2\beta)\times 10^5\,\text{GeV} \lesssim M_1 \lesssim (1+\tan^2\beta)\times 10^9\ \text{GeV}. \tag{2.30}$$

The corresponding values in the Standard Model can be attained by setting $\tan\beta = 0$ in the above inequalities.

It will turn out that for the models of interest $M_1 \sim (40-100)\times 10^9$ GeV. The results therefore appear to post-justify the flavour-dependent treatment only for $\tan\beta \gtrsim 10$. However as it turns out, our results for the three-flavour case are almost identical to those for the flavour-independent case. The reason is that the efficiency factors for the μ and τ flavours turn out to be equal, i.e. $\eta_{1,\mu} = \eta_{1,\tau}$, while the asymmetry for the electron flavour is zero, $\varepsilon_{1,e} = 0$, so there is no overall contribution to Y_B there. In this case one may define an efficiency factor $\eta^{\text{ind}} \equiv \eta_{1,\mu} = \eta_{1,\tau}$ and asymmetry $\varepsilon_1 \equiv \sum_\alpha \varepsilon_{1,\alpha}$ such that the BAU is proportional to $\eta^{\text{ind}}\varepsilon_1$, as will become clear from the following results. The only difference between the flavour-independent and flavour-dependent cases, in the considered models, is in the detailed solutions to the Boltzmann equations which involve differences in a numerical matrix A (defined below) which only appears logarithmically in determining the washouts. The main consequence of this is that the above condition $\tan\beta \gtrsim 10$ becomes relaxed, and our results are valid for any value of $\tan\beta$ to good approximation. However, for clarity, we shall perform the calculation using the full three-flavour treatment.

The total BAU Y_B is obtained as a sum over the individual contributions in each lepton flavour Y_{Δ_α}, by

$$Y_B = \frac{10}{31}\sum_\alpha Y_{\Delta_\alpha}, \tag{2.31}$$

The individual flavour contributions are in turn given by

$$Y_{\Delta_\alpha} = \eta_{1,\alpha}[Y_{N_1} + Y_{\tilde{N}_1}]\varepsilon_{1,\alpha}, \tag{2.32}$$

where $\eta_{1,\alpha}$ are efficiency factors and $\varepsilon_{1,\alpha}$ are the CP asymmetries. In the Boltzmann approximation for the MSSM, i.e. assuming the same statistics for fermions and bosons,

$$Y_{N_1} \approx Y_{\tilde{N}_1} \approx \frac{45}{\pi^4 g_*}, \qquad g_* = 228.75, \tag{2.33}$$

where g_* is the effective number of degrees of freedom in the MSSM. The factors $Y_{N_1,\tilde{N}_1}$ are (s)neutrino number densities and may be interpreted as normalisation constants.

The expression (per flavour index) for the CP asymmetry is [108]

$$\varepsilon_{1,\alpha} = \frac{1}{8\pi} \frac{\mathrm{Im}\left[(\lambda_\nu^\dagger)_{1\alpha}(\lambda_\nu^\dagger\lambda_\nu)_{12}(\lambda_\nu^\intercal)_{2\alpha}\right]}{(\lambda_\nu^\dagger\lambda_\nu)_{11}} g^{\mathrm{MSSM}}\left(\frac{M_2^2}{M_1^2}\right). \tag{2.34}$$

The loop factor $g^{\mathrm{MSSM}}(x)$ is given by

$$g^{\mathrm{MSSM}}(x) = \sqrt{x}\left(\frac{2}{1-x} - \ln\left(\frac{1+x}{x}\right)\right). \tag{2.35}$$

For large x, i.e. $M_1 \ll M_2$, we have

$$g^{\mathrm{MSSM}}\left(\frac{M_2^2}{M_1^2}\right) \approx -3\frac{M_1}{M_2}. \tag{2.36}$$

For the CSD(n) matrix λ_ν defined in Eq. 2.27, the flavour dependent asymmetries are

$$\begin{aligned} \varepsilon_{1,e} &= 0, \\ \varepsilon_{1,\mu} &= -\frac{3}{8\pi}\frac{M_1}{M_2}(n-1)n\,\frac{\mathrm{Im}[a^{*2}b^2]}{|a|^2}, \\ \varepsilon_{1,\tau} &= -\frac{3}{8\pi}\frac{M_1}{M_2}(n-1)(n-2)\,\frac{\mathrm{Im}[a^{*2}b^2]}{|a|^2}. \end{aligned} \tag{2.37}$$

Note that

$$\varepsilon_{1,\tau} = \left(\frac{n-2}{n}\right)\varepsilon_{1,\mu}. \tag{2.38}$$

We define the phase η that is relevant for leptogenesis as

$$\eta \equiv -\arg[a^{*2}b^2]. \tag{2.39}$$

This naming convention is not coincidental, as it will be shown to be equal to that which appears in the CSD(n) neutrino mass matrix m^ν.

Having established the factor $Y_{N_1} + Y_{\tilde{N}_1}$ and the $\varepsilon_{1,\alpha}$ asymmetries, it remains to determine the (flavour-dependent) efficiency factors $\eta_{1,\alpha}$. These arise from solutions to the supersymmetric flavour-dependent Boltzmann equations given in [108]. These equations do not have simple analytical solutions, and are more readily solved numerically. Generically, the efficiency factors $\eta_{1,\alpha}$ depend in a rather complicated fashion on λ_ν. This is doubly true in cases where the right-handed neutrino mass matrix is not already diagonal; moving into the flavour basis adds a layer of complexity to the result. Exactly this scenario is encountered in Chapter 4, where a similar leptogenesis calculation is performed in a $\Delta(27) \times SO(10)$ SUSY GUT. However, in the minimal CSD(n) framework presented here, we will find that $\eta_{1,\alpha}$ essentially depends only on the input mass parameter m_a, in such a way that we may use results available in [108] to calculate $\eta_{1,\alpha}$. We therefore defer a detailed discussion of the Boltzmann equations to Chapter 4.

As seen in [108], $\eta_{1,\alpha}$ may be expressed as a function of two quantities: $\log_{10}|A_{\alpha\alpha}K_\alpha|$ (no sum) and $K = \sum_\alpha K_\alpha$. $A_{\alpha\alpha}$ are the diagonal elements of a numerical matrix A. In the MSSM and in the three-flavour regime, it is given by the numerical 3×3 matrix

$$A = \begin{pmatrix} -\frac{93}{110} & \frac{6}{55} & \frac{6}{55} \\ \frac{3}{40} & -\frac{19}{30} & \frac{1}{30} \\ \frac{3}{40} & \frac{1}{30} & -\frac{19}{30} \end{pmatrix}. \tag{2.40}$$

The elements of A depend on which interactions are in thermal equilibrium at the temperatures where leptogenesis takes place. The parameters K_α are referred to as decay factors, and essentially describe the degree to which the asymmetry is washed out: $K_\alpha \gg 1$ may be considered strong washout, while $K_\alpha < 1$ is weak washout. They are themselves functions of so-called effective neutrino mass parameters $\tilde{m}_{1,\alpha}$, such that

$$K_\alpha = \frac{\tilde{m}_{1,\alpha}}{m^*_{\mathrm{MSSM}}}, \tag{2.41}$$

where $m^*_{\mathrm{MSSM}} \approx (1.58 \times 10^{-3}\ \mathrm{eV}) \sin^2\beta$ is the equilibrium neutrino mass, and

$$\tilde{m}_{1,\alpha} = (\lambda_\nu^\dagger)_{1\alpha}(\lambda_\nu)_{\alpha 1}\frac{v_u^2}{M_1}. \tag{2.42}$$

With λ_ν given in Eq. 2.27, and recalling that $v_u = v\sin\beta$, the mass parameters are

$$\tilde{m}_{1,e} = 0, \qquad \tilde{m}_{1,\mu} = \tilde{m}_{1,\tau} = |a|^2\frac{v^2\sin^2\beta}{M_1}. \tag{2.43}$$

Because $\tilde{m}_{1,\mu} = \tilde{m}_{1,\tau}$ we also obtain $K_\mu = K_\tau$. From Eq. 2.40 we obtain $A_{\mu\mu} = A_{\tau\tau} = -19/30$. Thus we conclude that $\eta_{1,\mu} = \eta_{1,\tau}$. Furthermore, the expression for $\tilde{m}_{1,\mu} = \tilde{m}_{1,\tau}$ in Eq. 2.43 corresponds exactly to the definition for the dominant input mass parameter m_a in the light neutrino mass matrix m^ν, as defined in Eq. 2.20 (for general CSD(n)) and Eq. 2.23 (for two right-handed neutrinos). It provides us with another immediate link between leptogenesis parameters and the neutrino mass matrix.

We may now return to the expression for the observed asymmetry Y_B as per Eqs. 2.31 and 2.32, where

$$Y_B = \frac{10}{31}\sum_\alpha \eta_{1,\alpha}[Y_{N_1} + Y_{\tilde{N}_1}]\varepsilon_{1,\alpha}. \tag{2.44}$$

Inserting the approximations for Y_{N_1} and $Y_{\tilde{N}_1}$ from Eq. 2.33 and the asymmetries $\varepsilon_{1,\alpha}$ from Eq. 2.37 yields

$$\begin{aligned} Y_B &= \frac{10}{31}\left(\eta_{1,\mu}\left[2\frac{45}{\pi^4 g_*}\right]\varepsilon_{1,\mu} + \eta_{1,\tau}\left[2\frac{45}{\pi^4 g_*}\right]\frac{n-2}{n}\varepsilon_{1,\mu}\right) \\ &= \frac{10}{31}\eta_{1,\mu}\left[2\frac{45}{\pi^4 g_*}\right]\left(\frac{2n-2}{n}\right)\left(-\frac{3}{8\pi}\frac{M_1}{M_2}(n-1)n\ \frac{\mathrm{Im}[a^{*2}b^2]}{|a|^2}\right). \end{aligned} \tag{2.45}$$

Expressing this in terms of the phase η defined in Eq. 2.39, noting that $\mathrm{Im}[a^{*2}b^2]/|a^2| = -|b|^2 \sin\eta$, we arrive at

$$Y_B = \frac{675}{31\pi^5 g_*}\frac{M_1}{M_2}\eta_{1,\mu}\ (n-1)^2|b|^2\sin\eta. \tag{2.46}$$

Finally, we note that $|b|^2/M_2 \propto m_b$, the subdominant input mass parameter in m^ν. Thus the final baryon asymmetry Y_B in Eq. 2.46 depends explicitly on m_b and η (which will shortly be shown to be identical to that in m^ν) and implicitly on m_a through the efficiency factor $\eta_{1,\alpha}$. The dependence on the integer n is also clear. Note in particular that the case $n = 1$ gives $Y_B = 0$, i.e. that TB mixing cannot give a non-zero baryon asymmetry, reproducing the known result.

2.4.3 Constraining leptogenesis with neutrino data

In order to constrain leptogenesis in CSD(n) we use information about low energy neutrino masses and mixing. As discussed earlier (see Eqs. 2.16 – 2.18), the lepton matrices and seesaw mechanism are defined by

$$\mathcal{L}^{LR} + \mathcal{L}^R_\nu = -H_d Y^e_{ij}\overline{L_{Li}}e_{Rj} - H_u Y^\nu_{ij}\overline{L_{Li}}\nu_{Rj} - \tfrac{1}{2}(M_R)_{ij}\overline{\nu^c_{Ri}}\nu_{Rj} + \text{h.c.} \tag{2.47}$$

The seesaw formula in this basis is $m^\nu = -v_u^2 Y^\nu M_R^{-1}(Y^\nu)^\intercal$, where m^ν is defined by $\mathcal{L}^L_\nu = -\frac{1}{2}m^\nu_{ij}\overline{\nu^c_{Li}}\nu_{Lj} + \text{h.c.}$. There is a simple dictionary between the seesaw basis and the SUSY basis in Eq. 2.26, as follows: $Y^\nu = (\lambda_\nu)^*$, while $M_R = (M^c)^* = M^c$. Hence the CSD(n) relations in Eq. 2.27 become, in the seesaw basis,

$$Y^\nu = \begin{pmatrix} 0 & b^* \\ a^* & nb^* \\ a^* & (n-2)b^* \end{pmatrix}, \qquad M_R = \begin{pmatrix} M_1 & 0 \\ 0 & M_2 \end{pmatrix}. \tag{2.48}$$

Recall that the seesaw mechanism produces the effective neutrino mass matrix

$$m^\nu = m_a \begin{pmatrix} 0 & 0 & 0 \\ 0 & 1 & 1 \\ 0 & 1 & 1 \end{pmatrix} + m_b e^{i\eta} \begin{pmatrix} 1 & n & (n-2) \\ n & n^2 & n(n-2) \\ (n-2) & n(n-2) & (n-2)^2 \end{pmatrix}, \tag{2.49}$$

where $m_a = v_u^2|a|^2/M_1$, $m_b = v_u^2|b|^2/M_2$, and the phase η is defined as

$$\eta \equiv \arg[a^2/b^2]. \tag{2.50}$$

This definition of the phase η is consistent with Eq. 2.39, providing the link between leptogenesis and low energy neutrino phenomenology. The sign of η fixes the leptonic Dirac phase δ_{CP}. Specifically, a positive η uniquely leads to negative δ_{CP}, and *vice*

versa. As experimental data hints at $\delta_{\rm CP} \sim -\pi/2$, the *a posteriori* preferred solution has positive η. The sign of η also has high energy cosmological significance: as seen in Eq. 2.46, it controls the sign and magnitude of the BAU. As noted earlier, $N^c_{\rm atm} \ll N^c_{\rm sol}$ and positive η predict a positive BAU, as desired.

The remainder of this section is devoted to the numerical CSD(n) results for both neutrino phenomenology and leptogenesis. The dependence on m_b is made apparent by rewriting Eq. 2.46 as

$$Y_B = \frac{675}{31\pi^5 g_*} \frac{M_1 m_b}{v_u^2} \eta_{1,\mu} (n-1)^2 \sin\eta. \tag{2.51}$$

We will limit our analysis to those values of n which produce reasonable fits to data, namely $n = 3, 4, 5$, as only these give $\chi^2 < 50$. For convenience, the relevant results from Table 2.2 are reproduced in Table 2.9, along with their predictions for the lepton mixing angles, CP violating phase and neutrino masses. Note that we have now fixed η to be positive, corresponding to negative $\delta_{\rm CP}$. This will ensure the correct sign of the baryon asymmetry.

We reiterate that values of m_a, m_b and η that may be characterised as providing "good" fits (or at least fits with χ^2 close to the minimal value) lie comfortably within $\pm 10\%$ of their respective best fit values. We are left with an expression for Y_B that is linear in M_1, multiplied by a numerical factor that ultimately depends only on n. Taking into account the variability of the mass matrix parameters, we estimate that the numerical factor may also vary by up to $\pm 10\%$ without significantly impacting the fits to neutrino masses and mixing angles. In terms of placing bounds on M_1, this far outweighs the current error on the experimental value for Y_B, which is approximately $\pm 0.6\%$. It is also worth noting that CSD(2) predicts a best fit with $\eta = 0$, while CSD(n) with $n > 5$ predict best fits with $\eta = \pi$, both giving $\sin\eta = 0$, which implies a zero baryon asymmetry. This further justifies neglecting those cases here.

n	m_a (meV)	m_b (meV)	η (rad)	θ_{12} (°)	θ_{13} (°)	θ_{23} (°)	$\delta_{\rm CP}$ (°)	m_2 (meV)	m_3 (meV)	χ^2
3	27.3	2.62	2.17	34.4	8.39	44.5	-92.2	8.69	49.5	3.98
4	36.6	1.95	2.63	34.3	8.72	38.4	-120	8.61	49.8	8.82
5	45.9	1.55	2.88	34.2	9.03	34.4	-142	8.53	50.0	33.8

Table 2.9: Best fit parameters for CSD(n) with two right-handed neutrinos, for $3 \leq n \leq 5$.

With m_a fixed by the fit, we may estimate $\log_{10}(A_{\mu\mu}K_\mu) = \log_{10}(A_{\tau\tau}K_\tau)$, from the results in Eqs. 2.40 – 2.43, with which we obtain the efficiency factors from the solutions to the Boltzmann equations given in [108]. Hence, for $n = (3, 4, 5)$, we obtain the corresponding efficiency factors $\eta_{1,\mu} = (0.0236, 0.0166, 0.0126)$. Inserting numerical values also for m_b and η from Table 2.9 into Eq. 2.51, we arrive at the predictions for

the right-handed neutrino masses[11]

$$\begin{aligned}
&\text{CSD}(3): \quad Y_B \sim 2.2 \times 10^{-11} \left[\frac{M_1}{10^{10}\ \text{GeV}}\right] \quad \Rightarrow \quad M_1 \sim 4.0 \times 10^{10}\ \text{GeV}, \\
&\text{CSD}(4): \quad Y_B \sim 1.5 \times 10^{-11} \left[\frac{M_1}{10^{10}\ \text{GeV}}\right] \quad \Rightarrow \quad M_1 \sim 5.8 \times 10^{10}\ \text{GeV}, \\
&\text{CSD}(5): \quad Y_B \sim 0.86 \times 10^{-11} \left[\frac{M_1}{10^{10}\ \text{GeV}}\right] \quad \Rightarrow \quad M_1 \sim 10 \times 10^{10}\ \text{GeV}.
\end{aligned} \tag{2.52}$$

With M_1 fixed in each case, $|a|$ may be calculated to be $\mathcal{O}(10^{-3})$ using $m_a = v_u^2|a|^2/M_1$, since m_a is known. On the other hand only the combination $m_b = v_u^2|b|^2/M_2$ is fixed by neutrino data and the separate parameters $|b|$ and M_2 are not determined from leptogenesis.

2.5 Summary

In this chapter we have described the sequential dominance framework, which provides a natural understanding of the smallness of neutrino mass and large lepton mixing in the context of the type-I seesaw mechanism. We have analysed the phenomenology of the CSD(n) class of models, where the dominant right-handed neutrino couples to the three families of left-handed neutrinos with strengths proportional to $(0, 1, 1)$, while the subdominant right-handed neutrino couples with strengths proportional to $(1, n, n-2)$, for an integer n, and shown how these couplings can arise from the vacuum alignments of flavons that are triplets under a discrete family symmetry.

Models with both two and three right-handed neutrinos have been considered, in the flavour basis, for $1 \leq n \leq 9$. A χ^2 fit shows that good agreement with experimental global fits can be attained for $n = 3, 4$. In particular, CSD(3) with two right-handed neutrinos yields a very minimal and successful model of neutrinos, involving only three free parameters: two mass parameters $m_{a,b}$ and a phase η.

This phase has significance for both leptonic CP violation and leptogenesis. The Dirac CP phase δ_{CP} is predicted by the fit to be approximately $\pm\pi/2$ for CSD(3), and $\pm 2\pi/3$ for CSD(4), and 0 or π for other n. Within CSD(n), we have also calculated the contribution to the baryon asymmetry of the Universe Y_B from thermal leptogenesis. The flavoured CP asymmetries are found to be proportional to $\sin\eta$. Coupled with the requirement that $Y_B > 0$ requires $\eta > 0$, which predicts $\delta_{\text{CP}} < 0$, in agreement with current experimental hints. These results represent a promising foundational step for a more complete model of leptons, and cosmology.

[11] We have used $\sin\beta \approx 1$ which is a good approximation for $\tan\beta \gtrsim 3$.

Chapter 3

An $A_4 \times SU(5)$ model

As noted in the Introduction, the Standard Model, although highly successful, leaves many unanswered questions in its wake, such as: what (if anything) stabilises the Higgs boson mass? Does charge quantisation and the apparent unification of gauge forces at high scale originate from grand unification? What is the origin of the three families of quarks and leptons and their pattern of masses, mixing and CP violation? Why is CP so accurately conserved by the strong interactions? In this chapter we discuss a proposed model capable of addressing all the above questions. The basic ingredients of the model are supersymmetry together with an $SU(5)$ grand unified theory, flavoured by an A_4 family symmetry. The majority of this chapter is adapted from work published in [2], which defines the model, while the discussion on leptogenesis was originally published in [3].

3.1 The minimal flavoured GUT

The model is minimal in the sense that $SU(5)$ is the smallest GUT group and A_4 is the smallest family symmetry group that admits triplet representations. Also, below the GUT scale, the model yields the minimal supersymmetric Standard Model (MSSM) supplemented by a minimal two right-handed neutrino seesaw mechanism. It is realistic in the sense that it provides a successful (and natural) description of the fermion mass and mixing spectrum, including spontaneous CP violation, while resolving the strong CP problem. It is fairly complete in the sense that GUT and flavour symmetry breaking are addressed, including doublet-triplet splitting, Higgs mixing and the origin of the MSSM μ term, all of which are detailed in Section C.1 of Appendix C. We emphasise the predictive nature of the model in the lepton sector, realising the very successful CSD(3) vacuum alignments analysed in the previous chapter. Here they originate from the vacuum alignment of A_4 triplets, fully determined by the field content and symmetries. The single phase η in the neutrino mass matrix is fixed to a discrete choice. We select

$\eta = 2\pi/3$ from the nine complex roots of unity arising from spontaneous CP violation of a $\mathbb{Z}_9 \times \mathbb{Z}_6$ discrete symmetry, by a mechanism proposed in [120]. Such a spontaneous CP-violating scenario had been proposed previously in order to account for the smallness of CP violation in the soft SUSY sector [121, 122].

We also employ a $\mathbb{Z}_4^R$ discrete R symmetry as the origin of MSSM matter parity (as in [123, 124]), ensuring in principle a viable WIMP dark matter candidate. Doublet-triplet splitting is achieved via the missing partner (MP) mechanism [125, 126], as advocated for flavoured GUTs in [127]. The model predicts very sparse charged lepton and down-type quark Yukawa matrices, with five texture zeroes, and Yukawa elements involving simple $SU(5)$ Clebsch-Gordan (CG) ratios of 4/9 and 9/2 for the first and second families, respectively, with $m_\tau/m_b = 1$ for the third family, all in excellent agreement with their experimental values run up to the GUT scale [128, 129]. Quark mixing originates predominantly from a non-diagonal and naturally hierarchical up-type quark Yukawa matrix, controlled by the $\mathbb{Z}_9$ symmetry. Quark CP violation, however, comes exclusively from a single off-diagonal element in the down-type quark Yukawa matrix. By contrast, to excellent approximation all lepton mixing and CP violation originates from the neutrino mass matrix, whose structure is controlled by the A_4 and the $\mathbb{Z}_6$ symmetries via CSD(3).

Although there have been several attempts in the literature at constructing an $A_4 \times SU(5)$ SUSY GUT of flavour (for an incomplete list see e.g. [130–139]), many of the previous models predicted mixing very close to tri-bimaximal and are by now excluded. For some examples of $SU(5)$ SUSY GUTs with different family symmetries, see [140–143]. It will take some time and (experimental) effort to resolve all these models. The most promising models are those that make testable predictions while being theoretically complete and consistent.

This is a non-minimal model from the perspective of counting degrees of freedom, as there are many different chiral superfields in this model, indeed almost exactly a hundred. It is however important to note that we are explicitly presenting a renormalisable model. Any non-renormalisable terms generated below the Planck scale are required to have a specific well-defined realization through multiple renormalisable terms involving heavy messenger fields that can be integrated out around the GUT scale. The resulting effective theory is actually more predictive than otherwise, with a normal neutrino mass hierarchy, a zero lightest neutrino mass, and all lepton mixing angles and CP phases predicted. We would argue that the model presented here is amongst the most viable and complete SUSY GUTs of flavour consistent with current data.

3.2 The Yukawa sector

3.2.1 Field content and symmetries

The model involves a superpotential invariant under $A_4 \times SU(5) \times \mathbb{Z}_9 \times \mathbb{Z}_6$ as well as a $\mathbb{Z}_4^R$ discrete R symmetry and CP at the GUT scale, where all symmetries, including CP, are spontaneously broken along supersymmetric flat directions to give the MSSM. The purpose of this section is to describe those aspects of the model pertaining to the Yukawa sector, i.e. the quark and lepton masses and mixing. The flavour sector of the model is very important in our approach, since we make a serious attempt to understand and, where possible, predict the experimentally observable fermion masses and mixing matrices.

Field	Representation				
	A_4	$SU(5)$	$\mathbb{Z}_9$	$\mathbb{Z}_6$	$\mathbb{Z}_4^R$
F	3	$\bar{5}$	0	0	1
T_1	1	10	5	0	1
T_2	1	10	7	0	1
T_3	1	10	0	0	1
N_1^c	1	1	7	3	1
N_2^c	1	1	8	3	1
Γ	1	1	0	3	1
H_5	1	5	0	0	0
$H_{\bar{5}}$	1	$\bar{5}$	2	0	0
H_{24}	$1'$	24	3	0	0
Λ_{24}	$1'$	24	0	0	0
H_{45}	1	45	4	0	2
$H_{\overline{45}}$	1	$\overline{45}$	5	0	0
ξ	1	1	2	0	0
θ_1	1	1	1	3	0
θ_2	1	1	1	4	0
ϕ_e	3	1	0	0	0
ϕ_μ	3	1	3	0	0
ϕ_τ	3	1	7	0	0
ϕ_1	3	1	3	2	0
ϕ_2	3	1	1	3	0
ϕ_3	3	1	3	1	0
ϕ_4	3	1	2	1	0
ϕ_5	3	1	6	2	0
ϕ_6	3	1	5	2	0

(a) Matter and symmetry-breaking superfields with even R charge.

Field	Representation				
	A_4	$SU(5)$	$\mathbb{Z}_9$	$\mathbb{Z}_6$	$\mathbb{Z}_4^R$
X_1	1	$\bar{5}$	7	0	1
X_2	1	5	2	0	1
X_3	1	$\bar{5}$	6	0	1
X_4	1	5	3	0	1
X_5	$1''$	$\bar{5}$	3	0	1
X_6	$1'$	5	6	0	1
X_7	1	$\bar{5}$	2	0	1
X_8	$1''$	5	7	0	1
X_9	$1'$	$\bar{5}$	0	0	1
X_{10}	$1'$	5	0	0	1
X_{11}	1	$\bar{5}$	1	3	1
X_{12}	1	5	7	5	1
X_{13}	1	$\bar{5}$	2	3	1
X_{14}	1	5	6	5	1
Σ_i	1	5	i	0	0
$\overline{\Sigma}_i$	1	$\bar{5}$	i	0	2

(b) Messenger superfields. The 16 Σ messengers are indexed by their (non-zero) $\mathbb{Z}_9$ charge $i = 1, \ldots, 8$.

Table 3.1: Superfields which specify the Yukawa sector of the model.

The $\mathbb{Z}_N$ symmetries are Abelian discrete groups which denote discrete roots of complex roots of unity. For example, a $\mathbb{Z}_9$ charge of n is equivalent to a charge $e^{2\pi ni/9}$. Such symmetries are often referred to as shaping symmetries, which serve to forbid unwanted terms in the superpotential. From a model-building perspective, these choices of N are free, as are the field charges, although in this model N are chosen as multiples of three, as these can lead to discrete phase choices in the fermion mass matrices that include the value $2\pi/3$, identified in the previous chapter as particularly suitable for CSD(3) in the neutrino sector. How this may arise is discussed in Section C.1 of Appendix C. Meanwhile, under the R symmetry $\mathbb{Z}_4^R$, the superpotential has an overall charge of 2.

Table 3.1a shows the matter superfields F, T_i that contain the quarks and leptons, as well as the right-handed neutrino superfields N_i^c and double-seesaw superfield Γ, all of which carry unit $\mathbb{Z}_4^R$ charge. Apart from the $A_4 \times SU(5)$ assignments of $F \sim (3, \bar{5})$, $T_i \sim (1, 10)$, $N_i^c \sim (1, 1)$, under $\mathbb{Z}_9$ they transform as $F \sim 0$, $T_i \sim (5, 7, 0)$, $N_i^c \sim (7, 8)$. Unlike the rest of the quarks and leptons, the right-handed neutrinos are further charged under $\mathbb{Z}_6$ (as are some of the symmetry-breaking scalars). Table 3.1a also contains the six Higgs superfields, generally denoted H (but also Λ) which serve to break the $SU(5)$ gauge symmetry. The two light MSSM Higgs doublet superfields H_u and H_d will emerge from H_5 and a mixture of $H_{\bar{5}}$ and $H_{\overline{45}}$. The superfield ξ which breaks $\mathbb{Z}_9$ is particularly central to this theory, as it is responsible for both right-handed neutrino masses and the up-type quark mass hierarchy. Finally we have the θ_i superfields which break $\mathbb{Z}_6$ and help to control neutrino Dirac masses, and nine A_4-breaking triplet flavons generally denoted ϕ, with various vacuum alignments, responsible for large lepton mixing.

With these assignments, only the top quark gets a mass from a renormalisable Yukawa coupling $H_5 T_3 T_3$ (which has $\mathbb{Z}_4^R$ charge 2 as required for an allowed superpotential term). All the other quark and lepton Yukawa couplings must arise through higher-order terms. This provides the basic reason why most of the Standard Model Yukawa couplings appear to be so small. Also the hierarchy among lighter quarks is addressed: more precisely, the observed hierarchy of Yukawa couplings between the three families will be explained via a discrete $\mathbb{Z}_9$ version of the Froggatt-Nielsen mechanism [58]. Originally conceived in terms of a global $U(1)$ symmetry, the mechanism involves the superfield ξ which gains a VEV $\langle\xi\rangle$ slightly below the scale M at which the symmetry (in our case, $\mathbb{Z}_9$) breaks, e.g. $\langle\xi\rangle / M \sim 0.1$. Fermions couple to different powers of ξ, such that the Yukawa matrices are populated by powers of $\langle\xi\rangle / M$. This introduces hierarchies in the Yukawa matrices. In this model, the low VEV of ξ controls the hierarchy in the up-type quark sector, and also, in part, the smallness of the down quark and electron.

In order to enhance predictivity we need the messengers listed in Table 3.1b, which is the price we pay for having a renormalisable theory at the GUT scale. We denote these superfields either as fermion messengers, X_i, or scalar messengers, Σ_i, depending on whether they carry similar quantum numbers to, respectively, the quarks and leptons (with odd $\mathbb{Z}_4^R$ charge) or the symmetry-breaking scalars (with even $\mathbb{Z}_4^R$ charge). The

fermion messengers X_i carry similar quantum numbers to down-type quarks and charged leptons (and neutrinos). Scalar messengers Σ_i have quantum numbers similar to H_5 (the superfield that gives the top quark a renormalisable mass term). The Σ_i messengers do not get VEVs, which means we need not consider the effect of diagrams with Σ_i in external legs to the masses of Standard Model fermions.

The messengers group themselves in pairs of two superfields with a renormalisable bare mass coupling which respects all the symmetries. Their masses are therefore expected to be around the GUT scale. Although there will be in general distinct masses for different pairs, for simplicity we take the masses of all such pairs to be M and set this equal to the GUT scale in our numerical estimates. We emphasise that the successful predictions of the model in the lepton sector (namely predicting the PMNS matrix) is independent of the specific values of these mass parameters.

3.2.2 Up-type quarks

Apart from the top quark mass, which originates from a renormalisable Yukawa coupling, the remaining up-type quark Yukawa couplings appear from higher-order terms that result from combining several renormalisable terms involving Σ_i messengers and the GUT singlet superfield ξ. To be precise, the up-type quark Yukawa couplings arise from tower diagrams shown in Figure 3.1. For example, the most suppressed coupling arises from the first diagram in Figure 3.1. Other (less suppressed) couplings arise from the diagrams where at the base one has the respective $T_i T_j$, with a shorter tower leading up to H_5. The renormalisable $H_5 T_3 T_3$ operator responsible for the top quark mass is the last diagram in Figure 3.1. Due to the cyclic nature of the $\mathbb{Z}$ symmetries, we are able to write down terms like $M\Sigma_2\overline{\Sigma}_7$, which as an overall $\mathbb{Z}_9$ charge of 9, equivalent to 0.

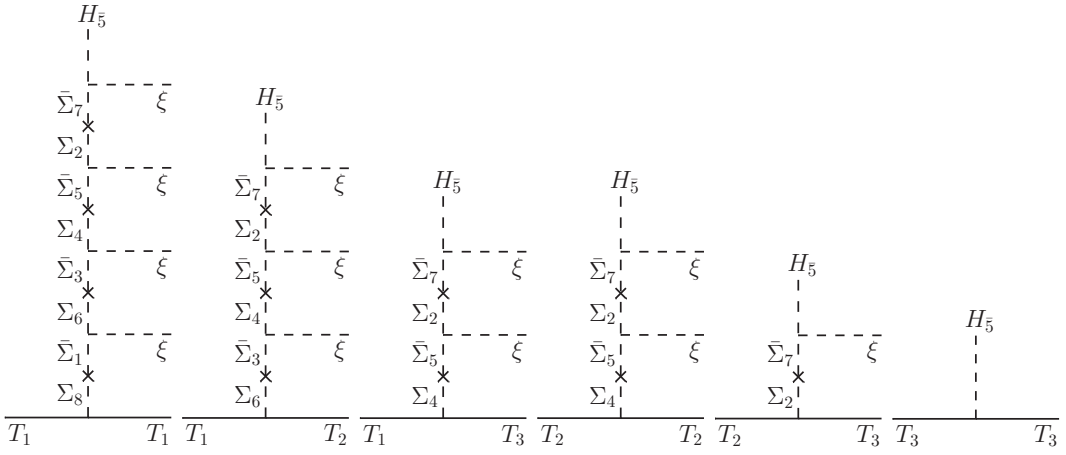

Figure 3.1: Diagrams responsible for the up-type quark Yukawa couplings.

The effective superpotential responsible for the up-type Yukawa couplings is

$$W_{\rm up} = u_{ij} H_5 T_i T_j \left(\frac{\xi}{M}\right)^{n_{ij}}. \tag{3.1}$$

The resulting symmetric Yukawa matrix for up-type quarks is

$$Y^u_{ij} = u_{ij}\left(\frac{\langle\xi\rangle}{M}\right)^{n_{ij}} \sim \begin{pmatrix} \tilde{\xi}^4 & \tilde{\xi}^3 & \tilde{\xi}^2 \\ & \tilde{\xi}^2 & \tilde{\xi} \\ & & 1 \end{pmatrix}, \tag{3.2}$$

where $\tilde{\xi} = \langle\xi\rangle/M \sim 0.1$. The explicit form of Y^u is given in Eq. 3.14 and includes the coefficients u_{ij}, which are $\mathcal{O}(1)$ and, by enforcing CP conservation at the GUT scale, necessarily real. Thus, the hierarchy of the up quark masses as well as the CKM mixing angles are given by powers of $\tilde{\xi}$. Due to the structure of this matrix, any phase introduced by $\langle\xi\rangle$ can be reabsorbed by appropriate redefinition of the three T_i fields, so Y^u does not contain a source of CP violation.

3.2.3 Down-type quarks and charged leptons

When considering the Yukawa structures of down quarks and charged leptons we must inevitably discuss A_4 triplet flavons. As a point of terminology, we refer to as "flavons" any superfields that are GUT singlets transforming non-trivially under the family symmetry and that get VEVs. In particular not only A_4 but also $\mathbb{Z}_9$ and $\mathbb{Z}_6$ are family symmetries, so we also refer to ξ as a flavon. The assignments of all the flavons under the family symmetries appear in Table 3.1a. Indeed, since the three families of F transform as a triplet of A_4, all terms like $T_i H_{\bar{5}} F$ require a contraction with at least one A_4 triplet flavon to be invariant.

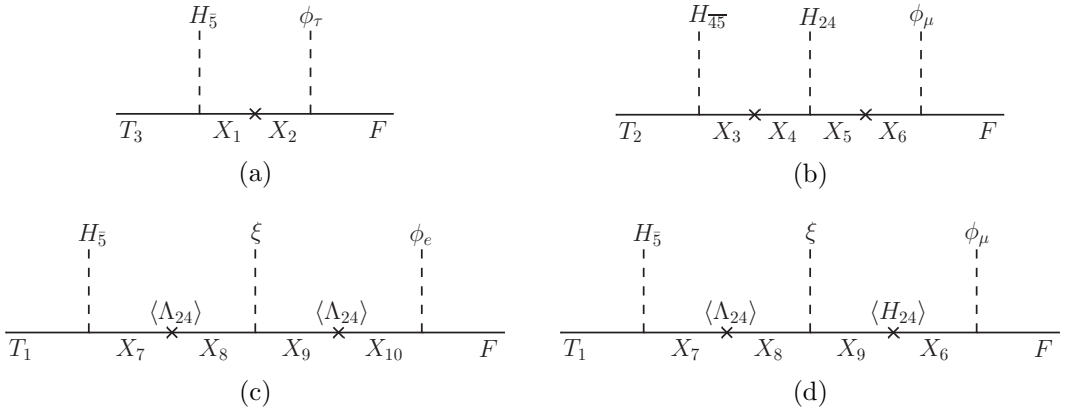

Figure 3.2: Diagrams responsible for the down-type quark and charged lepton Yukawa terms.

The relevant diagrams are shown in Figure 3.2. After integrating out the messengers X, which acquire large masses as a result of either explicit mass terms or GUT-scale Higgs

VEVs, we obtain effective operators of the form

$$\begin{aligned} W_{\text{down}} = d_{33}\frac{H_{\bar{5}}}{M}T_3(\phi_\tau F) + d_{22}\frac{H_{\overline{45}}H_{24}}{M^2}T_2(\phi_\mu F) + d_{11}\frac{H_{\bar{5}}\xi}{\langle\Lambda_{24}\rangle^2}T_1(\phi_e F) \\ + d_{12}\frac{H_{\bar{5}}\xi}{\langle\Lambda_{24}\rangle\langle H_{24}\rangle}T_1(\phi_\mu F), \end{aligned} \tag{3.3}$$

where d_{ij} are $\mathcal{O}(1)$ couplings. The light MSSM doublet H_d is a combination of the doublets inside $H_{\bar{5}}$ and $H_{\overline{45}}$, as discussed in Section C.1.2, hence the d_{22} term also leads to a relevant Yukawa coupling. The alignments of the respective VEVs of $\phi_{e,\mu,\tau}$ (discussed in Section 3.4) are

$$\langle\phi_e\rangle = v_e\begin{pmatrix}1\\0\\0\end{pmatrix}, \quad \langle\phi_\mu\rangle = v_\mu\begin{pmatrix}0\\1\\0\end{pmatrix}, \quad \langle\phi_\tau\rangle = v_\tau\begin{pmatrix}0\\0\\1\end{pmatrix}, \tag{3.4}$$

such that, apart from the term multiplying d_{12}, the contraction appearing with $T_{1,2,3}$ isolates the respective $F_{1,2,3}$ family. This would lead to diagonal Yukawa structures if not for the additional term connecting $T_1(\phi_\mu F)$ (see Figure 3.2d).

The resulting effective Yukawa matrices are, schematically,

$$Y^d_{LR} \sim Y^e_{RL} \sim \begin{pmatrix} \frac{\langle\xi\rangle v_e}{v^2_{\Lambda_{24}}} & \frac{\langle\xi\rangle v_\mu}{v_{\Lambda_{24}}v_{H_{24}}} & 0 \\ 0 & \frac{v_{H_{24}}v_\mu}{M^2} & 0 \\ 0 & 0 & \frac{v_\tau}{M} \end{pmatrix}, \tag{3.5}$$

where $v_{\Lambda_{24}}$ and $v_{H_{24}}$ are the respective VEVs of Λ_{24} and H_{24} (defined in Eq. 3.6 below). The off-diagonal term in Y^e also provides a tiny contribution to left-handed charged lepton mixing, $\theta^e_{12} \sim m_e/m_\mu$, which may safely be neglected. It also introduces CP violation to the CKM matrix via the phase of $\langle\xi\rangle$.

Furthermore, because the underlying renormalisable theory is known, the diagrams in Figure 3.2 are the only contributions for each family. The $SU(5)$ contractions and associated CG coefficients appearing for each family are unique [127–129]. With GUT-scale symmetry breaking as discussed in Appendix C, each of the scalars here get a VEV with the group structure

$$\begin{aligned} \langle H_{\bar{5}}\rangle^a &= \delta^a_5\ v_d/\sqrt{2}, \\ \langle H_{\overline{45}}\rangle^{ab}_c &= (\delta^{[a}_c - \delta^{[a}_5\delta^5_c - 4\delta^{[a}_4\delta^4_c)\delta^{b]}_5\ v_d/\sqrt{2}, \\ \langle H_{24}\rangle^a_b &= \text{diag}(2,2,2,-3,-3)\ v_{H_{24}}, \\ \langle\Lambda_{24}\rangle^a_b &= \text{diag}(2,2,2,-3,-3)\ v_{\Lambda_{24}}, \end{aligned} \tag{3.6}$$

where the indices run over $a, b, c = 1, \ldots, 5$. This leads to the GUT-scale predictions

$$\frac{Y^e_{33}}{Y^d_{33}} = 1, \qquad \frac{Y^e_{22}}{Y^d_{22}} = \frac{9}{2}, \qquad \frac{Y^e_{11}}{Y^d_{11}} = \frac{Y^e_{21}}{Y^d_{12}} = \frac{4}{9}. \tag{3.7}$$

The explicit forms of Y^d and Y^e, including CG and d_{ij} coefficients, are given later in Eqs. 3.15 and 3.16, respectively.

3.2.4 Neutrinos

In order to obtain the CSD(3) vacuum alignment in this model we couple the neutrinos to a set of flavons, distinguished by the $\mathbb{Z}_6$ symmetry. Of the superfields in Table 3.1a, only the right-handed neutrinos and some of the flavons are charged under this symmetry. For clarity, we relabel two of the flavon fields as $\phi_{\text{atm}} \equiv \phi_3$ and $\phi_{\text{sol}} \equiv \phi_4$, to highlight their role in producing neutrino mixing. We also write $N^c_{\text{atm}} \equiv N^c_1$ to denote the right-handed neutrino that dominantly leads to the atmospheric neutrino mass, and $N^c_{\text{sol}} \equiv N^c_2$ as that which contributes mainly to the solar neutrino mass. The relevant terms in the superpotential giving neutrino masses are thus

$$W_\nu = y_1 H_5 F \frac{\phi_{\text{atm}}}{\langle\theta_2\rangle} N^c_{\text{atm}} + y_2 H_5 F \frac{\phi_{\text{sol}}}{\langle\theta_2\rangle} N^c_{\text{sol}} + y_3 \frac{\xi^2}{M_\Gamma} N^c_{\text{atm}} N^c_{\text{atm}} + y_4 \xi N^c_{\text{sol}} N^c_{\text{sol}}, \tag{3.8}$$

where M_Γ refers to the mass scale of the superfield Γ. The flavons ϕ_{atm} and ϕ_{sol} gain VEVs

$$\langle\phi_{\text{atm}}\rangle = v_{\text{atm}} \begin{pmatrix} 0 \\ 1 \\ 1 \end{pmatrix}, \qquad \langle\phi_{\text{sol}}\rangle = v_{\text{sol}} \begin{pmatrix} 1 \\ 3 \\ 1 \end{pmatrix}, \tag{3.9}$$

where v_{atm} and v_{sol} are generally complex. Denoting the phases of VEVs as $\rho_i = \arg v_i$, only the relative phase $\rho_{\text{atm}} - \rho_{\text{sol}}$ between the VEVs is physically relevant. The flavon ξ (already responsible for the up-type quark masses) is also acting as a Majoron [144] by generating hierarchical right-handed neutrino masses.

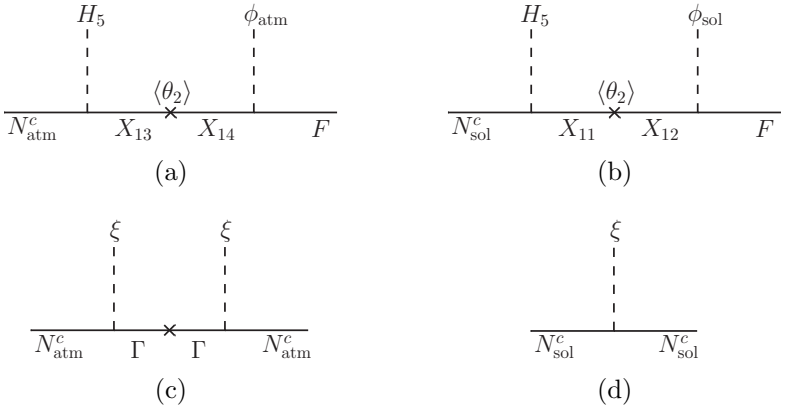

Figure 3.3: Diagrams responsible for the Dirac neutrino Yukawa terms.

At the effective level, the Dirac terms result from coupling the neutrinos (and H_5) to $\phi_{\rm atm}$ and $\phi_{\rm sol}$ via the flavon θ_2 (an A_4 singlet carrying $\mathbb{Z}_6$ charge). The corresponding diagrams with associated messengers appear in Figure 3.3. In turn, the Majorana mass term for $N^c_{\rm atm}$ is also non-renormalisable and we refer to Γ as the respective messenger. It couples only to $N^c_{\rm atm}$ and simply provides the non-renormalisable mass term for $N^c_{\rm atm}$, suppressed relative to the mass of $N^c_{\rm sol}$. As Γ has the quantum numbers of a third right-handed neutrino, one can also consider this field as mediating a double-seesaw mechanism. The mixing term $\xi^6 N^c_{\rm atm} N^c_{\rm sol}/M^5$, though allowed by the symmetries, is absent as there is no combination of messengers able to produce it. We write $\langle\xi\rangle = |v_\xi| e^{i\rho_\xi}$, where ρ_ξ is chosen from a discrete set of available phases, as shown in Appendix C. This phase originates from the spontaneous breaking of a discrete Abelian symmetry, in this case $\mathbb{Z}_9$.

We will now show that ρ_ξ and $\rho_{\rm atm} - \rho_{\rm sol}$ fix the relative phases within the effective neutrino mass matrix and consequently the leptonic mixing angles. Recall from the discussion in Chapter 2 (see Eqs. 2.16 – 2.18) that low-scale neutrino parameters are defined in the seesaw basis, which differs from the one in which the superpotential is defined (the SUSY basis) by complex conjugation. Within this model, let us assume that the charged lepton Yukawa matrix is essentially diagonal, i.e. corrections from the off-diagonal element Y^e_{21} are negligible. The superpotential in Eq. 3.8 leads, in the SUSY basis, to neutrino matrices

$$\lambda_\nu = \begin{pmatrix} 0 & b \\ a & 3b \\ a & b \end{pmatrix}, \qquad M^c = \begin{pmatrix} \dfrac{y_3 \langle\xi\rangle^2}{M_\Gamma} & 0 \\ 0 & y_4 \langle\xi\rangle \end{pmatrix}, \tag{3.10}$$

where $a = y_1 v_{\rm atm}/\langle\theta_2\rangle$ and $b = y_2 v_{\rm sol}/\langle\theta_2\rangle$. The corresponding matrices Y^ν and M_R in the seesaw basis are given by $Y^\nu = (\lambda_\nu)^*$ and $M_R = (M^c)^*$. The seesaw formula yields the light neutrino matrix

$$m^\nu = m_a \begin{pmatrix} 0 & 0 & 0 \\ 0 & 1 & 1 \\ 0 & 1 & 1 \end{pmatrix} + m_b e^{i\eta} \begin{pmatrix} 1 & 3 & 1 \\ 3 & 9 & 3 \\ 1 & 3 & 1 \end{pmatrix}, \tag{3.11}$$

where $m_a = v_u^2 |a|^2/(y_3 |v_\xi|^2/M)$ and $m_b = v_u^2 |b|^2/(y_4 |v_\xi|)$. We have multiplied throughout by an overall phase which we subsequently drop, keeping only the (physical) relative phase

$$\eta \equiv -\rho_\xi + 2(\rho_{\rm atm} - \rho_{\rm sol}), \tag{3.12}$$

where we recall the above definitions of phases,

$$\rho_\xi \equiv \arg\langle\xi\rangle, \qquad \rho_{\rm atm} - \rho_{\rm sol} \equiv \arg[v_{\rm atm} v^*_{\rm sol}], \tag{3.13}$$

and that CP conservation at high energies ensures that y_i and M are real.

By arguments given in Sections 3.4 (discussing vacuum alignment) and C.1 (discussing GUT breaking), we can restrict the physical phase η to one of the nine complex roots of unity. The values $\eta = \pm 2\pi/3$ are preferred by CSD(3). Note that the model predicts a normal neutrino mass hierarchy, namely $m_3 > m_2 \gg m_1 = 0$, which will be tested in the near future. The sign of η has phenomenological significance, as it fixes the leptonic Dirac phase δ^ℓ. Specifically, a positive η uniquely leads to negative δ^ℓ, and *vice versa*. As experimental data hints at $\delta^\ell \sim -\pi/2$, the *a posteriori* preferred solution has positive $\eta = +2\pi/3$. We saw in the last chapter that the sign of η also has cosmological significance: a positive η, together with the requirement that the baryon asymmetry of the Universe (BAU) is positive, implies that the lightest right-handed neutrino should be $N_1^c = N_{\rm atm}^c$, while $N_2^c = N_{\rm sol}^c$ is heavier, which is the natural ordering in our model.

3.3 Numerical fit to data

The structure of the Yukawa matrices and neutrino mass matrix is set by the theory, up to $\mathcal{O}(1)$ coefficients. The VEVs of the fields ξ, Λ_{24} and H_{24} are at or near the GUT scale, but otherwise undetermined. This freedom coincides with the choice of coefficients in the Yukawa matrices, providing no extra degrees of freedom in the determination of the Yukawas other than to provide the appropriate scale. The same is true for the flavon fields ϕ_e, ϕ_μ and ϕ_τ, which provide the necessary hierarchy in the down-type quark and charged lepton Yukawa sector.

The neutrino matrix m^ν is given in Eq. 3.11. Letting v_f represent the VEV of a field f, the Yukawa matrices are

$$Y^u = \begin{pmatrix} u_{11}|\tilde{\xi}^4| & u_{12}|\tilde{\xi}^3| & u_{13}|\tilde{\xi}^2| \\ u_{12}|\tilde{\xi}^3| & u_{22}|\tilde{\xi}^2| & u_{23}|\tilde{\xi}| \\ u_{13}|\tilde{\xi}^2| & u_{23}|\tilde{\xi}| & u_{33} \end{pmatrix}, \tag{3.14}$$

$$Y^d = \frac{1}{\sqrt{2}} \begin{pmatrix} \frac{1}{4} d_{11} \frac{|v_\xi v_e|}{|v_{\Lambda_{24}}|^2} & d_{12} \frac{|v_\xi v_\mu|}{|v_{\Lambda_{24}} v_{H_{24}}|} e^{i\zeta} & 0 \\ 0 & 2 d_{22} \frac{|v_{H_{24}} v_\mu|}{M^2} & 0 \\ 0 & 0 & d_{33} \frac{|v_\tau|}{M} \end{pmatrix}, \tag{3.15}$$

$$Y^e = \frac{1}{\sqrt{2}} \begin{pmatrix} \frac{1}{9} d_{11} \frac{|v_\xi v_e|}{|v_{\Lambda_{24}}|^2} & 0 & 0 \\ d_{12} \frac{|v_\xi v_\mu|}{|v_{\Lambda_{24}} v_{H_{24}}|} e^{i\zeta} & 9 d_{22} \frac{|v_{H_{24}} v_\mu|}{M^2} & 0 \\ 0 & 0 & d_{33} \frac{|v_\tau|}{M} \end{pmatrix}. \tag{3.16}$$

As already remarked, the phases in Y^u from powers of $\langle\xi\rangle = |v_\xi|e^{i\rho_\xi}$ can be removed by field redefinitions. Without loss of generality we have rephased fields such that the only phase appearing in Y^d and Y^e is the phase ζ as shown in Eqs. 3.15 and 3.16, so all quark CP violation originates from the single phase ζ appearing in Y^d_{12}. In turn, ζ is determined by a combination of phases coming from various field VEVs; more precisely

$$\zeta = \rho_\xi - 2\rho_{H_{24}} - \rho_{\Lambda_{24}}. \tag{3.17}$$

As long as it is reasonably far from zero, it can produce the necessary CP violation. Different choices of ζ do not affect the goodness-of-fit, corresponding simply to different but equally valid choices of $\mathcal{O}(1)$ coefficients. For our fit we choose $\zeta = \pi/3$. Note that the corresponding phase in Y^e_{21} does not contribute to leptonic CP violation, since this term does not affect left-handed mixing, to an accuracy of $\mathcal{O}(m_e/m_\mu)$.

To fit the real coefficients u_{ij}, d_{ij}, m_a and m_b, we minimise a χ^2 function, previously defined in Eq. 2.22, given by

$$\chi^2 = \sum_{i=1}^{N} \left(\frac{P_i(x) - \mu_i}{\sigma_i} \right)^2, \tag{3.18}$$

relating the physical predictions $P_i(x)$ for a given set of input parameters x to the best-fit value μ_i and associated error σ_i.

As in Chapter 2, the fit presented here uses best fit values and errors from the NuFit collaboration, version 2.0 [105], for PMNS parameters θ^ℓ_{ij} and neutrino mass-squared differences Δm^2_{ij}. These are given in Table 2.1. At the time of publication of [2], on which much of this chapter is based, these were the most up-to-date values. Recall also from Section 2.3.3 that the errors σ_i are equivalent to the standard deviation of a fit to a Gaussian distribution. For most parameters, this is a valid interpretation, with the exception of the (lepton) atmospheric angle θ^ℓ_{23}, which has a bimodal distribution. For a normal hierarchy, the distribution is roughly centered on $\theta^\ell_{23} = 45°$, with a local minimum in both the first and second octant. The best fit value is in the first octant, with $\theta^\ell_{23} = 42.3°$. As in Chapter 2, we approximate its distribution by a Gaussian about $42.3°$, setting $\sigma_{\theta^\ell_{23}} = 1.6°$.

In the fit of this $A_4 \times SU(5)$ model, $N = 18$, corresponding to six mixing angles θ^ℓ_{ij} (leptons) and θ^q_{ij} (quarks), the CKM phase δ^q, nine Yukawa eigenvalues for the quarks and charged leptons, and two neutrino mass-squared differences Δm^2_{21} and Δm^2_{31}. We use the PDG parametrisation of the PMNS and CKM matrices. In the NuFit 2.0 global fit the leptonic phase δ^ℓ is poorly constrained at 1σ (and completely unconstrained at 3σ), so is not fitted but left as a pure prediction of the model, as are the (completely unconstrained) Majorana phases α_{21} and α_{31}. As the model predicts only two massive left-handed neutrinos, i.e. $m_1 = 0$, one Majorana phase is zero, which we take to be $\alpha_{31} = 0$.

The running of best-fit and error values to the GUT scale are generally dependent on supersymmetry parameters, notably $\tan\beta$, as well as contributions from supersymmetric threshold corrections. We extract the GUT scale CKM parameters and all Yukawa couplings (with associated errors) from [145] for judicious choices of $\tan\beta$. In further reference to [145], we choose for the parameter $\bar{\eta}_b$ parametrising the threshold corrections a value $\bar{\eta}_b = -0.24375$; a non-zero value is required primarily to account for a (small) difference in b and τ Yukawa couplings. The data to which we compare the model (including the threshold correction) is given in Table 3.2. This parametrisation of the supersymmetric threshold corrections and running is discussed in Appendix B.

Parameter	Best fit $\pm 1\sigma$	
	$\tan\beta = 5$	$\tan\beta = 10$
$\theta_{12}^q\,/^\circ$	13.027 ± 0.0407	13.027 ± 0.0407
$\theta_{13}^q\,/^\circ$	0.1802 ± 0.0140	0.1802 ± 0.0140
$\theta_{23}^q\,/^\circ$	2.054 ± 0.192	2.054 ± 0.192
$\delta^q\,/^\circ$	69.21 ± 3.09	69.21 ± 3.09
$y_u\,/10^{-6}$	2.92 ± 0.906	2.88 ± 0.893
$y_c\,/10^{-3}$	1.43 ± 0.0501	1.41 ± 0.0493
$y_t\,/10^{-1}$	5.34 ± 0.171	5.20 ± 0.157
$y_d\,/10^{-6}$	4.81 ± 0.529	4.84 ± 0.533
$y_s\,/10^{-5}$	9.52 ± 0.514	9.59 ± 0.518
$y_b\,/10^{-3}$	6.95 ± 0.0896	7.01 ± 0.0914
$y_e\,/10^{-6}$	1.97 ± 0.0118	1.98 ± 0.0119
$y_\mu\,/10^{-4}$	4.16 ± 0.0249	4.19 ± 0.0251
$y_\tau\,/10^{-3}$	7.07 ± 0.0364	7.15 ± 0.0371

Table 3.2: Experimental CKM and charged fermion Yukawa parameters, run up to the GUT scale, assuming the MSSM [145]. The SUSY-breaking scale is set at 1 TeV. We have included an overall contribution from threshold corrections corresponding to $\bar{\eta}_b = -0.225$ which affects primarily the b quark Yukawa coupling y_b.

Minimisation by differential evolution was performed in Mathematica, yielding the set of physical parameters in Table 3.3 and corresponding $\mathcal{O}(1)$ input coefficients in Table 3.4, with an associated $\chi^2 = 7.98$ for $\tan\beta = 5$ and $\chi^2 = 7.84$ for $\tan\beta = 10$. The largest single contribution to χ^2 is from the fit to the atmospheric angle θ_{23}^ℓ. The non-zero Majorana phase is predicted to be $\alpha_{21} = 72^\circ$, and is insensitive to $\tan\beta$, as indeed are all the mixing angles and phases.

In this fit, the VEVs of ξ, Λ_{24}, H_{24} and the three $\phi_{e,\mu,\tau}$ are fixed by hand in terms of the scale M, which is taken to be the GUT scale, i.e. $M \approx 3 \times 10^{16}$ GeV. Similarly, the Higgs doublet VEV enters only implicitly through m_a and m_b, but is understood to

take the value $v_H = 174$ GeV. We set

$$\begin{aligned} v_\xi &= 6 \times 10^{-2} M, \qquad v_{\Lambda_{24}} = M, \qquad v_{H_{24}} = 3 \times 10^{-1} M, \\ v_e &= 10^{-3} M, \qquad v_\mu = 10^{-3} M, \qquad v_\tau = 5 \times 10^{-2} M. \end{aligned} \tag{3.19}$$

The value of v_ξ is chosen to accommodate not only the fit to Y^u parameters but also to control the μ-term. Meanwhile the approximate factor 3 split between $v_{\Lambda_{24}}$ and $v_{H_{24}}$ assists in establishing a hierarchy between the e and μ families. With the above numerical values for the VEVs, the Yukawa matrices can be expressed in terms only of $\mathcal{O}(1)$ coefficients and the complex phase ζ, as

$$\begin{aligned} Y^u &= \begin{pmatrix} 1.296 \times 10^{-5} \cdot u_{11} & 2.16 \times 10^{-4} \cdot u_{12} & 3.6 \times 10^{-3} \cdot u_{13} \\ 2.16 \times 10^{-4} \cdot u_{21} & 3.6 \times 10^{-3} \cdot u_{22} & 6 \times 10^{-2} \cdot u_{23} \\ 3.6 \times 10^{-3} \cdot u_{31} & 6 \times 10^{-2} \cdot u_{32} & u_{33} \end{pmatrix}, \\ Y^d &= \frac{1}{\sqrt{2}} \begin{pmatrix} 1.5 \times 10^{-5} \cdot d_{11} & 2 \times 10^{-4} \cdot d_{12} e^{i\zeta} & 0 \\ 0 & 6 \times 10^{-4} \cdot d_{22} & 0 \\ 0 & 0 & 5 \times 10^{-2} \cdot d_{33} \end{pmatrix}, \\ Y^e &= \frac{1}{\sqrt{2}} \begin{pmatrix} 6.67 \times 10^{-6} \cdot d_{11} & 0 & 0 \\ 2 \times 10^{-4} \cdot d_{12} e^{i\zeta} & 2.7 \times 10^{-3} \cdot d_{22} & 0 \\ 0 & 0 & 5 \times 10^{-2} \cdot d_{33} \end{pmatrix}. \end{aligned} \tag{3.20}$$

In order to understand the significance of the χ^2 fit, and assess the strength of the model overall, it is prudent to enumerate the parameters and predictions of the model. The nominal parameter count at the GUT scale is very large, owing to the diverse field content. However, at the scale where we are able to make predictions, many of these parameters combine to give a constrained set of free parameters that need to be determined. Notably, the VEVs of Higgs and flavon fields such as those given in Eq. 3.19 do not constitute true degrees of freedom, as they can be absorbed by redefining other parameters.

Relevant parameters that require consideration include: six u_{ij}, four d_{ij}, masses m_a and m_b, phases η and ζ, the threshold factor $\bar{\eta}_b$, and $\tan\beta$, for a total of 16 input parameters. However three of these parameters, namely $\tan\beta$, η and ζ, are fixed prior to the fit. Finally, the factor $\bar{\eta}_b$ affects only the coupling y_b and is fitted by hand. The model fits 18 observables, ten in the quark sector and eight in the lepton sector. In addition the model predicts the leptonic CP phase δ^ℓ, two Majorana phases (one of which is zero) and a massless physical neutrino.

Parameter	Value	
	$\tan\beta = 5$	$\tan\beta = 10$
θ_{12}^q /°	13.027	13.027
θ_{13}^q /°	0.180	0.180
θ_{23}^q /°	2.054	2.054
δ^q /°	69.18	69.18
y_u /10^{-6}	2.92	2.88
y_c /10^{-3}	1.43	1.41
y_t /10^{-1}	5.34	5.20
y_d /10^{-6}	4.30	4.33
y_s /10^{-5}	9.51	9.58
y_b /10^{-3}	7.05	7.13
θ_{12}^ℓ /°	34.3	34.3
θ_{13}^ℓ /°	8.67	8.67
θ_{23}^ℓ /°	45.8	45.8
δ^ℓ /°	−86.7	−86.7
Δm_{21}^2 /10^{-5} eV^2	7.38	7.38
Δm_{31}^2 /10^{-3} eV^2	2.48	2.48
y_e /10^{-6}	1.97	1.98
y_μ /10^{-4}	4.16	4.19
y_τ /10^{-3}	7.05	7.13

Table 3.3: Best fit physical quark and lepton parameters.

Parameter	Value	
	$\tan\beta = 5$	$\tan\beta = 10$
u_{11}	0.9566	0.9182
u_{12}	0.7346	0.7087
u_{13}	0.7198	0.6910
u_{22}	0.5961	0.5768
u_{23}	0.3224	0.3095
u_{33}	0.5435	0.5218
d_{11}	2.133	4.236
d_{12}	0.8363	1.661
d_{22}	1.108	2.200
d_{33}	1.021	2.034
m_a /meV	26.57	26.57
m_b /meV	2.684	2.684

Table 3.4: Best fit input quark Yukawa coefficients u_{ij} and d_{ij}, and neutrino mass parameters m_a and m_b, with fixed $\eta = 2\pi/3$, $\zeta = \pi/3$.

3.4 Flavon alignment

Thus far it has simply been assumed that the A_4 triplet VEVs are aligned in special directions, corresponding to CSD(3). These alignments are in fact also fixed by a renormalisable superpotential, which we present here, including all terms allowed by the symmetries. In doing so, the role of the $\mathbb{Z}_6$ symmetry becomes clearer. The method is that of F-term alignment, which necessitates the addition of several new fields. This set of superfields A_i and O_{ij} with $\mathbb{Z}_4^R$ charge 2, i.e. the driving sector, is listed in Table 3.5. The alignment superpotential is[1]

$$\begin{aligned} W_{\text{align}} \sim\ & A_\mu\phi_\mu\phi_\mu + A_\tau\phi_\tau\phi_\tau + A_2(\phi_2\phi_2 + \phi_2\theta_1) \\ & + O_{e\mu}\phi_e\phi_\mu + O_{e\tau}\phi_e\phi_\tau + O_{\mu\tau}\phi_\mu\phi_\tau \\ & + O_{e3}\phi_e\phi_3 + O_{23}\phi_2\phi_3 + O_{12}\phi_1\phi_2 + O_{13}\phi_1\phi_3 \\ & + O_{\mu5}\phi_\mu\phi_5 + O_{25}\phi_2\phi_5 + O_{\mu6}\phi_\mu\phi_6 + O_{56}\phi_5\phi_6 + O_{64}\phi_6\phi_4 + O_{14}\phi_1\phi_4. \end{aligned} \tag{3.21}$$

The inclusion of the $\mathbb{Z}_6$ symmetry is necessary to ensure each driving field is isolated from all others, such that their F terms depend only on flavons. This leads to an array of vanishing F-term conditions that force mutual orthogonality between many of the vacuum alignments. As F terms and the orthogonality conditions necessary to produce CSD(3) were discussed in Section 2.2 of the previous chapter, we shall not repeat them here, and state only the results, namely

$$\begin{aligned} &\langle\phi_e\rangle \propto \begin{pmatrix}1\\0\\0\end{pmatrix}, \qquad \langle\phi_\mu\rangle \propto \begin{pmatrix}0\\1\\0\end{pmatrix}, \qquad \langle\phi_\tau\rangle \propto \begin{pmatrix}0\\0\\1\end{pmatrix}, \\ &\langle\phi_1\rangle \propto \begin{pmatrix}2\\-1\\1\end{pmatrix}, \qquad \langle\phi_2\rangle \propto \begin{pmatrix}1\\1\\-1\end{pmatrix}, \qquad \langle\phi_3\rangle \propto \begin{pmatrix}0\\1\\1\end{pmatrix}, \\ &\langle\phi_4\rangle \propto \begin{pmatrix}1\\3\\1\end{pmatrix}, \qquad \langle\phi_5\rangle \propto \begin{pmatrix}1\\0\\1\end{pmatrix}, \qquad \langle\phi_6\rangle \propto \begin{pmatrix}1\\0\\-1\end{pmatrix}. \end{aligned} \tag{3.22}$$

The VEVs (containing two zero entries) of the flavons $\phi_{e,\mu,\tau}$ appear in the down-type quark and charged lepton Yukawa matrices Y^d, Y^e, while the flavons $\phi_{3,4}$ (redubbed $\phi_{\text{atm,sol}}$) appear in the neutrino Yukawa matrix Y^ν and subsequently the mass matrix after seesaw, m^ν. It is the special structure of these vacuum alignments, combined with the phase η in m^ν, that leads to the very successful prediction of the leptonic mixing angles (as described in Section 3.3). The remaining VEVs are not directly relevant to

[1] Note that the O (and P) fields that are neutral under $\mathbb{Z}_6$ couple to $H_5H_{\bar{5}}\xi^n$ (with some power of ξ), e.g. $P_{22}H_5H_{\bar{5}}$. We do not discuss these further as the respective F terms do not affect the alignment nor the origin of the μ-term.

the masses and mixings of Standard Model fermions, but help shape the VEVs of $\phi_{\rm atm}$ and $\phi_{\rm sol}$.

Field	Representation				
	A_4	$SU(5)$	$\mathbb{Z}_9$	$\mathbb{Z}_6$	$\mathbb{Z}_4^R$
A_μ	3	1	3	0	2
A_τ	3	1	4	0	2
A_2	3	1	7	0	2
$O_{e\mu}$	1	1	6	0	2
$O_{e\tau}$	1	1	2	0	2
$O_{\mu\tau}$	1	1	8	0	2
O_{e3}	1	1	6	5	2
O_{23}	1	1	5	2	2
O_{12}	1	1	5	1	2
O_{13}	1	1	3	3	2
$O_{\mu 5}$	1	1	0	4	2
O_{25}	1	1	2	1	2
$O_{\mu 6}$	1	1	1	4	2
O_{56}	1	1	7	2	2
O_{64}	1	1	2	3	2
O_{14}	1	1	4	3	2

(a) Alignment superfields.

Field	Representation				
	A_4	$SU(5)$	$\mathbb{Z}_9$	$\mathbb{Z}_6$	$\mathbb{Z}_4^R$
P_{ee}	1	1	0	0	2
$P_{\mu\mu}$	1	1	3	0	2
P_{22}	1	1	7	0	2
P_{e4}	1	1	7	5	2
P_{1e}	1	1	6	4	2
P_{44}	1	1	5	4	2
P_{34}	1	1	4	4	2
$P_{33}^{1,2}$	1	1	3	4	2
$P_{2\tau}$	1	1	1	3	2

(b) Phase-fixing superfields.

Table 3.5: Superfields driving family symmetry breaking.

With the direction of the A_4 triplet flavons ϕ fixed, we turn now to a discussion of how to fix the relative phase $\rho_{\rm atm} - \rho_{\rm sol} \equiv \arg[v_{\rm atm} v_{\rm sol}^*]$ to a discrete choice. We present a mechanism which does this by adding a number of fields P_{ij} that are A_4 and $SU(5)$ singlets, also given in Table 3.5, and which resemble the O_{ij} fields except they do not force orthogonality between the flavons ϕ.

These fields and their respective charge assignments result in the invariant superpotential terms

$$\begin{aligned} W_{\rm phase} = {} & P_{ee}(\phi_e\phi_e + M^2 + P_{ee}^2) + P_{\mu\mu}(\phi_\mu\phi_\mu + Z_2 Z_3 + P_{\mu\mu}^2) \\ & + P_{e4}(\phi_e\phi_4 + \theta_1\theta_2) + P_{22}(\phi_2\phi_2 + \theta_1\theta_1) \\ & + P_{1e}(\phi_1\phi_e + \phi_6\phi_\tau) + P_{44}(\phi_4\phi_4 + \phi_5\phi_\tau) + P_{34}(\phi_3\phi_4 + \phi_6\phi_e) \\ & + P_{33}^{1,2}(\phi_3\phi_3 + \phi_1\phi_\mu + \phi_5\phi_e) + P_{2\tau}(\phi_2\phi_\tau + \phi_3\phi_6 + \phi_4\phi_5), \end{aligned} \tag{3.23}$$

where each term technically has an associated real coupling λ which is $\mathcal{O}(1)$ and may be made positive by field redefinitions. We omit these for simplicity as they have no effect on the general argument presented here, with one caveat: the two superfields $P_{33}^{1,2}$ have exactly the same quantum numbers but different λ couplings to flavons. Due to this duplication there are two independent relations between the flavon VEVs involving

different λ couplings which leads to an additional constraint on the phases of the respective VEVs. Exact values of these λ are not specified; it suffices that they are not equal. Furthermore, the primary role of the SU(5) adjoint fields Z_2 and Z_3, which couple to $P_{\mu\mu}$, is in the GUT-breaking mechanism. Their phases are fixed separately by other superpotential terms (see Eq. C.1).

We begin the analysis of the terms in Eq. 3.23 by noting they do not affect the alignments of the flavons ϕ. The corresponding F terms for each field P_{ij} produces a set of coupled equations that admit a solution where none of the A, O, and P fields but all the flavons obtain a VEV. Omitting the λ coefficients, these VEVs have the structure

$$\begin{aligned}
&v_e \sim M, && v_\mu \sim (v_{Z_2} v_{Z_3})^{\frac{1}{2}},\\
&v_\tau \sim (v_{Z_2}\ v_{Z_3})^{-\frac{1}{3}} M^{\frac{5}{3}}, && v_1 \sim (v_{Z_2} v_{Z_3})^{-\frac{1}{2}}\ v_3^2,\\
&v_2 \sim (v_{Z_2} v_{Z_3})^{-\frac{1}{6}} M^{-\frac{7}{3}}\ v_3^3, && v_4 \sim (v_{Z_2} v_{Z_3})^{-\frac{1}{6}} M^{\frac{1}{3}}\ v_3,\\
&v_5 \sim M^{-1}\ v_3^2, && v_6 \sim (v_{Z_2} v_{Z_3})^{-\frac{1}{6}} M^{-\frac{2}{3}}\ v_3^2,\\
&v_{\theta_1} \sim (v_{Z_2} v_{Z_3})^{\frac{1}{6}} M^{-\frac{7}{3}}\ v_3^3, && v_{\theta_2} \sim (v_{Z_2} v_{Z_3})^{-\frac{1}{6}} M^{\frac{11}{3}}\ v_3^{-2},\\
&v_O = \ v_P = \ v_A = \ 0.
\end{aligned} \tag{3.24}$$

Regarding the magnitudes of the VEVs, two comments are in order. We assumed above that M sets the scale of the VEV of ϕ_e, which is in contradiction with our previous assumption that it be $\mathcal{O}(10^{-3})M$. This violates our simplifying assumption that all mass scales are equal, and demonstrates that some spectrum of mass scales is in fact required in this model. As for the VEV v_3, it is driven to a specific scale Λ_3 radiatively [146].[2] Writing $\rho_i \equiv \arg v_i$, this VEV structure gives (up to multiples of π) the phase relation

$$\rho_4 = \frac{2\pi n}{3} - \frac{1}{6}(\rho_{Z_2} + \rho_{Z_3}) + \rho_3, \tag{3.25}$$

where n is an integer, and similar relations for the other flavons as linear combinations of ρ_3, $(\rho_{Z_2} + \rho_{Z_3})$ and multiples of $2\pi/3$. This is an important equation since it fixes the relative phase $\rho_3 - \rho_4 = \rho_{\text{atm}} - \rho_{\text{sol}}$ in terms of $\frac{1}{6}(\rho_{Z_2} + \rho_{Z_3})$. We show in Appendix C that $\rho_{Z_2} + \rho_{Z_3} = \frac{2\pi k'}{3}$, where we also establish that $\rho_\xi = \frac{2\pi k}{9}$, for integers k, k'. From Eq. 3.12, $\eta \equiv -\rho_\xi + 2(\rho_{\text{atm}} - \rho_{\text{sol}})$, so we conclude that η is one of the nine complex roots of unity.

3.5 Aspects of GUT breaking

Let us now summarise features of the complete model related to the breaking of $SU(5)$ down to the Standard Model, including the resolution to the doublet-triplet splitting problem. We also find that new proton decay operators are naturally suppressed in this

[2] For examples of this mechanism in other models, see e.g. [147–151].

model due to the presence of flavour symmetries. The bulk of this discussion on GUT breaking is deferred to Section C.1 of Appendix C.

GUT breaking in this model arises from a superpotential involving adjoint Higgs superfields H_{24}, Λ_{24}, and the flavon ξ, and is driven by three $SU(5)$ adjoints $Z_{1,2,3}$. These were briefly encountered in the term $P_{\mu\mu} Z_2 Z_3$ which appears in the flavon driving superpotential in Eq. 3.23. The superpotential, given in Eq. C.1, contains two non-renormalisable terms which come from renormalisable diagrams involving new adjoint messengers Υ. All adjoints acquire GUT-scale VEVs which break $SU(5)$ to the Standard Model gauge group. The $\mathbb{Z}_4^R$ R symmetry is also broken at this scale, with a residual $\mathbb{Z}_2$ matter parity remaining.

Doublet-triplet splitting proceeds by the MP mechanism, which requires the addition of several new particles: at least one pair in the $\mathbf{50} + \overline{\mathbf{50}}$ representations of $SU(5)$, and (at least) one $\mathbf{75}$, which acquires a GUT-scale VEV. In this model, we label the $\mathbf{50}$ and $\overline{\mathbf{50}}$ by Ω_i, and the $\mathbf{75}$ by Π_i; they are listed in Table C.1b, giving rise to the superpotential in Eq. C.5. The mechanism works as follows: first, we forbid any terms where the Higgs superfields $H_{5,\bar{5}}$ and $H_{45,\overline{45}}$ (all containing MSSM-like doublets) couple to adjoint Higgs, which would give the doublets GUT-scale masses. They couple instead to the $\mathbf{50} + \overline{\mathbf{50}}$ superfields Ω_i, which do not contain $SU(2)$ doublets (that are not also colour non-singlets). The Higgs doublet mass matrix is therefore zero at this stage, while the triplet mass matrix, which mixes triplets within the 5-, 45- and 50-dimensonal Higgs superfields, is populated by elements depending on $\langle \Pi_i \rangle \sim M$, with all eigenvalues at the GUT scale. The MSSM μ term instead arises due to a single term $H_5 H_{\overline{45}} \Pi_1 \xi^8 / M^8$ allowed by the symmetries and messengers. As $\langle \xi \rangle \ll M$, this term is highly suppressed, giving $\mu \ll M$.

A classic problem in any GUT is that it allows for interactions that mediate proton decay, which must be kept under control. We find in this model that proton decay from new operators is strongly suppressed, due to the presence of multiple symmetries. Most dangerous are the "dimension-5" operators which lead to B-violating operators like $qqq\ell$ at the low scale (for a discussion of dimension-6 operators we refer the reader to [127]). In $SU(5)$, the relevant terms resemble $TTTF$, which are forbidden by the symmetries of the model. However, related higher-order operators are allowed of the form

$$T_i T_j T_k F \frac{Z\phi}{M^3} \left(\frac{\xi}{M} \right)^{n_{ijk}}, \tag{3.26}$$

where the extra superfields shown are needed for such terms to be invariant under the symmetries. Since we are working with a renormalisable theory, in order for such effective term to be present at the GUT scale with $M \sim M_{\mathrm{GUT}}$, there must be messengers allowing them. In this case, an analysis of the $SU(5)$ index structure revels there should either be messengers that in $SU(5)$ representations $\overline{\mathbf{10}}$ or $\mathbf{5}$ that are also charged under $\mathbb{Z}_4^R$.

As one can confirm from Table 3.1b, our model has neither: $\overline{\mathbf{10}}$ messengers were not used, and the $\mathbf{5}$ messengers are all neutral under $\mathbb{Z}_4^R$. We conclude therefore that our symmetry content, together with the existing set of messengers, do not allow any such GUT scale-suppressed operators that would lead to excessively fast proton decay to be generated. The operators in Eq. 3.26 may in principle be generated by physics at the Planck scale, with the scale M replaced by the Planck mass, leading to highly suppressed proton decay.

3.6 The strong CP problem

This model has the rather serendipitous benefit of containing a possible solution to the strong CP problem, of the Nelson-Barr type [152–155]. Before demonstrating how this solution appears in the model, let us review the problem itself. Although generally not written down, the Standard Model allows the term

$$\frac{g_s^2 \theta_0}{32\pi^2} G\widetilde{G}, \tag{3.27}$$

where G is the gluon field strength and $\tilde{G}$ its dual. The phase θ_0 can *a priori* take any value; it is reasonable to assume it is $\mathcal{O}(1)$. This term breaks CP, which is problematic as there is no evidence that CP is broken in the strong sector – all known CP violation is mediated by W bosons.

One may imagine that some form of CP symmetry may be enforced that prohibits the dangerous topological term. However, the effective angle θ_0 also receives corrections from the quark mass matrices, encoded in an angle $\theta_q = \arg\det[M^u M^d]$. Therefore we should consider the physical angle $\bar{\theta} = \theta_0 - \theta_q$. The most stringent experimental bounds on $\bar{\theta}$ come from measurements of the neutrino electron dipole moment [156], and set an upper bound

$$\bar{\theta} < 10^{-10}. \tag{3.28}$$

Some degree of CP violation must exist in the quark mass matrices due to a non-zero phase δ^q, suggesting that even if $\theta_0 = 0$ is enforced by the theory, strong CP violation might re-emerge in θ_q.

In short, ensuring such an extremely small value is non-trivial. It is possible that there is simply a cancellation of one in 10^{10} such that the physical angle $\bar{\theta}$ is sufficiently small, although this fine-tuning is aesthetically unappealing. It is also interesting to compare this to CP violation related to the weak interaction in the quark sector. The relevant quantity is the Jarlskog invariant $J^q \sim \det[Y^u Y^{u\dagger}, Y^d Y^{d\dagger}]$, which, when compared to data, is required to be non-vanishing, and indeed in the standard parameterisation, requires a large phase angle $\delta^q \sim 1$.

In the literature there are two popular mechanisms for solving the strong CP problem, based on very different physical principles.[3] Perhaps the most popular solution is the Peccei-Quinn mechanism [158, 159]. The key ingredients are a global $U(1)_{PQ}$ symmetry and one new scalar field φ charged under the symmetry. Moreover, some coloured particles (either known or newly imagined ones) are also charged under this $U(1)_{PQ}$, which is spontaneously broken by the VEV of φ, giving rise to a Goldstone mode known as the axion. This axion couples via a QCD anomaly to $G\tilde{G}$, giving rise to a term that of the same form as the topological term in Eq. 3.27. In the vacuum, the axion naturally relaxes the total topological term to zero, thereby solving the strong CP problem. The QCD axion is also an excellent dark matter candidate, offering an alternative to the WIMP paradigm.

An alternative, which does not rely on the introduction of new symmetries or field content *per se*, is known as the Nelson-Barr resolution. The idea relies on being able to set θ_0 and θ_q individually to zero. The former is rather trivially done by assuming a CP symmetry at the high scale that forbids the term proportional to θ_0. Next, one must ensure that after spontaneous violation of CP, one maintains $\bar{\theta} < 10^{-10}$ and in particular $\theta_q < 10^{-10}$, while at the same time allowing a large CKM phase δ^q. We proceed by example, showing how this is achieved in this $A_4 \times SU(5)$ model, demonstrating also the practical difficulties associated with this approach.

The solution lies in the particular forms of the quark Yukawa matrices. Recall from Eqs. 3.2 and 3.5 that the quark Yukawa matrices take the form

$$Y^u \sim \begin{pmatrix} \tilde{\xi}^4 & \tilde{\xi}^3 & \tilde{\xi}^2 \\ & \tilde{\xi}^2 & \tilde{\xi} \\ & & 1 \end{pmatrix}, \qquad Y^d \sim \begin{pmatrix} \frac{\langle\xi\rangle v_e}{v^2_{\Lambda_{24}}} & \frac{\langle\xi\rangle v_\mu}{v_{\Lambda_{24}} v_{H_{24}}} & 0 \\ 0 & \frac{v_{H_{24}} v_\mu}{M^2} & 0 \\ 0 & 0 & \frac{v_\tau}{M} \end{pmatrix}, \tag{3.29}$$

where $\tilde{\xi} = \langle\xi\rangle / M$, and v_i denote the VEVs of various superfields. First, note that Y^u can be made explicitly real by rephasing quark fields. If $\rho_\xi = \arg\langle\xi\rangle$, all phases may be eliminated by multipling the first row and column by $e^{-2i\rho_\xi}$, and the second row and column by $e^{-i\rho_\xi}$. Next, the diagonal elements of Y^d can also be made real by appropriate rephasings. A single phase remains in the (1,2) element of Y^d, which sources the CKM phase. On the other hand, the determinant of Y^d is real, simply given by the product of the diagonal entries, due to the fact that the (2,1) element is zero. In other words, $\arg\det[Y^u Y^d]$ is zero. But this is simply the definition of θ_q, nominally suggesting that the strong CP problem has been solved, as a result of particular matrix structures in the model. This is similar to the original proposal by Nelson and Barr, where the triangular

[3] In principle a third possibility exists: if the up quark is massless, there is one additional degree of freedom in the quark mass matrix which may be used to rotate away the strong CP angle, i.e. it becomes unphysical. However, a massless up quark is now ruled out by experiment [23] and lattice QCD [157].

form of Yukawa matrices was proposed, although in our model θ_q vanishes due to the triangular form of Y^d only, with Y^u being non-triangular and real.

On the other hand, the triangular matrix structure relies on a zero Yukawa coupling Y^d_{21}, which can conceivably be spoiled by higher-order corrections, violating the bound $\theta_q < 10^{-10}$. For a successful resolution of the strong CP problem, such corrections to the Yukawa matrices must be forbidden or sufficiently suppressed. Encouragingly, in our model such higher order corrections are absent at the field theory level with the specified messenger sector. Pollution in the Yukawa matrix would arise from the coupling of the bilinears $T_2 H_{\bar{5}}$ or $T_2 H_{\overline{45}}$ to the bilinear $\phi_e F$. Since these terms are non-renormalisable, we require messengers to form them. The messengers that could produce such terms are the X_i fields in Table 3.1b, but the only allowed connection to $\phi_e F$ with these messengers is $T_1 H_{\bar{5}}$ (contributing to Y^d_{11}). The required $Y^d_{21} = 0$ appears protected from higher-order corrections.

Before declaring victory, we must also consider the effect of corrections arising from interactions at the Planck scale, since such operators only have to respect the symmetries of the model, and do not require a specified messenger sector to generate them. The lowest-order contribution comes from the term[4]

$$T_2 H_{\bar{5}} \frac{\phi_e}{M_P} F. \tag{3.30}$$

With a general choice of phase, such a term would lead to $\theta_q \sim 10^{-4}$, which is far too big. This contribution to θ_q may be avoided by a judicious choice of GUT-breaking phases. As stated in Eq. 3.17, the physical phase in the down-type quark Yukawa matrix is $\zeta = \rho_\xi - 2\rho_{H_{24}} - \rho_{\Lambda_{24}}$. The new Planck-suppressed term has a phase $\zeta' = -\rho_\xi + 2\rho_{\Lambda_{24}}$. Choosing a relation between phases $2\rho_{H_{24}} = \rho_{\Lambda_{24}}$ gives $\zeta = -\zeta'$ and the contribution to θ_q vanishes. As shown in Section C.1 (see Eq. C.2), these phases are discretised, given as third roots of real $\mathcal{O}(1)$ parameters λ_i, which are coefficients of the renormalisable GUT-breaking superpotential. The relation $2\rho_{H_{24}} = \rho_{\Lambda_{24}}$ which makes the contribution to θ_q vanish, occurs in one in three cases.

The second-largest contribution comes from a term

$$T_2 H_{\bar{45}} \frac{\xi^2 \phi_e}{M_P^3} F, \tag{3.31}$$

giving $\theta_q \sim 10^{-14}$ which is several orders of magnitude below the current experimental bound. Any other Planck-suppressed terms allowed by the symmetries are at higher order, so we need not consider them. Finally, extra contributions may come from supersymmetry-breaking terms. If we assume that there is no extra CP violation in this sector, which is controlled by the (spontaneously) CP-violating flavons, such contributions to $\bar{\theta}$ are also expected to be negligible [160]. In summary, the model can

[4] This term would also give a contribution to lepton angles of $\mathcal{O}(10^{-3})$ which is negligible.

resolve the strong CP problem without introducing an axion, even in the presence of higher-order operators.

3.7 Leptogenesis

In Section 2.4 it was shown that the CSD(n) vacuum alignments can, for $3 \leq n \leq 5$, explain the observed baryon asymmetry of the Universe through N_1 leptogenesis. That calculation first appeared in [3], which also discusses leptogenesis in the $A_4 \times SU(5)$ model of this chapter. In fact, the implementation of CSD(3) in this model conforms closely to the simplest scenario, characterised by two right-handed neutrinos with a diagonal mass matrix M_R, a diagonal charged lepton Yukawa matrix Y^e, and the two columns of the neutrino Yukawa matrix Y^ν populated by the CSD(n) alignments proportional to $(0, 1, 1)$ and $(1, n, n-2)$. The main deviation in the current model from this setup is that Y^e is not quite diagonal: it contains also a non-zero $(1, 2)$ element. However, its effect on the leptogenesis calculation is negligible: the necessary basis transformation that makes Y^e diagonal induces negligible corrections (of $\mathcal{O}(1\%)$) to the CSD(3) alignment.

As such, we can immediately apply the results from Chapter 2 to this model. We recall that the leptogenesis calculation is performed in the SUSY basis, defined as in Eq. 2.26 by

$$W_\nu = y^i_{\rm atm} H L_i N^c_{\rm atm} + y^i_{\rm sol} H L_i N^c_{\rm sol} + M_{\rm atm} N^c_{\rm atm} N^c_{\rm atm} + M_{\rm sol} N^c_{\rm sol} N^c_{\rm sol}, \tag{3.32}$$

with diagonal charged leptons and right-handed neutrinos, and where the columns of the neutrino Yukawa matrix λ_ν are $y_{\rm atm} = (0, a, a)$ and $y_{\rm sol} = (b, nb, (n-2)b)$. We immediately identify the right-handed neutrino masses $M_1 = M_{\rm atm}$ and $M_2 = M_{\rm sol}$. This may be compared to the superpotential in Eq. 3.8 that defines the neutrino sector in the $A_4 \times SU(5)$ model,

$$W_\nu = y_1 H_5 F \frac{\phi_{\rm atm}}{\langle\theta_2\rangle} N^c_{\rm atm} + y_2 H_5 F \frac{\phi_{\rm sol}}{\langle\theta_2\rangle} N^c_{\rm sol} + y_3 \frac{\xi^2}{M_\Gamma} N^c_{\rm atm} N^c_{\rm atm} + y_4 \xi N^c_{\rm sol} N^c_{\rm sol}, \tag{3.33}$$

we identify the parameters a, b, M_1 and M_2 as

$$a = y_1 \frac{v_{\rm atm}}{\langle\theta_2\rangle}, \quad b = y_2 \frac{v_{\rm sol}}{\langle\theta_2\rangle}, \quad M_1 = y_3 \frac{(v_\xi)^2}{M_\Gamma}, \quad M_2 = y_4 v_\xi. \tag{3.34}$$

For convenience we can also specify the parameters of m^ν,

$$m_a = \frac{v_u^2 |a|^2}{M_1} = \left| \frac{y_1^2 v_u^2 v_{\rm atm}^2 M_\Gamma}{y_3 \langle\theta_2\rangle^2 v_\xi^2} \right|, \qquad m_b = \frac{v_u^2 |b|^2}{M_2} = \left| \frac{y_2^2 v_u^2 v_{\rm sol}^2}{y_4 \langle\theta_2\rangle^2 v_\xi} \right|. \tag{3.35}$$

As noted in Section 2.4, the Yukawa matrices λ_ν and Y^ν corresponding to the SUSY and seesaw bases, respectively, are related by conjugation, i.e. $Y^\nu = (\lambda_\nu)^*$.

Recall that the final asymmetry Y_B may be written as a sum over lepton flavour contributions, $Y_B = (10/31)\sum_\alpha Y_{\Delta_\alpha}$, where

$$Y_{\Delta_\alpha} = \eta_{1,\alpha}[Y_{N_1} + Y_{\tilde{N}_1}]\varepsilon_{1,\alpha}. \tag{3.36}$$

The CP asymmetry $\varepsilon_{1,\alpha}$ arises from the interference between diagrams describing right-handed neutrino decays, while the efficiency factors $\eta_{1,\alpha}$ contain information about washout. In CSD(n), we find (see Eq. 2.51)

$$Y_B = \frac{675}{31\pi^5 g_*}\frac{M_1 m_b}{v_u^2}\eta_{1,\mu}(n-1)^2 \sin\eta. \tag{3.37}$$

The dependence on the model parameters m_b, M_1 and M_2 is explicit, while the efficiency factors $\eta_{1,\alpha}$ depend on m_a.

The relevant best fit input parameters from our model are given in Table 3.4, with corresponding physical predictions in Table 3.3. In order to calculate $\eta_{1,\alpha}$ one generally needs to solve the associated Boltzmann equations. However, by the arguments presented in the Chapter 2, in the CSD(n) framework we may use known results from [108] to estimate $\eta_{1,\alpha}$. The parameters $\tilde{m}_{1,\alpha}$ were also discussed earlier (see Eq. 2.43), where it was shown that $\tilde{m}_{1,\mu} = \tilde{m}_{1,\tau} = m_a$. The model fit gives $m_a = 26.57$ meV, which implies $\log_{10}(A_{\mu\mu}K_\mu) = \log_{10}(A_{\tau\tau}K_\tau) = 1.027$. With this we obtain, from the solutions given in [108],

$$\eta_{1,\mu} = \eta_{1,\tau} \approx 0.0236. \tag{3.38}$$

The decay asymmetries given in Eq. 2.37 are calculated by

$$\begin{aligned}\varepsilon_{1,\mu} = 3\varepsilon_{1,\tau} &= \frac{9}{4\pi}\frac{M_1 m_b}{v^2 \sin^2\beta}\sin\eta \\ &\approx 6.01\times 10^{-7}\left[\frac{M_1}{10^{10}\text{ GeV}}\right].\end{aligned} \tag{3.39}$$

Using the above estimates, we may obtain from Eq. 2.51 the BAU for this model,

$$Y_B \approx 2.2\times 10^{-11}\left[\frac{M_1}{10^{10}\text{ GeV}}\right]. \tag{3.40}$$

Comparison with the experimental value of Y_B thus fixes the lightest right-handed neutrino mass to

$$M_1 \approx 3.9\times 10^{10}\text{ GeV}. \tag{3.41}$$

As shown in Eq. 3.34, in this model the right-handed neutrino mass is $M_1 = y_3(v_\xi)^2/M_\Gamma$, where M_Γ is the renormalizable mass of the messenger Γ that allows this term and can be $M_\Gamma \sim M_P$. This fixes the arbitrary dimensionless constant to be $y_3 \sim 0.3$, hence the BAU is achieved without extra tuning of parameters. Fixing the mass M_1 also fixes the parameter a in the Yukawa matrix to be $a \approx 0.006$, defined in Eq. 3.34.

3.8 Summary of features

We have presented a SUSY GUT based on $SU(5)$ with an $A_4 \times \mathbb{Z}_9 \times \mathbb{Z}_6$ family symmetry and a discrete $\mathbb{Z}_4^R$ R symmetry, which is broken to the MSSM with matter parity. It realises the CSD(3) vacuum alignments with (nearly) diagonal charged leptons, which successfully explains all observed neutrino masses and mixing with only three free parameters, while predicting a CP phase $\delta^\ell \approx \pm\pi/2$. It can also explain the observed baryon asymmetry of the Universe by thermal leptogenesis from the lightest right-handed neutrino. In the quark sector, mixing occurs from a discrete variant of the Froggatt-Nielsen mechanism, while CP violation arises from a single term in the down-type quark sector.

The model is renormalisable at the GUT scale, with both GUT and family symmetry breaking addressed (the former in an appendix), ensuring also doublet-triplet splitting via the missing partner mechanism, and a μ term as low as TeV scale. In addition, proton decay from higher-dimensional operators are shown to be strongly suppressed. The strong CP problem is resolved in the model without the inclusion of axions, due to the particular Yukawa matrix structures predicted by the model.

Chapter 4

A $\Delta(27) \times SO(10)$ model

Given the phenomenological success of the CSD(3) alignments and their incorporation into the $SU(5)$ SUSY GUT of the previous chapter, we wished to see if CSD(3) can also be realised in $SO(10)$, which features a more elegant and complete unification of quarks and leptons; $\Delta(27)$ was found to be a suitable candidate for the family symmetry. For a list of flavoured GUTs based on $SO(10)$ with discrete family symmetry, see [147, 148, 161–174]. Family and gauge unification leads in this model to distinct structures for the fermion mass matrices, and a successful fit of model parameters to the known masses and mixing parameters is found. The contents of this chapter are derived primarily from [4], where the model was first proposed, and [5], which discusses thermal leptogenesis.

4.1 Overview of the model

The model is based on $\Delta(27) \times SO(10)$, with a CP symmetry at the high scale. The choice of $\Delta(27)$ is primarily due to the fact that it has both triplet and antitriplet representations. It is not possible to construct any invariant with only two triplets (or two antitriplets), which is convenient as is immediately forbids many potentially dangerous terms involving the superfield Ψ, which is a spinorial **16** of $SO(10)$ and a triplet of $\Delta(27)$ and thereby unifies all known fermions into a single representation. In addition, the non-trivial singlets of $\Delta(27)$ are useful, as they are used to give rise to CP-violating phases that are related to the group rather than arbitrary parameters in the Lagrangian.[1] We therefore describe this as spontaneous geometrical CP violation [175–183], in this model in a novel form, as it fixes relative phases between distinct flavons. The model has many attractive features, including the use of only the lower-dimensional "named" representations of $SO(10)$, i.e. the singlet, fundamental, spinor or adjoint representations. $SO(10)$ is broken via $SU(5)$ with doublet-triplet splitting

[1] The latter scenario was encountered in the $A_4 \times SU(5)$ model of Chapter 3, where the single input phase η in the neutrino mass matrix was constrained to one of the ninth roots of unity.

achieved by a version of the Dimopoulos-Wilczek (DW) or missing VEV mechanism [184–186].

The model is renormalisable at the GUT scale, and also involves a discrete $\mathbb{Z}_9 \times \mathbb{Z}_{12} \times \mathbb{Z}_4^R$ symmetry. We identify all global symmetry groups other than $\mathbb{Z}_4^R$ as family (or flavour) symmetries, which are broken close to the GUT-breaking scale to yield the MSSM supplemented by a right-handed neutrino seesaw mechanism. $\mathbb{Z}_4^R$ is a discrete R symmetry and the origin of the MSSM matter parity which protects the LSP, a possible WIMP dark matter candidate.

The model is realistic in the sense that it provides a successful (and natural) description of the quark and lepton (including neutrino) mass and mixing spectra, including spontaneous CP violation. The low-scale Yukawa structure is dictated by the coupling of matter to $\Delta(27)$ antitriplets $\bar{\phi}$ whose VEVs are aligned in the CSD(3) directions by a superpotential. Light physical Majorana neutrinos masses emerge from a specific implementation of the seesaw mechanism within $SO(10)$. Furthermore, the model is fairly complete in the sense that both GUT and family symmetry breaking are addressed, including doublet-triplet splitting and the origin of the MSSM μ term.

The basic goal of the flavour sector in these models is to couple the Standard Model fermions to flavons $\bar{\phi}_{\rm atm}$, $\bar{\phi}_{\rm sol}$ and $\bar{\phi}_{\rm dec}$ which acquire CSD(3) VEVs

$$\bar{\phi}_{\rm atm} \propto \begin{pmatrix} 0 \\ 1 \\ 1 \end{pmatrix}, \quad \bar{\phi}_{\rm sol} \propto \begin{pmatrix} 1 \\ 3 \\ 1 \end{pmatrix}, \quad \bar{\phi}_{\rm dec} \propto \begin{pmatrix} 0 \\ 0 \\ 1 \end{pmatrix}. \tag{4.1}$$

We achieve this in a way that is compatible with an $SO(10)$ GUT, where all fermion states are united such that left- and right-handed fermions transform equally under the family symmetry. Since $SO(10)$ constrains the Dirac couplings of all leptons and quarks to be equal within a family, up to possible Clebsch-Gordan (CG) factors, it is actually rather non-trivial that the successful scheme in the lepton sector will translate to success in the quark sector. We find that we can attain good fits to data for quark and lepton masses, mixings and phases. In a sense this degree of unification is a significant improvement over the $SU(5)$ model in the previous chapter, wherein only the three generations of fermion $\bar{\mathbf{5}}$s were unified into a triplet of the A_4 family symmetry (while the $\mathbf{10}$s and neutrino $\mathbf{1}$s were family singlets).

4.2 Yukawa sector

4.2.1 Field content and superpotential

The most important field content is given in Table 4.1, while in Table 4.2 we list the messenger superfields with R charge 1, which are integrated out to give the superpotential in Eq. 4.3. The MSSM matter content is collected in Ψ. Higgs superfields are typically denoted by their $SO(10)$ representation, with two **10**s that couple respectively to the up-type and down-type MSSM matter at the low scale. Specifically, the two MSSM Higgs $SU(2)$ doublets H_u and H_d arise from H^u_{10} and H^d_{10}, where one only gets a VEV in the H_u direction and the other in the H_d direction. If we didn't have the two H_{10} we would get the erroneous relation

$$m^d_{ij} \tan\beta = m^u_{ij}, \tag{4.2}$$

which gives no CKM mixing. The $H_{\overline{16}}$ breaks $SO(10) \to SU(5)$ and gives masses to right-handed neutrinos.

Field	Representation				
	$\Delta(27)$	$SO(10)$	$\mathbb{Z}_9$	$\mathbb{Z}_{12}$	$\mathbb{Z}^R_4$
Ψ	3	16	0	0	1
H^u_{10}	1	10	6	0	0
H^d_{10}	1	10	5	0	0
H_{45}	1	45	0	0	0
H'_{45}	1	45	0	3	0
H_{DW}	1	45	6	0	2
$H_{\overline{16}}$	1	$\overline{16}$	6	0	0
H_{16}	1	16	2	0	2
$\bar{\phi}_{\text{dec}}$	$\bar{3}$	1	6	0	0
$\bar{\phi}_{\text{atm}}$	$\bar{3}$	1	1	0	0
$\bar{\phi}_{\text{sol}}$	$\bar{3}$	1	5	6	0
ξ	1	1	1	0	0

Table 4.1: Matter, Higgs and CSD(3) flavon superfields.

The flavons $\bar{\phi}_i$ are antitriplets under $\Delta(27)$, named in accordance with their respective roles in the CSD(3) scheme. The messengers are typically indexed by their $\mathbb{Z}_9$ charge, while each prime tick ($'$) corresponds to an additive $\mathbb{Z}_{12}$ charge of 3.

The H_{45} obtains a VEV that breaks $SU(5)$ to the Standard Model group, i.e. $SU(5) \to SU(3) \times SU(2) \times U(1)$. As we will see, it also provides the necessary CG coefficients to give the correct masses to Standard Model fermions. Since it has no $\mathbb{Z}$ charge and the messengers are in the **16** representation, these can have a renormalizable mass or a mass depending on $\langle H_{45} \rangle$.

Field	Representation				
	$\Delta(27)$	$SO(10)$	$\mathbb{Z}_9$	$\mathbb{Z}_{12}$	$\mathbb{Z}_4^R$
χ_i	1	16	$i \in \{1,5,6,7\}$	0	1
$\overline{\chi}_i$	1	$\overline{16}$	$i \in \{8,4,3,2\}$	0	1
χ_i''	1	16	$i \in \{5,6,7\}$	6	1
$\overline{\chi}_i''$	1	$\overline{16}$	$i \in \{4,3,2\}$	6	1
χ_6'	1	16	6	3	1
$\overline{\chi}_3'''$	1	$\overline{16}$	3	9	1
Ω_i	1	1	$i \in \{0,\ldots,8\}$	0	1
Ω_i''	1	1	$i \in \{3,4,5,6\}$	6	1

Table 4.2: Messengers with unit R charge.

The Yukawa superpotential that produces the quark and lepton mass matrices is

$$\begin{aligned}
W_Y = \Psi_i\Psi_j H_{10}^u \Bigg[& \bar{\phi}^i_{\rm dec}\bar{\phi}^j_{\rm dec} \sum_{n=0}^{2} \frac{\lambda^{(u)}_{{\rm dec},n}}{\langle H_{45}\rangle^n M_\chi^{2-n}} + \bar{\phi}^i_{\rm atm}\bar{\phi}^j_{\rm atm}\xi \sum_{n=0}^{3} \frac{\lambda^{(u)}_{{\rm atm},n}}{\langle H_{45}\rangle^n M_\chi^{3-n}} \\
& + \bar{\phi}^i_{\rm sol}\bar{\phi}^j_{\rm sol}\xi^2 \sum_{n=0}^{4} \frac{\lambda^{(u)}_{{\rm sol},n}}{\langle H_{45}\rangle^n M_\chi^{4-n}} + \bar{\phi}^i_{\rm sol}\bar{\phi}^j_{\rm dec}\xi\left(\frac{\lambda^{(u)}_{\rm sd,1}}{\langle H'_{45}\rangle^2 M_\chi} + \frac{\lambda^{(u)}_{\rm sd,2}}{\langle H'_{45}\rangle^2 \langle H_{45}\rangle}\right)\Bigg] \\
+ \Psi_i\Psi_j H_{10}^d \Bigg[& \bar{\phi}^i_{\rm dec}\bar{\phi}^j_{\rm dec}\xi \sum_{n=0}^{3} \frac{\lambda^{(d)}_{{\rm dec},n}}{\langle H_{45}\rangle^n M_\chi^{3-n}} + \bar{\phi}^i_{\rm atm}\bar{\phi}^j_{\rm atm}\xi^2 \sum_{n=0}^{4} \frac{\lambda^{(d)}_{{\rm atm},n}}{\langle H_{45}\rangle^n M_\chi^{4-n}} \\
& + \bar{\phi}^i_{\rm sol}\bar{\phi}^j_{\rm sol}\xi^3 \sum_{n=0}^{5} \frac{\lambda^{(d)}_{{\rm sol},n}}{\langle H_{45}\rangle^n M_\chi^{5-n}}\Bigg] \\
+ \Psi_i\Psi_j H_{\overline{16}} H_{\overline{16}} \Bigg[& \bar{\phi}^i_{\rm dec}\bar{\phi}^j_{\rm dec}\xi^3 \frac{\lambda^{(M)}_{\rm dec}}{M_\chi^2 M^4_{\Omega_{\rm dec}}} + \bar{\phi}^i_{\rm atm}\bar{\phi}^j_{\rm atm}\xi^4 \frac{\lambda^{(M)}_{\rm atm}}{M_\chi^3 M^4_{\Omega_{\rm atm}}} \\
& + \bar{\phi}^i_{\rm sol}\bar{\phi}^j_{\rm sol}\xi^5 \frac{\lambda^{(M)}_{\rm sol}}{M_\chi^4 M^4_{\Omega_{\rm sol}}}\Bigg],
\end{aligned} \tag{4.3}$$

where $\lambda^{(f)}_{i,n}$ are constants, presumed $\mathcal{O}(1)$. The singlet field ξ acquires a VEV slightly below the GUT scale, and is primarily responsible for the mass hierarchy between fermions through the Froggatt-Nielsen mechanism. In fact, the VEV of ξ arises in two different contexts: explicitly as in the superpotential above, as well as implicitly in the actual triplet flavon VEVs themselves, which are driven to slightly different scales by the superpotential. The details of this mechanism are discussed in Section C.2 of Appendix C. Each term in the above superpotential has an associated scale derived from the VEVs of the messengers that produce it. These are generally different, but for simplicity we refer to them all as M_χ when they are produced by pairs of $SO(10)$ spinor messengers χ and $\overline{\chi}$. We make a special note of cases where scale differences have important consequences

for the model, in particular writing $M_{\Omega_{\rm dec}}$, $M_{\Omega_{\rm atm}}$ and $M_{\Omega_{\rm sol}}$ as the combinations of messenger masses that appear in these respective terms.

While the superpotential in Eq. 4.3 is rather complex, due to the presence of multiple sums over λ parameters, mass scales, and the VEV of H_{45}, these sums result in a single numerical factor each at low scales. The apparent complexity of the exact superpotential obscures the quite simple and regular structure that ultimately dictates the fermion mass and Yukawa matrix structure. To see this structure more clearly, we suppress all numerical factors, which yields

$$\begin{aligned} W_Y = &\Psi_i \Psi_j H^u_{10} \left[\bar{\phi}^i_{\rm dec} \bar{\phi}^j_{\rm dec} + \bar{\phi}^i_{\rm atm} \bar{\phi}^j_{\rm atm} \xi + \bar{\phi}^i_{\rm sol} \bar{\phi}^j_{\rm sol} \xi^2 + \bar{\phi}^i_{\rm sol} \bar{\phi}^j_{\rm dec} \xi \right] \\ &+ \Psi_i \Psi_j H^d_{10} \xi \left[\bar{\phi}^i_{\rm dec} \bar{\phi}^j_{\rm dec} + \bar{\phi}^i_{\rm atm} \bar{\phi}^j_{\rm atm} \xi + \bar{\phi}^i_{\rm sol} \bar{\phi}^j_{\rm sol} \xi^2 \right] \\ &+ \Psi_i \Psi_j H_{\overline{16}} H_{\overline{16}} \xi^3 \left[\bar{\phi}^i_{\rm dec} \bar{\phi}^j_{\rm dec} + \bar{\phi}^i_{\rm atm} \bar{\phi}^j_{\rm atm} \xi + \bar{\phi}^i_{\rm sol} \bar{\phi}^j_{\rm sol} \xi^2 \right]. \end{aligned} \tag{4.4}$$

The first line will give up-type quark and neutrino Yukawa couplings, the second gives down-type quark and charged lepton Yukawa couplings, while the last line gives right-handed neutrinos Majorana masses. Each antitriplet flavon pair $\bar{\phi}^i \bar{\phi}^j$ corresponds to a numerical 3×3 matrix. With the exception of the pair $\bar{\phi}_{\rm sol} \bar{\phi}_{\rm dec}$, the resultant matrices are all rank 1. It is immediately clear that there is a large degree of uniformity in the Yukawa superpotential, which is reflected in the mass and Yukawa matrices presented shortly.

The renormalisable superpotential that gives Eq. 4.3 can be inferred from the diagrams that produce each term, which are given in Figures 4.1, 4.2 and 4.6. We now proceed to establish the fermion mass matrices, including the light neutrino mass matrix after seesaw.

4.2.2 Dirac mass matrices

The diagrams involving messengers that give the Yukawa terms in the up sector are shown in Figure 4.1, while the diagrams for the down sector are in Figure 4.2. Note that in these and all future diagrams, solid lines correspond to fields with odd R-charge, while dashed lines signify even R-charge.

There are several more diagrams that can be written wherein messenger pairs couple to the H_{45}. Specifically, since the H_{45} has no charge under any of the $\mathbb{Z}$ symmetries and is a real representation, it may replace a renormalizable mass diagram as in Figure 4.3. This is the reason for the sum of terms with different powers of $\langle H_{45} \rangle$ and M_χ appearing in the superpotential.

The H_{45} acquires a VEV with a magnitude $v_{45} \sim M_{\rm GUT}$, which breaks $SU(5)$ to the Standard Model group, and leads to CG relations which separate the fermion Yukawa

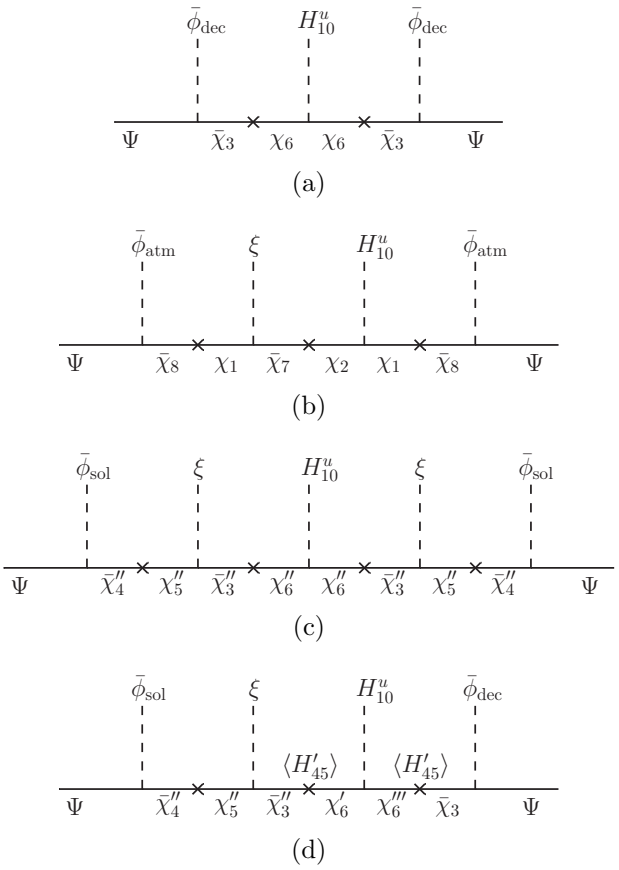

Figure 4.1: Diagrams coupling Ψ to H^u_{10}, giving the up-type quark and Dirac neutrino Yukawa terms.

couplings. As an example, consider the down-type quarks: at the low scale, the superpotential resembles

$$W_{\rm MSSM} \sim \bar{d}_L d_R H_d \left(\frac{y_1}{M_\chi^2} + \frac{y_2}{v_{45} M_\chi} + \frac{y_3}{v_{45}^2} \right). \tag{4.5}$$

We may use the parameters y_i to fit all the masses.[2] We assume H_{45} acquires a real VEV; the superpotential that fixes $\langle H_{45} \rangle$ is given in Section C.3 of Appendix C. The linear combinations of coefficients y_i thus yield a single effective real coefficient which is typically different for each generation, and different for each of the up, down, charged lepton, and neutrino sectors.

As noted above, a consequence of $SO(10)$ unification and the superpotential structure is that all fermion Dirac matrices have the same generic structure. More precisely, after the flavons acquire VEVs in the CSD(3) alignment, the Dirac mass matrices are given

[2] For the third family we have three y_i, with four for the second family, and five for the first family.

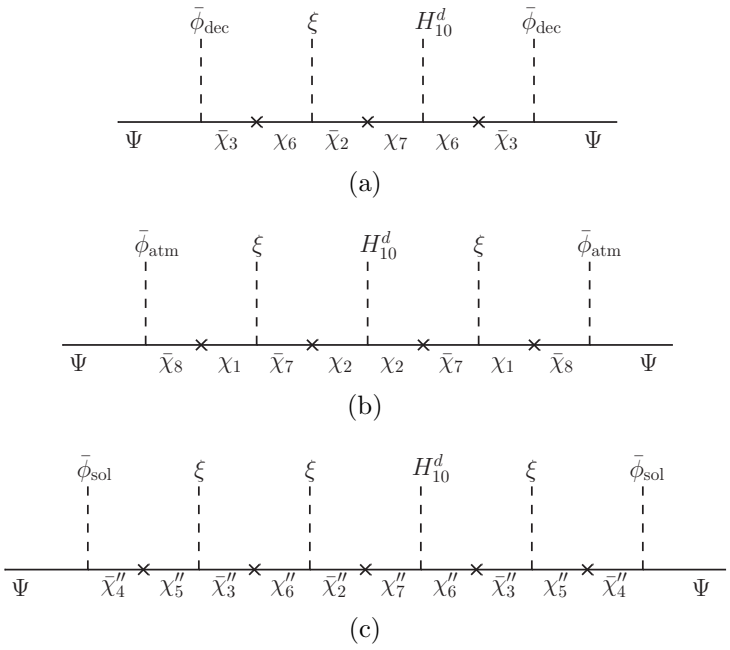

Figure 4.2: Diagrams coupling Ψ to H^d_{10}, giving the down-type quark and charged lepton Yukawa terms.

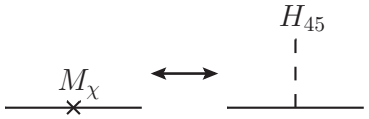

Figure 4.3: Diagram showing the replacement of a messenger mass term by a H_{45} VEV. The symmetries of the model allow for any mass insertion M_χ to be replaced by an $H_{45}\bar{\chi}\chi$ vertex, leading to extra superpotential terms.

by

$$\begin{aligned} m^f &= \mu^f_a \left\langle \bar{\phi}_{\rm atm} \right\rangle^i \left\langle \bar{\phi}_{\rm atm} \right\rangle^j + \mu^f_s \left\langle \bar{\phi}_{\rm sol} \right\rangle^i \left\langle \bar{\phi}_{\rm sol} \right\rangle^j + \mu^f_d \left\langle \bar{\phi}_{\rm dec} \right\rangle^i \left\langle \bar{\phi}_{\rm dec} \right\rangle^j \\ &= m^f_a e^{2i\rho_{\rm atm}} \begin{pmatrix} 0 & 0 & 0 \\ 0 & 1 & 1 \\ 0 & 1 & 1 \end{pmatrix} + m^f_s e^{2i\rho_{\rm sol}} \begin{pmatrix} 1 & 3 & 1 \\ 3 & 9 & 3 \\ 1 & 3 & 1 \end{pmatrix} + m^f_d e^{2i\rho_{\rm dec}} \begin{pmatrix} 0 & 0 & 0 \\ 0 & 0 & 0 \\ 0 & 0 & 1 \end{pmatrix}, \end{aligned} \tag{4.6}$$

where μ^f_i are coefficients derived from the $H^{u,d}_{10}$, H_{45} and ξ VEVs, and ρ_i are the phases of flavon VEVs. This structure however does not include an additional contribution to up quark mass matrix, which arises from a mixed term in W_Y (Eq. 4.3, line 2). Allowed by the symmetries and messengers, it is proportional to $\bar{\phi}_{\rm sol}\bar{\phi}_{\rm dec}$, and couples to H^u_{10} but not H^d_{10}. This term leads to the additional contribution to the up quark mass matrix

$$m^u_{sd}\, e^{i\rho_{sd}} \begin{pmatrix} 0 & 0 & 1 \\ 0 & 0 & 3 \\ 1 & 3 & 2 \end{pmatrix}. \tag{4.7}$$

This mixed term is not allowed for the H^d_{10} due to a lack of messengers able to produce it.

In Figure 4.4, we see how this mixed term would have had to be built with an H^d_{10}. Since there is no field χ'''_7 to build this diagram, it isn't allowed. There are no messengers that allow us to build other mixed terms (involving different pairs of flavons); even if there were, they would be highly suppressed. Without the term in Eq. 4.7, the fit to CKM parameters is quite poor, whereas with this term included, a good fit can be found.

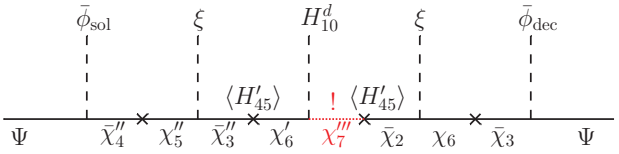

Figure 4.4: Hypothetical diagram that would produce a mixed term involving H^d_{10}, $\bar{\phi}_{\rm sol}$ and $\bar{\phi}_{\rm dec}$. As the required messenger χ'''_7 is absent, this term is forbidden.

The mixed term does not contribute to down-type quarks or charged leptons, since it only involves H^u_{10}. Furthermore, due to its structure it does not contribute to neutrino masses either. To see this we may decompose the contribution to neutrinos from the diagram in Figure 4.1d, at the $SU(5)$ level. We adopt the naming convention where the $SU(5)$ representation is labelled by its dimension, with its parent $SO(10)$ field given as a subscript. The left-handed neutrinos are in $\bar{\mathbf{5}}_\Psi$ and the right-handed neutrinos are the $\mathbf{1}_\Psi$. The hypothetical diagram would be in Figure 4.5. We see that the part of the diagram that is emphasized with a red circle involves one adjoint and two $SU(5)$ singlets. This is zero, therefore the whole diagram is zero.

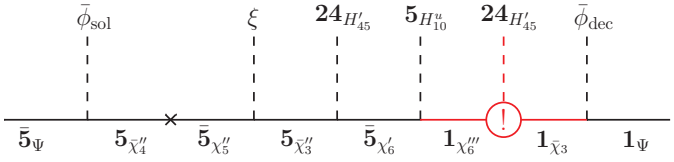

Figure 4.5: Null contribution from the $\bar{\phi}_{\rm sol}\bar{\phi}_{\rm dec}$ mixed term to neutrinos.

As $\langle H_{45}\rangle$ is assumed real, the only phases contributing to the mass matrices are therefore $\rho_{\rm atm}$, $\rho_{\rm sol}$ and $\rho_{\rm dec}$, the phases of $\langle\bar{\phi}_{\rm atm}\rangle$, $\langle\bar{\phi}_{\rm sol}\rangle$ and $\langle\bar{\phi}_{\rm dec}\rangle$ respectively, as well as ρ_ξ, the phase of $\langle\xi\rangle$. We define the dominant phase as the phase of the second (sol) matrix in the seesaw basis where the first (atm) matrix is real, i.e.

$$\eta \equiv -\arg\left[\frac{\langle\bar{\phi}_{\rm sol}\rangle^2}{\langle\bar{\phi}_{\rm atm}\rangle^2}\langle\xi\rangle\right] = -2(\rho_{\rm sol}-\rho_{\rm atm})-\rho_\xi. \tag{4.8}$$

Similarly the subdominant phase of the third (dec) matrix is

$$\eta' \equiv -\arg\left[\frac{\langle\bar{\phi}_{\rm dec}\rangle^2}{\langle\bar{\phi}_{\rm atm}\rangle^2}\frac{1}{\langle\xi\rangle}\right] = -2(\rho_{\rm dec}-\rho_{\rm atm})+\rho_\xi. \tag{4.9}$$

It will turn out that these definitions of the phases apply also for the effective neutrino mass matrix after seesaw.

4.2.3 Neutrinos

The right-handed neutrino Majorana terms (last two lines of Eq. 4.3) are produced by the diagrams in Figure 4.6. If we decompose these diagrams into $SU(5)$ components, the base line would be all singlets. Therefore there can be no contribution coming from the H_{45} nor the H'_{45} and there is no mixed term allowed. In other words, the diagrams shown are the only contributions to the right-handed neutrino mass matrix. Even though they appear suppressed by many orders of the messenger scales, these terms attain scales that are phenomenologically desirable. It is usual for the right-handed neutrino masses to be in the range $10^{10} - 10^{14}$ GeV. The VEV $H_{\overline{16}}$ breaks $SO(10) \to SU(5)$ and thus is at or slightly above the GUT scale, while the messenger scales, generically labelled M, are yet higher, such that messengers may be integrated out. Recalling that ξ gains a VEV roughly an order of magnitude below the GUT scale, we have $\xi < \langle H_{\overline{16}} \rangle \lesssim M$ and this way we may obtain the correct scale for right-handed neutrino masses.

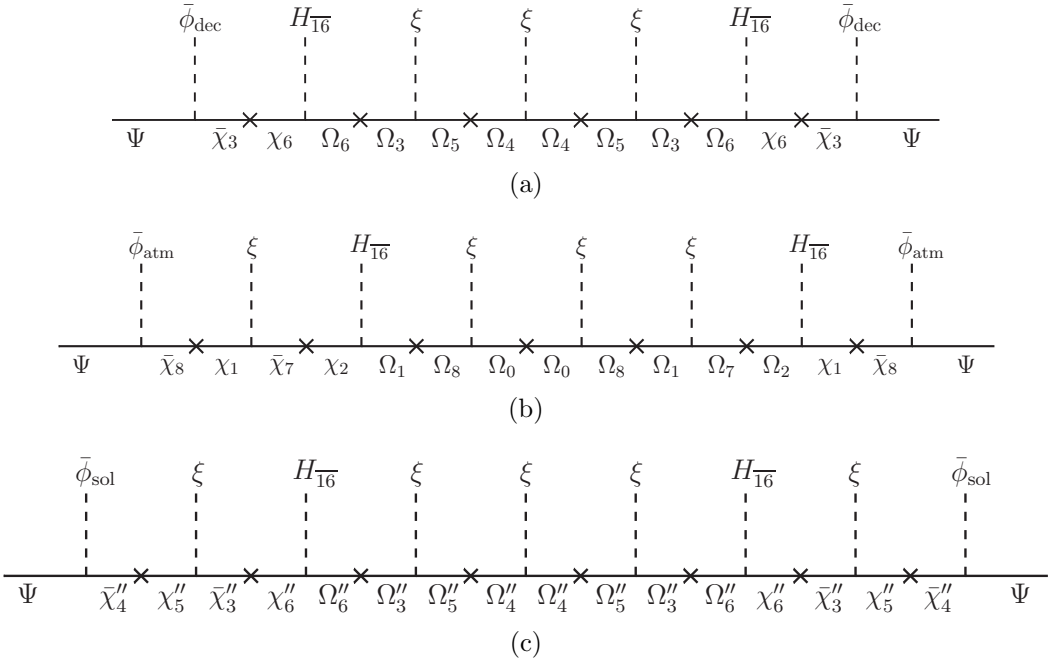

Figure 4.6: Diagrams responsible for the right-handed neutrino Majorana masses.

The right-handed Majorana mass matrix is constructed using the same flavon pairs as the Dirac matrices, and will have the same structure, as given in Eq. 4.6. It is also true, though not immediately obvious, that this mass matrix structure is realised also for the light Majorana neutrinos after seesaw. This will be proven shortly, but let us present here a heuristic description of this mechanism. To this end, it is helpful to consider the neutrino sector after breaking $SO(10) \to SU(5)$, where the left- and right-handed neutrinos ν and ν^c are contained respectively in a $\bar{\mathbf{5}}$ and $\mathbf{1}$ of $SU(5)$, in triplets of the family symmetry. We denote the $\bar{\mathbf{5}}$ by F and the singlet by N^c. The Dirac mass matrix

is then sourced by the terms

$$H_{10}^u \left[\frac{\lambda_{\rm atm}^{(\nu)} \xi}{M_\chi^3} (\bar{\phi}_{\rm atm} F)(\bar{\phi}_{\rm atm} N^c) + \frac{\lambda_{\rm sol}^{(\nu)} \xi^2}{M_\chi^4} (\bar{\phi}_{\rm sol} F)(\bar{\phi}_{\rm sol} N^c) + \frac{\lambda_{\rm dec}^{(\nu)}}{M_\chi^2} (\bar{\phi}_{\rm dec} F)(\bar{\phi}_{\rm dec} N^c) \right], \tag{4.10}$$

when the H_{10}^u, ξ and $\bar{\phi}$ fields acquire VEVs. Pairs of terms in parentheses, like (ϕF) and (ϕN^c), signify a contraction of a $\Delta(27)$ triplet-antitriplet pair, yielding a flavour singlet.

In a similar fashion, the right-handed Majorana matrix originates from the terms

$$\begin{aligned} \langle H_{\overline{16}} H_{\overline{16}} \rangle \Bigg[& \frac{\lambda_{\rm atm}^{(M)} \xi^4}{M_\chi^3 M_{\Omega_{\rm atm}}^4} (\bar{\phi}_{\rm atm} N^c)(\bar{\phi}_{\rm atm} N^c) + \frac{\lambda_{\rm sol}^{(M)} \xi^5}{M_\chi^4 M_{\Omega_{\rm sol}}^4} (\bar{\phi}_{\rm sol} N^c)(\bar{\phi}_{\rm sol} N^c) \\ & + \frac{\lambda_{\rm dec}^{(M)} \xi^3}{M_\chi^2 M_{\Omega_{\rm dec}}^4} (\bar{\phi}_{\rm dec} N^c)(\bar{\phi}_{\rm dec} N^c) \Bigg]. \end{aligned} \tag{4.11}$$

We have made a distinction between the average scales of the messengers that produce each of the above three terms, giving us three distinct mass scales for the Ω-type messengers, denoted $M_{\Omega_{\rm atm}}$, $M_{\Omega_{\rm sol}}$ and $M_{\Omega_{\rm dec}}$. We will see that the best fit to data suggests that the third effective neutrino mass is small, in accordance with the sequential dominance (SD) assumption. Implementing the seesaw mechanism, this translates to a requirement that the third right-handed neutrino is essentially decoupled. This implies its mass, which originates from the final term in Eq. 4.11, is very large. This can be achieved if $M_{\Omega_{\rm dec}} < M_{\Omega_{\rm atm}}, M_{\Omega_{\rm sol}}$.

Collecting the Higgs and ξ fields along with λ coefficients into generic parameters κ (with dimensions of inverse mass), we can write Eqs. 4.10 and 4.11 in the simplified form

$$\begin{aligned} & \kappa_{\rm atm}^{\nu} (\bar{\phi}_{\rm atm} F)(\bar{\phi}_{\rm atm} N^c) + \kappa_{\rm sol}^{\nu} (\bar{\phi}_{\rm sol} F)(\bar{\phi}_{\rm sol} N^c) + \kappa_{\rm dec}^{\nu} (\bar{\phi}_{\rm dec} F)(\bar{\phi}_{\rm dec} N^c) \\ & \quad + \kappa_{\rm atm}^{M} (\bar{\phi}_{\rm atm} N^c)(\bar{\phi}_{\rm atm} N^c) + \kappa_{\rm sol}^{M} (\bar{\phi}_{\rm sol} N^c)(\bar{\phi}_{\rm sol} N^c) + \kappa_{\rm dec}^{M} (\bar{\phi}_{\rm dec} N^c)(\bar{\phi}_{\rm dec} N^c), \end{aligned} \tag{4.12}$$

noting also that generically $\kappa^\nu \ll \kappa^M$. This can be written in block diagonal matrix form as

$$\begin{array}{c} \\ \bar{\phi}_{\rm atm} F \\ \bar{\phi}_{\rm atm} N^c \\ \bar{\phi}_{\rm sol} F \\ \bar{\phi}_{\rm sol} N^c \\ \bar{\phi}_{\rm dec} F \\ \bar{\phi}_{\rm dec} N^c \end{array} \begin{array}{c} \begin{array}{cccccc} \bar{\phi}_{\rm atm} F & \bar{\phi}_{\rm atm} N^c & \bar{\phi}_{\rm sol} F & \bar{\phi}_{\rm sol} N^c & \bar{\phi}_{\rm dec} F & \bar{\phi}_{\rm dec} N^c \end{array} \\ \begin{pmatrix} 0 & \kappa_{\rm atm}^{\nu} & & & & \\ \kappa_{\rm atm}^{\nu} & \kappa_{\rm atm}^{M} & & & & \\ & & 0 & \kappa_{\rm sol}^{\nu} & & \\ & & \kappa_{\rm sol}^{\nu} & \kappa_{\rm sol}^{M} & & \\ & & & & 0 & \kappa_{\rm dec}^{\nu} \\ & & & & \kappa_{\rm dec}^{\nu} & \kappa_{\rm dec}^{M} \end{pmatrix} \end{array}, \tag{4.13}$$

with all other elements zero. Diagonalisation gives, to $\mathcal{O}\big((\kappa^\nu/\kappa^M)^2\big)$, the effective Weinberg operators

$$-\frac{(\kappa^\nu_{\rm atm})^2}{\kappa^M_{\rm atm}}(\bar\phi_{\rm atm}F)(\bar\phi_{\rm atm}F)-\frac{(\kappa^\nu_{\rm sol})^2}{\kappa^M_{\rm sol}}(\bar\phi_{\rm sol}F)(\bar\phi_{\rm sol}F)-\frac{(\kappa^\nu_{\rm dec})^2}{\kappa^M_{\rm dec}}(\bar\phi_{\rm dec}F)(\bar\phi_{\rm dec}F). \quad (4.14)$$

These in turn reproduce a light neutrino Majorana mass matrix of the form given in Eq. 4.6.

Finally, we must take into account an overall complex conjugation of the Yukawa and right-handed Majorana matrices when shifting from the SUSY basis (in which the Yukawa superpotential is defined) to the seesaw basis. This basis change was discussed in Chapter 2 (see Eqs. 2.16 – 2.18) and we only repeat the conclusions, namely that

$$Y^\nu=(\lambda_\nu)^*, \qquad M_R=(M^c)^*, \quad (4.15)$$

where Y^ν, M_R are in the seesaw basis and λ_ν, M^c are in the SUSY basis. We proceed in the seesaw basis, wherein

$$\begin{aligned}
Y^\nu &= \kappa^{\nu*}_{\rm atm}v^{*2}_{\rm atm}\begin{pmatrix}0&0&0\\0&1&1\\0&1&1\end{pmatrix}+\kappa^{\nu*}_{\rm sol}v^{*2}_{\rm sol}\begin{pmatrix}1&3&1\\3&9&3\\1&3&1\end{pmatrix}+\kappa^{\nu*}_{\rm dec}v^{*2}_{\rm dec}\begin{pmatrix}0&0&0\\0&0&0\\0&0&1\end{pmatrix},\\
M_R &= \kappa^{M*}_{\rm atm}v^{*2}_{\rm atm}\begin{pmatrix}0&0&0\\0&1&1\\0&1&1\end{pmatrix}+\kappa^{M*}_{\rm sol}v^{*2}_{\rm sol}\begin{pmatrix}1&3&1\\3&9&3\\1&3&1\end{pmatrix}+\kappa^{M*}_{\rm dec}v^{*2}_{\rm dec}\begin{pmatrix}0&0&0\\0&0&0\\0&0&1\end{pmatrix},
\end{aligned} \quad (4.16)$$

using the effective parameters introduced in Eq. 4.12. To verify that the relative phases are again η and η' (as defined in Eqs. 4.8 and 4.9), we may insert VEVs of all fields (denoted v_f for given field f) to give an effective neutrino matrix

$$m^\nu=\mu_a e^{i\alpha}\begin{pmatrix}0&0&0\\0&1&1\\0&1&1\end{pmatrix}+\mu_b e^{i\beta}\begin{pmatrix}1&3&1\\3&9&3\\1&3&1\end{pmatrix}+\mu_c e^{i\gamma}\begin{pmatrix}0&0&0\\0&0&0\\0&0&1\end{pmatrix}, \quad (4.17)$$

where

$$\begin{aligned}
\mu_a &\equiv \left|\frac{(v_{H^u_{10}})^2}{(v_{H_{\overline{16}}})^2}\frac{(\lambda^{(\nu)}_{\rm atm})^2M^4_{\Omega_{\rm atm}}}{\lambda^{(M)}_{\rm atm}M^3_\chi}\frac{(v^2_{\rm atm}v_\xi)^2}{v^2_{\rm atm}v^4_\xi}\right|, & \alpha &\equiv -\arg\left[\frac{(v_{H^u_{10}})^2}{(v_{H_{\overline{16}}})^2}\frac{v^2_{\rm atm}}{v^2_\xi}\right],\\
\mu_b &\equiv \left|\frac{(v_{H^u_{10}})^2}{(v_{H_{\overline{16}}})^2}\frac{(\lambda^{(\nu)}_{\rm sol})^2M^4_{\Omega_{\rm sol}}}{\lambda^{(M)}_{\rm sol}M^4_\chi}\frac{(v^2_{\rm sol}v^2_\xi)^2}{v^2_{\rm sol}v^5_\xi}\right|, & \beta &\equiv -\arg\left[\frac{(v_{H^u_{10}})^2}{(v_{H_{\overline{16}}})^2}\frac{v^2_{\rm sol}}{v_\xi}\right],\\
\mu_c &\equiv \left|\frac{(v_{H^u_{10}})^2}{(v_{H_{\overline{16}}})^2}\frac{(\lambda^{(\nu)}_{\rm dec})^2M^4_{\Omega_{\rm dec}}}{\lambda^{(M)}_{\rm dec}M^2_\chi}\frac{v^4_{\rm dec}}{v^2_{\rm dec}v^3_\xi}\right|, & \gamma &\equiv -\arg\left[\frac{(v_{H^u_{10}})^2}{(v_{H_{\overline{16}}})^2}\frac{v^2_{\rm dec}}{v^3_\xi}\right],
\end{aligned} \quad (4.18)$$

and where messenger masses and λ couplings are all real due to CP conservation. As

before, the physical phases η and η' are defined as the relative phases between the three rank-1 matrices that make up m^ν, i.e.

$$\begin{aligned}\eta \equiv \beta - \alpha &= -\arg\left[\frac{v_{\rm sol}^2}{v_\xi}\right] + \arg\left[\frac{v_{\rm atm}^2}{v_\xi^2}\right] = -2(\rho_{\rm sol} - \rho_{\rm atm}) - \rho_\xi, \\ \eta' \equiv \gamma - \alpha &= -\arg\left[\frac{v_{\rm dec}^2}{v_\xi^3}\right] + \arg\left[\frac{v_{\rm atm}^2}{v_\xi^2}\right] = -2(\rho_{\rm dec} - \rho_{\rm atm}) + \rho_\xi,\end{aligned} \tag{4.19}$$

which is identical to Eqs. 4.8 and 4.9.

4.2.4 The seesaw mechanism with universal rank-1 structures

The heuristic argument above for how the seesaw mechanism is implemented was first presented for the case of tri-bimaximal mixing in [147, 187]. However one may worry that the combinations of right-handed neutrinos that are integrated out, namely $(\bar{\phi}_{\rm atm}N^c)$, $(\bar{\phi}_{\rm sol}N^c)$, $(\bar{\phi}_{\rm dec}N^c)$ are not mass eigenstates. One may also worry that the mechanism only works for tri-bimaximal mixing where the flavon alignments are mutually orthogonal. We now present a more rigorous discussion of how the seesaw mechanism is implemented in this model, showing that the above result is in fact robust. The core proof, that the effective neutrino mass matrix has the structure given in Eq. 4.6, does not depend on symmetry or the special CSD(3) alignments, requiring only that the Dirac and heavy Majorana matrices be expressable as linear combinations of the same three rank-1 matrices.

A symmetric $n \times n$ matrix M of rank n can be written as a sum over n rank-1 matrices M_i,

$$M = \sum_{i=1}^{n} M_i = \sum_{i=1}^{n} \alpha_i \phi_i \phi_i^\intercal, \tag{4.20}$$

where ϕ_i are column vectors of length n and α_i are constants. In our flavour model, ϕ_i can be identified with the flavon VEV alignments, up to a constant of proportionality. The neutrino Yukawa and right-handed Majorana matrices may be written

$$\begin{aligned}Y^\nu &= y_1 M_1 + y_2 M_2 + y_3 M_3, \\ M_R &= r_1 M_1 + r_2 M_2 + r_3 M_3,\end{aligned} \tag{4.21}$$

where $M_i \propto \phi\phi^\intercal$ and y_i, r_i are constants. Recalling the seesaw formula

$$m^\nu = -v_u^2 Y^\nu M_R^{-1} (Y^\nu)^\intercal, \tag{4.22}$$

determining m^ν requires finding the inverse of M_R. Applying once again the parametrisation in Eq. 4.20, we may express M_R^{-1} in terms of some other rank-1 matrices $\widetilde{M}_1$, $\widetilde{M}_2$ and $\widetilde{M}_3$. These are chosen such that the coefficients multiplying each rank-1 matrix

is $1/r_i$, i.e.

$$M_R^{-1} = \frac{1}{r_1}\widetilde{M}_1 + \frac{1}{r_2}\widetilde{M}_2 + \frac{1}{r_3}\widetilde{M}_3. \tag{4.23}$$

This defines the matrices $\widetilde{M}_i$. Their connection to the matrices M_i can be understood by taking the definition of the inverse,

$$\begin{aligned} I = M_R M_R^{-1} &= (r_1 M_1 + r_2 M_2 + r_3 M_3)\left(\frac{\widetilde{M}_1}{r_1} + \frac{\widetilde{M}_2}{r_2} + \frac{\widetilde{M}_3}{r_3}\right) \\ &= M_1\widetilde{M}_1 + \frac{r_2}{r_1}M_2\widetilde{M}_1 + \frac{r_3}{r_1}M_3\widetilde{M}_1 + \frac{r_1}{r_2}M_1\widetilde{M}_2 + M_2\widetilde{M}_2 + \frac{r_3}{r_2}M_3\widetilde{M}_2 \\ &\quad + \frac{r_1}{r_3}M_1\widetilde{M}_3 + \frac{r_2}{r_3}M_2\widetilde{M}_3 + M_3\widetilde{M}_3 \end{aligned} \tag{4.24}$$

The requirement that the definitions in Eqs. 4.21 and 4.23 hold simultaneously for any r_i fixes the products $M_i\widetilde{M}_j$, giving

$$\begin{aligned} M_1\widetilde{M}_1 + M_2\widetilde{M}_2 + M_3\widetilde{M}_3 &= I, \\ M_i\widetilde{M}_j &= 0, \text{ for } i \neq j. \end{aligned} \tag{4.25}$$

By a similar consideration of the equivalent relation $I = M_R^{-1}M_R$, we obtain also

$$\begin{aligned} \widetilde{M}_1 M_1 + \widetilde{M}_2 M_2 + M_3\widetilde{M}_3 &= I, \\ \widetilde{M}_i M_j &= 0, \text{ for } i \neq j. \end{aligned} \tag{4.26}$$

Now consider the trivial relation $M_R \equiv M_R M_R^{-1} M_R$. Expanding M_R and M_R^{-1} in terms of their respective rank-1 matrices, and matching coefficients r_i, we arrive at the rule

$$M_i\widetilde{M}_i M_i = M_i, \tag{4.27}$$

which is simply the pseudoinverse of M_i [188].

Returning to the seesaw formula, and noting that $Y^\nu = (Y^\nu)^\intercal$, we have

$$\begin{aligned} m^\nu &= -v_u^2 Y^\nu M_R^{-1} Y^\nu \\ &= -v_u^2 (y_1 M_1 + y_2 M_2 + y_3 M_3)\left(\frac{\widetilde{M}_1}{r_1} + \frac{\widetilde{M}_2}{r_2} + \frac{\widetilde{M}_3}{r_3}\right)(y_1 M_1 + y_2 M_2 + y_3 M_3). \end{aligned} \tag{4.28}$$

Expanding the parentheses and using Eqs. 4.25, 4.26 and 4.27, we arrive at

$$m^\nu = -v_u^2\left(\frac{y_1^2}{r_1}M_1 + \frac{y_2^2}{r_2}M_2 + \frac{y_3^2}{r_3}M_3\right), \tag{4.29}$$

which is the same form as Y^ν and M_R.

This proof can also be understood in the language of vacuum alignments, as demonstrated in [5]. Recalling Eq. 4.20, we express each rank-1 matrix by $M_i = \phi_i \phi_i^\intercal$, where it is understood that ϕ represents the VEV of a triplet flavon. Again, the neutrino Yukawa and right-handed Majorana matrices are written $Y^\nu = \sum_i y_i M_i$ and $M_R = \sum_i r_i M_i$, respectively, as in Eq. 4.21. Now let us consider a new set of column vectors $\tilde{\phi}_i$, $\tilde{\phi}_i$, $\tilde{\phi}_i$, which are orthogonal to the original ones, and satisfy the conditions

$$\tilde{\phi}_i^\intercal \phi_j = \delta_{ij}, \qquad i, j = a, b, c. \tag{4.30}$$

For example, for the column vectors corresponding to CSD(3),

$$\phi_1 = (0, 1, 1), \quad \phi_2 = (1, 3, 1), \quad \phi_3 = (0, 0, 1), \tag{4.31}$$

the corresponding column vectors which satisfy Eq. 4.30 are

$$\tilde{\phi}_1 = (-3, 1, 0), \quad \tilde{\phi}_2 = (1, 0, 0), \quad \tilde{\phi}_3 = (2, -1, 1). \tag{4.32}$$

Given these new vectors, we can define some new rank-1 matrices $\widetilde{M}_i = \tilde{\phi}_i \tilde{\phi}_i^\intercal$. Then the inverse of the heavy right-handed Majorana matrix is uniquely given by Eq. 4.23, in terms of r_i (the coefficients of M_R). It can easily be verified explicitly that this result satisfies $M_R M_R^{-1} = I$ using Eq. 4.30, which implies that the cross-terms vanish, i.e. $M_i \widetilde{M}_j = 0$. It is also worth noting that the orthogonality condition in Eq. 4.30 is sufficient for immediately computing the unique solution for the inverse. As such, this derivation reverses the earlier argument, wherein the orthogonality condition (Eqs. 4.25 and 4.26) arises from the requirement that the identity hold for any coefficients r_i multiplying the rank-1 matrices. Now, starting with the orthogonality of vectors ϕ, $\tilde{\phi}$ (Eq. 4.30), we uniquely fix the coefficients of the inverse M_R^{-1} to be $1/r_i$. Both formulations are equivalent, and valid for any linearly independent vectors ϕ.

4.2.5 Renormalisability of the top quark

The superpotential in Eq. 4.3 is written as a set of effective terms, divided by various powers of messenger scales which are $\mathcal{O}(M_{\mathrm{GUT}})$. The degree of suppresion in each term is largely controlled by the power of the singlet ξ, which as noted above acts as a Froggatt-Nielsen (super)field. We assume all terms containing at least one power of ξ/M can be safely expressed by an effective term after integrating out messengers. Only one term does not contain any insertions of ξ, and requires more care. Specifically, the first term in Eq. 4.3 is primarily responsible for the up-type third family fermions (notably, the top quark), and is written naively as

$$\Psi_i \Psi_j H_{10}^u \overline{\phi}_{\mathrm{dec}}^i \overline{\phi}_{\mathrm{dec}}^j \sum_{n=0}^{2} \frac{\lambda_{\mathrm{dec},n}^{(u)}}{\langle H_{45} \rangle^n M_\chi^{2-n}}. \tag{4.33}$$

When $\bar{\phi}_{\rm dec}$ gets a VEV like $(0, 0, v_{\rm dec})$, with $v_{\rm dec}$ assumed to be near the GUT scale, these terms reduce to

$$v_{\rm dec}^2 \Psi_3 \Psi_3 H_{10}^u \sum_{n=0}^{2} \frac{\lambda_{{\rm dec},n}^{(u)}}{\langle H_{45} \rangle^n M_\chi^{2-n}}. \tag{4.34}$$

In fact we can only consistently write these non-renormalisable terms when $\langle \bar{\phi}_{\rm dec} \rangle \ll M_\chi$, but we actually have $\langle \bar{\phi}_{\rm dec} \rangle \approx M_\chi$ so simple integration of the messengers is not possible. It turns out the physical top (and third Dirac neutrino) are not exactly aligned with the third component of Ψ. We therefore need to work out the mixing between the messengers and Ψ. Such mixing technically occurs for all terms, but as noted above, this is only necessary in practice for the least-suppressed term above.

To prove that this in fact gives us a renormalisable top mass, it is sufficient to examine the first term in the above sum (with $n = 0$). It is sourced by the renormalisable terms

$$W \sim \Psi \bar{\phi}_{\rm dec} \bar{\chi}_3 + M_\chi \chi_6 \bar{\chi}_3 + H_{10}^u \chi_6 \chi_6, \tag{4.35}$$

where we suppress $\mathcal{O}(1)$ couplings. In matrix form, this gives

$$W \sim \begin{pmatrix} \Psi_3 & \chi_6 & \bar{\chi}_3 \end{pmatrix} \begin{pmatrix} 0 & 0 & v_{\rm dec}/2 \\ 0 & \langle H_{10}^u \rangle & M_\chi/2 \\ v_{\rm dec}/2 & M_\chi/2 & 0 \end{pmatrix} \begin{pmatrix} \Psi_3 \\ \chi_6 \\ \bar{\chi}_3 \end{pmatrix}. \tag{4.36}$$

Since $\langle H_{10}^u \rangle \ll v_{\rm dec} \sim M_\chi$, diagonalising this mass matrix reveals two heavy and one light eigenstate, the latter being at the electroweak scale and which we can associate with the third family, and crucially with the top quark. Supposing $v_{\rm dec} \approx M_\chi$, the electroweak scale eigenstate is

$$t \approx \frac{1}{\sqrt{2}} \left(\Psi_3 + \chi_6 \right). \tag{4.37}$$

In other words the third family up-type fermion, specifically the top quark, is a linear combination of Ψ_3 and χ_6, where the latter has a renormalizable coupling to the Higgs. The other eigenstates have masses at the GUT scale and are therefore identified as messenger eigenstates. We will revisit this topic of the renormalisability of the third family in the next chapter in the context of an $S_4 \times SO(10)$ model.

4.3 Family symmetry and GUT breaking

In this section we summarise how the flavour symmetries and GUT group are broken at high scale to the MSSM group with R parity, deferring the details of the discussion to Appendix C. Family symmetry breaking, and the specific implementation of the F-term alignment mechanism which produces the CSD(3) alignments, is given in full

in Section C.2. The product rules for triplets and antitriplets of $\Delta(27)$ are listed in Appendix A. Meanwhile, GUT breaking, doublet-triplet splitting, and the smallness of the μ term are all addressed in Section C.3.

4.3.1 Flavon alignments

Here we sketch the method for obtaining CSD(3), and give key results. The CSD(3) alignments, which fully break the flavour symmetries (with no residual symmetries remaining), are obtained by initially considering the "special" alignments of $\Delta(27)$. They are characterised by having either two zeros (e.g. $(0,0,1)$) or three equal magnitudes, with phases that are powers of $\omega = e^{i2\pi/3}$ (e.g. $(1,1,1)$ or $(1,\omega,\omega^2)$). They may be procured by coupling triplet and antitriplet flavons ϕ and $\bar{\phi}$ to driving fields A_i, $\overline{A}_i$, which are also triplets or antitriplets. A number of singlet driving fields O_i are introduced whose F terms force orthogonalities between flavons, ultimately fixing the VEVs of three antitriplets to the CSD(3) alignments; these alone couple directly to Ψ. All flavons and driving fields involved in this mechanism are given in Tables C.2a and C.2b.

All flavon VEVs are also driven to particular scales. To do this, we introduce driving fields P_i and messengers ζ_i (listed in Table C.3) which force additional relations. Denoting the magnitudes of flavon VEVs v_i, the relevant flavons turn out to be related by

$$v_{\rm sol}^2 \propto \omega^2 \left(\frac{\xi}{M_\zeta}\right)^7 v_{\rm dec}^2, \qquad v_{\rm atm}^2 \propto \left(\frac{\xi}{M_\zeta}\right)^8 v_{\rm dec}^2, \tag{4.38}$$

where the constants of proportionality are given as a product of various real $\mathcal{O}(1)$ renormalisable couplings. Since $\langle\xi\rangle / M_\zeta < 1$, we conclude that $v_{\rm dec} \gg v_{\rm atm} \sim v_{\rm sol}$. These relations also result in fixed relative phases between flavons, such that the physical phases in the fermion mass matrices, defined in Eqs. 4.8 and 4.9, are given by

$$\begin{aligned} \eta &= -\arg\left[\frac{v_{\rm sol}^2}{v_{\rm atm}^2}\langle\xi\rangle\right] = -\arg[\omega^2], \\ \eta' &= -\arg\left[\frac{v_{\rm dec}^2}{v_{\rm atm}^2}\frac{1}{\langle\xi\rangle}\right] = 9\arg[\langle\xi\rangle]. \end{aligned} \tag{4.39}$$

These phases are in fact completely fixed. The VEV of ξ is fixed by the GUT-breaking potential given in Appendix C (see Eq. C.28), and fixes the phase of $\langle\xi\rangle$ to a ninth root of unity; by the cancellation of this phase we finally have

$$\eta = \frac{2\pi}{3}, \qquad \eta' = 0. \tag{4.40}$$

Strictly speaking these phases are fixed only up to a relative phase π, depending on the signs of the real constants. However, this additional phase is unphysical, as it may always be subsumed into other real parameters at the low scale.

4.3.2 GUT breaking

We proceed by summarising key features of GUT and R symmetry breaking. Here we are particularly interested in those aspects relevant for understanding the flavour puzzle. $SO(10)$ is broken by the VEV of a Higgs $\mathbf{16} + \overline{\mathbf{16}}$ pair to $SU(5)$, and then by the VEVs of Higgs **45**s to the Standard Model group. Symmetry breaking arises from a rather complicated superpotential (see Eq. C.28) involving adjoints H_{45}, H'_{45}, H_{DW}, spinors $H_{16,\overline{16}}$, and two driving singlets Z, Z''. Their F terms ensure all the above fields get non-zero VEVs, which break both the GUT and R symmetry at the GUT scale. Various higher-order terms are realised in the renormalisable theory by diagrams involving new messenger superfields Z_i, Σ_i, Υ, with associated scales M_Z, M_Σ, M_Υ. The superpotential also contains several terms like $Z\phi_i\bar{\phi}_j\xi^n$, i.e. coupling Z to flavon triplet-antitriplet pairs and some power of ξ, which are allowed by the symmetries and messengers, which links the flavon and Higgs VEVs.

Of particular interest are the VEVs of H_{45} and ξ, which play important roles in the Yukawa sector. As H_{45} is a pure singlet under all flavour symmetries, we may write down infinitely many terms involving progressively higher powers of H_{45}. For simplicity we keep only the first two terms, which are of the form $X(\lambda_{10}H_{45} + \lambda_{11}H_{45}^3/M_\Upsilon^2)$, where X is a combination of other superfields (see Eq. C.28 for the exact form). Its own F-term equation gives H_{45} a VEV,

$$v_{45} = \sqrt{-\frac{\lambda_{10}}{\lambda_{11}}} M_\Upsilon. \tag{4.41}$$

By a choice of λ parameters, we may take v_{45} as real. The VEV of ξ is fixed by the F-term conditions for $H_{10}^{u,d}$ and given in terms of some real $\mathcal{O}(1)$ coefficients λ by

$$\langle\xi\rangle = \left(\frac{\lambda_5\lambda_7}{\lambda_8\lambda_6}\right)^{1/9} M_\Sigma. \tag{4.42}$$

In other words, its phase is given by $\rho_\xi = 2\pi n/9$ for some integer n.

Doublet-triplet splitting is achieved by implementing the DW mechanism. The idea is that Higgs **10**s, $H_{10}^{u,d}$, are given masses through their coupling to a **45**, H_{DW}, whose VEV is aligned in such a way that only the triplet components in the **10**s couple to $\langle H_{DW}\rangle$, while the doublets do not couple to the VEV. For this reason, the mechanism is sometimes known as the "missing VEV mechanism". In $SO(10)$, the VEV may be written as

$$\langle H_{DW}\rangle = v_{DW}\,\mathrm{diag}(1,1,1,0,0) \otimes i\sigma_2, \tag{4.43}$$

where σ_2 is a 2×2 Pauli matrix. The alignment $(1,1,1,0,0)$ may be viewed as "$SU(5)$-like";[3] the first three components therefore couple to the $SU(3)$ part, while the zero components couple to the $SU(2)$ part.

[3] Note however that the alignment $(1,1,1,0,0)$ is not a valid alignment in an $SU(5)$ GUT, as it is not traceless. In $SO(10)$, due to the product with σ_2, the tracelessness condition is automatically fulfilled.

This leaves several massless Higgs doublets: two in each H_{10}, as well as one in each of H_{16} and $H_{\overline{16}}$. In the MSSM, only two of these are massless, while the others should also acquire large masses, so as not to spoil successful gauge coupling unification. In other words, we also have a "doublet-doublet" splitting problem. The solution in this model is similar in nature to that of the previous $A_4 \times SU(5)$ model: we write down the superpotential compatible with the symmetries and field content involving two or more of the Higgs superfields containing $SU(2)$ doublets, which also couple to various powers of ξ. We write down the mass matrix, and find that there is one eigenvalue which is suppressed by $\xi^8/M^7 \ll M$, which we identify as the μ term. With the freedom due to $\mathcal{O}(1)$ parameters and messenger scales, we can arrange for $\mu \sim 1$ TeV without significant tuning. Moreover we identify the MSSM Higgs doublets arising almost entirely from a single **10** each with negligible mixing, i.e. $H_u \approx \mathbf{2}(H^u_{10})$ and $H_d \approx \mathbf{2}(H^d_{10})$.

4.3.3 Proton decay

As in the previous $A_4 \times SU(5)$ model, a characteristic feature of $SO(10)$ GUTs is the prediction of proton decay, mediated by extra gauge bosons or by the triplets accompanying the Higgs doublets. We must ensure that our model does not lead to an unacceptable decay rate, and obeys the bound on the proton lifetime, which we assume to be $\tau_p > 10^{32}$ years. We do not here consider the individual predictions for different decay modes, which have different associated experimental bounds giving $\tau_p > 10^{31-33}$ years [23]. In SUSY $SO(10)$ GUTs the main source for proton decay comes from triplet Higgsinos, whose decay width is dependent on SUSY breaking and the specific coupling texture of the triplets. In general the constraints are barely met when the triplets are at the GUT scale [189, 190], as in this model.

Again we find that that proton decay from dangerous dimension-5 operators resembling $qqq\ell$ is strongly suppressed, due to the presence of multiple symmetries (for a discussion of dimension-6 operators we refer the reader to [127]). As all matter is contained in the same $\Psi \sim (3, 16)$ representation of $SO(10)$, we consider $\Psi\Psi\Psi\Psi$. However this is forbidden by $\Delta(27)$, which does not allow products of only triplets (or only antitriplets) unless there are three of them – or some multiple of three. To build this effective term at higher order we require at minimum one $\bar{\phi}$, as well as some superfield with R charge 2; one such candidate is the field Z, which is a singlet under all other symmetries and plays a role in GUT breaking (see Section C.3). To ensure the $\mathbb{Z}_{9,12}$ symmetries are respected may require additional fields such as ξ. We are therefore interested in terms like

$$\Psi\Psi\Psi\Psi \frac{Z\bar{\phi}}{M^3} \left(\frac{\xi}{M}\right)^n , \tag{4.44}$$

for some integer n. In the renormalisable theory, for this type of effective term to be present at $M \sim M_{\rm GUT}$ requires appropriate messengers. Specifically, we would need

messengers that are $\Delta(27)$ triplets, which are completely absent from our model. Hence such terms can not be produced at (or below) the GUT scale.

They may, however, arise with Planck-scale suppression $M \sim M_P$. The lowest-order term arising from fields that aquire non-vanishing VEVs (and therefore contribute to proton decay) is

$$\Psi\Psi\Psi\Psi\frac{Z\bar{\phi}_{\text{dec}}\xi^3}{M_P^6}, \tag{4.45}$$

which would generate proton decay terms of the type

$$gQQQL\frac{\langle X\rangle}{M_P^2}, \tag{4.46}$$

where g is a dimensionless coupling and $\langle X\rangle$ is a generic VEV of a field, as discussed in [191]. These terms must be suppressed enough to generate a proton lifetime $\tau_p > 10^{32}$ years, which is achieved when

$$g\langle X\rangle < 3 \times 10^9 \text{ GeV}. \tag{4.47}$$

In our model,

$$\langle X\rangle = \frac{\langle Z\rangle v_{\text{dec}} \langle\xi\rangle^3}{M_P^4} \sim 150 \text{ GeV}, \tag{4.48}$$

such that with $\mathcal{O}(1)$ dimensionless couplings, proton decay is very suppressed.

4.4 Numerical fit

4.4.1 Mass matrices

We turn to a numerical fit of all known quark and lepton mass and mixing parameters. At the low scale, the VEVs of flavons and messenger fields combine to give the mass

matrices

$$\begin{aligned}
\frac{m^u}{v_u} &= y_1^u \begin{pmatrix} 0 & 0 & 0 \\ 0 & 1 & 1 \\ 0 & 1 & 1 \end{pmatrix} + y_2^u e^{i\eta} \begin{pmatrix} 1 & 3 & 1 \\ 3 & 9 & 3 \\ 1 & 3 & 1 \end{pmatrix} + y_3^u e^{i\eta'} \begin{pmatrix} 0 & 0 & 0 \\ 0 & 0 & 0 \\ 0 & 0 & 1 \end{pmatrix} + y_4^u e^{i\eta_4^u} \begin{pmatrix} 0 & 0 & 1 \\ 0 & 0 & 3 \\ 1 & 3 & 2 \end{pmatrix}, \\
\frac{m^d}{v_d} &= y_1^d \begin{pmatrix} 0 & 0 & 0 \\ 0 & 1 & 1 \\ 0 & 1 & 1 \end{pmatrix} + y_2^d e^{i\eta} \begin{pmatrix} 1 & 3 & 1 \\ 3 & 9 & 3 \\ 1 & 3 & 1 \end{pmatrix} + y_3^d e^{i\eta'} \begin{pmatrix} 0 & 0 & 0 \\ 0 & 0 & 0 \\ 0 & 0 & 1 \end{pmatrix}, \\
\frac{m^e}{v_d} &= y_1^e \begin{pmatrix} 0 & 0 & 0 \\ 0 & 1 & 1 \\ 0 & 1 & 1 \end{pmatrix} + y_2^e e^{i\eta} \begin{pmatrix} 1 & 3 & 1 \\ 3 & 9 & 3 \\ 1 & 3 & 1 \end{pmatrix} + y_3^e e^{i\eta'} \begin{pmatrix} 0 & 0 & 0 \\ 0 & 0 & 0 \\ 0 & 0 & 1 \end{pmatrix}, \\
m^\nu &= \mu_a \begin{pmatrix} 0 & 0 & 0 \\ 0 & 1 & 1 \\ 0 & 1 & 1 \end{pmatrix} + \mu_b e^{i\eta} \begin{pmatrix} 1 & 3 & 1 \\ 3 & 9 & 3 \\ 1 & 3 & 1 \end{pmatrix} + \mu_c e^{i\eta'} \begin{pmatrix} 0 & 0 & 0 \\ 0 & 0 & 0 \\ 0 & 0 & 1 \end{pmatrix}.
\end{aligned} \tag{4.49}$$

We recall that $\eta = 2\pi/3$ and $\eta' = 0$, while the remaining phase η_4^u is free.

Assuming all superpotential terms have $\mathcal{O}(1)$ couplings, we may derive a "natural" scale for each of the coefficients y_i^f. Firstly, we recall that there are several messenger scales present in our model. The ones that appear in y_i^f are M_χ, M_ζ, $M_{\Omega_{\rm dec}}$, $M_{\Omega_{\rm sol}}$ and $M_{\Omega_{\rm atm}}$. As previously established, we have $\langle\xi\rangle \lesssim M_\zeta < M_\chi$. More specifically, we will assume the ratios

$$\frac{\langle\xi\rangle}{M_\zeta} \gtrsim 0.5, \qquad \frac{\langle\xi\rangle}{M_\chi} \lesssim 0.1. \tag{4.50}$$

We further define the GUT scale by $M_{\rm GUT} \equiv v_{45} \lesssim M_\chi$. Finally, as discussed previously, we assume that $M_{\Omega_{\rm atm}} \approx M_{\Omega_{\rm sol}} > M_{\Omega_{\rm dec}}$, by roughly one order of magnitude.

The coefficients y_i^f derive from can be obtained from the superpotential in Eq. 4.3. For a given fermion type $f = u, d, e$, they take a generic form

$$\begin{aligned}
y_1^f &= \bar{\phi}_{\rm atm}\bar{\phi}_{\rm atm}\xi^{N-2} \sum_{n=0}^{N} \frac{\lambda_{X,n}^{(f)}}{\langle H_{45}\rangle^n M_\chi^{N-n}}, \\
y_2^f &= \bar{\phi}_{\rm sol}\bar{\phi}_{\rm sol}\xi^{N-2} \sum_{n=0}^{N} \frac{\lambda_{X,n}^{(f)}}{\langle H_{45}\rangle^n M_\chi^{N-n}}, \\
y_3^f &= \bar{\phi}_{\rm dec}\bar{\phi}_{\rm dec}\xi^{N-2} \sum_{n=0}^{N} \frac{\lambda_{X,n}^{(f)}}{\langle H_{45}\rangle^n M_\chi^{N-n}},
\end{aligned} \tag{4.51}$$

where λ are $\mathcal{O}(1)$ couplings and N is a number between two and five. We will assume there are no large cancellations between terms in the sums. The flavon VEVs were discussed briefly above (and in more detail in Appendix C); they may be approximated

by

$$\langle \bar{\phi}_{\rm dec} \rangle \sim M_{\rm GUT}, \quad \langle \bar{\phi}_{\rm atm} \rangle \sim \frac{\langle \xi \rangle^4}{M_\zeta^4} M_{\rm GUT}, \quad \langle \bar{\phi}_{\rm sol} \rangle \sim \frac{\langle \xi \rangle^{7/2}}{M_\zeta^{7/2}} M_{\rm GUT}. \tag{4.52}$$

We note immediately that these VEVs have large powers of $\langle \xi \rangle / M_\zeta$, which is primarily bounded below (see Eq. 4.50). This translates to only a loose upper bound on the fitting parameters.

We expect the fitted coefficients y_i^f to be of the approximate scales

$$\begin{aligned} &y_1^u \gtrsim 4 \times 10^{-4}, && y_1^e \gtrsim 4 \times 10^{-5}, && y_1^d \gtrsim 4 \times 10^{-5}, && \mu_a \sim 10^{-2} \text{ eV}, \\ &y_2^u \gtrsim 8 \times 10^{-5}, && y_2^e \gtrsim 8 \times 10^{-6}, && y_2^d \gtrsim 8 \times 10^{-6}, && \mu_b \sim 10^{-3} \text{ eV}, \\ &y_3^u \sim 1, && y_3^e \sim 10^{-1}, && y_3^d \sim 10^{-1}, && \mu_c \sim 10^{-3} \text{ eV}, \\ &y_4^u \gtrsim 5 \times 10^{-4}. \end{aligned} \tag{4.53}$$

Smaller parameter values than given above are allowed, as there may be cancellations within the sums that make up each parameter, although this scenario is indicative of some tuning. Nevertheless, we see how $SO(10)$ unification implies similar hierarchies among all charged fermions. It also suggests up-type quark masses are larger than for down-type quarks and charged leptons, by roughly one order of magnitude, due to one fewer insertion of $\langle \xi \rangle$. This is welcome as far as the second and third family are concerned, but potentially problematic for the first family, given that the up quark is lighter than the down quark.

4.4.2 Best fit results

To fit the real coefficients $y^u_{1,2,3,4}$, $y^d_{1,2,3}$, $y^e_{1,2,3}$, and $\mu_{a,b,c}$ as well as the phase η^u_4, we minimise a χ^2 function that relates the physical predictions $P_i(x)$ for a given set of input parameters x to their current best-fit values μ_i and their associated errors, denoted σ_i. The χ^2 function, first defined in Eq. 2.22, is given by

$$\chi^2 = \sum_{i=1}^{N} \left(\frac{P_i(x) - \mu_i}{\sigma_i} \right)^2. \tag{4.54}$$

Neutrino masses and PMNS parameters are obtained from the NuFit collaboration. As in Chapters 2 and 3, the most recent global fit results at the time of publication of [4], on which much of this chapter is based, was NuFit 2.0 [105].

In further reference to previous discussions (see Sections 2.3.3, 3.3), the errors σ_i are equivalent to the standard deviation of a fit to a Gaussian distribution, which is a good representation of the data for most physical parameters; the exception is the (lepton) atmospheric angle θ^l_{23}, which has a bimodal distribution. For a normal hierarchy (as

predicted by the model), the distribution is broadly centered on maximal atmospheric angle, i.e. $\theta_{23}^l \sim 45°$, with a small preference for θ_{23}^l to be in the first octant. We wish to extend the scope of the previous analyses, which simply assumed the preference for the first octant was true. As such, we here consider two possible scenarios when performing our fit.

- Scenario 1: we assume that the (weak) preference for $\theta_{23}^l < 45°$ is true, and approximate its distribution by a Gaussian about $\mu_{\theta_{23}^l} = 42.3°$, setting $\sigma_{\theta_{23}^l} = 1.6°$ as the error.
- Scenario 2: we remain octant-agnostic by assuming a Gaussian distribution centred at the midpoint between the two 1σ bounds, i.e. $\mu_{\theta_{23}^l} = 45.9°$ with $\sigma_{\theta_{23}^l} = 3.5°$.

A separate χ^2 fit was performed for each scenario.

Here, $N = 18$, corresponding to six mixing angles θ_{ij}^l (neutrinos) and θ_{ij}^q (quarks), the CKM phase δ^q, nine Yukawa eigenvalues for the quarks and charged leptons, and two neutrino mass-squared differences Δm_{21}^2 and Δm_{31}^2. We note however that the free input parameters controlling the quark and lepton sectors are distinct, and thus the two sectors may be considered separately, constrained only by the requirement that related parameters are of comparable scales. We use the PDG parametrisation of the PMNS and CKM matrices. Experimentally, the leptonic phase δ^ℓ is poorly constrained and left as a pure prediction of the model, as are the (completely unconstrained) Majorana phases α_{21} and α_{31}. The bound on the sum of neutrino masses coming from cosmology is not included in the fit but is anyway easily met for strongly hierarchical neutrinos predicted by the SD framework.

The running of best-fit and error values to the GUT scale are generally dependent on supersymmetry parameters, notably $\tan\beta$, as well as contributions from supersymmetric threshold corrections. These are discussed in Appendix B. We extract the GUT-scale CKM parameters and all Yukawa couplings (with associated errors) from [145] for $\tan\beta = 5$. The value of $\tan\beta$ is found not to have a significant impact on the quality of our model, so we only present results for $\tan\beta = 5$ here. Furthermore, we find that our model is essentially unaffected by threshold corrections, so we simply assume them to be zero. Using the notation defined in [145], and summarised in Appendix B, this is equivalent to setting the parameters $\bar{\eta}_i$ to zero.

Table 4.3 shows the best fit of the model to quark masses and CKM parameters, as well as the 1σ ranges from experimental data (run up to the GUT scale) for reference. The corresponding set of model parameters is given in Table 4.4. Table 4.5 shows the analogous best fit of the model to lepton masses and PMNS parameters, also with data 1σ ranges, where applicable. It includes also predictions for currently unmeasured parameters, including the two Majorana CP phases and the effective neutrino mass

Parameter	Value	Data fit 1σ range
$\theta^q_{12}/^\circ$	13.020	$12.985 \to 13.067$
$\theta^q_{13}/^\circ$	0.2023	$0.1866 \to 0.2005$
$\theta^q_{23}/^\circ$	2.238	$2.202 \to 2.273$
$\delta^q/^\circ$	69.89	$66.12 \to 72.31$
m_u /MeV	0.602	$0.351 \to 0.666$
m_c /MeV	249.5	$240.1 \to 257.5$
m_t /GeV	93.37	$89.84 \to 95.77$
m_d /MeV	0.511	$0.744 \to 0.929$
m_s /MeV	15.80	$15.66 \to 17.47$
m_b /GeV	0.947	$0.925 \to 0.948$

Table 4.3: Best fit quark sector observables at the GUT scale, with experimental 1σ ranges from [145]. The SUSY-breaking scale is set to 1 TeV, $\tan\beta = 5$, and no threshold corrections are assumed.

Parameter	Value
$y^u_1/10^{-5}$	3.478
$y^u_2/10^{-4}$	2.075
$y^u_3/10^{-1}$	5.389
$y^u_4/10^{-3}$	5.774
η^u_4	1.629π
$y^d_1/10^{-4}$	-3.199
$y^d_2/10^{-5}$	2.117
$y^d_3/10^{-2}$	2.792
η	$2\pi/3$
η'	0

Table 4.4: Quark sector input parameter values, with η, η' fixed by the theory.

$|m_{\beta\beta}|$. The corresponding input parameters are given in Table 4.6. The total χ^2 is 17.3 and 16.7 for scenario 1 and 2, respectively (see discussion on θ^l_{23} above).

In the quark sector there are seven real input parameters plus three phases, two of which are fixed by the model, that we fit to six quark masses and four CKM parameters.[4] The quark contribution to the total χ^2 is 16.0, by far the largest contribution, and consists almost entirely of an approximately 3.5σ deviation in the down quark mass m_d.

In the lepton sector there are six real input parameters plus two fixed discrete phases that we fit to three charged lepton masses, two neutrino mass-squared differences and three mixing angles (a total of eight observables). The associated contribution to the total χ^2 is 1.3 and 0.7 for scenario 1 and 2, respectively. Note the two different data

[4] Note that in [4], a fit was conducted with several extra phases in the quark sector, giving a better fit with $\chi^2 \approx 2$. These phases resulted from assuming an imaginary VEV of the $SO(10)$ adjoint H_{45} (see Table 4.1) which appears in sums in Eq. 4.3. The model fixes its VEV to be either strictly real or imaginary. However, this would necessarily introduce extra phases in the lepton sector, spoiling the predictivity of the CSD(n) scheme with fixed $\eta = 2\pi/3$. It was then discovered that a good fit can be achieved even in the more predictive case where $\langle H_{45} \rangle$ is real, and all (but one) phases are fixed.

Parameter	Value		Data fit 1σ range
	Scenario 1	Scenario 2	
θ_{12}^l /°	33.13	32.94	32.83 → 34.27
θ_{13}^l /°	8.59	8.55	8.29 → 8.68
θ_{23}^l /°	40.81		40.63 → 43.85
		46.65	42.40 → 49.40
δ^ℓ /°	280	275	192 → 318
m_e /MeV	0.342	0.342	0.340 → 0.344
m_μ /MeV	72.25	72.25	71.81 → 72.68
m_τ /GeV	1.229	1.229	1.223 → 1.236
$\Delta m_{21}^2 / 10^{-5}$ eV^2	7.58	7.46	7.33 → 7.69
$\Delta m_{31}^2 / 10^{-3}$ eV^2	2.44	2.47	2.41 → 2.50
m_1 /meV	0.32	0.38	
m_2 /meV	8.64	8.65	
m_3 /meV	49.7	49.7	
$\sum m_i$ /meV	58.7	59.4	
α_{21} /°	264	264	
α_{31} /°	323	333	
$\lvert m_{\beta\beta}\rvert$ /meV	2.46	2.42	

Table 4.5: Best fit lepton observables at the GUT scale, with experimental 1σ ranges from [105, 145]. The SUSY-breaking scale is set to 1 TeV, $\tan\beta = 5$, and no threshold corrections are assumed.

Parameter	Value	
	Scenario 1	Scenario 2
$y_1^e / 10^{-3}$	2.217	-1.966
$y_2^e / 10^{-5}$	-1.025	1.027
$y_3^e / 10^{-2}$	3.366	3.790
μ_a /meV	26.60	25.90
μ_b /meV	2.571	2.546
μ_c /meV	2.052	2.461
η	$2\pi/3$	
η'	0	

Table 4.6: Lepton sector input parameter values, with η, η' fixed by the theory.

fit 1σ ranges for θ_{23}^l in Table 4.5, depending on the choice of scenario. Although the fit does not constitute a full analysis of the parameter space, it agrees with the results of the more dedicated numerical analysis of CSD(n) models in Chapter 2. The most significant different between the $SO(10)$ model presented here and the idealised model considered previously is that the charged lepton mass matrix is non-diagonal. In fact, small charged lepton corrections appear to improve the fit slightly.

It is also worth noting that on one hand the model successfully fits all measured lepton parameters, and predicts a Dirac CP phase $\delta^\ell \sim -\pi/2 = 270^\circ$, which is in good agreement with the current hints from data. In fact, when this model was first conceived [4], the NuFit global fit [105] preferred $\delta^\ell \approx 306^\circ$, while more recent results [36] suggest $\delta^\ell \approx 261^\circ$, which is somewhat closer to the predicted values in Table 4.5.

On the other hand, two generic predictions for the lepton sector, namely a normal neutrino hierarchy and a very small effective neutrino mass $m_{\beta\beta} \lesssim 3$ meV, are unfortunately very difficult to test directly. Nevertheless these predictions would rule the model out in the event that an inverted neutrino ordering is observed. As noted in the Introduction, an inverted ordering is currently disfavoured by global fits to neutrino oscillation data albeit to low significance, and is also being constrained by cosmology which may be able to settle this question decisively within the foreseeable future.

4.5 Leptogenesis

Conventional wisdom when discussing leptogenesis in $SO(10)$ suggests that the lightest right-handed neutrino N_1 has a mass that is too low to produce the correct baryon asymmetry of the Universe (BAU). It can be understood as follows: there is a very strong hierarchy in the up-type quark masses, with $m_u : m_c : m_t \sim 10^{-5} : 10^{-3} : 1$, while the hierarchy among neutrinos is comparatively mild. Assuming a normal ordering $m_1 < m_2 < m_3$, we have $m_1 : m_2 : m_3 \sim 10^{-2} : 10^{-1} : 1$. If up-type quark and neutrino Dirac couplings are assumed equal in naive $SO(10)$, producing the correct hierarchy in the neutrino Majorana masses after seesaw requires a large hierarchy in the right-handed neutrino masses M_i that is stronger even than the quark hierarchy, like $10^6 : 10^{10} : 10^{15}$. The typically cited lower bound [192] on the lightest mass M_1 which can successfully realise N_1 leptogenesis is

$$M_1 \gtrsim 10^9 \text{ GeV}. \tag{4.55}$$

While this bound is slightly malleable [109], a mass $M_1 \sim 10^6$ GeV is too light for traditional leptogenesis. Typically one proceeds by considering N_2 leptogenesis [193, 194], which has been studied in detail for $SO(10)$-inspired models [195–199] (for further work on leptogenesis in $SO(10)$, see [200–205]). We here show that in a flavoured $SO(10)$ SUSY GUT model where the naive quark and neutrino Yukawa structures may be modified, N_1 leptogenesis is indeed possible, and the N_1 mass can be made to respect

the traditional bound. This section is chiefly based on our work in [5], showing how leptogenesis may be realised in the above $\Delta(27) \times SO(10)$ model.

4.5.1 Mass and Yukawa parameters

As discussed previously, a compelling feature of the model is that the mass matrices in each sector (including the light neutrinos after seesaw) have the same universal structure, and the phases and mixing angles are guided by the flavour symmetry. In particular the phases in both quark and lepton sectors are determined by relative phases of flavons.[5] This leads also to a rather predictive scenario for leptogenesis, which ultimately allows us to constrain some of the free parameters of the model (and indirectly the mass of the right-handed neutrinos) in order to obtain the correct baryon asymmetry.

For the following calculation, we use the notation consistent with [5], which is slightly different to that used previously within this chapter. We write the charged lepton and neutrino Yukawa matrices $Y^{e,\nu}$ and right-handed neutrino mass matrix M_R as

$$\begin{aligned} Y^{e,\nu} &= y^{e,\nu}_{\rm atm} \begin{pmatrix} 0 & 0 & 0 \\ 0 & 1 & 1 \\ 0 & 1 & 1 \end{pmatrix} + y^{e,\nu}_{\rm sol} e^{i\eta} \begin{pmatrix} 1 & 3 & 1 \\ 3 & 9 & 3 \\ 1 & 3 & 1 \end{pmatrix} + y^{e,\nu}_{\rm dec} e^{i\eta'} \begin{pmatrix} 0 & 0 & 0 \\ 0 & 0 & 0 \\ 0 & 0 & 1 \end{pmatrix}, \\ M_R &= M_{\rm atm} \begin{pmatrix} 0 & 0 & 0 \\ 0 & 1 & 1 \\ 0 & 1 & 1 \end{pmatrix} + M_{\rm sol} e^{i\eta} \begin{pmatrix} 1 & 3 & 1 \\ 3 & 9 & 3 \\ 1 & 3 & 1 \end{pmatrix} + M_{\rm dec} e^{i\eta'} \begin{pmatrix} 0 & 0 & 0 \\ 0 & 0 & 0 \\ 0 & 0 & 1 \end{pmatrix}. \end{aligned} \tag{4.56}$$

The model fixes $\eta = 2\pi/3$, $\eta' = 0$, while the effective couplings $y^{e,\nu}_i$ and M_i (with $i = {\rm atm}, {\rm sol}, {\rm dec}$) are real and dimensionless with the natural hierarchies

$$\begin{aligned} y^{e,\nu}_{\rm dec} &\gg y^{e,\nu}_{\rm atm} \gg y^{e,\nu}_{\rm sol}, \\ M_{\rm dec} &\gg M_{\rm atm} > M_{\rm sol}. \end{aligned} \tag{4.57}$$

These relations are a direct consequence of the superpotential in Eq. 4.3 and the symmetry-breaking sector that fixes the flavon VEVs, although, apart from these general expectations, we shall regard the y_i and M_i as free parameters. The subscripts $i = {\rm atm}, {\rm sol}, {\rm dec}$ differ from those in Eq. 4.51, where simply $i = 1, 2, 3$, respectively. This is done to emphasise the connection of each parameter to the flavons $\phi_{\rm atm}$, $\phi_{\rm sol}$, $\phi_{\rm dec}$, and to the SD framework. Similarly, we write the light neutrino matrix as

$$m^\nu = \mu_{\rm atm} \begin{pmatrix} 0 & 0 & 0 \\ 0 & 1 & 1 \\ 0 & 1 & 1 \end{pmatrix} + \mu_{\rm sol} e^{i\eta} \begin{pmatrix} 1 & 3 & 1 \\ 3 & 9 & 3 \\ 1 & 3 & 1 \end{pmatrix} + \mu_{\rm dec} e^{i\eta'} \begin{pmatrix} 0 & 0 & 0 \\ 0 & 0 & 0 \\ 0 & 0 & 1 \end{pmatrix}, \tag{4.58}$$

[5] The quark sector is largely not relevant for leptogenesis calculations, with the exception of the top mass m_t, which appears when $\Delta L = 1$ scatterings like $qt \to H \to \ell N$ are taken into account.

where $\mu_i \equiv (y_i^\nu v_u)^2/M_i$ and $\mu_{\rm atm} \gg \mu_{\rm sol} \gtrsim \mu_{\rm dec}$.[6]

Low-scale experimental data can only fix the combination of neutrino Dirac and Majorana parameters encoded in the μ_i, and do not allow the three right-handed neutrino mass parameters $M_{\rm atm}$, $M_{\rm sol}$, $M_{\rm dec}$ to be disentangled from the Yukawa couplings $y^\nu_{\rm atm}$, $y^\nu_{\rm sol}$, $y^\nu_{\rm dec}$. Leptogenesis on the other hand is a high-scale phenomenon: the requirement that the BAU is produced entirely from thermal N_1 leptogenesis may constrain the Yukawa couplings $y^\nu_{\rm atm}$, $y^\nu_{\rm sol}$, which enables the right-handed neutrino mass parameters $M_{\rm atm}$ and $M_{\rm sol}$ to be constrained, thereby also the lightest two right-handed neutrino mass eigenvalues M_1 and M_2, assuming the third mass M_3 to be much heavier. The relation between the parameters $M_{\rm atm}$, $M_{\rm sol}$ and the eigenvalues M_1, M_2 is rather complicated since the mass matrix M_R is not diagonal, but according to SD we should have $M_{\rm dec} \approx M_3$ much heavier than the others and thus essentially decoupled.

Before proceeding with the calculation of the BAU, let us recapitulate the results of the leptogenesis analysis in Chapter 2 (see Section 2.4), which is based on the work in [3]. There we discussed N_1 leptogenesis in a class of models with CSD(n) vacuum alignments, leading to rather a rather simple expression for the final BAU in terms of the parameters of the light neutrino mass matrix m^ν (see Eq. 2.46). A special case of this class of models was considered in Chapter 3, in the context of an $A_4 \times SU(5)$ model.

Previous results depended crucially on several features of said class of CSD(n) models, namely 1) diagonal charged leptons, 2) only two right-handed neutrinos with 3) a diagonal Majorana mass matrix, as well as 4) a neutrino Yukawa matrix Y^ν where each column is proportional to one of the CSD(n) vacuum alignments. To elaborate on the final point, the first and second columns of Y^ν resembled $(0, a, a)$ and $(b, nb, (n-2)b)$ respectively, where a, b are complex numbers (see e.g. Eq. 2.27) collecting various $\mathcal{O}(1)$ couplings and (magnitudes of) flavon VEVs. Notably, each element of Y^ν was expressed in terms of only one complex free parameter, greatly simplifying the resultant expression for the BAU. In particular, the only phase dependence was a single explicit factor $\sin\eta$, with $\eta = \arg[b^2/a^2]$.

None of the above conditions apply here. It is immediately apparent that neither the charged leptons nor the right-handed neutrinos are diagonal (conditions 1 and 3, respectively), and unification under $\Delta(27) \times SO(10)$ demands three right-handed neutrinos rather than two (condition 2). Finally, the CSD(3) alignments are not neatly arranged in columns of Y^ν (condition 4), which is now necessarily symmetric due to $SO(10)$ unification. As a consequence, each element of Y^ν is a non-trivial combination of real parameters y_i and η, while its phase will depend on the relative magnitudes of these parameters.

[6] For completeness, all effective parameters are given explicitly in terms of VEVs and $\mathcal{O}(1)$ parameters at the end of this section (see Eq. 4.84).

Despite the increased complexity, it is tempting to derive also in this scenario analytical estimates for the CP asymmetries $\epsilon_{1,\alpha}$ akin to those in Eq. 2.37. To do so requires transforming into the flavour basis where charged leptons and right-handed neutrinos are diagonal, which modifies Y^ν. Analytical approximations for this basis transformation are discussed in Appendix D along with some estimates for the resultant CP asymmetries. However, the resultant neutrino Yukawa matrix in the flavour basis depends rather intricately on all the input parameters, and the physical consequences are not easily discerned. Only in the limit where rather severe simplifications are made do the analytical approximations for the CP asymmetries yield distinct predictions. It was concluded that the limited scope of the approximate expressions did not provide much additional value, and are therefore not presented in [5], which relies entirely on numerical solutions to the Boltzmann equations.

To conclude this discussion, we define the neutrino Yukawa matrix λ_ν, in the flavour basis. The charged lepton and right-handed neutrino mass matrices may be diagonalised by a set of unitary matrices generically labelled U, V, such that

$$\begin{aligned} V_{eL} Y^e V_{eR}^\dagger &= \mathrm{diag}(y_e, y_\mu, y_\tau), \\ V_{eL} Y^{e\dagger} Y^e V_{eL}^\dagger &= \mathrm{diag}(y_e^2, y_\mu^2, y_\tau^2) = V_{eR} Y^e Y^{e\dagger} V_{eR}^\dagger, \\ U_N M^N U_N^T &= \mathrm{diag}(M_1, M_2, M_3). \end{aligned} \tag{4.59}$$

As Y^e in Eq. 4.56 is complex-symmetric, we have $V_{eR}^\dagger = V_{eL}^T$. λ_ν is thus given by

$$\lambda_\nu^* = V_{eL} Y^\nu U_N^T, \tag{4.60}$$

where the complex conjugation accounts for the shift between seesaw and leptogenesis bases, as discussed in earlier chapters (see e.g. Section 2.4).

4.5.2 Boltzmann equations

Having defined the lepton matrices that consitute the primary model input into the leptogenesis calculations, we proceed to establish the Boltzmann equations for flavoured N_1 leptogenesis, whose solution ultimately yields the desired BAU. This calculation primarily follows the method described in [108].

As we are considering thermal leptogenesis, we assume a reheating temperature $T > M_1$. Moreover, the model establishes a strong hierarchy in right-handed neutrino mass eigenvalues $M_1 \ll M_2 \ll M_3$, demonstrated in Appendix D. We may therefore use the approximation whereby an asymmetry is generated only by the lightest right-handed neutrino. Under these conditions, as in Chapter 2 (see Eqs. 2.31 and 2.32), we may

parametrise the final BAU Y_B as

$$Y_B = \frac{10}{31}\left[Y_{N_1} + Y_{\tilde{N}_1}\right]_{z\ll 1} \sum_\alpha \varepsilon_{1,\alpha}\eta_\alpha. \tag{4.61}$$

Each $\varepsilon_{1,\alpha}$ is the CP asymmetry of N_1 neutrinos in a particular lepton flavour α, while η_α (previously labelled $\eta_{1,\alpha}$) is an efficiency factor which contains the dependence on washout from inverse decays and scattering, and is typically different for each flavour α. $Y_{N_1,\tilde{N}_1}$ are (s)neutrino number densities and serve as normalisation factors. In the fully flavoured regime, calculating η_α requires solving the Boltzmann equations in terms of the decay factors K_α and a numerical 3×3 flavour coupling matrix A. As will be seen shortly, η_α typically takes values $0 < \eta_\alpha \lesssim 0.2$.

The flavoured decay asymmetries $\varepsilon_{1,\alpha}$ are defined by

$$\varepsilon_{1,\alpha} = \frac{\Gamma_{1\alpha} - \bar{\Gamma}_{1\alpha}}{\Gamma_1 + \bar{\Gamma}_1}, \tag{4.62}$$

where $\Gamma_{1\alpha}$, $\bar{\Gamma}_{1\alpha}$ are the decay rates of N_1 neutrinos decaying, respectively, into $\ell_\alpha H_u$ lepton-Higgs or $\bar{\ell}_\alpha H_u^*$ antilepton-Higgs pairs, in a given flavour α. Γ_1 and $\bar{\Gamma}_1$ are the corresponding total decay rates (summed over flavour). An analogous decay asymmetry $\varepsilon_{1,\tilde{\alpha}}$ may be defined for neutrinos decaying into $\tilde{\ell}_\alpha \tilde{H}$ slepton-Higgsino pairs, and similarly we may define $\varepsilon_{\tilde{1},\alpha}$, and $\varepsilon_{\tilde{1},\tilde{\alpha}}$ for $\tilde{N}_1$ sneutrino decays. In the MSSM, to which the $SO(10)$ model reduces, all these decay rates are equal, i.e. $\varepsilon_{1,\alpha} = \varepsilon_{1,\tilde{\alpha}} = \varepsilon_{\tilde{1},\alpha} = \varepsilon_{\tilde{1},\tilde{\alpha}}$.

Assuming M_3 is large enough that the N_3 neutrino does not participate in leptogenesis, in the hierarchical approximation $M_1 \ll M_2$, $\varepsilon_{1,\alpha}$ can be expressed as

$$\varepsilon_{1,\alpha} = \frac{1}{8\pi} \frac{\mathrm{Im}\left[(\lambda_\nu^\dagger)_{1\alpha}(\lambda_\nu^\dagger\lambda_\nu)_{12}(\lambda_\nu^\intercal)_{2\alpha}\right]}{(\lambda_\nu^\dagger\lambda_\nu)_{11}} g^{\mathrm{MSSM}}\left(\frac{M_2^2}{M_1^2}\right). \tag{4.63}$$

λ_ν is the neutrino Yukawa matrix in the flavour basis. Recall from Eq. 2.36 that the factor g^{MSSM} is, in the limit where $M_1 \ll M_2$, well approximated by

$$g^{\mathrm{MSSM}}\left(\frac{M_2^2}{M_1^2}\right) \approx -3\frac{M_1}{M_2}. \tag{4.64}$$

Given the highly non-trivial mass and Yukawa matrix structures, to rigorously show that N_1 leptogenesis can be achieved in this model, we cannot rely on approximations to these matrices, which may only be valid in small regions of parameter space. Moreover, unlike the discussions in Chapters 2 and 3, the efficiency factors η_α are not fixed by the fit to neutrino mixing data (recall that in those calculations, η_α depended only on the input parameter m_a in the neutrino mass matrix m^ν, which was known to good precision). Rather, we solve the Boltzmann equations for the evolution of the N_1 neutrino and

$B-L$ asymmetry densities numerically. This allows us to derive bounds on the neutrino Yukawa couplings by performing a scan over parameter space.

The solutions are chiefly dependent on the decay factors K_α (themselves dependent on the neutrino Dirac matrix) and the matrix A that encodes flavour coupling effects that modify the lepton asymmetries in individual flavours. In the three-flavour case, K_α and the total decay factor K are defined by

$$K_\alpha = \frac{v_u^2 (\lambda_\nu^\dagger)_{1\alpha} (\lambda_\nu)_{\alpha 1}}{m_\star M_1}, \qquad K = \sum_\alpha K_\alpha, \tag{4.65}$$

where $m_\star \simeq 1.58 \times 10^{-3}$ eV is the equilibrium neutrino mass (in the MSSM). Recall that in the three-flavour case, the numerical matrix A in the MSSM is given by

$$A = \begin{pmatrix} -93/110 & 6/55 & 6/55 \\ 3/40 & -19/30 & 1/30 \\ 3/40 & 1/30 & -19/30 \end{pmatrix}. \tag{4.66}$$

The N_1 neutrino density is given by Y_{N_1}, with the density at thermal equilibrium given by $Y_{N_1}^{\rm eq}$. We define $\Delta Y_{N_1} = Y_{N_1} - Y_{N_1}^{\rm eq}$, as well as corresponding $\Delta Y_{\tilde{N}_1} = Y_{\tilde{N}_1} - Y_{\tilde{N}_1}^{\rm eq}$ for the sneutrino density $Y_{\tilde{N}_1}$. The equilibrium density for leptons and sleptons are denoted $Y_\ell^{\rm eq}$ and $Y_{\tilde{\ell}}^{\rm eq}$. We use

$$Y_{N_1}^{\rm eq} = Y_{\tilde{N}_1}^{\rm eq} \approx \frac{45}{2\pi^4 g_*} z^2 \mathcal{K}_2(z), \qquad Y_\ell^{\rm eq} = Y_{\tilde{\ell}}^{\rm eq} \approx \frac{45}{2\pi^4 g_*}. \tag{4.67}$$

The function $\mathcal{K}_2(z)$ and its companion $\mathcal{K}_1(z)$ which appears below are modified Bessel functions of the second kind.

The total $B/3 - L_\alpha$ asymmetries (including both fermion and scalar matter) are given by Y_{Δ_α}. The Boltzmann equations may be written as

$$\frac{dY_{N_1}}{dz} = -2 D f_1 \Delta Y_{N_1}, \tag{4.68}$$

$$\frac{dY_{\tilde{N}_1}}{dz} = -2 D f_1 \Delta Y_{\tilde{N}_1}, \tag{4.69}$$

$$\frac{dY_{\Delta_\alpha}}{dz} = 2\,\varepsilon_{1,\alpha} D f_1 (\Delta Y_{N_1} + \Delta Y_{\tilde{N}_1}) + W \frac{K_\alpha}{K} f_2 \sum_\beta A_{\alpha\beta} Y_{\Delta_\beta}. \tag{4.70}$$

The decay and washout terms D and W are defined as

$$D = K z \frac{\mathcal{K}_1(z)}{\mathcal{K}_2(z)}, \qquad W = K z \frac{\mathcal{K}_1(z)}{\mathcal{K}_2(z)} \frac{Y_{N_1}^{\rm eq} + Y_{\tilde{N}_1}^{\rm eq}}{Y_\ell^{\rm eq} + Y_{\tilde{\ell}}^{\rm eq}}. \tag{4.71}$$

The functions $f_1(z)$ and $f_2(z)$ parametrise the contributions from $\Delta L = 1$ scatterings. We use the results from [79], wherein they consider scatterings involving neutrinos and

top quarks but not gauge bosons, nor do they consider thermal effects. The functions may be approximated by

$$f_1(z) \approx f_2(z) \approx \frac{z}{a}\left[\ln\left(1+\frac{a}{z}\right)+\frac{K_S}{Kz}\right]\left(1+\frac{15}{8z}\right), \tag{4.72}$$

where

$$a = \frac{K}{K_S \ln(M_1/M_h)}, \tag{4.73}$$

while the ratio K_S/K is given by

$$\frac{K_S}{K} = \frac{9}{4\pi^2}\frac{m_t^2}{g_{N_1} v^2}, \tag{4.74}$$

where m_t is the top quark mass (at the leptogenesis scale), $M_h \approx 125$ GeV is the Higgs mass, and $g_{N_1} = 2$. In the limit where scattering effects are neglected, $f_1(z) = f_2(z) = 1$. The top mass is fitted by the $SO(10)$ model at the GUT scale, at $m_t = 92.8$ GeV. Assuming the running between GUT and leptogenesis scales is relatively minor, we use this benchmark value.

Let us rewrite the parametrisation in Eq. 4.61 as $Y_B = Y_0 \sum_\alpha \varepsilon_{1,\alpha}\eta_\alpha$, where $Y_0 = (10/31)[Y_{N_1} + Y_{\tilde{N}_1}]_{z\ll 1}$ is now interpreted as a normalisation constant that ensures $0 \leq \eta_\alpha \leq 1$. We may factor out the decay asymmetry $\varepsilon_{1,\alpha}$ from the Boltzmann equation for each of the three Y_{Δ_α} in Eq. 4.70, leading to a set of equations for the efficiency factors η_α. Furthermore, if we neglect the small off-diagonal elements of the matrix A, the efficiencies in each flavour decouple and may be solved individually in terms of the decay factors K_α. More precisely, for fixed $K/|A_{\alpha\alpha}K_\alpha|$, $\eta_\alpha(z \to \infty)$ is a function only of $A_{\alpha\alpha}K_\alpha$. Eq. 4.70 may be rewritten as

$$Y_0 \frac{d\eta_\alpha}{dz} = 2D f_1(\Delta Y_{N_1} + \Delta Y_{\tilde{N}_1}) + W\frac{A_{\alpha\alpha}K_\alpha}{K} f_2 Y_0 \eta_\alpha. \tag{4.75}$$

4.5.3 Results

The above final step, i.e. assuming A to be diagonal, is not strictly speaking necessary when solving the above equations numerically, as the increased computational load of using the full A matrix is negligible. However, it allows us to examine the properties of η_α independently of the details of the Yukawa matrix and of the lepton flavour α, using instead K_α as inputs. In Figure 4.7 we show the variation in η_α, in agreement with the results in [108]. The grey lines show η_α when scatterings are switched off, i.e. $f_1 = f_2 = 1$.

In the solutions presented below, we will solve Eqs. 4.68 – 4.70 in terms of the full A-matrix. The only relevant parameters in the $\Delta(27) \times SO(10)$ model which are not fixed by the fit to lepton data are either the set of three neutrino Dirac couplings y_i^ν or the

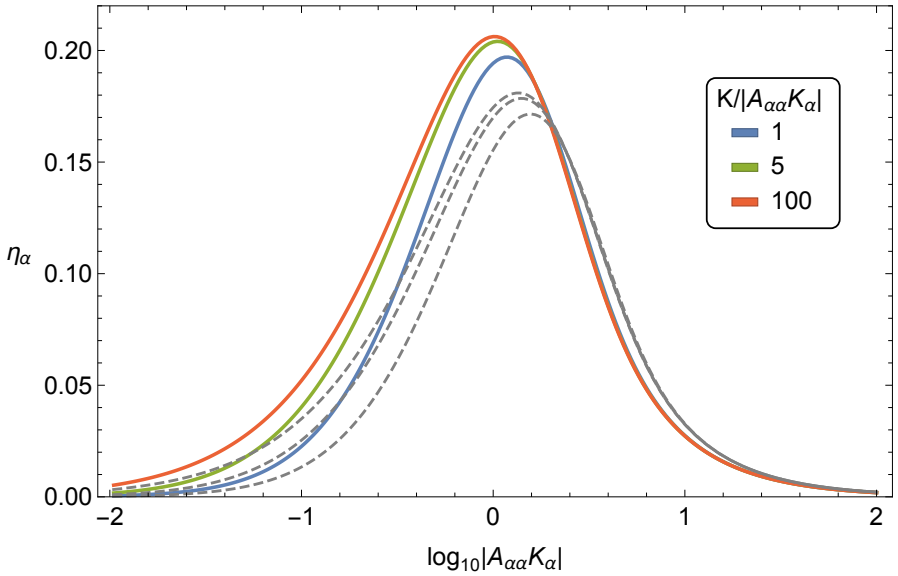

Figure 4.7: Variation in the efficiency factor η_α with $|A_{\alpha\alpha}K_\alpha|$. K_α are decay constants and $A_{\alpha\alpha}$ the diagonal elements of a numerical coupling matrix. The grey lines show η_α when scatterings are switched off.

three right-handed neutrino Majorana couplings M_i ($i = \text{dec}, \text{atm}, \text{sol}$). Once either set has been chosen, the other is fixed by the seesaw relation $\mu_i = (v_u y_i^\nu)^2/M_i$. We choose as inputs the Dirac couplings.

Due to the structure of $SO(10)$, we anticipate these to be roughly equal to the up-type quark Yukawa couplings. As we will find, there exists some tension between the up-quark and neutrino sectors. We begin by noting that the third neutrino does not significantly affect the results. Thus it is most interesting to examine the $y^\nu_{\text{atm}} - y^\nu_{\text{sol}}$ space, while setting $y^\nu_{\text{dec}} = 0.5$. Given the seesaw relation and that $\mu_3 \sim 1$ meV, the third neutrino N_3 has a mass $M_3 \approx M_{\text{dec}} \sim M_{\text{GUT}}$.

Figure 4.8 shows the values of the neutrino Dirac parameters y^ν_{atm} and y^ν_{sol} which produce the correct Y_B, to within 10% and 20% (darker and lighter shades, respectively) as well as satisfying the phenomenological requirements for correct neutrino masses and lepton mixing. Each distinct region of parameter space in Figure 4.8 is marked in a different colour, which correlate also with the colours in Figures 4.9 and 4.10. Although the dotted line (indicating $y_{\text{atm}} = \pm y_{\text{sol}}$) in Figure 4.8 shows that the successful leptogenesis points always satisfy $y^\nu_{\text{atm}} > y^\nu_{\text{sol}}$, the hierarchy is not that strong, bearing in mind that the rank-1 matrix associated with y^ν_{atm} in Eq. 4.56 has numerically smaller entries than that associated with y^ν_{sol}. Consequently both rank-1 matrices will contribute significantly to the second column of the Yukawa matrix over the successul leptogenesis regions, reaffirming the earlier conclusion that any analytical approximation is highly non-trivial.

Figures 4.9 and 4.10 show the corresponding right-handed neutrino mass parameters giving the correct Y_B to within 20%, satisfying also the phenomenological requirements for correct neutrino masses and lepton mixing. Figure 4.9 shows input mass parameters

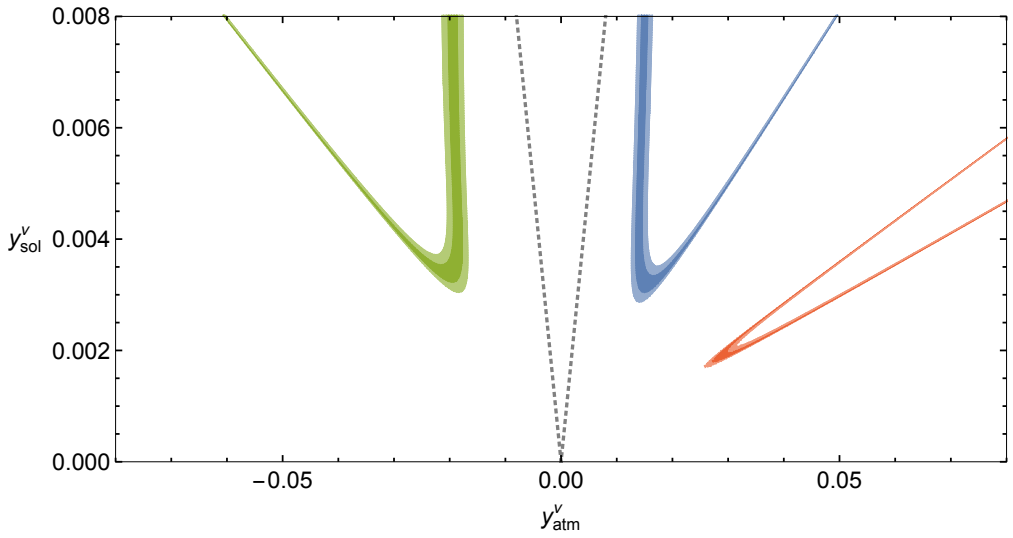

Figure 4.8: Regions where Y_B is within 20% (light bands) and 10% (darker bands) of the observed value. Colours mark separated regions in parameter space, with corresponding regions in Figures 4.9 and 4.10. Dotted lines correspond to $y^{\nu}_{\rm atm} = \pm y^{\nu}_{\rm sol}$.

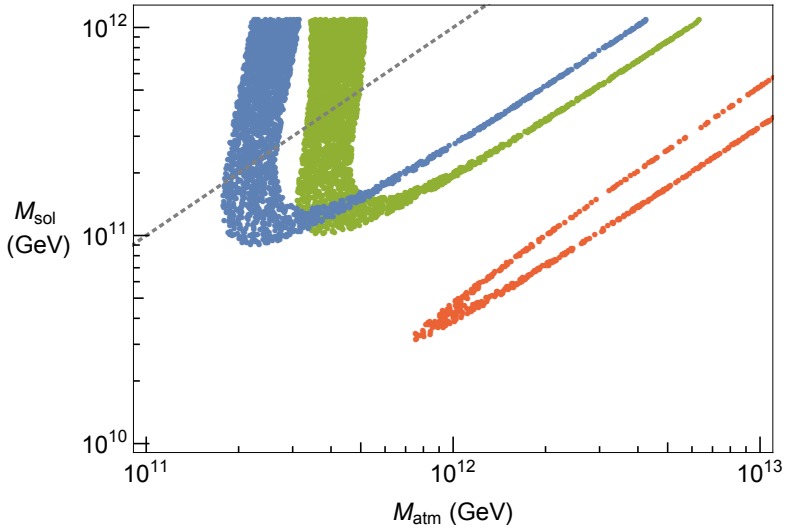

Figure 4.9: Allowed values of input parameters $M_{\rm atm}$, $M_{\rm sol}$, giving Y_B within 20% of the observed value. The dotted line corresponds to $M_{\rm atm} = M_{\rm sol}$.

$M_{\rm atm}$, $M_{\rm sol}$ while Figure 4.10 shows mass eigenvalues M_1, M_2. The assumed strong hierarchy $M_1 \ll M_2$ is always realised for successful leptogenesis, as seen in Figure 4.10 where all points satisfy $M_1 < 0.1 M_2$, i.e. they lie above the dot-dashed line corresponding to $M_1 = 0.1 M_2$.

There is however no such strong hierarchy between the mass parameters $M_{\rm sol,atm}$ in Figure 4.9. Although successful leptogenesis points satisfy $M_{\rm sol} < M_{\rm atm}$ over much of parameter space (the dotted line in Figure 4.9 marks where $M_{\rm atm} = M_{\rm sol}$), it should be noted that the trace of the matrix associated with $M_{\rm sol}$ in Eq. 4.56 is about five times larger than that associated with $M_{\rm atm}$. We conclude that both these mass matrices will

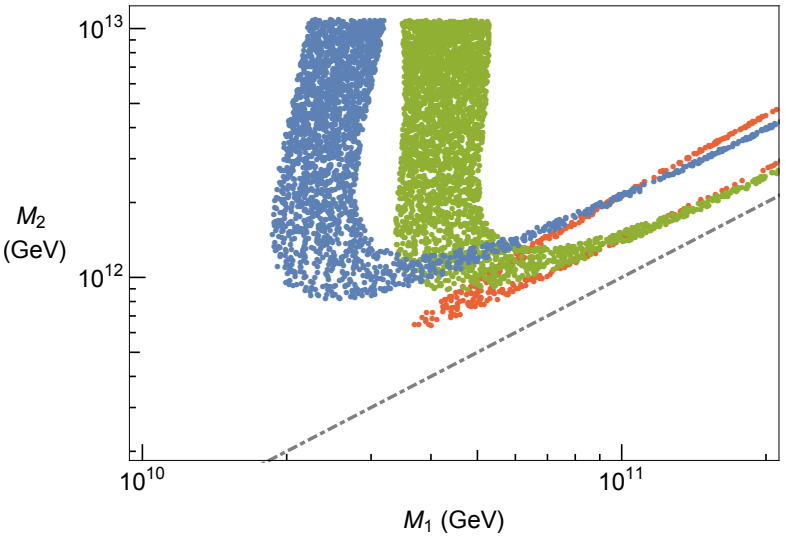

Figure 4.10: Allowed values of right-handed neutrino mass eigenvalues M_1, M_2, giving Y_B within 20% of the observed value. The dot-dashed line corresponds to $M_1 = 0.1 M_2$.

be important in determining the eigenvalues M_1 and M_2 over the successful leptogenesis regions, and simple approximations are generally not reliable.

We find a lower bound on the parameters giving successful leptogenesis, with $y^\nu_{\rm atm} \gtrsim 0.01$ and $y^\nu_{\rm sol} \gtrsim 0.002$. The narrow red region arises from very particular choices of y^ν_i that also give the weakest hierarchy of right-handed neutrino masses $M_1/M_2 \sim 0.1$. Note that the mass M_3 does not appear in the approximated decay asymmetries and its effect on leptogenesis is always negligible. M_3 is therefore only constrained by the relation imposed by SD, namely $M_3 \gg M_{1,2}$.

The effective neutrino couplings y^ν_i that yield viable leptogenesis (as shown by Figure 4.8) are within acceptable ranges when compared to the rough approximations given in Eq. 4.57. We note however that the y^ν_i are different to the effective up-type quark couplings y^u_i, as given by the fit, required to obtain correct GUT scale masses m_u, m_c and m_t. This would rule out N_1 leptogenesis in a naive $SO(10)$ model, and while it can be accommodated in this model, there is a price to pay as the y^ν_i necessarily differ from the y^u_i. In particular, $y^\nu_{\rm atm}$ is larger than its corresponding quark parameter by an $\mathcal{O}(100)$ factor. We will return to this point below.

It is interesting to compare this model to the one introduced in Chapter 3, based on $A_4 \times SU(5)$ with two right-handed neutrinos. In that model the neutrino Yukawa and right-handed Majorana mass matrices may be written as

$$Y^\nu = \begin{pmatrix} 0 & b\, e^{i\eta/2} \\ a & 3b\, e^{i\eta/2} \\ a & b\, e^{i\eta/2} \end{pmatrix}, \qquad M_R = \begin{pmatrix} M_{\rm atm} & 0 \\ 0 & M_{\rm sol} \end{pmatrix}, \tag{4.76}$$

where a and b are real numbers and $M_{\rm atm} = M_1 \ll M_2 = M_{\rm sol}$. It was found in this scenario that $Y_B \propto +\sin\eta$, which gives the correct sign of the BAU since η is fixed (in both models) to be positive by low energy neutrino phenomenology.

To make the connection between models, in the present $SO(10)$ model let us first consider the regions of parameter space where $y^\nu_{\rm atm} \gg y^\nu_{\rm sol}$ and $M_{\rm atm} \gg M_{\rm sol}$, and the third neutrino is entirely decoupled (i.e. $M_{\rm dec} \to \infty$). In these regions of parameter space, which however do not correspond to the successful leptogenesis regions we have seen, the matrices in Eq. 4.56 approximate to

$$Y^\nu \approx \begin{pmatrix} y^\nu_{\rm sol}\, e^{i\eta} & 3y^\nu_{\rm sol} \\ 3y^\nu_{\rm sol}\, e^{i\eta} & y^\nu_{\rm atm} \\ y^\nu_{\rm sol}\, e^{i\eta} & y^\nu_{\rm atm} \end{pmatrix}, \qquad M_R \approx \begin{pmatrix} M_{\rm sol} e^{i\eta} & 0 \\ 0 & M_{\rm atm} \end{pmatrix}. \tag{4.77}$$

By the arguments presented in [108], this implies $Y_B \propto -\sin\eta$. This can be understood intuitively by noting that Eqs. 4.76 and 4.77 differ by a column swap in Y^ν. Under this swap, the relative phase between columns flips sign. This gives the wrong sign of the asymmetry and an antimatter Universe, confirmed by the exact numerical solutions which show that these regions of parameter space are not allowed, precisely because they would lead to the wrong sign of the BAU. The correct sign can be achieved, however, in the regions of parameter space where the above assumptions of a strong hierarchy between 'atm' and 'sol' are relaxed. These correspond to the successful regions shown in Figures 4.8 and 4.9.

We finally note that enforcing the hierarchy $M_{\rm atm} \ll M_{\rm sol}$ in the present model, as predicted by the $SU(5)$ model, does not recover the matrix structure of that model (as seen in Eq. 4.76). In this limit, which also requires $y^\nu_{\rm atm} \ll y^\nu_{\rm sol} \ll y^\nu_{\rm dec}$, the $SO(10)$ matrices proportional to $y^\nu_{\rm atm}$ and $M_{\rm atm}$ are negligible, and the total Yukawa and mass matrices approximate to

$$Y^\nu \approx y^\nu_{\rm sol}\, e^{i\eta} \begin{pmatrix} 1 & 3 & 1 \\ 3 & 9 & 3 \\ 1 & 3 & \dfrac{y^\nu_{\rm dec}}{y^\nu_{\rm sol} e^{i\eta}} \end{pmatrix}, \qquad M_R \approx M^\nu_{\rm sol}\, e^{i\eta} \begin{pmatrix} 1 & 3 & 1 \\ 3 & 9 & 3 \\ 1 & 3 & \dfrac{M^\nu_{\rm dec}}{M^\nu_{\rm sol} e^{i\eta}} \end{pmatrix}, \tag{4.78}$$

which are markedly different from the form of Eq. 4.76.

4.5.4 Connecting quark and neutrino parameters

$SO(10)$ unification suggests a deep relationship between quarks and leptons, and while the above leptogenesis analysis involves only leptons, the results allow us to make statements also about the quark sector. For instance, in naive $SO(10)$ GUT models, the Yukawa couplings of up-type quarks and neutrinos are the same. By the seesaw mechanism, one derives an expected range for each of the heavy right-handed neutrino masses

$M_{1,2,3}$ like $10^6 : 10^{10} : 10^{15}$. In this model the relation $Y^u = Y^\nu$ does not hold exactly, due to the presence of an adjoint Higgs H_{45}.

To see this more clearly, let us recast the Yukawa superpotential in Eq. 4.3 in terms of modified couplings $\tilde{\lambda}$, as

$$\begin{aligned} W_Y^0 = {} & \Psi_i \Psi_j H_{10}^u \left[\bar{\phi}^i_{\rm dec} \bar{\phi}^j_{\rm dec} \frac{\tilde{\lambda}^{(u)}_{\rm dec}}{M_\chi^2} + \bar{\phi}^i_{\rm atm} \bar{\phi}^j_{\rm atm} \xi \frac{\tilde{\lambda}^{(u)}_{\rm atm}}{M_\chi^3} + \bar{\phi}^i_{\rm sol} \bar{\phi}^j_{\rm sol} \xi^2 \frac{\tilde{\lambda}^{(u)}_{\rm sol}}{M_\chi^4} \right] \\ & + \Psi_i \Psi_j H_{10}^d \left[\bar{\phi}^i_{\rm dec} \bar{\phi}^j_{\rm dec} \xi \frac{\tilde{\lambda}^{(d)}_{\rm dec}}{M_\chi^3} + \bar{\phi}^i_{\rm atm} \bar{\phi}^j_{\rm atm} \xi^2 \frac{\tilde{\lambda}^{(d)}_{\rm atm}}{M_\chi^4} + \bar{\phi}^i_{\rm sol} \bar{\phi}^j_{\rm sol} \xi^3 \frac{\tilde{\lambda}^{(d)}_{\rm sol}}{M_\chi^5} \right] \\ & + \Psi_i \Psi_j H_{\overline{16}} H_{\overline{16}} \left[\bar{\phi}^i_{\rm dec} \bar{\phi}^j_{\rm dec} \xi^3 \frac{\tilde{\lambda}^{(M)}_{\rm dec}}{M_\chi^2 M^4_{\Omega_{\rm dec}}} + \bar{\phi}^i_{\rm atm} \bar{\phi}^j_{\rm atm} \xi^4 \frac{\tilde{\lambda}^{(M)}_{\rm atm}}{M_\chi^3 M^4_{\Omega_{\rm atm}}} \right. \\ & \left. + \bar{\phi}^i_{\rm sol} \bar{\phi}^j_{\rm sol} \xi^5 \frac{\tilde{\lambda}^{(M)}_{\rm sol}}{M_\chi^4 M^4_{\Omega_{\rm sol}}} \right], \end{aligned} \tag{4.79}$$

where

$$\begin{aligned} \frac{\tilde{\lambda}^{(u,d,M)}_{\rm dec}}{M_\chi^2} &= \sum_{n=0}^{2} \frac{\lambda^{(u,d,M)}_{{\rm dec},n}}{\langle H_{45} \rangle^n M_\chi^{2-n}}, \\ \frac{\tilde{\lambda}^{(u,d,M)}_{\rm atm}}{M_\chi^2} &= \sum_{n=0}^{3} \frac{\lambda^{(u,d,M)}_{{\rm atm},n}}{\langle H_{45} \rangle^n M_\chi^{3-n}}, \\ \frac{\tilde{\lambda}^{(u,d,M)}_{\rm sol}}{M_\chi^2} &= \sum_{n=0}^{4} \frac{\lambda^{(u,d,M)}_{{\rm sol},n}}{\langle H_{45} \rangle^n M_\chi^{4-n}}. \end{aligned} \tag{4.80}$$

The alignment of $\langle H_{45} \rangle$ dictates the CG coefficients associated with quarks and leptons, such that the $\tilde{\lambda}$ factors are generally different between these sectors. For example, if the VEV $\langle H_{45} \rangle$ is aligned in the $B - L$ direction then $\langle H_{45} \rangle = v_{45}/3$ for quarks and $\langle H_{45} \rangle = -v_{45}$ for leptons. For a general alignment, the practical consequence is that the real parameters in the mass matrices also differ. However, we assume that $\langle H_{45} \rangle$ is real, such that phases only arise from the phases of flavon VEVs $\langle \phi \rangle$ and $\langle \xi \rangle$.

The quark mass matrices can thus be written as

$$\begin{aligned} Y^u &= y^u_{\rm atm} \begin{pmatrix} 0 & 0 & 0 \\ 0 & 1 & 1 \\ 0 & 1 & 1 \end{pmatrix} + y^u_{\rm sol} e^{i\eta} \begin{pmatrix} 1 & 3 & 1 \\ 3 & 9 & 3 \\ 1 & 3 & 1 \end{pmatrix} + y^u_{\rm dec} \begin{pmatrix} 0 & 0 & 0 \\ 0 & 0 & 0 \\ 0 & 0 & 1 \end{pmatrix} + y^u_{\rm sd} e^{i\eta^u} \begin{pmatrix} 0 & 0 & 1 \\ 0 & 0 & 3 \\ 1 & 3 & 2 \end{pmatrix}, \\ Y^d &= y^d_{\rm atm} \begin{pmatrix} 0 & 0 & 0 \\ 0 & 1 & 1 \\ 0 & 1 & 1 \end{pmatrix} + y^d_{\rm sol} e^{i\eta} \begin{pmatrix} 1 & 3 & 1 \\ 3 & 9 & 3 \\ 1 & 3 & 1 \end{pmatrix} + y^d_{\rm dec} \begin{pmatrix} 0 & 0 & 0 \\ 0 & 0 & 0 \\ 0 & 0 & 1 \end{pmatrix}. \end{aligned} \tag{4.81}$$

We are most concerned with the relationship between up-type quark and neutrino Yukawa couplings. The difference may be parametrised by δ_i, such that

$$y_i^u = y_i^\nu + \delta_i \tag{4.82}$$

There is an additional parameter $y_{\rm sd}^u$ in Y^u not present in Y^ν. If we were to set this and the three δ_i to zero, there would be no difference between the up-type quark and neutrino Yukawa couplings, and the model would follow the expectation of naive $SO(10)$ models: three independent parameters, $y_{\rm dec}^u = y_{\rm dec}^\nu$, $y_{\rm atm}^u = y_{\rm atm}^\nu$, and $y_{\rm sol}^u = y_{\rm sol}^\nu$, which can be eliminated in terms of the GUT scale values for up, charm and top Yukawa couplings y_u, y_c, y_t.

The numerical fit to the data indicates (see Table 4.3) that $y_{\rm atm}^u \sim 10^{-5}$. This is the root of a fine-tuning in the model that arises when we compare it to $y_{\rm atm}^\nu$, which, in order to have viable leptogenesis, requires $y_{\rm atm}^\nu \sim 10^{-3} - 10^{-2}$, according to Figure 4.8. This mismatch between up-type quark and neutrino couplings is a typical problem for leptogenesis in $SO(10)$ GUT models, and would invalidate leptogenesis in naive $SO(10)$ models where the couplings need to be equal.

In the model in question it can be accommodated through a cancellation between $y_{\rm atm}^\nu$ and $\delta_{\rm atm}$ both of order $10^{-3} - 10^{-2}$, leaving $y_{\rm atm}^u \sim 10^{-5}$. It should be noted that in this model, $y_{\rm atm}^\nu \sim 10^{-3} - 10^{-2}$ is indeed the expected order of magnitude for the Dirac neutrino coupling (due to the powers of the superfield ξ). It is $y_{\rm atm}^u \sim 10^{-5}$, required by the fit, that turns out to be anomalously small, which is linked to the mass of the (first generation) up quark, m_u.

For completeness, we write down the Yukawa (and right-handed Majorana) matrices in terms of model parameters. They are

$$\begin{aligned}
(Y_{ij}^u)^* \sim (Y_{ij}^\nu)^* &= \frac{\tilde{\lambda}_{\rm atm}^{(u)}}{M_\chi^3} \langle \bar{\phi}_{\rm atm}^i \bar{\phi}_{\rm atm}^j \xi \rangle + \frac{\tilde{\lambda}_{\rm sol}^{(u)}}{M_\chi^4} \langle \bar{\phi}_{\rm sol}^i \bar{\phi}_{\rm sol}^j \xi^2 \rangle + \frac{\tilde{\lambda}_{\rm dec}^{(u)}}{M_\chi^2} \langle \bar{\phi}_{\rm dec}^i \bar{\phi}_{\rm dec}^j \rangle \,, \\
(Y_{ij}^d)^* \sim (Y_{ij}^e)^* &= \frac{\tilde{\lambda}_{\rm atm}^{(d)}}{M_\chi^4} \langle \bar{\phi}_{\rm atm}^i \bar{\phi}_{\rm atm}^j \xi^2 \rangle + \frac{\tilde{\lambda}_{\rm sol}^{(d)}}{M_\chi^5} \langle \bar{\phi}_{\rm sol}^i \bar{\phi}_{\rm sol}^j \xi^3 \rangle + \frac{\tilde{\lambda}_{\rm dec}^{(d)}}{M_\chi^3} \langle \bar{\phi}_{\rm dec}^i \bar{\phi}_{\rm dec}^j \xi \rangle \,, \\
(M_{ij}^N)^* &= \langle H_{\overline{16}} \rangle^2 \left[\frac{\tilde{\lambda}_{\rm atm}^{(M)}}{M_\chi^3 M_{\Omega_{\rm atm}}^4} \langle \bar{\phi}_{\rm atm}^i \bar{\phi}_{\rm atm}^j \xi^4 \rangle + \frac{\tilde{\lambda}_{\rm sol}^{(M)}}{M_\chi^4 M_{\Omega_{\rm sol}}^4} \langle \bar{\phi}_{\rm sol}^i \bar{\phi}_{\rm sol}^j \xi^5 \rangle \right. \\
&\qquad \left. + \frac{\tilde{\lambda}_{\rm dec}^{(M)}}{M_\chi^2 M_{\Omega_{\rm dec}}^4} \langle \bar{\phi}_{\rm dec}^i \bar{\phi}_{\rm dec}^j \xi^3 \rangle \right] ,
\end{aligned} \tag{4.83}$$

where the complex conjugation arises when moving from the SUSY basis to the seesaw basis. We have neglected the additional mixed "sol-dec" term in Y^u for convenience, since it has no direct bearing on leptogenesis. The real input parameters of the matrices

can then be read off explicitly as

$$\begin{aligned}
y^u_{\rm atm} \sim y^\nu_{\rm atm} &= \tilde{\lambda}^{(u)}_{\rm atm} |v_{\rm atm}|^2 |v_\xi| / M_\chi^3, \\
y^u_{\rm sol} \sim y^\nu_{\rm sol} &= \tilde{\lambda}^{(u)}_{\rm sol} |v_{\rm sol}|^2 |v_\xi|^2 / M_\chi^4, \\
y^u_{\rm dec} \sim y^\nu_{\rm dec} &= \tilde{\lambda}^{(u)}_{\rm dec} |v_{\rm dec}|^2 / M_\chi^2, \\
y^d_{\rm atm} \sim y^e_{\rm atm} &= \tilde{\lambda}^{(d)}_{\rm atm} |v_{\rm atm}|^2 |v_\xi|^2 / M_\chi^4, \\
y^d_{\rm sol} \sim y^e_{\rm sol} &= \tilde{\lambda}^{(d)}_{\rm sol} |v_{\rm sol}|^2 |v_\xi|^3 / M_\chi^5, \\
y^d_{\rm dec} \sim y^e_{\rm dec} &= \tilde{\lambda}^{(d)}_{\rm dec} |v_{\rm dec}|^2 |v_\xi| / M_\chi^3, \\
M_{\rm atm} &= \tilde{\lambda}^{(M)}_{\rm atm} |v_{\rm atm}|^2 |v_\xi|^4 |v_{H_{\overline{16}}}|^2 / (M_\chi^3 M^4_{\Omega_{\rm atm}}), \\
M_{\rm sol} &= \tilde{\lambda}^{(M)}_{\rm sol} |v_{\rm sol}|^2 |v_\xi|^5 |v_{H_{\overline{16}}}|^2 / (M_\chi^4 M^4_{\Omega_{\rm atm}}), \\
M_{\rm dec} &= \tilde{\lambda}^{(M)}_{\rm dec} |v_{\rm dec}|^2 |v_\xi|^3 |v_{H_{\overline{16}}}|^2 / (M_\chi^2 M^4_{\Omega_{\rm atm}}), \\
\eta &= -\arg\left[v^2_{\rm sol} v_\xi / v^2_{\rm atm}\right], \\
\eta' &= -\arg\left[v^2_{\rm dec} / (v^2_{\rm atm} v_\xi)\right].
\end{aligned} \tag{4.84}$$

4.6 Summary of features

In this chapter we have presented a SUSY GUT of flavour, where all known fermions are united into a single $(3, 16)$ representation of the $\Delta(27) \times SO(10)$ group. Emphasis has been put on the Yukawa sector, where the CSD(3) vacuum alignments dictate the matrix structures of quarks and leptons. In particular, all mass matrices have nearly the same structure, given as sums over rank-1 matrices. This provides a simple interpretation of fermion structures without fine-tuning. We have shown that a good fit to data, i.e. a low χ^2, can be achieved in all sectors.

The model is both fairly complete and quite natural: hierarchies arise dynamically from a renormalisable superpotential that fixes all mass scales in terms of Higgs and flavon VEVs, shaped by an auxiliary $\mathbb{Z}_9 \times \mathbb{Z}_{12}$ symmetry. Although it requires a rather large field content (with no field larger than an $SO(10)$ adjoint), the model is capable of addressing many important problems in GUT model building, including proton decay, doublet-triplet splitting and the μ problem.

Furthermore, we have shown that, unlike in naive $SO(10)$, the observed baryon asymmetry of the Universe can be explained by the lightest right-handed neutrino decays in thermal N_1 leptogenesis. This required solving the flavoured Boltzmann equations numerically, which yielded predictions for the right-handed neutrino masses, or equivalently the elements of the neutrino Yukawa matrix.

Chapter 5

An $S_4 \times SO(10)$ model

The work presented thus far has had several core aims, chiefly that of explaining the observed masses and mixing patterns of both quarks and leptons, catalysed by the phenomenological success of sequential dominance in the lepton sector. We have shown how the CSD(3) alignment can be realised in SUSY GUTs based on both $SU(5)$ and $SO(10)$ with flavour symmetry, and discussed the implications for leptogenesis. These models followed the guiding principle of completeness: they are renormalisable theories with a specific field content that explicitly shows how the Yukawa structures are obtained, the symmetries are broken, the VEVs aligned, and how to recover the MSSM at low scales. To achieve all this, these models employ a large field content that resides primarily at the GUT scale, and most likely cannot ever be directly observed. Moreover, it is less clear which components are essential for resolving the flavour puzzle specifically.

Drawing from the knowledge gained in the construction of the $\Delta(27) \times SO(10)$ model of the previous chapter, as well as recent developments in flavour model building, we aimed to find a simpler model, where the origin of flavour is made apparent. Those efforts led to the work in [6], which forms the basis of this chapter, and discusses an $S_4 \times SO(10)$ SUSY GUT of flavour.

5.1 A simpler $SO(10)$ GUT of flavour

To begin, let us reiterate some key aspects of the flavour puzzle. We know that charged fermion masses are very hierarchical, with the up-type quark mass hierarchy $m_u \ll m_c \ll m_t$ being stronger than for the down-type quark masses $m_d \ll m_s \ll m_b$, which resemble more closely the charged lepton masses $m_e \ll m_\mu \ll m_\tau$. The lightest charged fermion is the electron, with $m_e \sim 0.5$ MeV. Quark mixing, encoded in the CKM matrix, is small and hierarchical. The discovery of neutrino mass and mixing makes the flavour problem more acute but also provides new features, namely small neutrino masses, and

large lepton mixing (encoded in the PMNS matrix U) resembling tri-bimaximal (TB) mixing, but with non-zero reactor angle. The origin, nature and ordering of the neutrino masses remain open questions, but cosmology suggests that all neutrino masses must be below about 100 meV [37], making them by far the lightest (known) fermions in nature.

The smallness of neutrino mass may originate in the type-I seesaw mechanism, wherein a natural way to obtain large lepton mixing and normal neutrino ordering is to assume the sequential dominance of right-handed neutrinos (which arise naturally in $SO(10)$), predicting $m_1 \ll m_2 \ll m_3 \sim 50$ meV. The magnitude of atmospheric and solar mixing is determined by ratios of Yukawa couplings, which can easily be large, while the reactor mixing is typically $U_{e3} \lesssim \mathcal{O}(m_2/m_3) \approx 0.17$, a prediction made over a decade before the reactor angle was measured.

To obtain precise predictions for mixing one can impose constraints on the Yukawa couplings, where the CSD(3) scheme is particularly successful, although in this model it appears in a slightly different form. The flavon vacuum alignments are fixed by a superpotential which we do not specify here, but is given in a recent publication [96], where they show that CSD(3) can be enforced by an S_4 symmetry. In particular, they find that the CSD(3) alignments preserve a generator of the symmetry (specifically, the SU generator). By comparison, $\Delta(27)$ cannot enforce the CSD(3) alignments by symmetry alone, requiring several orthogonality conditions between flavons and a rather complicated superpotential (found in Appendix C).

After implementing the seesaw mechanism, the flavon VEVs yield a light effective Majorana neutrino mass matrix,

$$m^\nu = \mu_1 Y_{11} + \mu_2 Y_{22} + \mu_3 Y_{33}, \tag{5.1}$$

where $Y_{ij} \sim \langle \phi_i \rangle \langle \phi_j \rangle^\intercal$, up to S_4 Clebsch-Gordan (CG) factors. While the ability to express mass matrices as sums over low-rank matrices was known previously, the prospects for model building were not fully explored. The $\Delta(27) \times SO(10)$ model applied the above structure universally across all fermion sectors, which seems quite appealing at first sight. However, it led to problems in the quark sector, which were fixed by adding an extra non-universal term in the up-type quark Yukawa matrix, together with some degree of fine-tuning between matrix coefficients in order to obtain the correct quark masses and mixing angles.

Against this backdrop, we present an $S_4 \times SO(10)$ SUSY GUT of flavour in which CSD(3) is embedded. Our guiding principles are firstly simplicity, involving the fewest number of low-dimensional fields, secondly naturalness, and thirdly completeness, which includes ensuring doublet-triplet splitting. What does natural mean? For us it means that we have a qualitative explanation of fermion mass and mixing hierarchies with all dimensionless parameters $\mathcal{O}(1)$, and in particular that the Yukawa matrices are obtained from sums of low-rank matrices, where each matrix in the sum naturally accounts for the

mass of a particular family, analogous to sequential dominance in the neutrino sector. This qualitative picture of "universal sequential dominance" is underpinned by a detailed quantitative fit of the fermion spectrum.

In order to achieve this, we shall introduce two Higgs **10**s, H_{10}^u and H_{10}^d, which will give rise at low energy to the MSSM Higgs doublets, H_u and H_d, respectively, with no appreciable Higgs mixing effects. Neutrinos and up-type quarks, which couple to H_{10}^u, have Yukawa matrices with the universal structure as in Eq. 5.1. The charged leptons and down-type quarks, which couple to H_{10}^d, have Yukawa matrices with a different universal structure where Y_{11} is replaced by $Y_{12} \sim \langle\phi_1\rangle \langle\phi_2\rangle^{\mathsf{T}}$. Quark mixing originates primarily in the down-type quark sector, with the down and strange quark masses successfully realised by having a zero entry in the (1,1) element of the down-type quark Yukawa matrix Y^d, as in the Gatto-Sartori-Tonin (GST) approach [206], with a milder hierarchy among down-type quarks as compared to up-type quarks.

The model accurately fits all available quark and lepton data, and predicts a leptonic CP phase δ^ℓ that deviates significantly from maximal. Since quark mixing dominantly originates from Y^d, analytical estimates for the quark mixing angles can be obtained. A hierarchy in the flavon VEVs fixes the scales of all but one parameter, with all dimensionless couplings in the renormalisable theory naturally $\mathcal{O}(1)$. The model reduces to the MSSM, and we demonstrate how a μ term of $\mathcal{O}$(TeV) can be realised, as well as doublet-triplet splitting, with Planck scale proton decay operators suppressed. In order to achieve the above we also require auxiliary $\mathbb{Z}_4^2$ and $\mathbb{Z}_4^R$ symmetries and a spectrum of messenger fields.

We would like to emphasise that the model presented here is very different from earlier models based on $S_4 \times SO(10)$ [166–169] (see also [170–172]).[1] Firstly, the full symmetry is different, since we invoke an extra $\mathbb{Z}_4^2 \times \mathbb{Z}_4^R$ symmetry, while earlier works use a $\mathbb{Z}_n$ [167–169]. Furthermore, we only allow small Higgs representations **10** (fundamental), **16** (spinor) and **45** (adjoint) and not the large Higgs representations such as the $\overline{\mathbf{126}}$ and **120** which are used in the other approaches. As a consequence our neutrino masses follow from a type-I seesaw mechanism, rather than a type-II seesaw employed in other papers. In further contrast, we do not allow Higgs mixing: the MSSM Higgs doublets H_u and H_d emerge directly from H_{10}^u and H_{10}^d, respectively, whereas in [166–169] they arise as unconconstrained linear combinations of doublets contained in 10- and 126-dimensional Higgs fields. In addition we consider doublet-triplet splitting. These features are largely absent from earlier works.

Another important difference is that we have used the CSD(3) vacuum alignments in [96], whereas the vacuum aligments used in most previous works were geared towards TB mixing, and do not naturally provide a large reactor angle. Indeed this model, as

[1] Previous works on $SO(10)$ models with non-Abelian discrete flavour symmetries are found in [147, 148, 161–165, 173, 174], and further flavoured GUTs can be found in citenonAbelian. More recently, a generalised approach to flavour symmetries in $SO(10)$ is considered in [207, 208].

those discussed earlier, is motivated by the success of CSD(3) in the neutrino sector, with an emphasis now on a simpler realisation in $SO(10)$ and a natural description of all hierarchies.

5.2 The model

5.2.1 Basic features

In the present model quarks and leptons are unified in ψ, a $(3', 16)$ representation of $S_4 \times SO(10)$, and with $H_{10}^{u,d}$ in $(1, 10)$ and ϕ_i in $(3', 1)$ representations. The idea is that the up-type quark Yukawa matrix Y^u and neutrino Yukawa matrix Y^ν arise from effective terms like

$$H_{10}^u(\psi\phi_1)(\psi\phi_1) + H_{10}^u(\psi\phi_2)(\psi\phi_2) + H_{10}^u(\psi\phi_3)(\psi\phi_3), \tag{5.2}$$

where the group contraction in each bracket is into an S_4 singlet. These non-renormalisable operators will have denominator scales of order $M_{\rm GUT}$, determined by the VEVs of additional Higgs adjoint **45**s, leading to various CG factors. The resultant Yukawa matrices Y^u and Y^ν are sums of rank-1 matrices as in Eq. 5.1, with independent coefficients multiplying each rank-1 matrix. We assume the flavon vacuum alignments

$$\langle\phi_1\rangle = v_1 \begin{pmatrix} 1 \\ 3 \\ -1 \end{pmatrix}, \quad \langle\phi_2\rangle = v_2 \begin{pmatrix} 0 \\ 1 \\ -1 \end{pmatrix}, \quad \langle\phi_3\rangle = v_3 \begin{pmatrix} 0 \\ 1 \\ 0 \end{pmatrix}. \tag{5.3}$$

We note that these alignments preserve the SU generator of S_4. These differ from the alignments considered previously, but give equivalent predictions for neutrino mixing parameters, and are considered a variant of CSD(3), as discussed in [96]. Their VEVs are driven to scales with the hierarchy

$$v_1 \ll v_2 \ll v_3 \sim M_{\rm GUT}, \tag{5.4}$$

so that each rank-1 matrix in the sum contributes dominantly to a particular family, giving a rather natural understanding of the hierarchical Yukawa couplings whereby $y_u \sim v_1^2/M_{\rm GUT}^2$, $y_c \sim v_2^2/M_{\rm GUT}^2$, $y_t \sim v_3^2/M_{\rm GUT}^2$, and similarly for the neutrino Yukawa couplings. In this discussion we shall not provide an explanation for this hierarchy of VEVs, nor shall we repeat the vacuum alignment superpotential responsible for the alignments in Eq. 5.3, found in [96]. Since the expansion breaks down for the third family, in the complete model we shall find a renormalisable explanation of the third-family Yukawa couplings. The right-handed neutrino Majorana mass matrix will also have the same universal form, leading to the seesaw mass matrix as in Eq. 5.1.

The down-type quark Yukawa matrix Y^d and charged lepton Yukawa matrix Y^e arise from terms like

$$H^d_{10}(\psi\phi_1)(\psi\phi_2) + H^d_{10}(\psi\phi_2)(\psi\phi_2) + H^d_{10}(\psi\phi_3)(\psi\phi_3), \tag{5.5}$$

introducing a mixed term involving ϕ_1 and ϕ_2, leading to a new rank-2 Yukawa structure $Y_{12} \sim \langle\phi_1\rangle \langle\phi_2\rangle^\intercal$. In the Yukawa matrices Y^d and Y^e, Y_{11} is replaced by Y_{12}, which has two consequences: it enforces a zero in the (1,1) element of Y^d, giving the GST relation for the Cabibbo angle, i.e. $\theta^q_{12} \approx \sqrt{y_d/y_s}$, and also leads to a milder hierarchy in the down and charged lepton sectors. Both features are welcome.

We need additional symmetries and fields to ensure the above structures, provide renormalisable third family Yukawa couplings, give the desired Clebsch-Gordan relations to distinguish down-type quarks from charged leptons, achieve doublet-triplet splitting, and obtain the MSSM Higgs doublets H_u and H_d from H^u_{10} and H^d_{10}, respectively.

5.2.2 Field content and superpotential

The full superfield content of the model is given in Table 5.1. It contains the following: a "matter" superfield ψ containing all known Standard Model fermions, three triplet flavons ϕ which acquire CSD(3) vacuum alignments, two Higgs **10**s containing one each of the electroweak-scale Higgs $SU(2)$ doublets, a spinor $H_{\overline{16}}$ which breaks $SO(10)$ (and, along with the singlet ρ, gives masses to the right-handed neutrinos), as well as several Higgs adjoints. The χ superfields are messengers that are integrated out below the GUT scale, and are given GUT-scale masses by the VEV of H^Z_{45}. We assume that the MSSM Higgs doublets H_u, H_d lie completely inside, respectively, the $SO(10)$ multiplets H^u_{10}, H^d_{10}. This is justified in Section C.4 of Appendix C.

Two $\mathbb{Z}_4$ shaping symmetries help to forbid unwanted mixed flavon Yukawa terms. We also assume a discrete R symmetry $\mathbb{Z}^R_4$, under which the superpotential has total charge two, and which is broken at the GUT scale by the H^{B-L}_{45} VEV to $\mathbb{Z}^R_2$, the usual R (or matter) parity in the MSSM, ensuring a stable LSP. It also controls the μ term and helps ensure that only two light Higgs doublets (and no Higgs triplets) are present in the effective MSSM. $\mathbb{Z}^R_4$ is the smallest R symmetry that can achieve the above, and is specially motivated within $SO(10)$ [124]. We shall also assume a spontaneously broken CP symmetry at the high scale.

At the GUT scale, the renormalisable Yukawa superpotential is given by

$$\begin{aligned} W^{(\mathrm{GUT})}_Y = {} & \psi\phi_a\overline{\chi}_a + \overline{\chi}_a\chi_a H^Z_{45} + \chi_a\chi_a H^u_{10} + \rho\chi_3 H_{\overline{16}} + M_\rho\rho\rho \\ & + \overline{\chi}_b\chi'_b\left(H^X_{45} + H^Y_{45}\right) + \chi'_b\chi'_b H^d_{10} + \chi_1\chi_2 H^d_{10}, \end{aligned} \tag{5.6}$$

Field	Representation				
	S_4	$SO(10)$	$\mathbb{Z}_4$	$\mathbb{Z}_4$	$\mathbb{Z}_4^R$
ψ	$3'$	16	1	1	1
H_{10}^u	1	10	0	2	0
H_{10}^d	1	10	2	0	0
$H_{\overline{16}}$	1	$\overline{16}$	2	1	0
H_{16}	1	16	1	2	0
$H_{45}^{X,Y}$	1	45	2	1	0
H_{45}^{Z}	1	45	1	2	0
H_{45}^{B-L}	1	45	2	2	2
ϕ_1	$3'$	1	0	0	0
ϕ_2	$3'$	1	2	0	0
ϕ_3	$3'$	1	0	2	0

(a) Matter, Higgs and flavon superfields.

Field	Representation				
	S_4	$SO(10)$	$\mathbb{Z}_4$	$\mathbb{Z}_4$	$\mathbb{Z}_4^R$
$\overline{\chi}_1$	1	$\overline{16}$	3	3	1
χ_1	1	16	0	3	1
$\overline{\chi}_2$	1	$\overline{16}$	1	3	1
χ_2	1	16	2	3	1
$\overline{\chi}_3$	1	$\overline{16}$	3	1	1
χ_3	1	16	0	1	1
χ_3'	1	16	3	2	1
χ_2'	1	16	1	0	1
ρ	1	1	2	2	1

(b) Messenger superfields.

Table 5.1: Field content giving the Yukawa superpotential in Eq. 5.6.

where we sum over indices $a = 1, 2, 3$ and $b = 2, 3$, and have suppressed $\mathcal{O}(1)$ coefficients λ that multiply each term. Furthermore, there are several crucial terms that appear suppressed by one Planck mass M_P. These are

$$W_Y^{(\text{Planck})} = \frac{\chi_a \chi_a H_{\overline{16}} H_{\overline{16}}}{M_P} + \frac{\psi\psi\phi_3 H_{10}^d}{M_P}, \tag{5.7}$$

where $a = 1, 2, 3$. The first term couples $H_{\overline{16}}$ to fermions via the messengers. The second is allowed by the symmetries and will be shown to contribute at the order of the smallest GUT-scale terms to the fermion Yukawa matrices, and thus cannot be ignored.

The adjoint Higgs superfields acquire VEVs at the GUT scale, i.e. $\langle H_{45}^k \rangle \sim M_{\text{GUT}}$, which are generally complex. $H_{45}^{X,Y,Z}$ gain different (Standard Model-preserving) VEVs, providing CG factors which separate the quark and lepton masses. The VEVs of ϕ_1 and ϕ_2 are assumed to acquire VEVs well below the GUT scale, i.e. $\langle \phi_{1,2} \rangle \ll M_{\text{GUT}}$, while $\langle \phi_3 \rangle \sim M_{\text{GUT}}$, which is therefore also the scale at which the flavour symmetry is broken, along with CP. We note that no residual CP symmetry remains at low scales. As $\langle \phi_3 \rangle$ is near the messenger scale, the process of integrating out messengers $\chi_3, \overline{\chi}_3$ is not trivial. The correct procedure and the consequences of having a flavon VEV near M_{GUT} are discussed in detail below, where we verify also that the third family Yukawa couplings are renormalisable at the electroweak scale.

The diagrams giving the mass and Yukawa matrices are drawn in Figures 5.1 – 5.3. The three diagrams in Figure 5.1 correspond to the ultraviolet completion of the three terms in Eq. 5.2, while those in Figure 5.2 are the completion of the terms in Eq. 5.5. The diagrams ensure correct S_4 group theory contractions and introduce CG coefficients due to the $H_{45}^{X,Y,Z}$ VEVs. These diagrams are analogous to how the seesaw mechanism

replaces the Weinberg operator for neutrino mass. Of course neutrino mass itself in this model is more subtle, since both the Dirac and right-handed Majorana masses arise from these diagrams.

Each diagram leads to a 3×3 matrix, whose internal structure is dictated by the vacuum alignment of the relevant flavon VEVs in Eq. 5.3. The Yukawa and mass matrices are consequently given as a sum over these matrices. A prominent feature is a texture zero in the (1,1) element of Y^d and Y^e, which realises the GST relation for the Cabibbo angle. The exact matrices that we fit to data are given below.

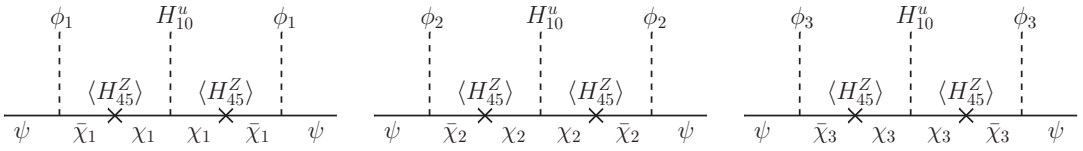

Figure 5.1: Diagrams coupling ψ to H^u_{10}, giving the up-type quark and Dirac neutrino Yukawa terms.

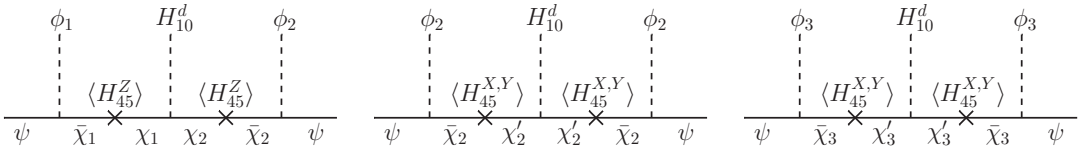

Figure 5.2: Diagrams coupling ψ to H^d_{10}, giving the down-type quark and charged lepton Yukawa terms.

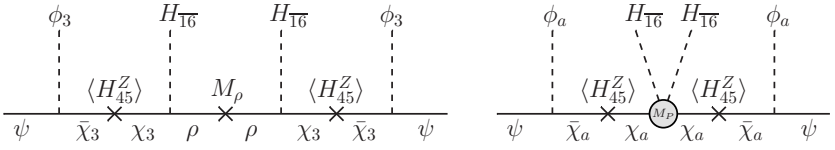

Figure 5.3: Diagrams coupling ψ to $H_{\overline{16}}$, giving the right-handed neutrino mass terms. One copy of the right-hand diagram may be drawn for each of $a = 1, 2, 3$, although for $a = 3$, its contribution is negligible compared to the left diagram.

Planck-scale operators suppressed by one power of the Planck mass M_P, beyond those in Eq. 5.7, are forbidden by the symmetries. However we expect additional effective operators arising in the model, suppressed by at least two powers of the Planck mass M_P^2. These include terms involving all possible contractions of S_4 multiplets ψ and ϕ_i, which are forbidden at the renormalisable level, but allowed by the symmetries. The largest of these terms can be $\mathcal{O}(M^2_{\rm GUT}/M^2_P) \sim 10^{-6}$. We will assume these contributions are negligible, but note that such corrections may pollute the texture zero in Y^d.

5.2.3 Clebsch-Gordan factors

An adjoint of $SO(10)$ can acquire a VEV aligned in the direction of any of the four $U(1)$ subgroup generators that commute with the Standard Model, or a combination thereof.

There are four such $U(1)$ symmetries, labelled $U(1)_X$, $U(1)_Y$, $U(1)_{B-L}$, $U(1)_{T_R^3}$. $U(1)_X$ arises from the breaking $SO(10) \to SU(5) \times U(1)_X$. $U(1)_Y$ is the Standard Model hypercharge which arises when $SU(5) \to SU(3) \times SU(2)_L \times U(1)_Y$. The other two $U(1)$ arise when $SO(10)$ is broken along the Pati-Salam chain, via a LR-symmetric gauge group. Their generators are not linearly independent; two of them may be expressed in terms of the other two. The VEVs of $H_{45}^{X,Y,Z}$ may be written as linear combinations of these alignments. Without loss of generality we may assume $\langle H_{45}^X \rangle$ and $\langle H_{45}^Y \rangle$ align in the "X" and "Y" directions, respectively, while $\langle H_{45}^Z \rangle$ is a linear combination of the two.

Fermions couple to these VEVs with strengths that depend on their associated $U(1)$ charges, which are different for quarks and leptons. H_{45}^{B-L} is assumed to gain a VEV in the direction that preserves $B - L$, generating GUT-scale masses for Higgs triplets via the Dimopoulos-Wilczek (DW) mechanism [184–186]. Our implementation of the DW mechanism is described in Appendix C.

Up-type quarks and Dirac neutrinos couple to H_{45}^Z (see Figure 5.1). As $\langle H_{45}^Z \rangle$ is arbitrary, there is no hard prediction for the ratio between quark and neutrino Yukawa couplings within a family. However, as all flavons ϕ_a couple to this VEV in the same way, flavour unification demands that the same ratio hold for all families. Therefore, once Y^u is determined, Y^ν is also fixed, such that $Y^\nu \propto Y^u$ to good approximation, up to an overall CG factor, with small deviations for the third family.

Meanwhile, the down-type quarks and charged leptons couple to H_{45}^X and H_{45}^Y (see Figure 5.2). Unlike the up sector, where matter always couples to the same $SO(10)$ adjoint VEV, each diagram like Figure 5.2 involving a different flavon will couple to a different linear combination of VEVs. This introduces CG factors non-trivially into Y^d and Y^e. As such, there is no fixed relationship between down-type quark and charged lepton Yukawa couplings, neither within a family, nor across families. They are nevertheless expected to be of the same order.

5.2.4 Renormalisability of the third family

Next, we show that naive integration over messenger fields is not possible for the third family, due to the large VEV of ϕ_3. We reiterate that there is an assumed hierarchy of flavon VEVs, such that $v_1 \ll v_2 \ll v_3 \sim M_{\text{GUT}}$, implying it is not possible to formally integrate out the messengers χ_3 which couple to the flavon ϕ_3.

To explore this further, let us single out the terms in W_Y involving these fields and H_{10}^u (the same method applies to terms coupling to H_{10}^d). Suppressing $\mathcal{O}(1)$ couplings, the relevant terms are

$$W_Y^{(3)} = \psi\phi_3\overline{\chi}_3 + H_{45}^Z\chi_3\overline{\chi}_3 + \chi_3\chi_3 H_{10}^u. \tag{5.8}$$

After fields acquire VEVs (with $\langle\phi_3\rangle = v_3(0,0,1)$), we have

$$W_Y^{(3)} = v_3\psi_3\overline{\chi}_3 + \langle H_{45}^Z\rangle\,\chi_3\overline{\chi}_3. \tag{5.9}$$

These two terms are of comparable order.

Naïvely, ψ_3 may be interpreted as the set of third-family particles. The problem with this picture is that it has a large coupling to $\overline{\chi}_3$, which induces a mass for ψ_3 via the second term in Eq. 5.9. This clearly does not correspond to the physical third-family states (top quark and third Dirac neutrino), which are massless above the electroweak scale. To obtain the physical (massless) states, which we label t, we rotate into a physical basis $(\psi_3, \chi_3) \to (t, \chi)$, such that t does not couple to $\overline{\chi}_3$. This basis change is given by

$$\psi_3 = \frac{\langle H_{45}^Z\rangle\, t + v_3\,\chi}{r}, \quad \chi_3 = \frac{-v_3\, t + \langle H_{45}^Z\rangle\,\chi}{r}; \quad r = \sqrt{v_3^2 + \langle H_{45}^Z\rangle^2}. \tag{5.10}$$

Physically, it may be interpreted as follows: inside the original superpotential W_Y lie the terms

$$\mathcal{W}_Y \supset \chi_3\chi_3 H_{10}^u \supset \frac{v_3^2}{v_3^2 + \langle H_{45}^Z\rangle^2}\, t\, t\, H_{10}^u, \tag{5.11}$$

which generate renormalisable mass terms for the top quark and the third Dirac neutrino at the electroweak scale.

The factors that multiply the renormalisable Yukawa couplings can in principle modify the third row and column of a given fermion Yukawa matrix independently of any particular vacuum alignment. They depend on the alignment of the $SO(10)$ adjoint VEV in question, and the corresponding CG factors. In principle this can alter the relation $Y^\nu \propto Y^u$, which is the natural prediction. For simplicity, we assume these coefficients are all 1.

5.2.5 Proton decay

As noted in previous chapters, we must consider also the model predictions for proton decay. We reach similar conclusions for the present model as in earlier discussions. Recall that the proton lifetime is constrained by experiment to $\tau_p \gtrsim 10^{32}$ years [23].[2] In SUSY $SO(10)$ GUTs, proton decay can be mediated by heavy gauge bosons and or Higgs $SU(3)$ triplets, with the dominant contribution involving triplet Higgsinos. The decay width depends on details of SUSY breaking and the coupling texture of the triplets. It has been shown that the experimental constraints are met when triplets are at the GUT scale [189, 190]. As shown in Appendix C, this is the case here.

[2] As noted in the previous chapter, the proton lifetime bounds vary with the decay mode, giving $\tau_p > 10^{31-33}$ years. For simplicity, we consider only a single bound here.

The existence of additional fields in the model may also allow proton decay from effective terms of the type

$$gQQQL\frac{\langle X\rangle}{M_P^2}. \tag{5.12}$$

Such terms must obey the constraint $g\langle X\rangle < 3\times 10^9$ GeV. In our model, the largest contribution of this type comes from the term

$$\psi\psi\psi\psi\frac{H_{45}^{B-L}(H_{45}^{X,Y}H_{45}^{Z})^2}{M_P^6} \quad\Rightarrow\quad \langle X\rangle = \frac{(M_{GUT})^5}{M_P^4}\sim 10^3 \text{ GeV}. \tag{5.13}$$

The constraint on $\langle X\rangle$ is easily met, so proton decay from such terms is highly suppressed.

5.3 Mass matrices and analytical estimates

5.3.1 Mass matrices

We present here the Yukawa and mass matrices, which will be used in the numerical fits below. A detailed derivation is given below, in Section 5.3.3. We begin by defining numerical matrices

$$\begin{aligned} Y_{11} &= \begin{pmatrix}1&1&3\\1&1&3\\3&3&9\end{pmatrix}, \qquad Y_{22} = \begin{pmatrix}0&0&0\\0&1&1\\0&1&1\end{pmatrix}, \qquad Y_{33} = \begin{pmatrix}0&0&0\\0&0&0\\0&0&1\end{pmatrix}, \\ Y_{12} &= \begin{pmatrix}0&1&1\\1&2&4\\1&4&6\end{pmatrix}, \qquad Y_P = \begin{pmatrix}0&0&-1\\0&2&0\\-1&0&0\end{pmatrix}. \end{aligned} \tag{5.14}$$

We note that all matrices derive from triplet products like $(\psi\phi_i)(\psi\phi_j)$, with S_4 singlet contractions in each bracket, except Y_P which derives from the Planck-suppressed operator $\psi\psi\phi_3 H_{10}^d$.

The up, down, charged lepton and Dirac neutrino Yukawa matrices (Y^u, Y^d, Y^e and Y^ν respectively) and right-handed neutrino mass matrix $M^{\rm R}$ arising from Figures 5.1 – 5.3, assuming that the MSSM Higgs doublets H_u and H_d arise from H_{10}^u and H_{10}^d, respectively, may then be expressed as

$$\begin{aligned} Y^u &= y_1^u e^{i\eta}Y_{11} + y_2^u Y_{22} + y_3^u e^{i\eta'}Y_{33}, \\ Y^\nu &= y_1^\nu e^{i\eta}Y_{11} + y_2^\nu Y_{22} + y_3^\nu e^{i\eta'}Y_{33}, \\ M^{\rm R} &= M_1^{\rm R} e^{i\eta}Y_{11} + M_2^{\rm R} Y_{22} + M_3^{\rm R} e^{i\eta'}Y_{33}, \\ Y^d &= y_{12}^d e^{i\frac{\eta}{2}}Y_{12} + y_2^d e^{i\alpha_d}Y_{22} + y_3^d e^{i\beta_d}Y_{33} + y^P e^{i\gamma}Y_P, \\ Y^e &= y_{12}^e e^{i\frac{\eta}{2}}Y_{12} + y_2^e e^{i\alpha_e}Y_{22} + y_3^e e^{i\beta_e}Y_{33} + y^P e^{i\gamma}Y_P. \end{aligned} \tag{5.15}$$

The flavon VEVs v_a are complex, with the fixed phase relation

$$\eta = \arg\left[\frac{v_1}{v_2}\right]^2 = -\frac{2\pi}{3}, \tag{5.16}$$

given (up to a sign) by the superpotential that fixes the alignments. The remaining phase η' is determined by the fit.

The light neutrino mass matrix is obtained by the seesaw mechanism. Both Y^ν and $M^{\rm R}$ have the same structure, namely both are sums over the same rank-1 matrices Y_{11}, Y_{22} and Y_{33}. By the proof given in the previous chapter (see Section 4.2.4), the light neutrino matrix m^ν will also have this structure, i.e.

$$\begin{aligned} m^\nu &= \mu_1 e^{i\eta} Y_{11} + \mu_2 Y_{22} + \mu_3 e^{i\eta'} Y_{33} \\ &= \mu_1 e^{i\eta} \begin{pmatrix} 1 & 1 & 3 \\ 1 & 1 & 3 \\ 3 & 3 & 9 \end{pmatrix} + \mu_2 \begin{pmatrix} 0 & 0 & 0 \\ 0 & 1 & 1 \\ 0 & 1 & 1 \end{pmatrix} + \mu_3 e^{i\eta'} \begin{pmatrix} 0 & 0 & 0 \\ 0 & 0 & 0 \\ 0 & 0 & 1 \end{pmatrix}, \end{aligned} \tag{5.17}$$

where the parameters μ_i are given in terms of the parameters y_i^ν and $M_i^{\rm R}$ simply by

$$\mu_i = v_u^2 \frac{(y_i^\nu)^2}{M_i^{\rm R}}. \tag{5.18}$$

As shown in the Introduction, the flavons yield a light neutrino mass matrix m^ν, where the normal hierarchy $m_1 \ll m_2 \ll m_3$ then corresponds to $\mu_3 \lesssim \mu_1 \ll \mu_2$. Achieving this hierarchy after seesaw implies that the right-handed neutrino masses are very hierarchical, as we will see below.[3]

5.3.2 Analytical estimates

The mass matrices involve the following real free parameters: y_i^u, y_i^d, y_i^e, μ_i, and y^P (a total of 13). Recalling that η is fixed by flavon vacuum alignment, we have the following further free parameters: η', $\alpha_{d,e}$, $\beta_{d,e}$, and γ (a total of six). The scales of the real parameters are mostly fixed by the scales of the flavon VEVs, $v_{1,2,3}$. We set the flavon VEV scales to some appropriate values,

$$v_1 \approx 0.002 M_{\rm GUT}, \quad v_2 \approx 0.05 M_{\rm GUT}, \quad v_3 \approx 0.5 M_{\rm GUT}, \tag{5.19}$$

where we set $M_{\rm GUT} \simeq 10^{16}$ GeV. The terms giving $M_{1,2}^{\rm R}$ and y^P in $M^{\rm R}$ and $Y^{d,e}$ derive from terms suppressed by one Planck mass M_P. As they arise from unspecified dynamics, the scale of these parameters is not very well defined. For definiteness, we set

[3] While the model does not mathematically forbid an inverted hierarchy, we have checked that the corresponding predictions for neutrino masses and mixing angles would always give a bad fit to data. It would also require parameter choices that strongly violate the naturalness principle employed here.

$M_P \simeq 10^{19}$ GeV and again assume the associated coefficients are close to one. Recall also that $M_3^{\rm R}$ is at the GUT scale due to the term $\rho\chi_3 H_{\overline{16}}$.

We may estimate the parameters of the matrices defined in Eq. 5.15 as follows: set all $\mathcal{O}(1)$ coefficients to exactly one, and ignore CG factors by setting all adjoint Higgs VEVs to $M_{\rm GUT} \simeq 10^{16}$ GeV. Then the Yukawa couplings are estimated to be

$$\begin{aligned} y_1^u \sim y_1^\nu \sim\ & v_1^2/M_{\rm GUT}^2 && \approx 4\times 10^{-6}, \\ y_2^u \sim y_2^\nu \sim y_2^d \sim\ & y_2^e \sim\ v_2^2/M_{\rm GUT}^2 && \approx 2.5\times 10^{-3}, \\ y_3^u \sim y_3^\nu \sim y_3^d \sim\ & y_3^e \sim\ v_3^2/M_{\rm GUT}^2 && \approx 0.25, \\ y_{12}^d \sim y_{12}^e \sim\ & v_1 v_2/M_{\rm GUT}^2 && \approx 1\times 10^{-4}, \\ y^P \sim\ & \quad v_3/M_P && \approx 5\times 10^{-4}. \end{aligned} \tag{5.20}$$

The right-handed neutrino mass parameters are estimated to be

$$M_1^{\rm R} \sim 4\times 10^7 \text{ GeV}, \quad M_2^{\rm R} \sim 2.5\times 10^{10} \text{ GeV}, \quad M_3^{\rm R} \sim 10^{16} \text{ GeV}. \tag{5.21}$$

This very strong hierarchy implies negligible right-handed neutrino mixing, such that the mass eigenvalues closely correspond to the above values. As each parameter contains several $\mathcal{O}(1)$ coefficients λ and CG factors, the above numbers only represent order of magnitude estimates.

As we will see in the numerical fit below, the above estimates are in good agreement with the values that produce a good fit to data, with a single exception: the parameter $M_1^{\rm R}$, which is primarily responsible for the lightest right-handed neutrino mass, should be a factor $\mathcal{O}(0.01)$ times the estimate above in order to give the correct light neutrino mass spectrum. This can be understood by inserting the above estimates for y_1^ν and $M_1^{\rm R}$ into the expression for μ_1 in Eq. 5.18, which suggests $\mu_1 \sim 0.01$ meV, whereas we will see the fit prefers a value of $\mathcal{O}(1)$ meV. The necessary factor can be achieved by assuming one or more coefficients deviates from unity.

One may also obtain approximate expressions for the quark mixing angles in terms of quark Yukawa couplings as follows. The very strong hierarchy in the three real parameters of Y^u is correlated with that in the physical Yukawa eigenvalues of up, charm and top quarks. We therefore expect negligible contributions from the up sector to quark mixing. This implies that not only do the four real parameters in the down sector, y_i^d and y^P, fix the down-type Yukawa eigenvalues, they also must reproduce the observed CKM mixing angles.

Let us consider Y^d, keeping only the leading terms in each element. For simplicity, we ignore free phases. As noted above, $y_{12}^d \sim y^P < y_2^d \ll y_3^d$. We also define $y_2' =$

$y_2^d + 2y_{12}^d + 2y^P$. Then

$$Y^d \approx \begin{pmatrix} 0 & y_{12}^d & y_{12}^d - y^P \\ y_{12}^d & y_2' & y_2' + 2(y_{12}^d - y^P) \\ y_{12}^d - y^P & y_2' + 2(y_{12}^d - y^P) & y_3^d \end{pmatrix}. \tag{5.22}$$

In the small angle approximation, the mixing angles can be estimated by

$$\theta_{12}^q \approx \frac{Y_{12}^d}{Y_{22}^d} = \frac{y_{12}^d}{y_2'}, \quad \theta_{13}^q \approx \frac{Y_{13}^d}{Y_{33}^d} = \frac{y_{12}^d - y^P}{y_3^d}, \quad \theta_{23}^q \approx \frac{Y_{23}^d}{Y_{33}^d} = \frac{y_2' + 2(y_{12}^d - y^P)}{y_3^d}. \tag{5.23}$$

The down-type Yukawa eigenvalues are given by $y_d \approx (y_{12}^d)^2/y_2'$, $y_s \approx y_2'$, $y_b \approx y_3^d$. Solving for y_{12}^d, y_2' and y_3^d, we have, to good approximation, $y_{12}^d \approx \sqrt{y_d y_s}$, $y_2' \approx y_s$, $y_3^d \approx y_b$. Reintroducing these into our estimates for mixing angles, we get

$$\theta_{12}^q \approx \sqrt{\frac{y_d}{y_s}}, \quad \theta_{13}^q \approx \frac{\sqrt{y_d y_s} - y^P}{y_b}, \quad \theta_{23}^q \approx \frac{y_s + 2(\sqrt{y_s y_d} - y^P)}{y_b}. \tag{5.24}$$

Note that the first equality is exactly the GST relation [206], which is in good agreement with data. In fact, the GST relation, which predicts $\theta_{12}^q \simeq 0.224$ for the central values of y_d and y_s, is in mild tension with experimental data, which gives $\theta_{12}^q \simeq 0.227$. Possible modifications to the GST result have been proposed [209], e.g. adding a correction like $\sqrt{y_u/y_c}$, which can be realised by a texture zero also in Y^u. Alternatively, one may exploit the statistical uncertainties on each of the down and strange quark masses. A small deviation from their central values can predict a slightly different θ_{12}^q.

On the other hand, the mixing angles θ_{13}^q and θ_{23}^q are less precisely estimated, as the parameter y^P can be as large as y_{12}^d, and the final result will depend on the relative phase between y_{12}^d and y^P. Note however that both mixing angles depend in the same way on $y_{12}^d - y^P$. Generally, the approximations in Eq. 5.24 predict some tension between θ_{13}^q and θ_{23}^q, which are too large and too small, respectively. This tension cannot be resolved simply by tuning y^P.

5.3.3 Full derivation of matrices

For completeness, we here derive the precise forms of the Yukawa and Majorana mass matrices, taking into account the vacuum alignments of the adjoint Higgs superfields.

The renormalisable superpotential given by Eqs. 5.6 and 5.7, with explicit $\mathcal{O}(1)$ couplings, is

$$\begin{aligned} W_Y = {} & \lambda_a^\phi \psi \phi_a \overline{\chi}_a + \lambda_a^\chi \chi_a \overline{\chi}_a H_{45}^Z + \chi_a \chi_a \left(\lambda_a^u H_{10}^u + \lambda_a^N \frac{H_{\overline{16}} H_{\overline{16}}}{M_P} \right) \\ & + \overline{\chi}_b \chi_b' \left(\lambda_b^X H_{45}^X + \lambda_b^Y H_{45}^Y \right) + \lambda_b^d \chi_b' \chi_b' H_{10}^d \\ & + \lambda_{12}^d \chi_1 \chi_2 H_{10}^d + \lambda_3^\rho \rho \chi_3 H_{\overline{16}} + M_\rho \rho \rho + \lambda_P^d \frac{\psi \psi \phi_3 H_{10}^d}{M_P}, \end{aligned} \tag{5.25}$$

where a sum over $a = 1, 2, 3$ and $b = 2, 3$ is understood. Recall from Eq. 5.3 the flavon vacuum alignments $\langle \phi_1 \rangle = v_1(1, 3, -1)$, $\langle \phi_2 \rangle = v_2(0, 1, -1)$, $\langle \phi_3 \rangle = v_3(0, 1, 0)$. The singlet product which occurs in $\psi \phi_a$ above, i.e. $3' \times 3' \to 1$, is given by $(AB) = A_1 B_1 + A_2 B_3 + A_3 B_2$. To account for this nontrivial product as well as the field redefinition $\psi_2 \to -\psi_2$ (this overall sign is unphysical), we define the vectors $\langle \tilde{\phi}_i \rangle = I_{S_4} \langle \phi_i \rangle$, where

$$I_{S_4} = \begin{pmatrix} 1 & 0 & 0 \\ 0 & 0 & -1 \\ 0 & 1 & 0 \end{pmatrix}. \tag{5.26}$$

This gives

$$\langle \tilde{\phi}_1 \rangle = v_1 \begin{pmatrix} 1 \\ 1 \\ 3 \end{pmatrix}, \quad \langle \tilde{\phi}_2 \rangle = v_2 \begin{pmatrix} 0 \\ 1 \\ 1 \end{pmatrix}, \quad \langle \tilde{\phi}_3 \rangle = v_3 \begin{pmatrix} 0 \\ 0 \\ 1 \end{pmatrix}. \tag{5.27}$$

Next, we introduce notation to specify the relevant components of a VEV $\langle H_{45}^k \rangle$, corresponding to unique CG factors. The index k labels the adjoint, i.e. $k = X, Y, Z$, or $B - L$. After the GUT is broken and ψ is decomposed into MSSM gauge multiplets, the part of an adjoint VEV which couples to a given multiplet f is denoted

$$H_{45}^k \to \langle H_{45}^k \rangle_f, \tag{5.28}$$

where $f = Q, u^c, d^c, L, e^c$, or ν^c. The $H_{\overline{16}}$ gets a VEV in the direction which preserves $SU(5)$, which we call the (singlet) ν^c direction. Its VEV only affects the right-handed neutrino mass matrix and is simply denoted $v_{\overline{16}}$.

We extract the Yukawa matrices from diagrams in Figures 5.1 – 5.3. Taking into account nontrivial S_4 products (as above), we have

$$
\begin{aligned}
Y^u_{ij} &= \sum_{a=1,2} \lambda^u_a \frac{(\lambda^\phi_a)^2 \langle\tilde\phi_a\rangle_i \langle\tilde\phi_a\rangle_j}{(\lambda^\chi_a)^2 \langle H^Z_{45}\rangle_Q \langle H^Z_{45}\rangle_{u^c}} + \frac{(\lambda^\phi_3)^2 \langle\tilde\phi_3\rangle_i \langle\tilde\phi_3\rangle_j}{(\lambda^\phi_3)^2 v_3^2 + (\lambda^\chi_3)^2 \langle H^Z_{45}\rangle_Q \langle H^Z_{45}\rangle_{u^c}}, \\
Y^\nu_{ij} &= \sum_{a=1,2} \lambda^u_a \frac{(\lambda^\phi_a)^2 \langle\tilde\phi_a\rangle_i \langle\tilde\phi_a\rangle_j}{(\lambda^\chi_a)^2 \langle H^Z_{45}\rangle_L \langle H^Z_{45}\rangle_{\nu^c}} + \frac{(\lambda^\phi_3)^2 \langle\tilde\phi_3\rangle_i \langle\tilde\phi_3\rangle_j}{(\lambda^\phi_3)^2 v_3^2 + (\lambda^\chi_3)^2 \langle H^Z_{45}\rangle_L \langle H^Z_{45}\rangle_{\nu^c}}, \\
M^{\rm R}_{ij} &= \sum_{a=1,2} \frac{\lambda^N_a v_{\overline{16}}^2}{M_P} \frac{(\lambda^\phi_a)^2 \langle\tilde\phi_a\rangle_i \langle\tilde\phi_a\rangle_j}{(\lambda^\chi_a)^2 \langle H^Z_{45}\rangle_{\nu^c} \langle H^Z_{45}\rangle_{\nu^c}} \\
&\quad + v_{\overline{16}}^2 \left(\frac{(\lambda^\rho_3)^2}{M_\rho} + \frac{\lambda^N_3}{M_P} \right) \frac{(\lambda^\phi_3)^2 \langle\tilde\phi_3\rangle_i \langle\tilde\phi_3\rangle_j}{(\lambda^\phi_3)^2 v_3^2 + (\lambda^\chi_3)^2 \langle H^Z_{45}\rangle_{\nu^c} \langle H^Z_{45}\rangle_{\nu^c}}, \\
Y^d_{ij} &= \lambda^d_2 \frac{(\lambda^\phi_2)^2 \langle\tilde\phi_2\rangle_i \langle\tilde\phi_2\rangle_j}{[\lambda^X_2 \langle H^X_{45}\rangle + \lambda^Y_2 \langle H^Y_{45}\rangle]_Q [\lambda^X_2 \langle H^X_{45}\rangle + \lambda_2 Y \langle H^Y_{45}\rangle]_{d^c}} \\
&\quad + \lambda^d_3 \frac{(\lambda^\phi_3)^2 \langle\tilde\phi_3\rangle_i \langle\tilde\phi_3\rangle_j}{(\lambda^\phi_3)^2 v_3^2 + [\lambda^X_3 \langle H^X_{45}\rangle + \lambda^Y_3 \langle H^Y_{45}\rangle]_Q [\lambda^X_3 \langle H^X_{45}\rangle + \lambda_3 Y \langle H^Y_{45}\rangle]_{d^c}} \\
&\quad + \lambda^d_{12} \frac{\lambda^\phi_1 \lambda^\phi_2 \langle\tilde\phi_1\rangle_i \langle\tilde\phi_2\rangle_j}{\lambda^\chi_1 \lambda^\chi_2 \langle H^Z_{45}\rangle_Q \langle H^Z_{45}\rangle_{d^c}} + \lambda^d_P \frac{Y_P v_3}{M_P}, \\
Y^e_{ij} &= \lambda^d_2 \frac{(\lambda^\phi_2)^2 \langle\tilde\phi_2\rangle_i \langle\tilde\phi_2\rangle_j}{[\lambda^X_2 \langle H^X_{45}\rangle + \lambda^Y_2 \langle H^Y_{45}\rangle]_L [\lambda^X_2 \langle H^X_{45}\rangle + \lambda_2 Y \langle H^Y_{45}\rangle]_{e^c}} \\
&\quad + \lambda^d_3 \frac{(\lambda^\phi_3)^2 \langle\tilde\phi_3\rangle_i \langle\tilde\phi_3\rangle_j}{(\lambda^\phi_3)^2 v_3^2 + [\lambda^X_3 \langle H^X_{45}\rangle + \lambda^Y_3 \langle H^Y_{45}\rangle]_L [\lambda^X_3 \langle H^X_{45}\rangle + \lambda_3 Y \langle H^Y_{45}\rangle]_{e^c}} \\
&\quad + \lambda^d_{12} \frac{\lambda^\phi_1 \lambda^\phi_2 \langle\tilde\phi_1\rangle_i \langle\tilde\phi_2\rangle_j}{\lambda^\chi_1 \lambda^\chi_2 \langle H^Z_{45}\rangle_L \langle H^Z_{45}\rangle_{e^c}} + \lambda^d_P \frac{Y_P v_3}{M_P}.
\end{aligned}
\tag{5.29}
$$

The last term in Eq. 5.25 is a singlet coming from three S_4 triplets and gives rise to the final terms in Y^d and Y^e, where Y_P is the numerical matrix defined in Eq. 5.14.

5.4 Numerical fit

5.4.1 χ^2 minimisation and Monte Carlo methods

Our model determines the Yukawa couplings and mixing parameters at the GUT scale, which is also the highest flavour-breaking scale. As in the analyses of Chapters 3 and 4, the values from experiments must be run up to the GUT scale, taking into account supersymmetric radiative threshold corrections. This analysis has been performed in [145], and their parametrisation of the corrections is summarised in Appendix B. Most parameters do not significantly affect the fit, so are simply set to reasonable values. Specifically, we set $M_{\rm SUSY} = 1$ TeV, $\tan\beta = 5$ and $\bar\eta_q = \bar\eta_\ell = 0$. We also find that a good fit can be achieved for a rather large value $\bar\eta_b = -0.8$. The choices of SUSY

parameters $\tan\beta$ and $\bar{\eta}_b$ are here empirically determined to give a good fit of the model to data. It is clear from the fit that large (negative) $\bar{\eta}_b$ is required, affecting primarily the bottom quark Yukawa coupling y_b. In order to keep y_b perturbative, we must assume reasonably small $\tan\beta$. In the region of $5 < \tan\beta < 10$ or so, the fit is rather insensitive to the exact choice. Neutrino data is taken from the NuFit global fit, version 3.0 [36].

To find the best fit of the model to data, we minimise a χ^2 function, defined as in Eq. 2.22 by

$$\chi^2 = \sum_i \left(\frac{P_i(\theta) - P_i^{\text{obs}}}{\sigma_i} \right)^2 , \tag{5.30}$$

where P_i^{obs} and σ_i are the experimental best fits and errors, respectively, and we have used θ instead of x to denote the input parameters. As already noted, in order for a minimum χ^2 to correspond to the maximum likelihood, the statistical uncertainties should be symmetric (Gaussian). In earlier fits based on the NuFit 2.0 data, we needed to carefully consider the bimodality of the atmospheric mixing angle θ_{23}^ℓ; experimental data could not conclusively resolve the octant, i.e whether θ_{23}^ℓ is larger or smaller than 45°. While this remains true in the current global fit, the preference for the first octant (for normal ordering) is stronger, with a central value 41.6°. We will assume this is the true value.

For our model, the input parameters are $\theta = \{y_i^u, y_i^d, y_i^e, y_P, \mu_i, \eta', \alpha_{d,e}, \beta_{d,e}, \gamma\}$, and the observables are given by $P_i \in \{\theta_{ij}^q, \delta^q, y_{u,c,t}, y_{d,s,b}, \theta_{ij}^\ell, y_{e,\mu,\tau}, \Delta m_{ij}^2\}$. As the lepton CP phase δ^ℓ is (still) not well measured, we do not include it in the fit, leaving it as a pure prediction. While we fit to the neutrino mass-squared differences, the model predicts the masses outright, including the lightest neutrino mass m_1, as well as the Majorana phases $\alpha_{21,31}$.

χ^2 minimisation is an effective tool for finding a best fit point parameter space, and for comparing models to each other. For this model we went further, supplementing the fit with a Markov Chain Monte Carlo (MCMC) analysis, allowing us to gain more insight into the model predictions, in particular the likely ranges for mass and mixing parameters in the model. The broad aim is to estimate the probability distribution of parameters in the model, given the available data.[4] In the language of Bayesian inference, this is the posterior probability density. Once this is known, we may identify regions of highest posterior density (hpd), which correspond to the most likely predicted values of physical parameters, and construct so-called 95% credible intervals, which contain those parameter values that collectively have a 95% chance of being the true predicted value by the model (given the data). These are analogous to, but philosophically very different from, the often cited confidence intervals associated with frequentist analyses. Confidence intervals correspond to those values of a parameter where, in 95% of iterations of an experiment repeated many times, the measured value of an experiment will lie.

[4] These methods for exploring the parameter space were foreshadowed in the analysis of CSD(n) in Chapter 2, where we plotted χ^2 as functions of the inputs (see Figures 2.1 and 2.2).

To estimate the posterior distributions we used the Metropolis-Hastings algorithm [210], which repeatedly samples from the parameter space, preferentially revisiting regions that correspond to higher likelihood (a lower χ^2). It falls within a particular class of Monte Carlo methods based on Markov chains, which have as a key characteristic that the each iteration depends only on the last sample, and has no "memory" of previous iterations. The algorithm works as follows:

1. Generate a set of input parameters θ.
2. Calculate the relevant observables $P_i(\theta)$.
3. Calculate the likelihood $L(\theta)$, defined as
$$L(\theta) \equiv \exp\left[-\frac{\chi^2}{2}\right], \tag{5.31}$$
in terms of the standard χ^2 test statistic, defined above.
4. Generate a new set of input parameters θ'. There is some freedom in how this new set is selected, discussed below.
5. Calculate $L(\theta')$ and the acceptance ratio
$$\alpha \equiv \frac{L(\theta')}{L(\theta)}, \tag{5.32}$$
which describes the relative likelihood of the two points in parameter space.
6. If $\alpha > 1$, we automatically accept θ' as the new starting point, so $\theta' \to \theta$. If $\alpha < 1$, we accept θ' only with probability α, i.e. the new starting point is randomly chosen to be either θ', with a probability α, or θ, with a probability $1 - \alpha$.
7. Repeat from step 2.

A few additional notes on the method are in order. The random choice when $\alpha < 1$ allows for the possibility of moving from a point in parameter space with lower χ^2 to a (somewhat) higher one. This ensures one does not get trapped in a shallow local minimum. In a large and complicated parameter space such as the one considered here, several local minima may exist; it is important that the MCMC algorithm can sample from all such regions. In the infinite limit, the chain will visit (and revisit) each region for an amount of time proportional to the likelihood (itself proportional to the posterior probability).

Meanwhile, the shape of the distribution from which the next point θ' is chosen is a free parameter in the algorithm, and affects the rate of convergence. Conventionally, the proposal distribution is chosen such that no more than half of proposed sets θ' are accepted. A common choice, which we employed, is to choose each new θ'_j from a normal

distribution centered around the previous θ_j, with some appropriate standard deviation σ, typically a few percent of the mean value. We set $\sigma = 2\%$.

The initial starting set constitutes another free choice, chosen from physical considerations within the model itself. In this model with universal sequential dominance, we have rather well-defined expectations for the natural values of the input parameters. For instance, we anticipate y_3^u to be closely related to the top quark mass; $y_3^u = y_t$ thus serves as an appropriate starting point. However, we allow an initial burn-in period, which allows the algorithm to "forget" the initial state. To calculate a hpd interval, one plots the posterior distribution and identifies the region(s) with the tallest peaks; these do not need to be connected.

5.4.2 Results

Observable	Data		Model	
	Central value	1σ range	Best fit	Interval
θ_{12}^ℓ /°	33.57	32.81 → 34.32	33.62	31.69 → 34.46
θ_{13}^ℓ /°	8.460	8.310 → 8.610	8.455	8.167 → 8.804
θ_{23}^ℓ /°	41.75	40.40 → 43.10	41.96	39.47 → 43.15
δ^ℓ /°	261.0	202.0 → 312.0	300.9	280.7 → 308.4
y_e /10^{-5}	1.017	1.011 → 1.023	1.017	1.005 → 1.029
y_μ /10^{-3}	2.147	2.134 → 2.160	2.147	2.121 → 2.173
y_τ /10^{-2}	3.654	3.635 → 3.673	3.654	3.616 → 3.692
Δm_{21}^2 /10^{-5} eV^2	7.510	7.330 → 7.690	7.515	7.108 → 7.864
Δm_{31}^2 /10^{-3} eV^2	2.524	2.484 → 2.564	2.523	2.443 → 2.605
m_1 /meV			0.441	0.260 → 0.550
m_2 /meV			8.680	8.435 → 8.888
m_3 /meV			50.24	49.44 → 51.05
$\sum m_i$ /meV		< 230	59.36	58.49 → 60.19
α_{21}			67.90	-25.19 → 87.49
α_{31}			164.2	19.98 → 184.5

Table 5.2: Model predictions in the lepton sector, at the GUT scale, with experimental 1σ ranges from [105, 145]. We set $\tan\beta = 5$, $M_{\rm SUSY} = 1$ TeV and $\bar{\eta}_b = -0.8$. The lepton contribution to the total χ^2 is 0.03. δ^ℓ as well as the neutrino masses m_i are pure predictions of our model. The model interval is a Bayesian 95% credible interval.

We present the best fit (minimum χ^2) of the model to physical observables (Yukawa couplings and neutrino mass and mixing parameters) in Tables 5.2 and 5.3, which also include the central values and 1σ ranges from data. Figure 5.4 shows the associated pulls, and Table 5.4 shows the corresponding input parameter values. The fit gives $\chi^2 \approx 3.4$. A second minimum with $\chi^2 \approx 4$ was also found, leading primarily to a different prediction for δ^ℓ, as discussed below, although we shall not present the full fit parameters for this case.

Observable	Data		Model	
	Central value	1σ range	Best fit	Interval
θ_{12}^q /°	13.03	$12.99 \to 13.07$	13.02	$12.94 \to 13.10$
θ_{13}^q /°	0.039	$0.037 \to 0.040$	0.039	$0.036 \to 0.041$
θ_{23}^q /°	0.445	$0.438 \to 0.452$	0.439	$0.426 \to 0.450$
δ^q /°	69.22	$66.12 \to 72.31$	69.21	$63.22 \to 73.94$
$y_u / 10^{-6}$	2.988	$2.062 \to 3.915$	3.012	$1.039 \to 4.771$
$y_c / 10^{-3}$	1.462	$1.411 \to 1.512$	1.493	$1.445 \to 1.596$
y_t	0.549	$0.542 \to 0.556$	0.547	$0.532 \to 0.562$
$y_d / 10^{-5}$	2.485	$2.212 \to 2.758$	2.710	$2.501 \to 2.937$
$y_s / 10^{-4}$	4.922	$4.656 \to 5.188$	5.168	$4.760 \to 5.472$
y_b	0.141	$0.136 \to 0.146$	0.137	$0.126 \to 0.143$

Table 5.3: Model predictions in the quark sector at the GUT scale, with experimental 1σ ranges from [145]. We set $\tan\beta = 5$, $M_{\rm SUSY} = 1$ TeV and $\bar{\eta}_b = -0.8$. The quark contribution to the total χ^2 is 3.38. The model interval is a Bayesian 95% credible interval.

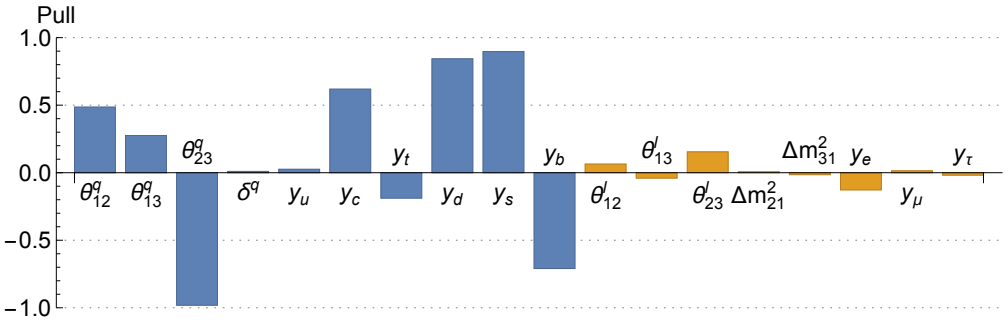

Figure 5.4: Pulls for the best fit of the model to data. Quark parameters are given in blue, and lepton parameters in yellow. The corresponding best fit values are shown in Tables 5.2 and 5.3.

Parameter	Value
$y_1^u / 10^{-6}$	3.009
$y_2^u / 10^{-3}$	1.491
y_3^u	0.549
$y_{12}^d / 10^{-4}$	-1.186
$y_2^d / 10^{-4}$	6.980
y_3^d	0.137
$y^P / 10^{-4}$	1.243

Parameter	Value
$y_{12}^e / 10^{-4}$	1.558
$y_2^e / 10^{-3}$	2.248
$y_3^e / 10^{-2}$	3.318
μ_1 /meV	2.413
μ_2 /meV	27.50
μ_3 /meV	2.900

Parameter	Value
α_d	0.043π
β_d	0.295π
α_e	1.692π
β_e	1.755π
γ	0.918π
η'	1.053π

Table 5.4: Best fit input parameter values. The model has 13 real parameters: y_i^u, y_i^d, y_i^e, μ_i and y^P. While η is fixed by flavon alignment to $-2\pi/3$, there are six additional free phases: η', $\alpha_{d,e}$, $\beta_{d,e}$ and γ. The total χ^2 is 3.4.

We see from Tables 5.2, 5.3 and Figure 5.4 that both quark and lepton sectors are fitted to within 1σ of the values predicted by global fits to experiment. The biggest pulls are in down-type quark Yukawa couplings $y_{d,s,b}$ and θ^q_{23}. As shown in Section 5.3.2, θ^q_{23} is approximately given by the ratio y_s/y_b, which is typically too small. Furthermore, attempts to increase θ^q_{23}, e.g. by tuning y^P, tends to increase θ^q_{13}, which is then too large. This tension can be ameliorated by assuming large threshold corrections, i.e. by setting $\bar{\eta}_b = -0.8$, although some tension remains among the above parameters, which deviate by about 1σ.

Tables 5.2 and 5.3 also include a Bayesian 95% credible interval for each observable. The interval for a given parameter corresponds to the hpd region, marginalised over the other parameters. Recall that this may be interpreted as follows: given the data, there is a 95% probability that the true model value of that observable resides in the stated interval. For many observables, these probability distributions are essentially Gaussian, centred around the best fit value. This is not always the case: the distributions for θ^ℓ_{12} and θ^ℓ_{23} are asymmetric, consisting of two partially overlapping peaks. Moreover, the hpd region for δ^ℓ consists of two completely distinct intervals, which contain the best fit values 300.9° (as seen in Table 5.2) and 233.9° (corresponding to a second best fit point with $\chi^2 \approx 4$). Their associated 95% credible intervals are given by $280.7 < \delta^\ell < 308.3$ and $225.1 < \delta^\ell < 253.2$, respectively. We note that neither region includes maximal CP violation $\delta^\ell = 270^\circ$, which is close to the prediction from CSD(3) with diagonal charged leptons. In short, charged-lepton corrections induce a deviation from maximal CP phase, which can either be positive or negative, depending on the phases of Y^e.

5.5 Summary of features

We have constructed a rather simple, natural and complete $SO(10)$ model of flavour with a discrete $S_4 \times \mathbb{Z}_4^2 \times \mathbb{Z}_4^R$ symmetry, where all Yukawa matrices derive from the VEVs of triplet flavons with CSD(3) alignments. It is simple in the sense that the field content is reasonably minimal, with small Higgs representations of $SO(10)$ consisting of two **10**s which contain the MSSM doublets, a Higgs spinor pair $\mathbf{16} + \overline{\mathbf{16}}$, and three adjoint Higgs **45**s, which provide necessary Clebsch-Gordan factors that distinguish charged leptons and down-type quarks. It is natural in the sense that Yukawa and mass matrices consist of sums of low-rank matrices, each of which contributes dominantly to a particular family, i.e. universal sequential dominance. It is complete in the sense that it is renormalisable, and addresses doublet-triplet splitting, the μ-problem, Higgs mixing and proton decay.

The model successfully reproduces all observed fermion masses and mixing. Analytical estimates are underpinned by a detailed numerical analysis, employing also Monte Carlo methods to give credible intervals for all predicted parameters. There is no tuning of

$\mathcal{O}(1)$ parameters necessary to explain the mass hierarchies of charged fermions, accounting also for the milder hierarchy in down-type quarks compared to up-type quarks. The model simultaneously realises large lepton mixing and small quark mixing, as well as the GST relation for the Cabibbo angle, $\theta_{12}^q \approx \sqrt{y_d/y_s}$ via a texture zero in the down-type Yukawa matrix Y^d. In the lepton sector an excellent fit to data is found, predicting a normal neutrino hierarchy and lightest neutrino mass $m_1 \lesssim 0.5$ meV. The CP phase δ^ℓ was not fitted, but left as a pure prediction. Two distinct regions are preferred, with corresponding best fit values $\delta^\ell \approx 301^\circ$ and 234°. We emphasise that the model predicts significant deviation from both zero and maximal CP violation.

Chapter 6

Conclusion

In the previous four chapters of this thesis we have discussed various aspects of the flavour puzzle and their potential resolutions within SUSY GUTs with discrete family symmetries. Before discussing the impact and outlook for the future, let us reiterate the most compelling features of the work presented within this thesis. They can be summarised in a number of key concepts: naturalness, completeness, simplicity, predictivity.

In Chapter 2 we discussed the sequential dominance framework, with particular focus on a numerical analysis of the CSD(n) class of models describing neutrino mass and mixing, considering models of both two and three right-handed neutrinos. We showed how CSD(n) can arise from the vacuum alignments of family triplet flavons ϕ. A χ^2 fit was performed for integer $n \leq 9$, and an excellent agreement with data was found for the case $n = 3$, with also $n = 4$ showing promise. In particular CSD(3) with two right-handed neutrinos offers a highly predictive and successful setup, where the entire PMNS matrix is essentially fixed by a single phase η in the neutrino mass matrix. It also predicts a the leptonic CP-violating phase δ^ℓ very close to maximal, which coincides with current experimental hints. These rather small values of n are promising from the perspective of model building, as they are more readily achieved in indirect models of flavour based on orthogonality arguments.

We found that the χ^2 measure offers a simple and effective way of examining parameter space, and for comparing models, and has been dispatched for every model considered within this thesis. However, the interpretation and robustness of the χ^2 statistic is subject to a number of subtleties, which we have also addressed at every step. These include the non-Gaussianity of the data (i.e. the results of a particular global fit) and the decision about whether to include δ^ℓ in the χ^2 fit or leave it as a pure prediction of the model. Additionally, we have considered how best to treat those parameters which do not significantly affect the fit, such as the "decoupled" neutrino mass parameter m_c and associated phase, and those which may be fixed by theory, such as n, or the phase η, which may be fixed by a discrete symetry.

We have also considered the cosmological consequences in general CSD(n) models, by studying thermal leptogenesis, showing that the observed baryon asymmetry of the Universe can be explained through decays of the lightest right-handed neutrino N_1. This process can depend strongly on flavour effects, and the predictions for the BAU depend on the value of n; interestingly, the smallest value giving non-zero BAU is found to be $n = 3$. In this highly constrained framework, we can also make a direct link between the phase η which controls the PMNS matrix parameters and the phase which appears in the CP asymmetries ε_i appearing in leptogenesis calculations. Notably, we showed that a preference for $\delta^\ell \sim -\pi/2$ in oscillation experiments implies, in CSD(n), that the BAU is positive.

The above analysis serves as a promising start for a more complete resolution to the flavour puzzle. We subsequently constructed several models based on CSD(3) with a unifying gauge group, each of which has its own strengths and shortcomings. In Chapter 3 we constructed a "minimal" model based on $A_4 \times SU(5)$, so called because A_4 is the smallest group that admits triplet representations – a partial explanation for the origin of three families of fermions – and $SU(5)$ is the smallest GUT group that contains the Standard Model. With only two active right-handed neutrinos, it also realises the most minimal and predictive incarnation of CSD(3).

The second guiding principle was completeness: we aimed to construct a model that resolves as many open questions in particle physics as possible simultaneously. Charge quantisation is guaranteed by the GUT group, as is gauge coupling unification, which is protected from dangerous corrections by ensuring only the two MSSM Higgs doublets remain at low scales. GUT breaking, proton decay, doublet-triplet splitting and the μ problem are also addressed and resolved. The focus, however, was on the viability of the Yukawa sector, where the model predicts quark and lepton masses and mixing patterns are in agreement with data. In the quark sector, mixing occurs from a discrete variant of the Froggatt-Nielsen mechanism, while CP violation arises from a single term in the down-type quark sector. The lepton sector realises a rather "clean" implementation of CSD(3) considered previously, ensuring a good fit. As a consequence, the successful predictions for leptogenesis in CSD(n) are also carried over into this model. Serendipitously, the model can also resolve the strong CP problem of QCD without relying on axions, due to the highly constrained nature of the quark Yukawa matrices, itself a result of the family symmetries.

While $SU(5)$ offers perhaps the simplest "upgrade" of the Standard Model with CSD(n) into a fully fledged GUT, the presumed existence of heavy right-handed neutrinos heavily favours $SO(10)$, where they are automatic. We therefore constructed two successful models based on $SO(10)$, where CSD(3) arises from $\Delta(27)$ and S_4, respectively. Both have the enviable feature that all known fermions are contained at the high scale within a single representation Ψ (or ψ) of the symmetries at high scale. However, beyond this

point there are many differences, both in the approach taken to model building and the physical predictions.

In the $\Delta(27) \times SO(10)$ presented in Chapter 4, the emphasis once again lay on completeness. Symmetry breaking, proton decay and doublet-triplet splitting were addressed, as were doublet-doublet splitting and the μ term. $SO(10)$ offers a much greater challenge for explaining flavour than $SU(5)$, as total unification of fermions within a family naïvely implies that they couple identically to Higgs doublets and that the Yukawa matrices are all equal, giving incorrect mass relations between fermions and no flavour mixing. In order to produce a viable model, new perspectives are required. Here, by coupling Ψ to flavons, we developed a framework – universal sequential dominance – where both the hierarchies among fermions and non-zero mixing can be explained in a transparent and rather simple way. All Yukawa matrices are given as sums over rank-1 matrices, with each part understood to be responsible for one non-zero eigenvalue. This replicates the CSD(3) prediction for the form of the neutrino mass matrix in all sectors. *A priori*, this has no reason to work for quarks, and even in the lepton sector we needed to be careful that corrections coming from a decidedly non-diagonal charged lepton Yukawa matrix do not spoil the successful CSD(3) predictions for the PMNS parameters. With a small tweak in the up-type quark sector, we could indeed achieve a good fit of the model to data.

While completeness is an admirable goal, both the above models necessarily have very large field content. Sharp predictions are made possible by having a renormalisable theory at the GUT scale, with the immediate consequence that we require a rather large number of messenger superfields in order to attain exactly the desired superpotential. In the $S_4 \times SO(10)$ model presented in Chapter 5, our focus lay instead on minimality, here interpreted as employing the smallest possible field content, and naturalness, where all hierarchies (such as those between fermion masses) arise dynamically, and renormalisable superpotential terms all have $\mathcal{O}(1)$ coupling strengths. Certainly this model is more minimal than previous efforts, with a considerably smaller field content, and a rather simple superpotential responsible for all Yukawa and mass terms. This simplicity is partly due to the absence of a singlet flavon (in the previous two models labelled ξ) acting as a Froggatt-Nielsen field.

It also realises a more sophisticated implementation of universal sequential dominance, explaining all fermion hierarchies by assuming only a rather mild hierarchy in the VEVs of flavons, i.e. $\langle\phi_1\rangle < \langle\phi_2\rangle < \langle\phi_3\rangle$, each separated by one order of magnitude. In this sense the hierarchy conundrum, although not entirely resolved, has been considerably ameliorated. The milder hierarchy among down-type quarks compared to up-type quarks is explained by a mixed term involving $\phi_1\phi_2$, giving a texture zero in the (1,1) element of Y^d, realising the GST relation. We therefore have a natural explanation for a comparatively large Cabibbo angle, and why the up quark (originating from a term involving ϕ_1^2) is so light.

Neutrino mixing arises in accordance with CSD(3), whose phenomenological success is now well-established, although we must necessarily take into account mixing coming from charged leptons. One effect is to alter the standard prediction for the CP-violating phase δ^ℓ: in standard CSD(3), it is maximal, i.e. $\delta^\ell \approx 270°$, while the numerical fit above shows is necessarily deviates from maximal. This prediction may be tested in future experiments. In the analysis of this model we also supplemented the standard χ^2 fit with new numerical tools, namely Monte Carlo methods and credible intervals. This enabled us to more fully understand the parameter space.

Moreso than the previous two models, the $S_4 \times SO(10)$ model is a work in progress. While the low-scale Yukawa predictions are rather well understood from the analysis presented within this thesis, several assumptions are made that need to be addressed if the model is to be truly complete. We have not, for instance, proved that the CSD(3) alignments, derived elsewhere in a non-GUT framework, can be realised within this model. To do so, we must show that the additional field content necessary for fixing the VEV alignments are compatible with all the symmetries of the present model, and that no new terms appear in the effective Yukawa superpotential which spoil the predictive matrix structures. However, recall that the vacuum alignments preserve a generator of S_4, and as such are at least partially motivated purely on symmetry grounds. There is consequently a reasonable expectation that these alignments can arise naturally in any model with spontaneously broken S_4.

Although doublet-triplet splitting and the μ problem have been considered in this model, we have not shown explicitly how $SO(10)$ is broken to the MSSM. This should be addressed in a complete model. Similarly, we have not discussed leptogenesis within this model, although some generic inferences can be made as to how a baryon asymmetry may be generated in this model. The structure of the neutrino Yukawa matrix Y^ν is tightly constrained to resemble the up-type quark matrix Y^u, up to an overall $\mathcal{O}(1)$ factor. The seesaw relation and the numerical fit to light neutrino masses thereby strongly constrain the right-handed neutrino masses. We conclude that the lightest right-handed neutrino N_1 with a mass $M_1 \sim 10^6$ GeV is too light to produce the observed BAU, and that N_2 thermal leptogenesis will be required. The second-to-lightest right-handed neutrino in our model has a mass of $\mathcal{O}(10^{10})$ GeV, which is in the preferred range. However, in N_2 leptogenesis one must account for washout due to inverse decays into N_1. To verify that thermal leptogenesis is indeed viable, one should calculate all relevant parameters, e.g. decay asymmetries, efficiency factors, taking into account also flavour effects. The resultant constraints on the neutrino Yukawa couplings may test the prediction in this model of $Y^\nu \propto Y^u$.

Beyond the specific models presented here, and beyond CSD(n), there are a number of topic in SUSY GUTs, and particularly those of flavour, which merit further study. First, we note that the earlier models reproduce the MSSM with conserved matter parity at low scale, itself broken at TeV scale. This is among the most studied supersymmetric

extensions of the Standard Model and among the most constrained. In a more complete phenomenological study, experimental constraints on SUSY observables would also be taken into account. As we have seen, to achieve a good fit to data for all quarks and fermions, we must assume some SUSY threshold corrections to the running of Yukawa parameters. For instance in Chapter 3, these corrections ensured the equality of bottom quark and tau lepton masses at the GUT scale, as predicted by the model. What underlying SUSY model is thus required in order to reproduce the necessary corrections? This would be a natural and compelling avenue for probing the SUSY GUTs discussed.

Furthermore, while the $SU(5)$ model in Chapter 3 contains a solution to the strong CP problem by the Nelson-Barr mechanism, no such solution is available in the $SO(10)$ models of Chapters 4 and 5. A natural candidate solution is to introduce a Peccei-Quinn symmetry and an axion. It may be realised rather trivially by introducing the axion as a new field which is essentially decoupled from the existing fields. However, as these models already contain a number of gauge singlets – notably, family symmetry triplet flavons – and spontaneously broken global symmetries, it is interesting to examine whether an axionic solution to the strong CP problem can be realised more compactly with the available field content. Some early efforts in this direction have been made, but are as yet inconclusive.

Finally, a complete model ought also to include a candidate inflaton.[1] Again, it is possible that a member of the flavon sector, which contains many scalars including singlet and triplet flavons as well as driving fields, may be the inflaton. Such a scenario, proposed in [100], is worth further study. While deemed beyond the scope of this thesis, the author has studied inflation in another context [211], namely whether "resonant" leptogenesis may be realised in a model of chaotic sneutrino inflation involving two nearly-degenerate heavy right-handed neutrino superfields, whose scalar parts are responsible for inflation.

[1] This presumes, of course, that inflation is the correct description of the early moments of the Universe, which is widely accepted, although many variations on the theme have been proposed.

Appendix A

Properties of discrete groups

A.1 S_4 and A_4

The group theory properties of S_4 and A_4 are well-known. Here we summarise the relevant group properties, including the Kronecker products, as presented in [212]. S_4 has five irreducible matrix representations: two triplets $\mathbf{3}$ and $\mathbf{3'}$, which are independent, one doublet $\mathbf{2}$, and two singlet representations $\mathbf{1}$ and $\mathbf{1'}$. The A_4 subgroup has only one triplet representation $\mathbf{3}$, and three singlets $\mathbf{1}$, $\mathbf{1'}$ and $\mathbf{1''}$. All group elements can be expressed as products of generators S, T and U. The form of these generators depend on the choice of basis. For the $S_4 \times SO(10)$ model presented in Chapter 5, we use the basis where the generator T is diagonal, with elements of unit length and phases that are products of $\omega = e^{i2\pi/3}$ [55]. Note that the $A_4 \times SU(5)$ model in Chapter 3 employs another basis, which we will describe shortly. The matrix representations in the diagonal-T basis are given in Table A.1.

Representation	S_4 / A_4	$\mathbf{3}, \mathbf{3'}$ / $\mathbf{3}$	$\mathbf{2}$ / $(\mathbf{1''}, \mathbf{1'})$	$\mathbf{1}, \mathbf{1'}$ / $\mathbf{1}$
Generator	S	$\frac{1}{3}\begin{pmatrix} -1 & 2 & 2 \\ 2 & -1 & 2 \\ 2 & 2 & -1 \end{pmatrix}$	$\begin{pmatrix} 1 & 0 \\ 0 & 1 \end{pmatrix}$	1
	T	$\begin{pmatrix} 1 & 0 & 0 \\ 0 & \omega^2 & 0 \\ 0 & 0 & \omega \end{pmatrix}$	$\begin{pmatrix} \omega & 0 \\ 0 & \omega^2 \end{pmatrix}$	1
	U	$\begin{pmatrix} 1 & 0 & 0 \\ 0 & 0 & 1 \\ 0 & 1 & 0 \end{pmatrix}$	$\begin{pmatrix} 0 & 1 \\ 1 & 0 \end{pmatrix}$	± 1

Table A.1: Generators of the S_4 and A_4 groups in the diagonal-T basis.

The Kronecker products of the group representations are basis-independent, but the values of the Clebsch-Gordan coefficients depend on the basis. Let us consider first

S_4. In a given product $\mathbf{x}^{(\prime)} \otimes \mathbf{y}^{(\prime)} \to \mathbf{z}^{(\prime)}$, where $\mathbf{x}$, $\mathbf{y}$, $\mathbf{z}$ denote the dimensions of the representations, we indicate the number of primes which appear by n, e.g. $\mathbf{3} \otimes \mathbf{3'} \to \mathbf{3'}$ has $n = 2$ primes. The product rules can then be given in a compact form, as follows. Products involving at least one singlet or doublet are given by

$$\begin{aligned}
\mathbf{1}^{(\prime)} \otimes \mathbf{1}^{(\prime)} &\to \mathbf{1}^{(\prime)} && \alpha\beta, \\
\mathbf{1}^{(\prime)} \otimes \mathbf{2} &\to \mathbf{2} && \alpha \begin{pmatrix} \beta_1 \\ (-1)^n \beta_2 \end{pmatrix}, \\
\mathbf{1}^{(\prime)} \otimes \mathbf{3}^{(\prime)} &\to \mathbf{3}^{(\prime)} && \alpha \begin{pmatrix} \beta_1 \\ \beta_2 \\ \beta_3 \end{pmatrix}, \\
\mathbf{2} \otimes \mathbf{2} &\to \mathbf{1}^{(\prime)} && \alpha_1\beta_2 + (-1)^n \alpha_2\beta_1, \\
\mathbf{2} \otimes \mathbf{2} &\to \mathbf{2} && \begin{pmatrix} \alpha_2\beta_2 \\ \alpha_1\beta_1 \end{pmatrix}, \\
\mathbf{2} \otimes \mathbf{3}^{(\prime)} &\to \mathbf{3}^{(\prime)} && \alpha_1 \begin{pmatrix} \beta_2 \\ \beta_3 \\ \beta_1 \end{pmatrix} + (-1)^n \alpha_2 \begin{pmatrix} \beta_3 \\ \beta_1 \\ \beta_2 \end{pmatrix},
\end{aligned} \tag{A.1}$$

while products of two triplets going into either a singlet, doublet or another triplet are given by

$$\begin{aligned}
\mathbf{3}^{(\prime)} \otimes \mathbf{3}^{(\prime)} &\to \mathbf{1}^{(\prime)} && \alpha_1\beta_1 + \alpha_2\beta_3 + \alpha_3\beta_2, \\
\mathbf{3}^{(\prime)} \otimes \mathbf{3}^{(\prime)} &\to \mathbf{2} && \begin{pmatrix} \alpha_2\beta_2 + \alpha_3\beta_1 + \alpha_1\beta_3 \\ (-1)^n(\alpha_3\beta_3 + \alpha_1\beta_2 + \alpha_2\beta_1) \end{pmatrix}, \\
\mathbf{3}^{(\prime)} \otimes \mathbf{3}^{(\prime)} &\to \mathbf{3}^{(\prime)} && \begin{pmatrix} \alpha_2\beta_3 - \alpha_3\beta_2 \\ \alpha_1\beta_2 - \alpha_2\beta_1 \\ \alpha_3\beta_1 - \alpha_1\beta_3 \end{pmatrix} \ [n \text{ even}], \\
\mathbf{3}^{(\prime)} \otimes \mathbf{3}^{(\prime)} &\to \mathbf{3}^{(\prime)} && \begin{pmatrix} 2\alpha_1\beta_1 - \alpha_2\beta_3 - \alpha_3\beta_2 \\ 2\alpha_3\beta_3 - \alpha_1\beta_2 - \alpha_2\beta_1 \\ 2\alpha_2\beta_2 - \alpha_3\beta_1 - \alpha_1\beta_3 \end{pmatrix} \ [n \text{ odd}].
\end{aligned} \tag{A.2}$$

The A_4 product rules in this basis can be found by dropping all primes, and identifying the two components of the S_4 doublet by $\mathbf{1''}$ and $\mathbf{1'}$. The non-trivial products are given

by

$$\begin{aligned}
&\mathbf{1}' \otimes \mathbf{1}'' \to \mathbf{1} && \alpha\beta, \\
&\mathbf{1}' \otimes \mathbf{3} \to \mathbf{3} && \alpha \begin{pmatrix} \beta_3 \\ \beta_1 \\ \beta_2 \end{pmatrix}, \\
&\mathbf{1}'' \otimes \mathbf{3} \to \mathbf{3} && \alpha \begin{pmatrix} \beta_2 \\ \beta_3 \\ \beta_1 \end{pmatrix}, \\
&\mathbf{3} \otimes \mathbf{3} \to \mathbf{1} && \alpha_1\beta_1 + \alpha_2\beta_3 + \alpha_3\beta_2, \\
&\mathbf{3} \otimes \mathbf{3} \to \mathbf{1}' && \alpha_3\beta_3 + \alpha_1\beta_2 + \alpha_2\beta_1, \\
&\mathbf{3} \otimes \mathbf{3} \to \mathbf{1}'' && \alpha_2\beta_2 + \alpha_3\beta_1 + \alpha_1\beta_3, \\
&\mathbf{3} \otimes \mathbf{3} \to \mathbf{3} + \mathbf{3} && \begin{pmatrix} 2\alpha_1\beta_1 - \alpha_2\beta_3 - \alpha_3\beta_2 \\ 2\alpha_3\beta_3 - \alpha_1\beta_2 - \alpha_2\beta_1 \\ 2\alpha_2\beta_2 - \alpha_3\beta_1 - \alpha_1\beta_3 \end{pmatrix} + \begin{pmatrix} \alpha_2\beta_3 - \alpha_3\beta_2 \\ \alpha_1\beta_2 - \alpha_2\beta_1 \\ \alpha_3\beta_1 - \alpha_1\beta_3 \end{pmatrix}.
\end{aligned} \tag{A.3}$$

However, in the $A_4 \times SU(5)$ model of Chapter 3, we use instead the basis where S is diagonal, called the real basis, as the generators S, T and U are all real [213]. In the triplet representation, we then have

$$S = \begin{pmatrix} 1 & 0 & 0 \\ 0 & -1 & 0 \\ 0 & 0 & -1 \end{pmatrix}, \qquad T = \begin{pmatrix} 0 & 1 & 0 \\ 0 & 0 & 1 \\ 1 & 0 & 0 \end{pmatrix}. \tag{A.4}$$

This yields the product rules for two triplets

$$\begin{aligned}
&\mathbf{3} \otimes \mathbf{3} \to \mathbf{1} && \alpha_1\beta_1 + \alpha_2\beta_2 + \alpha_3\beta_3, \\
&\mathbf{3} \otimes \mathbf{3} \to \mathbf{1}' && \alpha_1\beta_1 + \omega^2\alpha_2\beta_2 + \omega\alpha_3\beta_1, \\
&\mathbf{3} \otimes \mathbf{3} \to \mathbf{1}'' && \alpha_1\beta_1 + \omega\alpha_2\beta_2 + \omega^2\alpha_3\beta_1, \\
&\mathbf{3} \otimes \mathbf{3} \to \mathbf{3_1} + \mathbf{3_2} && \begin{pmatrix} \alpha_2\beta_3 \\ \alpha_3\beta_1 \\ \alpha_1\beta_2 \end{pmatrix} + \begin{pmatrix} \alpha_3\beta_2 \\ \alpha_1\beta_3 \\ \alpha_2\beta_1 \end{pmatrix}.
\end{aligned} \tag{A.5}$$

A.2 $\Delta(27)$

$\Delta(27)$ belongs to a class of discrete non-Abelian groups known as $\Delta(3n^2)$. These are isomorphic to the semidirect product of the cyclic group $\mathbb{Z}_3$ with $\mathbb{Z}_n \times \mathbb{Z}_n$; $n = 2$ gives the familiar A_4 group, while $n = 3$ gives $\Delta(27)$. The $\Delta(3n^2)$ class has been studied in detail in [214]. The key aspects relevant to model building are the representations of the group and their product rules. $\Delta(27)$ contains two irreducible triplet representations and nine singlets, which are labelled 1_{rs}, with $r, s = 0, 1, 2$. It is also the smallest in this class to contain a conjugate representation, referred to as an antitriplet.

The $\Delta(27)$ rules for taking the product of a triplet $A = (a_1, a_2, a_3)$ and an antitriplet $\bar{B} = (\bar{b}^1, \bar{b}^2, \bar{b}^3)$ are

$$\begin{aligned}
[A\bar{B}]_{00} &\equiv (a_1\bar{b}^1 + a_2\bar{b}^2 + a_3\bar{b}^3)_{00} \\
[A\bar{B}]_{01} &\equiv (a_1\bar{b}^3 + a_2\bar{b}^1 + a_3\bar{b}^2)_{01} \\
[A\bar{B}]_{02} &\equiv (a_1\bar{b}^2 + a_2\bar{b}^3 + a_3\bar{b}^1)_{02} \\
[A\bar{B}]_{10} &\equiv (a_1\bar{b}^1 + \omega^2 a_2\bar{b}^2 + \omega a_3\bar{b}^3)_{10} \\
[A\bar{B}]_{11} &\equiv (\omega a_1\bar{b}^3 + a_2\bar{b}^1 + \omega^2 a_3\bar{b}^2)_{11} \\
[A\bar{B}]_{12} &\equiv (\omega^2 a_1\bar{b}^2 + \omega a_2\bar{b}^3 + a_3\bar{b}^1)_{12} \\
[A\bar{B}]_{20} &\equiv (a_1\bar{b}^1 + \omega a_2\bar{b}^2 + \omega^2 a_3\bar{b}^3)_{20} \\
[A\bar{B}]_{21} &\equiv (\omega^2 a_1\bar{b}^3 + a_2\bar{b}^1 + \omega a_3\bar{b}^2)_{21} \\
[A\bar{B}]_{22} &\equiv (\omega a_1\bar{b}^2 + \omega^2 a_2\bar{b}^3 + a_3\bar{b}^1)_{22}
\end{aligned} \tag{A.6}$$

where $\omega \equiv e^{i2\pi/3}$. The product of two triplets or two antitriplets yields, respectively, an antitriplet or a triplet. There are three possible products that can be made in each case, labelled I (identity), S (symmetric) and A (antisymmetric). Defining triplets $A = (a_1, a_2, a_3)$, $B = (b_1, b_2, b_3)$ and antitriplets $\bar{A} = (\bar{a}^1, \bar{a}^2, \bar{a}^3)$, $\bar{B} = (\bar{b}^1, \bar{b}^2, \bar{b}^3)$, their products are given by

$$\begin{aligned}
[AB]_I &\equiv (a_1b_1, a_2b_2, a_3b_3)_{02} \\
[\bar{A}\bar{B}]_I &\equiv (\bar{a}^1\bar{b}^1, \bar{a}^2\bar{b}^2, \bar{a}^3\bar{b}^3)_{01} \\
[AB]_S &\equiv (a_2b_3 + a_3b_2, a_3b_1 + a_1b_3, a_1b_2 + a_2b_1)_{02} \\
[\bar{A}\bar{B}]_S &\equiv (\bar{a}^2\bar{b}^3 + \bar{a}^3\bar{b}^2, \bar{a}^3\bar{b}^1 + \bar{a}^1\bar{b}^3, \bar{a}^1\bar{b}^2 + \bar{a}^2\bar{b}^1)_{01} \\
[AB]_A &\equiv (a_2b_3 - a_3b_2, a_3b_1 - a_1b_3, a_1b_2 - a_2b_1)_{02} \\
[\bar{A}\bar{B}]_A &\equiv (\bar{a}^2\bar{b}^3 - \bar{a}^3\bar{b}^2, \bar{a}^3\bar{b}^1 - \bar{a}^1\bar{b}^3, \bar{a}^1\bar{b}^2 - \bar{a}^2\bar{b}^1)_{01}
\end{aligned} \tag{A.7}$$

Note that the bar on antitriplets serve merely a reminder of their assignment under $\Delta(27)$.

Appendix B

Running Yukawa parameters

In order to compare models defined at the GUT scale, as in Chapters 3, 4 and 5, to experimental data which describes fermion mass and mixing parameters at Standard Model scales, we must take into account two things: renormalisation group running and SUSY threshold effects. These effects have been examined by others in [145], where they develop a useful parametrisation of the SUSY threshold effects, and also perform the running, producing data sets which may be incorporated into model-building efforts. This section summarises the key features of that work relevant to the analyses in the above-mentioned chapters.

B.1 Parametrisation of threshold corrections

In supersymmetric extensions of the Standard Model, there are corrections to the Yukawa couplings induced by loops involving SUSY particles, which become relevant at (or near) the scale at which SUSY is broken. Furthermore, these couplings are run from the SUSY scale to the GUT scale using the renormalisation group equations. The MSSM contains a large number of parameters which describe the soft breaking of SUSY and resultant sparticle spectrum. In the absence of a model of SUSY breaking, we know neither the scale of SUSY breaking, nor the sparticle mass spectrum. In such cases one commonly assumes a common scale $M_{\rm SUSY}$ where all superpartners are integrated out simultaneously. From considerations of the electroweak hierarchy problem, this scale should not significantly exceed ~ 1 TeV.

Corrections to the Yukawa couplings at the threshold $M_{\rm SUSY}$ can be parametrised. In [145], they introduce a set of parameters η_i, which account for contributions which are $\tan\beta$-enhanced, noting that others are expected to give corrections at less-than-percent level. A connection is made between the Standard Model and MSSM Yukawa matrices

via matching conditions

$$\begin{aligned} Y^u_{\rm SM} &\simeq Y^u_{\rm MSSM} \sin\bar{\beta}, \\ Y^d_{\rm SM} &\simeq (\mathbb{1} + {\rm diag}(\bar{\eta}_q, \bar{\eta}_q, \bar{\eta}_b))\, Y^d_{\rm MSSM} \cos\bar{\beta}, \\ Y^e_{\rm SM} &\simeq (\mathbb{1} + {\rm diag}(\bar{\eta}_\ell, \bar{\eta}_\ell, 1))\, Y^e_{\rm MSSM} \cos\bar{\beta}. \end{aligned} \tag{B.1}$$

For more details on the origin of these parameters, we refer the reader to the original paper. We do however note here that corrections to the τ Yukawa coupling y_τ are subsumed into a redefinition $\beta \to \bar{\beta}$. In the limit where threshold corrections to y_τ are negligible, this reduces to the usual β. In all cases in this thesis, such a scenario is assumed.

The models described in this thesis reduce to the MSSM. As such, we are concerned with the MSSM Yukawa couplings, so we may rearrange Eq. B.1 to give an expression for each MSSM coupling, as

$$\begin{aligned} y^{\rm MSSM}_{u,c,t} &\simeq y^{\rm SM}_{u,c,t} \csc\bar{\beta}, \\ y^{\rm MSSM}_{d,s} &\simeq (1+\bar{\eta}_q)^{-1}\, y^{\rm SM}_{d,s} \sec\bar{\beta}, \\ y^{\rm MSSM}_{b} &\simeq (1+\bar{\eta}_b)^{-1}\, y^{\rm SM}_{b} \sec\bar{\beta}, \\ y^{\rm MSSM}_{e,\mu} &\simeq (1+\bar{\eta}_\ell)^{-1}\, y^{\rm SM}_{e,\mu} \sec\bar{\beta}, \\ y^{\rm MSSM}_{\tau} &\simeq y^{\rm SM}_{\tau} \sec\bar{\beta}. \end{aligned} \tag{B.2}$$

The CKM matrix will also be altered by these threshold corrections. The authors note that, to good approximation, θ^q_{12} and δ^q are not affected by SUSY threshold corrections. The MSSM mixing angles (at $M_{\rm SUSY}$) are given by

$$\begin{aligned} \theta^{q,{\rm MSSM}}_{i3} &\simeq \frac{1+\bar{\eta}_b}{1+\bar{\eta}_q}\, \theta^{q,{\rm SM}}_{i3}, \\ \theta^{q,{\rm MSSM}}_{12} &\simeq \theta^{q,{\rm SM}}_{12}, \\ \delta^{q,{\rm MSSM}} &\simeq \delta^{q,{\rm SM}}. \end{aligned} \tag{B.3}$$

These values are then run up to the GUT scale using the renormalisation group errors, i.e. $y_i^{\rm MSSM} \to y_i^{\rm MSSM@GUT}$. Those may then be compared to the GUT model predictions. The analysis in [145] shows that the running depends primarily on the parameters $\bar{\eta}_b$ and $\bar{\beta}$. They provide the necessary GUT-scale values for the observables defined in Eqs. B.2 and B.3, as functions of these SUSY parameters.

Meanwhile, the neutrino mass and mixing parameters are expected to be largely insensitive to group running. As the experimental uncertainties are larger than in the quark sector, these will dominate the overall error.

Let us summarise the particular choices for SUSY parameters made in each model presented in this thesis. In all cases we assume $M_{\rm SUSY} = 1$ TeV. In the $A_4 \times SU(5)$ model

in Chapter 3, we set $\bar{\eta}_b = -0.24375$. Note that this does not imply five orders of precision, rather the datasets from which we extract quark couplings give the input values in discrete intervals; for $\bar{\eta}_b$, they are multiples of ± 0.01875. All other threshold parameters are set to zero, while for $\tan\beta$ we consider two cases, $\tan\beta = 5$ and 10. In the $\Delta(27) \times SO(10)$ model of Chapter 4, we find the fit is rather insensitive to threshold corrections, and simply set all $\bar{\eta}_i$ parameters to zero. As it was found that $\tan\beta$ has only marginal effects on the quality of the fit (as long as it was not much larger than 10), we also assume $\tan\beta = 5$ for convenience.

Conversely, in the $S_4 \times SO(10)$ model of Chapter 5 the threshold corrections play a crucial role in achieving a good fit to data. It is sufficient to assume only one of the threshold parameters, namely $\bar{\eta}_b$, is non-zero, however it must take a rather large negative value $\bar{\eta}_b = -0.8$. This has two primary effects. One is to shift the bottom quark Yukawa coupling by an amount proportional to $\bar{\eta}_b$, the second is to alter the relative running of quark masses and CKM mixing angles $\theta^q_{13,23}$ such that the tension (described in Chapter 5) between Yukawa and CKM parameters is sufficiently ameliorated. The effect on group running is dominated by $\bar{\eta}_b$. Any particular choice of $\bar{\eta}_q$ will scale the d and s Yukawa couplings as well as θ^q_{13} and θ^q_{23} without affecting the running, a shift which can largely be subsumed into the free parameters $y^d_{1,2}$. We do find that the running of fermion Yukawa couplings can change noticeably for large $\tan\beta \gtrsim 25$. However, generically the model prefers a smaller value of $\tan\beta$, so we focus on this region of parameter space.[1] For $5 \lesssim \tan\beta \lesssim 15$, the Yukawa couplings run uniformly regardless of the precise value of $\tan\beta$. The shift by an overall factor $\cos\beta$ in $Y^{d,e}$ can again be subsumed into the parameters $y^{d,e}_{1,2,3}$. For definiteness, we set $\tan\beta = 5$.

[1] One must also be careful that the corrections, which are calculated at one loop, remain perturbative. For large $\tan\beta$, the b coupling can easily be larger than 1, beyond which we cannot trust one-loop results.

Appendix C

Symmetry breaking in models

C.1 GUT breaking in $A_4 \times SU(5)$

In this section we discuss the aspects of the model described in Chapter 3 that relate to grand unification, including how the R symmetry and the GUT gauge group are spontaneously broken. We then describe the details of the missing partner (MP) mechanism giving heavy Higgs triplets.

C.1.1 $SU(5)$ and $\mathbb{Z}_4^R$ breaking

We refer to the superfields involved in GUT and R symmetry breaking as the scalar sector. This includes several superfields found in Table 3.1a, and repeated in Table C.1a for convenience. In addition we introduce new superfields given in Table C.1b.

The Υ messengers form pairs; their mass scale, unprotected by any symmetry, is near the highest scale of the theory, which we represent generically as M. The GUT breaking superpotential with non-renormalisable terms is then

$$\begin{aligned} W_{\text{GUT}} = Z_1 \left(M\Lambda_{24} + \frac{\lambda_1}{M^2} H_{24}\xi^3 + \lambda_2 Z_1^2 \right) + Z_2 \left(\frac{\lambda_3}{M^2}\Lambda_{24}\xi^3 + \lambda_4 Z_2^2 \right) \\ + Z_3 \left(\lambda_5 H_{24}^2 + \lambda_6 Z_3^2 \right). \end{aligned} \tag{C.1}$$

We have five GUT adjoint superfields, three of which (the Z fields) are charged by 2 and two (Λ_{24} and H_{24}) by 0 under the R symmetry. Also appearing in W_{GUT} is the Majoron ξ, the GUT singlet field which we have seen is involved in giving mass to several Standard Model fermions and whose VEV breaks lepton number by giving the right-handed neutrinos their Majorana mass. The supression of the non-renormalisable terms in Eq. C.1 come precisely from the mass of the Υ messengers, as displayed in Fig. C.1.

Field	Representation				
	A_4	$SU(5)$	$\mathbb{Z}_9$	$\mathbb{Z}_6$	$\mathbb{Z}_4^R$
F	3	$\bar{5}$	0	0	1
T_1	1	10	5	0	1
T_2	1	10	7	0	1
T_3	1	10	0	0	1
H_5	1	5	0	0	0
$H_{\bar{5}}$	1	$\bar{5}$	2	0	0
H_{24}	$1'$	24	3	0	0
Λ_{24}	$1'$	24	0	0	0
H_{45}	1	45	4	0	2
$H_{\overline{45}}$	1	$\overline{45}$	5	0	0
ξ	1	1	2	0	0

(a) Relevant superfields from Table 3.1a.

Field	Representation				
	A_4	$SU(5)$	$\mathbb{Z}_9$	$\mathbb{Z}_6$	$\mathbb{Z}_4^R$
Z_1	$1''$	24	0	0	2
Z_2	$1''$	24	3	0	2
Z_3	$1'$	24	3	0	2
Υ_1	$1'$	24	7	0	0
Υ_2	$1''$	24	2	0	2
Υ_3	$1'$	24	5	0	0
Υ_4	$1''$	24	4	0	2
Υ_5	$1'$	24	4	0	0
Υ_6	$1''$	24	5	0	2
Υ_7	$1'$	24	2	0	0
Υ_8	$1''$	24	7	0	2
Υ_9	1	75	0	0	0
Υ_{10}	1	75	0	0	2
Υ_{11}	1	75	6	0	0
Υ_{12}	1	75	3	0	2
Ω_1	1	50	4	0	2
Ω_2	1	$\overline{50}$	3	0	0
Ω_3	1	50	1	0	2
Ω_4	1	$\overline{50}$	8	0	0
Π_1	1	75	6	0	2
Π_2	1	75	3	0	0

(b) Extended scalar sector.

Table C.1: Superfields that govern GUT and R-symmetry breaking.

A renormalisable term of the form $Z_2 H_{24} \Pi_2$, allowed by the symmetries, has been dropped to make the discussion more transparent. This term mixes the VEVs of the GUT breaking scalars with the ones in the MP mechanism so they should be naturally around the same scale $M \sim M_{\text{GUT}}$. Beyond this, its practical effect is minimal: the fields obtain VEVs with or without this term. Since the VEVs get very complicated when this "mixing" term is included, we ignore it for simplicity, simply bearing in mind that VEVs from both sets of fields are related.

Figure C.1: Diagrams giving the non-renormalisable terms in Eq. C.1.

W_{GUT} has a non-trivial minimum

$$\begin{aligned} v_{Z_1} &= -\frac{i2^{2/3}\lambda_1\lambda_4^{1/3}\lambda_6^{1/6}}{3^{1/2}\lambda_2\lambda_3\lambda_5^{1/2}}M, & v_{H_{24}} &= \frac{\lambda_1\lambda_4^{1/3}\lambda_6^{1/3}}{\lambda_2^{2/3}\lambda_3\lambda_5}M, \\ v_{Z_2} &= \frac{i2^{1/3}\lambda_1\lambda_6^{1/6}}{3^{1/2}\lambda_2^{2/3}\lambda_3\lambda_5^{1/2}}M, & v_{\Lambda_{24}} &= \frac{2^{1/3}\lambda_1^2\lambda_4^{2/3}\lambda_6^{1/3}}{\lambda_2\lambda_3^2\lambda_5}M, \\ v_{Z_3} &= \frac{i\lambda_1\lambda_4^{1/3}}{3^{1/2}\lambda_2^{2/3}\lambda_3\lambda_5^{1/2}\lambda_6^{1/6}}M, & \langle\xi\rangle^3 &= \frac{2^{1/3}\lambda_4^{1/3}}{\lambda_2^{1/3}\lambda_3}M^3, \end{aligned} \tag{C.2}$$

where all the adjoint scalars get a VEV of the form $\langle\Phi_{24}\rangle = v_{\Phi_{24}}\ \text{diag}(2,2,2,-3,-3)$. By themselves, the F-terms associated with W_{GUT} also allow a trivial minimum where the magnitude of each VEV vanishes. But after SUSY is broken and we consider the effects of the small contribution from radiative breaking [215] to the scalar components of the GUT-breaking superfields (as we did for the A_4-breaking flavons in Section 3.4), the stationary point with vanishing magnitudes is no longer a minimum due to the radiatively induced negative squared mass term. To a very good approximation the true minima are given by the magnitudes in Eq. C.2, which are now a lower energy state than the trivial F-term solution. We conclude that Eq. C.1 can generate GUT and R-symmetry breaking at high scale, with $\mathbb{Z}_4^R$ broken to $\mathbb{Z}_2^R$ (standard R parity) by the Z_i VEVs.[1]

A slightly unappealing issue with W_{GUT} is that the minimum requires some non-$\mathcal{O}(1)$ choice of λ parameters if we are to obtain a hierarchy between the VEVs of H_{24} and Λ_{24}, and an appropriate value for $\langle\xi\rangle/M$ (as shown in Eq. 3.19). These requirements come from the successful fit to up and down quark and charged lepton masses (see Section 3.3) and partly also for the μ term, as will be discussed shortly. However, since the messengers will in general have different masses (recall we set them all equal to M only for simplicity), the λ parameters need not be as hierarchical as Eq. C.2 appears to indicate. For example, if the masses of messengers Σ are slighly larger than the GUT-scale masses of messengers Υ, this would allow all λ to be $\mathcal{O}(1)$.

We note also that, although we are considering a situation where the superpotential parameters (the M and λ couplings) are real due to CP conservation, the VEVs of the GUT-breaking scalars may be complex, since they depend on n^{th}-order roots of real numbers. As noted in Section 3.4, the phases of the fields ξ, Z_2 and Z_3 are relevant for establishing the physical phase η in the neutrino mass matrix, which controls neutrino masses and mixing. We see immediately that $\rho_\xi = \frac{2\pi k}{9}$, for integer k, i.e. one of nine roots of unity. While ρ_{Z_2} and ρ_{Z_3} individually can be any of six roots, originating in the factor $\lambda_5^{1/6}$, their product Z_2Z_3 cancels this factor such that the largest root is a third, giving $\rho_{Z_2} + \rho_{Z_3} = \frac{2\pi k'}{3}$, for integer k'.

[1] Because $\mathbb{Z}_4^R$ is broken at a high scale, the no-go theorem from [216] does not apply to our model and we verified that all the components of the $SU(5)$ adjoints acquire GUT-scale masses.

C.1.2 Doublet-triplet splitting, Higgs mixing and the μ term

Given that we have a number of GUT representations containing weak doublets and colour triplets we turn now to a brief discussion of how doublet-triplet splitting is achieved in this model via the MP mechanism, with the fields listed in Table C.1b. We have a superpotential

$$W_{\Pi} = \Pi_1 \left(\lambda_7 \Pi_1^2 + M\Pi_2 + \frac{\lambda_8}{M^2} \Pi_2^4 \right), \tag{C.3}$$

which gives Π, the **75**s of $SU(5)$, their VEVs

$$v_{\Pi_1} = -\frac{1}{16^{1/3} \lambda_7^{1/2} \lambda_8^{1/6}} M, \qquad v_{\Pi_2} = -\frac{1}{4\lambda_8^{1/3}} M, \tag{C.4}$$

which are aligned with the Standard Model singlet inside the $SU(5)$ **75**. The non-renormalisable term in W_{Π} comes from the diagram in Fig. C.2.

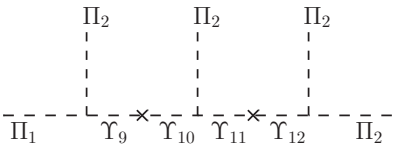

Figure C.2: Diagram giving the non-renormalisable term in W_{Π}.

With Eq. C.4, the MP mechanism proceeds through the superpotential

$$\begin{aligned} W_{\mathrm{MP}} = {} & H_{\bar{5}}\Omega_1\Pi_2 + H_5\Omega_2\Pi_1 + \xi\Omega_1\Omega_2 + H_{\overline{45}}\Omega_3\Pi_2 + MH_{\overline{45}}H_{45} + M\Omega_3\Omega_4 \\ & + H_{\bar{5}}H_{45}\Pi_2 + H_5 H_{\overline{45}}\Pi_1 \left(\frac{\xi}{M}\right)^8, \end{aligned} \tag{C.5}$$

where we have suppressed coupling constants for convenience. The very high-order non-renormalisable term at the end arises through the Σ messengers listed in Table 3.1b in Chapter 3.[2] Strictly speaking this term does not participate in splitting the masses of doublets and triplets, rather it is the source of the μ term in our model, as shown below.

The terms in W_{MP} generate mixing between the **45**s and **5**s of $SU(5)$. The mass matrix for the triplets contained in the **45**s and **5**s is

$$M_{\mathbf{3}} = \overline{\mathbf{3}}^{\intercal} \begin{pmatrix} 0 & v_{\Pi_2} & v_{\Pi_2} & 0 \\ v_{\Pi_1}\tilde{\xi}^8 & M & 0 & v_{\Pi_2} \\ v_{\Pi_1} & 0 & \langle\xi\rangle & 0 \\ 0 & 0 & 0 & M \end{pmatrix} \mathbf{3}, \tag{C.6}$$

[2] Recall that half the Σ_i participate in constructing up-type Yukawa terms, as illustrated in Figure 3.1.

where

$$\begin{aligned}\overline{\mathbf{3}} &= (\mathbf{3}(H_{\bar{5}}),\ \mathbf{3}(H_{\overline{45}}),\ \mathbf{3}(\Omega_2),\ \mathbf{3}(\Omega_4))\,,\\ \mathbf{3} &= (\mathbf{3}(H_5),\ \mathbf{3}(H_{45}),\ \mathbf{3}(\Omega_1),\ \mathbf{3}(\Omega_3))\,,\end{aligned} \tag{C.7}$$

and once again $\tilde{\xi} = v_\xi/M$. Taking $\langle \Pi_{1,2} \rangle \sim M$, the eigenvalues of this mass matrix are all of order M (i.e. at the GUT scale), leading us to conclude there are no light triplets. Conversely, for the doublets we have the matrix

$$M_2 = \begin{pmatrix}\mathbf{2}(H_{\bar{5}}) & \mathbf{2}(H_{\overline{45}})\end{pmatrix} \begin{pmatrix} 0 & v_{\Pi_2} \\ v_{\Pi_1}\tilde{\xi}^8 & M \end{pmatrix} \begin{pmatrix}\mathbf{2}(H_5) \\ \mathbf{2}(H_{45})\end{pmatrix}. \tag{C.8}$$

It is clear that were it not for $\tilde{\xi}^8$, the determinant of this mass matrix would vanish. We may rotate to the basis of the MSSM Higgs doublets $H_{u,d}$ and a pair of very heavy doublets $H^H_{u,d}$,

$$\begin{aligned}\begin{pmatrix}\mathbf{2}(H_{\bar{5}}) \\ \mathbf{2}(H_{\overline{45}})\end{pmatrix} &\approx \frac{1}{\sqrt{2}} \begin{pmatrix} 1 & -1 \\ 1 & 1 \end{pmatrix} \begin{pmatrix} H^H_d \\ H_d \end{pmatrix},\\ \begin{pmatrix}\mathbf{2}(H_5) \\ \mathbf{2}(H_{45})\end{pmatrix} &\approx \begin{pmatrix} \tilde{\xi}^8 & 1 \\ -1 & \tilde{\xi}^8 \end{pmatrix} \begin{pmatrix} H^H_u \\ H_u \end{pmatrix}.\end{aligned} \tag{C.9}$$

The usual MSSM term $\mu H_d H_u$ comes from this mechanism with

$$\mu \sim \frac{v_{\Pi_1} v_{\Pi_2}}{M} \tilde{\xi}^8, \tag{C.10}$$

where v_{Π_1} provides the necessary $\mathbb{Z}_4^R$ breaking. Using the approximate values from Eq. 3.19 for flavon and Higgs VEV magnitudes, we see that $\tilde{\xi}^8 \sim 1.6 \times 10^{-10} M_{\text{GUT}}$. If we choose the couplings at the vertices of the tower that generates the ξ^8 term to be ~ 0.5 we may get a term $\mu \sim \mathcal{O}(10^2 - 10^3)$ GeV without any fine-tuning.

C.2 Family symmetry breaking in $\Delta(27) \times SO(10)$

We turn now to the $\Delta(27) \times SO(10)$ model described in Chapter 4. In this section we show how the CSD(3) alignments are produced by F-term alignment and orthogonality arguments. We further write down a superpotential which drives the VEVs of the flavons, such that they acquire expectation values at a fixed scale (slightly below the GUT scale), with phases fixed to discrete roots of unity. In particular, the relative phases between $\bar{\phi}_{\text{atm}}$, $\bar{\phi}_{\text{sol}}$ and $\bar{\phi}_{\text{dec}}$ are constrained to discrete choices, which subsequently fixes the physical phases η, η' in the lepton mass matrices to exact values.

C.2.1 Obtaining the CSD(3) alignments

Field	Representation				
	$\Delta(27)$	$SO(10)$	$\mathbb{Z}_9$	$\mathbb{Z}_{12}$	$\mathbb{Z}_4^R$
$\bar{\phi}_{\text{dec}}$	$\bar{3}$	1	6	0	0
$\bar{\phi}_{\text{atm}}$	$\bar{3}$	1	1	0	0
$\bar{\phi}_{\text{sol}}$	$\bar{3}$	1	5	6	0
$\bar{\phi}_1$	$\bar{3}$	1	0	4	0
$\bar{\phi}_7$	$\bar{3}$	1	0	5	0
ϕ_0	3	1	2	6	0
ϕ_2	3	1	3	7	0
ϕ_8	3	1	1	8	0
ϕ_4	3	1	3	0	0
ϕ_6	3	1	0	11	0
σ_{00}^0	1_{00}	1	0	1	0
σ_{01}^0	1_{01}	1	0	1	0
σ_{01}^1	1_{01}	1	0	0	0

(a) Flavons.

Field	Representation				
	$\Delta(27)$	$SO(10)$	$\mathbb{Z}_9$	$\mathbb{Z}_{12}$	$\mathbb{Z}_4^R$
A_1	3	1	0	8	2
A_3	3	1	3	0	2
$\bar{A}_0$	$\bar{3}$	1	7	5	2
$\bar{A}_4$	$\bar{3}$	1	6	0	2
O_{02}	1_{02}	1	0	5	2
O_{00}	1_{00}	1	6	1	2
O_{00}^1	1_{00}	1	5	5	2
O_{01}^1	1_{01}	1	5	0	2
O_{02}^2	1_{02}	1	3	1	2
$O_{02}'^2$	1_{02}	1	6	0	2
O_{00}^2	1_{00}	1	0	8	2
O_{01}^2	1_{01}	1	0	8	2
O_{00}^3	1_{00}	1	8	11	2
$O_{00}'^3$	1_{00}	1	7	4	2
O_{01}^4	1_{01}	1	1	11	2
O_{00}^4	1_{00}	1	3	10	2

(b) Driving superfields.

Table C.2: Superfields responsible for obtaining CSD(3) vacuum alignments.

The flavons involved in this alignment mechanism are given in Table C.2a, and the necessary driving fields are given in Table C.2b. The special directions for $\Delta(27)$ are VEVs with two zeros, and VEVs with 3 equal magnitudes, with phases that are powers of $\omega = e^{i2\pi/3}$. There are three distinct ways to obtain either the $(0,0,1)$ class of VEV or the $(1,1,1)$ class of VEV [217]. One of the possibilities that we make use of here uses invariants built out of an antitriplet and triplet, and out of three triplets, of the type

$$c[A\bar{\phi}]_{00} + c_I[A[\phi\phi]_I]_{00} + c_S[A[\phi\phi]_S]_{00}, \tag{C.11}$$

where $\bar{\phi}$ is an antitriplet unrelated to triplet ϕ and A is itself a triplet, giving rise to three F terms

$$\begin{aligned} c\bar{\phi}^1 + c_I\phi_1\phi_1 + 2c_S\phi_2\phi_3 &= 0, \\ c\bar{\phi}^2 + c_I\phi_2\phi_2 + 2c_S\phi_3\phi_1 &= 0, \\ c\bar{\phi}^3 + c_I\phi_3\phi_3 + 2c_S\phi_1\phi_2 &= 0. \end{aligned} \tag{C.12}$$

To obtain the VEVs we require in the $(0,0,1)$ and $(1,1,1)$ classes of VEVs, an economical solution is the superpotential

$$\begin{aligned} W_{V0} = {} & c_a[\phi_0 \overline{A}_0]_{00}\sigma^0_{00} + c_b[\phi_0 \overline{A}_0]_{02}\sigma^0_{01} \\ & + c_c[A_1\overline{\phi}_1]_{00}M + c_d[A_1\overline{\phi}_1]_{02}\sigma^1_{01} \\ & + c_e[A_3\overline{\phi}_3]_{00}M + c_f[A_3[\phi_4\phi_4]_I]_{00} + c_g[A_3[\phi_4\phi_4]_S]_{00} \\ & + c_h[\phi_4\overline{A}_4]_{00}M + c_i[[\overline{\phi}_3\overline{\phi}_3]_I\overline{A}_4]_{00} + c_j[[\overline{\phi}_3\overline{\phi}_3]_S\overline{A}_4]_{00} \\ & + O_{02}[\phi_2\overline{\phi}_3]_{01} + O_{00}[\phi_2\overline{\phi}_1]_{00}, \end{aligned} \tag{C.13}$$

where the c_x $(x = a, \ldots, j)$ are coefficients that we show explicitly, and the coefficients for the other terms are not shown as they aren't relevant when taking the respective F term. The triplet flavon ϕ_0 is aligned to $(1, \omega, \omega^2)$ similarly to how the antitriplet flavon $\overline{\phi}_1$ is aligned to $(1,1,1)$, through the alignment antitriplet $\overline{A}_0$ or triplet A_1 and flavon singlets σ^0_{00}, σ^0_{01} VEVs with a relative phase of ω and σ^1_{01} taking a real VEV.

The antitriplet flavon $\overline{\phi}_3$ is aligned in a $(0,0,1)$ direction together with the triplet ϕ_4. This proceeds from the F terms of the components of A_3 and $\overline{A}_4$, which are of the type shown in Eq. C.12. Taken together the six equations only allow a discrete set of solutions where both flavons are aligned in the same direction. One of the solutions has them aligned like $(0,0,v_3)$ and $(0,0,v_4)$,[3] with their magnitudes v_3 and v_4 fixed. The relevant VEV magnitudes are

$$v_3^3 = -\frac{c_e c_h^2}{c_f c_i^2}M^3, \qquad v_4^3 = -\frac{c_e^2 c_h}{c_f^2 c_i}M^3, \qquad \langle\sigma^1_{01}\rangle = -\frac{c_c}{c_d}M. \tag{C.14}$$

We impose trivial CP symmetry on the flavons, including the triplets and antitriplets. This is consistent with the contractions that make invariants with the 1_{0i} set of singlets that we are using. Since the coupling constants c_x are forced to be real by CP conservation, up to minus signs (which can be reabsorbed into the real coefficients) the VEVs $v_{3,4}$ can have a phase only as a third root of unity while $\langle\sigma^1_{01}\rangle$ has to be real. We expect this mass scale M to be around the GUT scale and with $\mathcal{O}(1)$ c parameters, these VEVs should be at this scale also. The triplet ϕ_2 is then forced into the $(0, y_2, z_2)$ direction due to the alignment singlet O_{02} and the alignment singlet O_{00} ensures $y_2 = -z_2$ by orthogonality with $(1,1,1)$.

In order to have CSD(3) we want the directions $(0,1,1)$ and $(1,3,1)$. We can use a chain of orthogonality relations, where in $\Delta(27)$ they must be between triplet and antitriplets. Using the three directions above we can arrive at $(0,1,1)$ through orthogonality with ϕ_2 and ϕ_4, by

$$W_{V1} = O^1_{00}[\phi_2\overline{\phi}_5]_{00} + O^1_{01}[\phi_4\overline{\phi}_5]_{02}. \tag{C.15}$$

[3] The phenomenologically viable solution is where both flavons are aligned in the $(0,0,1)$ direction, another possibility is that they would both be aligned in the $(1,1,1)$ direction.

With this we obtain a $\bar{\phi}_5$ antitriplet in the $(0,1,1)$ direction (note the $[]_{02}$ contraction matches the first component of the antitriplet with the third component of the triplet, putting the zero in the right place in $\bar{\phi}_5$).

In order to get to $(1,3,1)$ we require a $(2,-1,1)$ direction, which itself requires $(1,1,-1)$. To obtain the latter we also duplicate the $\bar{\phi}_5$ direction in a triplet ϕ_6 (other than them having VEVs in the same direction, $\bar{\phi}_5$ and ϕ_6 are unrelated). This may be achieved by the superpotential

$$W_{V2} = O^2_{02}[\phi_6\bar{\phi}_3]_{01} + O'^2_{02}[\phi_2\bar{\phi}_7]_{01} + O^2_{00}[\phi_6\bar{\phi}_7]_{00} + O^2_{01}[\phi_6\bar{\phi}_7]_{02}. \tag{C.16}$$

The first two orthogonalities ensure a zero in the first component of ϕ_6, i.e. $(0, y_6, z_6)$, and that $\bar{\phi}_7$ is aligned in a direction (x_7, x_7, z_7). The other two mutual orthogonalities give $0x_7 + y_6x_7 + z_6z_7 = 0$ and $0x_7 + y_6z_7 + z_6x_7 = 0$, which complete the $(0,1,1)$ and $(1,1,-1)$ alignments. Strictly speaking, this alignment allows both an undesired solution where we get $(0,1,-1)$ with $(1,1,1)$ and the desired solution of $(0,1,1)$ with $(1,1,-1)$.

The next step is obtaining the $(2,-1,1)$ as a triplet. For this we want to use the $(0,1,1)$ antitriplet direction, and the antitriplet with the recently obtained $(1,1,-1)$ direction, by

$$W_{V3} = O^3_{00}[\phi_8\bar{\phi}_7]_{00} + O'^3_{00}[\phi_8\bar{\phi}_5]_{00}. \tag{C.17}$$

Finally, by orthogonality

$$W_{V4} = O^4_{01}[\phi_2\bar{\phi}_9]_{02} + O^4_{00}[\phi_8\bar{\phi}_9]_{00}, \tag{C.18}$$

one obtains the $(1,3,1)$ direction as an antitriplet. We did not need to align a $(1,0,-1)$ direction as the $[\ldots]_{02}$ contraction with the triplet $(0,1,-1)$ (ϕ_2) puts its zero together with the second component of the antitriplet $\bar{\phi}_9$.

Noting now that the VEVs of antitriplets $\bar{\phi}_3$, $\bar{\phi}_5$ and $\bar{\phi}_9$ are the desired directions for $\bar{\phi}_{\text{dec}}$, $\bar{\phi}_{\text{atm}}$, and $\bar{\phi}_{\text{sol}}$ respectively, we now rename them to match the notation used in earlier discussions, so $v_3 = v_{\text{dec}}$ and

$$\bar{\phi}_3 \equiv \bar{\phi}_{\text{dec}}, \qquad \bar{\phi}_5 \equiv \bar{\phi}_{\text{atm}}, \qquad \bar{\phi}_9 \equiv \bar{\phi}_{\text{sol}}. \tag{C.19}$$

This notation is also used in Table C.2b, which summarises the field content and their representation under the symmetries. For the sake of completeness we collect all alignment terms into one superpotential

$$W_V = W_{V0} + W_{V1} + W_{V2} + W_{V3} + W_{V4}, \tag{C.20}$$

such that, omitting the coefficients, we have

$$\begin{aligned} W_V = {} & [\phi_0\overline{A}_0]_{00}\sigma^0_{00} + [\phi_0\overline{A}_0]_{02}\sigma^0_{01} + [A_1\bar{\phi}_1]_{00}M + [A_1\bar{\phi}_1]_{02}\sigma^1_{01} \\ & + [A_3\bar{\phi}_3]_{00}M + [A_3[\phi_4\phi_4]_I]_{00} + [A_3[\phi_4\phi_4]_S]_{00} \\ & + [\phi_4\overline{A}_4]_{00}M + [[\bar{\phi}_3\bar{\phi}_3]_I\overline{A}_4]_{00} + [[\bar{\phi}_3\bar{\phi}_3]_S\overline{A}_4]_{00} \\ & + O_{02}[\phi_2\bar{\phi}_3]_{01} + O_{00}[\phi_2\bar{\phi}_1]_{00} + O^1_{00}[\phi_2\bar{\phi}_{\rm atm}]_{00} + O^1_{01}[\phi_4\bar{\phi}_{\rm atm}]_{02} \\ & + O^2_{02}[\phi_6\bar{\phi}_{\rm dec}]_{01} + O'^2_{02}[\phi_2\bar{\phi}_7]_{01} + O^2_{00}[\phi_6\bar{\phi}_7]_{00} + O^2_{01}[\phi_6\bar{\phi}_7]_{02} \\ & + O^3_{00}[\phi_8\bar{\phi}_7]_{00} + O'^3_{00}[\phi_8\bar{\phi}_{\rm atm}]_{00} + O^4_{01}[\phi_2\bar{\phi}_{\rm sol}]_{02} + O^4_{00}[\phi_8\bar{\phi}_{\rm sol}]_{00}. \end{aligned} \tag{C.21}$$

We summarise the alignments produced by the above superpotential as follows:

$$\begin{aligned} \langle\phi_0\rangle &\propto (1,\omega,\omega^2), & \langle\bar{\phi}_1\rangle &\propto (1,1,1), \\ \langle\phi_2\rangle &\propto (0,1,-1), & \langle\bar{\phi}_{\rm dec}\rangle &\propto (0,0,1), \\ \langle\phi_4\rangle &\propto (0,0,1), & \langle\bar{\phi}_{\rm atm}\rangle &\propto (0,1,1), \\ \langle\phi_6\rangle &\propto (0,1,1), & \langle\bar{\phi}_7\rangle &\propto (1,1,-1), \\ \langle\phi_8\rangle &\propto (2,-1,1), & \langle\bar{\phi}_{\rm sol}\rangle &\propto (1,3,1). \end{aligned} \tag{C.22}$$

C.2.2 Driving the flavon VEVs

To drive the flavon VEVs, we introduce a set of superfields given in Table C.3. They are GUT singlets with nontrivial representations under $\Delta(27)$ and the $\mathbb{Z}$ symmetries, and couple to the flavons.

Field	Representation				
	$\Delta(27)$	$SO(10)$	$\mathbb{Z}_9$	$\mathbb{Z}_{12}$	$\mathbb{Z}_4^R$
P_1	1_{00}	1	8	1	2
P_2	1_{00}	1	1	6	2
P_3	1_{01}	1	2	0	2
ζ_i	1_{00}	1	$i \in \{0,1,2,3\}$	1	2
$\bar{\zeta}_i$	1_{00}	1	$i \in \{0,6,7,8\}$	11	0
ζ'_i	1_{01}	1	$i \in \{3,4,5\}$	0	2
$\bar{\zeta}'_i$	1_{02}	1	$i \in \{4,5,6\}$	0	0

Table C.3: Field content for driving the flavon VEVs.

To obtain the necessary superpotential we need to add more messengers $\zeta, \bar{\zeta}$, with a characteristic mass M_ζ, also listed in Table C.3. The superpotential which drives the

flavons is

$$\begin{aligned} W_\phi = P_1 \left[\kappa_1 \left(\frac{\xi}{M_\zeta} \right)^4 \bar{\phi}_{\text{dec}} \phi_6 - \kappa_2 \bar{\phi}_{\text{atm}} \phi_6 \right] + P_2 \left[\kappa_3 \bar{\phi}_{\text{sol}} \phi_4 - \kappa_4 \bar{\phi}_{\text{dec}} \phi_0 \right] \\ + P_3 \left[\kappa_5 \bar{\phi}_{\text{sol}} \phi_0 - \kappa_6 \left(\frac{\xi}{M_\zeta} \right)^3 \bar{\phi}_{\text{atm}} \phi_4 \right], \end{aligned} \tag{C.23}$$

where κ_i are real dimensionless constants. To acquire a good fit to data without tuning, we need to assume that $\langle \xi \rangle \lesssim M_\zeta$. The F-term equations for the P fields give relationships between the VEVs of the flavons that couple to the Standard Model particles. The (nontrivial) representations of the P fields under $\Delta(27)$ are chosen specifically so that the pairs of flavon VEVs they are multiplied by do not give zero when they acquire VEVs.

The constants κ_i are forced to be real by CP conservation, but the VEV $\langle \phi_0 \rangle$ has complex components that introduce phases to the other VEVs. Specifically, the terms multiplied by the constants $\kappa_{4,5}$ obtain the following factors when contracting the $\Delta(27)$ triplets:

$$[\langle \bar{\phi}_{\text{sol}} \rangle \langle \phi_0 \rangle]_{02} = 2 v_{\text{sol}} v_0, \qquad [\langle \bar{\phi}_{\text{dec}} \rangle \langle \phi_0 \rangle]_{00} = \omega^2 v_{\text{dec}} v_0, \tag{C.24}$$

so we may effectively treat as κ_4 carrying a factor of ω^2.

Solutions to the F-term equations for the P fields yield VEVs for the important flavons $\bar{\phi}_{\text{sol}}$ and $\bar{\phi}_{\text{atm}}$, while $\langle \bar{\phi}_{\text{dec}} \rangle$ is given in Eq. C.14 (recall that $v_3 \equiv v_{\text{dec}}$). It is useful to note the relation $v_4 = c_j v_{\text{dec}}^2 / (c_h M)$, which can be seen from comparing the VEVs in Eq. C.14. We obtain

$$v_{\text{sol}}^2 = \omega^2 \frac{\kappa_4 \kappa_6 c_h}{2 \kappa_3 \kappa_5 c_j} \left(\frac{\xi}{M_\zeta} \right)^7 v_{\text{dec}}^2, \qquad v_{\text{atm}}^2 = \frac{\kappa_1^2}{4 \kappa_2^2} \left(\frac{\xi}{M_\zeta} \right)^8 v_{\text{dec}}^2, \tag{C.25}$$

where, since $\langle \xi \rangle / M_\zeta < 1$, we conclude that $v_{\text{dec}} \gg v_{\text{atm}} \sim v_{\text{sol}}$. Given these VEVs, the physical phases defined in Chapter 4 (see Eqs. 4.8, 4.9) are given by

$$\begin{aligned} \eta &= -\arg \left[\frac{v_{\text{sol}}^2}{v_{\text{atm}}^2} \langle \xi \rangle \right] = -\arg[\omega^2], \\ \eta' &= -\arg \left[\frac{v_{\text{dec}}^2}{v_{\text{atm}}^2} \frac{1}{\langle \xi \rangle} \right] = 9 \arg[\langle \xi \rangle], \end{aligned} \tag{C.26}$$

where the real coupling constants c_x, κ_i do not contribute to phases. These phases are in fact completely fixed. As will be shown shortly, the phase of $\langle \xi \rangle$ is a ninth root of unity; by the cancellation of this phase we finally have

$$\eta = \frac{2\pi}{3}, \qquad \eta' = 0. \tag{C.27}$$

Strictly speaking these phases are fixed only up to a relative phase π, depending on the signs of the real constants. However, this additional phase is unphysical, as it may

always be subsumed into other real parameters at the low scale.

C.3 GUT breaking in $\Delta(27) \times SO(10)$

Next, we describe how, in the model described in Chapter 4, $SO(10)$ is broken down to the MSSM via $SU(5)$. We also show how doublet-triplet splitting is achieved, and how only two light Higgs doublets are present below the GUT scale, as in the MSSM.

C.3.1 Breaking potential and diagrams

The superpotential that breaks $SO(10)$ is given by

$$\begin{aligned} W_{\text{GUT}} = {} & M^2 Z + \lambda_1 Z^3 + \lambda_2 Z Z''^2 + \lambda_3 Z'' H_{45}'^2 + \lambda_4 Z \frac{H_{45}'^4}{M_\Upsilon^2} \\ & + \frac{Z H_{16} H_{16}}{M_\Sigma} \left(\lambda_5 H_{10}^d + \lambda_6 \frac{\xi^8}{M_\Sigma^8} H_{10}^u \right) + \frac{Z H_{\overline{16}} H_{\overline{16}}}{M_\Sigma} \left(\lambda_8 \frac{\xi}{M_\Sigma} H_{10}^d + \lambda_7 H_{10}^u \right) \\ & + \lambda_9 Z H_{DW}^2 \frac{\xi^6}{M_Z^6} + H_{DW} \frac{\xi^3}{M_Z^2} \left(\lambda_{10} H_{45} + \lambda_{11} \frac{H_{45}^3}{M_\Upsilon^2} \right) + H_{16} H_{\overline{16}} \left(\lambda_{12} \xi + \frac{\lambda_{13}}{M_Z} \bar{\phi}_1 \phi_8 \right) \\ & + Z \left(\lambda_{14} \frac{\xi^6}{M_Z^6} \bar{\phi}_7 \phi_2 + \lambda_{15} \frac{\xi^8}{M_Z^8} \bar{\phi}_1 \phi_8 + \lambda_{16} \frac{\xi^5}{M_Z^5} \bar{\phi}_{\text{sol}} \phi_4 + \lambda_{17} \frac{\xi^2}{M_Z^2} \bar{\phi}_{\text{sol}} \phi_0 + \lambda_{18} \bar{\phi}_{\text{dec}} \phi_4 \right). \end{aligned} \tag{C.28}$$

The renormalisable diagrams that give rise to this superpotential are given[4] in Figure C.3 (giving lines 1 and 3) and Figure C.4 (giving line 2), and the corresponding messenger fields (Σ, Υ and Z_i) are detailed in Table C.4. Most fields are familiar from the Yukawa sector discussed previously, while the field H_{DW} is an $SO(10)$ adjoint that governs doublet-triplet splitting, as we will see shortly. Note that the model also includes Z_0 (but not $\bar{Z}_0$) which we label Z, and that Υ_6 has the same quantum number as H_{DW} (see Table 4.1). Requiring that all F terms vanish yields a set of equations that fixes the VEVs of the above superfields.

The first line contains terms involving different powers of Z, Z'' and H'_{45}, which ensures that their corresponding F-term conditions fix all VEVs to be non-zero. The exact expressions for the VEVs are complicated and thus are not shown, since they are not enlightening.

The second line has terms involving the fields $H_{10}^{u,d}$ that will be discussed carefully in the next section on doublet-triplet splitting. At this level, the fields $H_{10}^{u,d}$ have a zero VEV, so any term involving two of them does not contribute to the F-term equations.

[4] We omit those diagrams with seven or eight powers of ξ, as they are constructed in a similar way using the same messengers but are not particularly illuminating.

Field	Representation				
	$\Delta(27)$	$SO(10)$	$\mathbb{Z}_9$	$\mathbb{Z}_{12}$	$\mathbb{Z}_4^R$
Z	1	1	0	0	2
Z''	1	1	0	6	2
Z_i	1	1	$i \in \{1, ..., 8\}$	0	2
$\bar{Z}_i$	1	1	$i \in \{1, ..., 8\}$	0	0
$\overline{\Sigma}_{6,7}$	1	$\overline{16}$	$6, 7$	0	2
$\Sigma_{3,2}$	1	16	$3, 2$	0	0
$\tilde{\Sigma}_i$	1	16	$i \in \{0, ..., 8\}$	0	2
$\bar{\tilde{\Sigma}}_i$	1	$\overline{16}$	$i \in \{0, ..., 8\}$	0	0
$\overline{\Upsilon}_{3,2}$	1	45	$3, 2$	0	0
$\Upsilon_{6,7}$	1	45	$6, 7$	0	2
$\overline{\Upsilon}'''$	1	45	0	9	0
Υ'	1	45	0	3	2
$\overline{\Upsilon}''$	1	45	0	6	0
Υ''	1	45	0	6	2

Table C.4: Messenger superfields required for the doublet and triplet mass terms.

The F-term conditions coming from $H_{10}^{u,d}$ themselves relate the $H_{16,\overline{16}}$ VEVs and also fixes the VEV of ξ to be

$$\langle \xi \rangle = \left(\frac{\lambda_5 \lambda_7}{\lambda_8 \lambda_6} \right)^{1/9} M_\Sigma, \tag{C.29}$$

which subsequently fixes the phase of $\langle \xi \rangle$ to be one of the ninth roots of unity.

At this stage it is relevant to consider superfields H_{DW} and Υ_6, which have the same quantum numbers. In terms of superfields Υ_6^a, Υ_6^b, the mass term for the messenger pair reads $M_\Upsilon(c_a \Upsilon_6^a + c_b \Upsilon_6^b)\overline{\Upsilon}_3$. We define $\Upsilon_6 \equiv (c_a \Upsilon_6^a + c_b \Upsilon_6^b)$ and H_{DW} as the orthogonal combination. The F term with respect to $\overline{\Upsilon}_3$ forces Υ_6 to have a zero VEV, meaning it won't contribute elsewhere and justifies identifying it as half of the messenger pair. Therefore, the third line contains different powers of H_{DW} and H_{45} and gives them VEVs.

The model actually allows an infinity of terms involving H_{45}, each with a higher power of this field. We keep only the first two terms since they are enough to give the H_{45} a general VEV, whereas adding the other terms will make its VEV look more complicated, but will not affect the physics. Its own F-term equation fixes its VEV to be

$$v_{45} = \sqrt{-\frac{\lambda_{10}}{\lambda_{11}}} M_\Upsilon, \tag{C.30}$$

which must define the GUT scale, while we choose the signs of $\lambda_{10,11}$ so that it is real. The F term for ξ will fix the VEV of $H_{16,\overline{16}}$. The F terms coming from $H_{16,\overline{16}}$ will drive

the VEVs of the flavons $\bar{\phi}_7$ and ϕ_2 (seen on line 2).

The last line, allowed by the symmetries and messengers, only adds terms to the F terms for Z and ξ, relating their VEVs to the flavon ones. The flavon F terms will fix some of the O field VEVs. The VEVs $\langle H_{16,\overline{16}} \rangle$ specifically break $SO(10) \to SU(5)$. The VEVs $\langle H_{45}, H'_{45}, H_{DW} \rangle$ specifically break $SU(5) \to SU(3) \times SU(2) \times U(1)$. The VEV $\langle \xi \rangle$ completely breaks $\mathbb{Z}_9$. Finally, the VEVs $\langle Z, Z'' \rangle$, carrying 2 units of charge under $\mathbb{Z}_4^R$, break it into the usual $\mathbb{Z}_2^R$ R parity at the GUT scale.

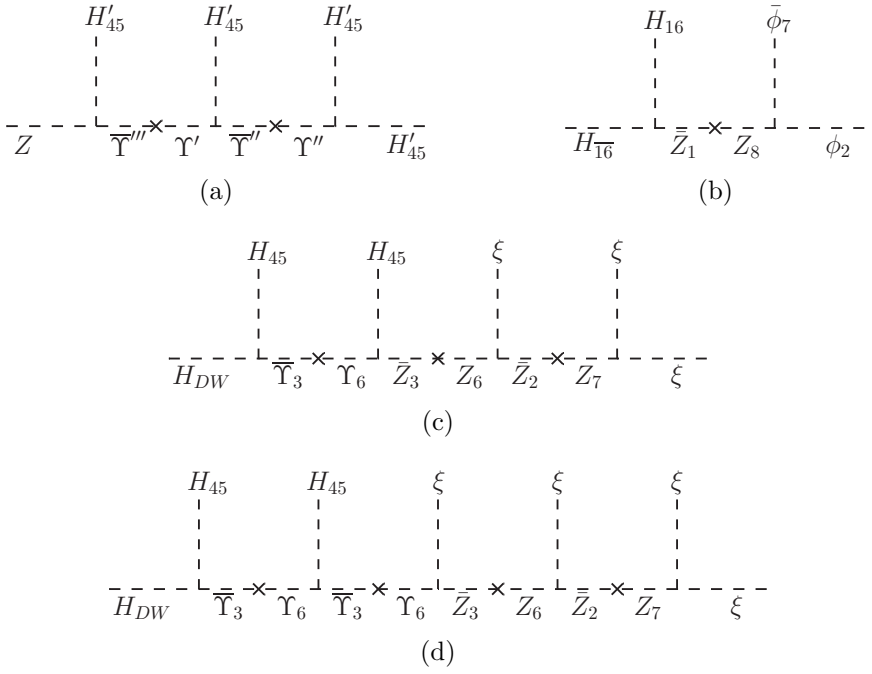

Figure C.3: Diagrams that give rise to GUT-breaking terms.

C.3.2 Obtaining two light Higgs doublets

The Higgs doublets and triplets contained within the $H_{10}^{u,d}$ and $H_{16,\overline{16}}$ superfields acquire masses, in a way dictated by the model such that all triplets are heavy, while only two light Higgs doublets remain at low scales, which we may associate with the MSSM Higgs doublets. Recall that this splitting of doublet and triplet masses is important because any light coloured Higgs states would lead to very rapid proton decay. We solve the doublet-triplet splitting by the familiar Dimopoulos-Wilczek (DW) mechanism [184–186]. In $SO(10)$ there is a further complication, as each **10** has two $SU(2)$ doublet states within it, and we have two additional doublets from the $H_{16,\overline{16}}$. Only two of these six doublets should be light, so as to reduce to the MSSM.

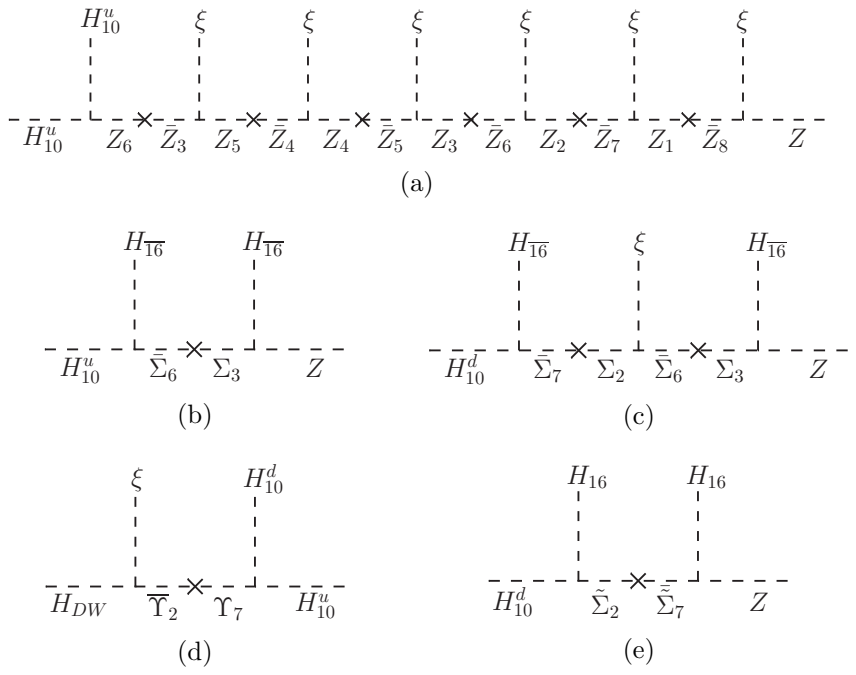

Figure C.4: Diagrams that give rise to doublet-triplet splitting.

The superpotential that gives masses to doublets is

$$W_\mu = Z H_{10}^u H_{10}^u \frac{\xi^6}{M_Z^6} + Z H_{10}^u H_{10}^d \frac{\xi^7}{M_Z^7} + Z H_{10}^d H_{10}^d \frac{\xi^8}{M_Z^8} + \xi H_{16} H_{\overline{16}} + \frac{Z}{M_\Sigma}\left(H_{16} H_{16} H_{10}^d + \frac{\xi^8}{M_\Sigma^8} H_{16} H_{16} H_{10}^u + H_{\overline{16}} H_{\overline{16}} H_{10}^u + \frac{\xi}{M_\Sigma} H_{\overline{16}} H_{\overline{16}} H_{10}^d \right), \tag{C.31}$$

where we suppress $\mathcal{O}(1)$ couplings for convenience. The corresponding diagrams that produce the non-renormalisable terms are given in Figure C.4. The second line is a reproduction of the second line in Eq. C.28, while the first line includes those terms involving more than one insertion of $H_{10}^{u,d}$, which had previously been omitted.

The fields $H_{16,\overline{16}}$ contain doublets that mix with the ones in $H_{10}^{u,d}$, and will also contribute to masses, since they both get VEVs above the GUT scale. Defining $\tilde{H}_{16,\overline{16}} = \langle H_{16,\overline{16}} \rangle / M_\Sigma$, we assume it to be reasonably close to 1. We similarly define $\tilde{\xi} \sim \langle \xi \rangle / M_Z \sim \langle \xi \rangle / M_\Sigma$, where M_Z and M_Σ are the typical scales of the messengers that produce Eq. C.31. We will find that they are necessarily different from the scale M_ζ that governs the flavon driving potential.

In order to make the connection to the two MSSM Higgs doublets, we denote the H_u-like doublets inside a given Higgs field by $\mathbf{2}_u(H)$, where $H \in \{H_{10}^u, H_{10}^d, H_{\overline{16}}\}$. The H_d-like doublets are named similarly, replacing the subindex $u \to d$. In other words, we collect

the Higgs doublets into two vectors

$$\begin{aligned}\mathbf{2}_u &= \left(\mathbf{2}_u(H^u_{10}),\ \mathbf{2}_u(H^d_{10}),\ \mathbf{2}_u(H_{\overline{16}})\right),\\ \mathbf{2}_d &= \left(\mathbf{2}_d(H^u_{10}),\ \mathbf{2}_d(H^d_{10}),\ \mathbf{2}_d(H_{16})\right).\end{aligned} \tag{C.32}$$

The doublet mass matrix can then be written as

$$M_{\mathbf{2}} = \mathbf{2}_d^{\intercal} \begin{pmatrix} \tilde{\xi}^6 & \tilde{\xi}^7 & \tilde{H}_{\overline{16}} \\ \tilde{\xi}^7 & \tilde{\xi}^8 & \tilde{\xi}\tilde{H}_{\overline{16}} \\ \tilde{H}_{16}\tilde{\xi}^8 & \tilde{H}_{16} & \xi/\langle Z\rangle \end{pmatrix} \langle Z\rangle\, \mathbf{2}_u. \tag{C.33}$$

Its eigenvalues $m_{\mathbf{2}}$ are

$$m_{\mathbf{2}} \sim \tilde{\xi}\langle Z\rangle, \quad \tilde{\xi}\langle Z\rangle, \quad \tilde{\xi}^8\langle Z\rangle. \tag{C.34}$$

Two doublets receive large masses, which we assume are slightly larger than $M_{\rm GUT}$ such that they don't upset gauge coupling unification. The remaining eigenvalue is suppressed by a factor $\tilde{\xi}^8$. We can choose the mass of the Z and Σ messengers so that $\tilde{\xi} \sim 0.03$, i.e. $\tilde{\xi}^8\langle Z\rangle \sim 1$ TeV. This generates the MSSM μ term $\tilde{\xi}^8\langle Z\rangle H_u H_d$ at the correct scale, where we make the connection between MSSM Higgs doublets and the doublets defined above by

$$H_u \approx \mathbf{2}_u(H^u_{10}), \qquad H_d \approx \mathbf{2}_d(H^d_{10}). \tag{C.35}$$

We turn to showing how all triplets acquire large masses via the DW mechanism. It is based on having an $SO(10)$ **45**, which we call H_{DW}, that obtains a VEV with the structure

$$\langle H_{DW}\rangle = \begin{pmatrix} 0 & \langle H_{U(5)}\rangle \\ -\langle H_{U(5)}\rangle & 0 \end{pmatrix}, \tag{C.36}$$

which is traceless regardless of the structure of $\langle H_{U(5)}\rangle$. We can actually choose $\langle H_{U(5)}\rangle = v_{45}\ \mathrm{diag}(1,1,1,0,0)$ such that it contributes only to the mass of the triplets. This alignment of $\langle H_{U(5)}\rangle$ is not possible in an $SU(5)$ adjoint representation (as its trace does not vanish) but is possible in $SO(10)$, and is the direction which preserves $B-L$. The field H_{DW} has R charge 2 and $\mathbb{Z}_9$ charge 6, allowing us to write the term

$$W_{DT} = H_{DW} H^u_{10} H^d_{10} \frac{\xi}{M_\Upsilon}, \tag{C.37}$$

where, due to the antisymmetry of $\langle H_{DW}\rangle$, only the mixed term is possible. The renormalisable diagram that produces this term is given in Figure C.4.

By analogy to Eq. C.32, we define Higgs triplets $\mathbf{3}_u(H)$ and $\mathbf{3}_d(H)$ arising from H^u_{10}, H^d_{10} and $H_{\overline{16}}$ by

$$\begin{aligned}\mathbf{3}_u &= \left(\mathbf{3}_u(H^u_{10}),\ \mathbf{3}_u(H^d_{10}),\ \mathbf{3}_u(H_{\overline{16}})\right),\\ \mathbf{3}_d &= \left(\mathbf{3}_d(H^u_{10}),\ \mathbf{3}_d(H^d_{10}),\ \mathbf{3}_d(H_{16})\right).\end{aligned} \tag{C.38}$$

The terms involving these triplets arising from the superpotential in Eq. C.31 produces the mass matrix

$$M_{\mathbf{3}} = \mathbf{3}_d^{\intercal} \begin{pmatrix} \tilde{\xi}^6 & \tilde{\xi}\,\langle H_{DW}\rangle / \langle Z\rangle & \tilde{H}_{\overline{16}} \\ \tilde{\xi}\,\langle H_{DW}\rangle / \langle Z\rangle & \tilde{\xi}^8 & \tilde{\xi}\tilde{H}_{\overline{16}} \\ \tilde{H}_{16}\,\tilde{\xi}^8 & \tilde{H}_{16} & \xi / \langle Z\rangle \end{pmatrix} \langle Z\rangle\, \mathbf{3}_u, \tag{C.39}$$

where the only structural difference between this and $M_{\mathbf{2}}$ in Eq. C.33 is in the (1,2) and (2,1) entries, which arise from Eq. C.37. All the eigenvalues of this matrix are at the scale $\tilde{\xi}\,\langle Z\rangle \sim M_{\mathrm{GUT}}$, i.e. there are no light triplet eigenstates, which gives doublet-triplet splitting.

C.4 GUT breaking in $S_4 \times SO(10)$

Finally, we turn to the model described in Chapter 5. As in the above discussions, the effective theory below the GUT scale contains more fields than the MSSM. In particular, the $H_{10}^{u,d}$ Higgs multiplets contain dangerous colour triplets mediating proton decay, and additional doublets that, if light, could spoil gauge coupling unification. Those extra fields need to be heavy, while ensuring the MSSM doublets are (initially) massless. This splitting can be achieved in our model. Note that we have not specified exactly how the GUT is broken. However, it is understood that GUT breaking occurs (as in the $\Delta(27) \times SO(10)$ model) when spinorial and adjoint Higgs superfields acquire VEVs, which break $SO(10)$ to the Standard Model via $SU(5)$. These are already present in the model.

The splitting mechanism involves superfields given in Table 5.1, as well as several new ones, given in Table C.5. The singlet ξ obtains a VEV slightly above the GUT scale. The H_{16} generates a mass for the $H_{\overline{16}}$ and also gets a VEV in the RH neutrino (ν^c) direction, thus breaking $SO(10) \to SU(5)$. H_{45}^{B-L} is the only R-charged field that gets a VEV, breaking $\mathbb{Z}_4^R$ to the usual R parity. This splitting mechanism needs three extra messenger pairs, listed in Table C.5.

With them, we may write the superpotential (ignoring dimensionless couplings)

$$\begin{aligned} W = {} & H_{45}^{B-L}\left(H_{10}^u H_{10}^d + \zeta_2\zeta_2 + H_{\overline{16}}\chi_u + H_{16}\bar{\chi}_d\right) \\ & + H_{\overline{16}}H_{10}^u\bar{\chi}_u + H_{16}H_{10}^d\chi_d + H_{16}H_{\overline{16}}\zeta_1 + \xi\left(\zeta_1\zeta_2 + \bar{\chi}_u\chi_u + \bar{\chi}_d\chi_d\right) \\ & + H_{45}^{B-L}\left(\frac{H_{\overline{16}}H_{\overline{16}}H_{10}^d}{M_P} + \frac{H_{16}H_{16}H_{10}^u}{M_P} + H_{10}^u H_{10}^d \frac{(H_{45}^{X,Y,Z})^4}{M_P^4}\right), \end{aligned} \tag{C.40}$$

Field	Representation				
	S_4	$SO(10)$	$\mathbb{Z}_4$	$\mathbb{Z}_4$	$\mathbb{Z}_4^R$
ξ	1	1	2	2	0
$\bar{\chi}_u$	1	$\overline{16}$	2	1	2
χ_u	1	16	0	1	0
$\bar{\chi}_d$	1	$\overline{16}$	1	0	0
χ_d	1	16	1	2	2
ζ_1	1	45	1	1	2
ζ_2	1	45	1	1	0

Table C.5: Messengers involved in doublet-triplet splitting.

where we assume that the VEV $\langle\xi\rangle \gtrsim M_{GUT}$, so that we may integrate out the messenger fields and obtain the effective superpotential

$$W_H = H_{45}^{B-L}\left(H_{10}^u H_{10}^d + \frac{(H_{16}H_{\overline{16}})^2}{\langle\xi\rangle^2} + \frac{H_{\overline{16}}H_{\overline{16}}H_{10}^u}{\langle\xi\rangle} + \frac{H_{16}H_{16}H_{10}^d}{\langle\xi\rangle} + \frac{H_{\overline{16}}H_{\overline{16}}H_{10}^d}{M_P} + \frac{H_{16}H_{16}H_{10}^u}{M_P} + H_{10}^u H_{10}^d \frac{(H_{45}^{X,Y,Z})^4}{M_P^4}\right). \tag{C.41}$$

The three terms suppressed by $\langle\xi\rangle$ are allowed by the integration of three messenger pairs.

We assume that the superfields $H_{\overline{16},16}$, H_{45}^k $(k = X, Y, Z, B-L)$ get GUT-scale VEVs, i.e. $v_{16,\overline{16}} \approx v_{45}^k \approx M_{GUT}$, through an unspecified mechanism. $H_{\overline{16},16}$ get VEVs in the ν^c direction. H_{45}^{B-L} gets a VEV aligned in the $B-L$ direction, which splits doublet and triplet Higgs masses through the DW mechanism, discussed earlier. The mechanism can be also understood by considering the decomposition of the $H_{10}^{u,d}$ into the Pati-Salam group. The triplets behave as a sextuplet of $SU(4)$ while the doublets are singlets. Since $U(1)_{B-L} \subset SU(4)$, the triplets get a mass from the first term of Eq. C.41 while the doublets do not. In the last term, all the $SO(10)$ adjoints can be contracted to a singlet, so they affect doublets and triplets equally.

To demonstrate the mechanism, we construct the doublet and triplet mass matrices. We define the dimensionless scale parameters $y = M_{\rm GUT}/M_P$, $z = M_{\rm GUT}/\langle\xi\rangle$. We label the up-type doublets inside a given Higgs representation H by $\mathbf{2}_u(H)$, and down-type doublets by $\mathbf{2}_d(H)$. We define triplets $\mathbf{3}_u(H)$ and $\mathbf{3}_d(H)$ analogously. H can be either

H_{10}^u, H_{10}^d or $H_{\overline{16},16}$. Doublets and triplets are collected in vectors

$$\begin{aligned}
\mathbf{2}_u &= \Big(\mathbf{2}_u(H_{10}^u),\ \mathbf{2}_u(H_{10}^d),\ \mathbf{2}_u(H_{\overline{16}})\Big)\,,\\
\mathbf{2}_d &= \Big(\mathbf{2}_d(H_{10}^d),\ \mathbf{2}_d(H_{10}^u),\ \mathbf{2}_d(H_{16})\Big)\,,\\
\mathbf{3}_u &= \Big(\mathbf{3}_u(H_{10}^u),\ \mathbf{3}_u(H_{10}^d),\ \mathbf{3}_u(H_{\overline{16}})\Big)\,,\\
\mathbf{3}_d &= \Big(\mathbf{3}_d(H_{10}^d),\ \mathbf{3}_d(H_{10}^u),\ \mathbf{3}_d(H_{16})\Big)\,.
\end{aligned} \tag{C.42}$$

The mass matrices $M_{\mathbf{2}}$ and $M_{\mathbf{3}}$ are given by

$$\begin{aligned}
M_{\mathbf{2}} &= \mathbf{2}_d^\intercal \begin{pmatrix} y^4 & 0 & y \\ 0 & -y^4 & z \\ y & z & z^2 \end{pmatrix} \mathbf{2}_u,\\
M_{\mathbf{3}} &= \mathbf{3}_d^\intercal \begin{pmatrix} 1 & 0 & y \\ 0 & -1 & z \\ y & z & z^2 \end{pmatrix} \mathbf{3}_u.
\end{aligned} \tag{C.43}$$

The triplet mass matrix $M_{\mathbf{3}}$ has three eigenvalues of $\mathcal{O}(M_{\rm GUT})$. The doublet mass matrix has two eigenvalues at $\mathcal{O}(M_{\rm GUT})$ and one at $\mathcal{O}(y^4 M_{\rm GUT})$, which we identify with the μ term. Since $y \approx 10^{-3}$ we have $\mu \sim 1$ TeV, which is the desired order. Furthermore, the light eigenvectors of $M_{\mathbf{2}}$ define the MSSM doublets $H_{u,d}$ as

$$H_u \approx \mathbf{2}_u(H_{10}^u) + \frac{y}{z}\mathbf{2}_u(H_{10}^d), \quad H_d \approx \mathbf{2}_d(H_{10}^d) + \frac{y}{z}\mathbf{2}_u(H_{10}^d), \tag{C.44}$$

where the contribution of $\mathcal{O}(y)$ is negligible, so that the MSSM doublets are located as required by the Yukawa structure of the model.

Appendix D

Approximations to lepton matrices in $\Delta(27) \times SO(10)$

The CP asymmetry ε in leptogenesis calculations is defined in the flavour basis, where the charged lepton and right-handed neutrino mass matrices are diagonal. In the $\Delta(27)\times SO(10)$ model of Chapter 4, they are decidedly non-diagonal. One may nevertheless attempt to parametrise the necessary basis transformation and derive an analytical approximation of the neutrino Yukawa matrix in the flavour basis. This appendix describes our efforts to do so, although it was concluded that the resultant expressions are too complicated to be practical.

D.1 Matrices and model fit results

We first recapitulate the key elements of the lepton Yukawa sector. Defining numerical matrices Y_i as

$$Y_{\text{atm}} = \begin{pmatrix} 0 & 0 & 0 \\ 0 & 1 & 1 \\ 0 & 1 & 1 \end{pmatrix}, \quad Y_{\text{sol}} = \begin{pmatrix} 1 & 3 & 1 \\ 3 & 9 & 3 \\ 1 & 3 & 1 \end{pmatrix}, \quad Y_{\text{dec}} = \begin{pmatrix} 0 & 0 & 0 \\ 0 & 0 & 0 \\ 0 & 0 & 1 \end{pmatrix}, \tag{D.1}$$

the charged lepton and neutrino Yukawa matrices, Y^e and Y^ν, and the left- and right-handed neutrino mass matrices, m^ν and M_R, may be written as

$$\begin{aligned} Y^e &= y^e_1 Y_{\text{atm}} + y^e_2 e^{i\eta} Y_{\text{sol}} + y^e_3 e^{i\eta'} Y_{\text{dec}}, \\ Y^\nu &= y^\nu_{\text{atm}} Y_{\text{atm}} + y^\nu_{\text{sol}} e^{i\eta} Y_{\text{sol}} + y^\nu_{\text{dec}} e^{i\eta'} Y_{\text{dec}}, \\ m^\nu &= \mu_{\text{atm}} Y_{\text{atm}} + \mu_{\text{sol}} e^{i\eta} Y_{\text{sol}} + \mu_{\text{dec}} e^{i\eta'} Y_{\text{dec}}, \\ M_R &= M_{\text{atm}} Y_{\text{atm}} + M_{\text{sol}} e^{i\eta} Y_{\text{sol}} + M_{\text{dec}} e^{i\eta'} Y_{\text{dec}}. \end{aligned} \tag{D.2}$$

The parameters μ_i are defined by the seesaw relation in sequential dominance, i.e.

$$\mu_i = \frac{v_u^2 (y_i^\nu)^2}{M_i}. \tag{D.3}$$

A numerical fit determines the parameters y_i^e and μ_i, but not y_i^ν and M_i separately, i.e. of the six degrees of freedom in the neutrino sector, only three are fixed. The best fit values are given in Table 4.6 and reproduced here in Table D.1.

Parameter	Value	
	Scenario 1	Scenario 2
$y_1^e\,/10^{-3}$	2.217	-1.966
$y_2^e\,/10^{-5}$	-1.025	1.027
$y_3^e\,/10^{-2}$	3.366	3.790
$\mu_{\rm atm}$ /meV	26.60	25.90
$\mu_{\rm sol}$ /meV	2.571	2.546
$\mu_{\rm dec}$ /meV	2.052	2.461
η	$2\pi/3$	
η'	0	

Table D.1: Lepton sector input parameter values, with η, η' fixed by the theory.

D.2 Charged lepton diagonalisation

As the charged leptons are strongly hierarchical, we expect small mixing in this sector, which suggests a perturbative approach is valid when diagonalising Y^e. Moreover, as Y^e is fixed by the fit, we can directly test this hypthesis. We write

$$Y^e = \begin{pmatrix} y_2^e e^{i\eta} & 3y_2^e e^{i\eta} & y_2^e e^{i\eta} \\ 3y_2^e e^{i\eta} & y_1^e + 9y_2^e e^{i\eta} & y_1^e + 3y_2^e e^{i\eta} \\ y_2^e e^{i\eta} & y_1^e + 3y_2^e e^{i\eta} & y_1^e + y_2^e e^{i\eta} + y_3^e \end{pmatrix} \tag{D.4}$$

As Eq. D.4 is symmetric, it may be diagonalised by a unitary matrix U via

$$U^e Y^e (U^e)^\intercal = \mathrm{diag}(y_e, y_\mu, y_\tau), \tag{D.5}$$

where U^e is defined as the unitary matrix that diagonalises the (Hermitian) squared matrix, i.e $U^e (Y^e)^\dagger Y^e (U^e)^\dagger = \mathrm{diag}(y_e^2, y_\mu^2, y_\tau^2)$. This unitary matrix may in turn be

parametrised in terms of three rotation angles θ^e_{12}, θ^e_{13} and θ^e_{23} and several phases, i.e.

$$\begin{aligned} U^e &= P^e_\delta R^e_{23} U^e_{13} R^e_{12} P^e_\varphi \\ &= \begin{pmatrix} \delta^e_e & 0 & 0 \\ 0 & \delta^e_\mu & 0 \\ 0 & 0 & \delta^e_\tau \end{pmatrix} \begin{pmatrix} 1 & 0 & 0 \\ 0 & c_{23} & s_{23} \\ 0 & -s_{23} & c_{23} \end{pmatrix} \begin{pmatrix} c_{13} & 0 & s_{13}e^{-i\delta} \\ 0 & 1 & 0 \\ -s_{13}e^{i\delta} & 0 & c_{13} \end{pmatrix} \begin{pmatrix} c_{12} & s_{12} & 0 \\ -s_{12} & c_{12} & 0 \\ 0 & 0 & 1 \end{pmatrix} \\ &\quad \times \mathrm{diag}(e^{-i\varphi^e_1/2}, e^{-i\varphi^e_2/2}, 1), \end{aligned} \tag{D.6}$$

where $c_{ij} = \cos\theta^e_{ij}$ and $s_{ij} = \sin\theta^e_{ij}$. Note that the Majorana phases $\varphi_{1,2}$ differ from those in the PDG parametrisation, where $P_\varphi \to P_\alpha = \mathrm{diag}(1, e^{i\alpha_{21}/2}, e^{i\alpha_{31}/2})$.

In the perturbative approximation, where $y^e_2 \ll y^e_1 \ll y^e_3$, the mixing angles (for charged leptons) are

$$\theta^e_{12} \approx \left|\frac{Y^e_{12}}{Y^e_{22}}\right| \approx \frac{3y^e_2}{y^e_1 + 9y^e_2\cos\eta}, \tag{D.7}$$

$$\theta^e_{13} \approx \left|\frac{Y^e_{13}}{Y^e_{33}}\right| \approx \frac{y^e_2}{y^e_3}, \tag{D.8}$$

$$\theta^e_{23} \approx \left|\frac{Y^e_{23}}{Y^e_{33}}\right| \approx \frac{y^e_1 + 3y^e_2\cos\eta}{y^e_3}. \tag{D.9}$$

Inserting the best fit values from Table D.1, this approximation gives

$$\theta^e_{12} \approx 0.770^\circ, \qquad \theta^e_{13} \approx 0.0174^\circ, \qquad \theta^e_{23} \approx 3.842^\circ. \tag{D.10}$$

Exact numerical diagonalisation gives

$$\theta_{12} = 0.806^\circ, \qquad \theta_{13} = 0.0195^\circ, \qquad \theta_{23} = 3.825^\circ, \tag{D.11}$$

showing that the approximation works well.

D.3 Right-handed neutrino diagonalisation

The right-handed neutrino Majorana matrix has a very strong hierarchy between the third matrix and the first two, i.e. $M_{\mathrm{atm,sol}} \ll M_{\mathrm{dec}}$, per the sequential dominance assumption. The consequence of this hierarchy in Majorana mass coefficients is that we naturally assume small mixing between the first two families of right-handed neutrinos and the third. We define a diagonalising matrix U^M analogously to U^e above, such that $U^M M_R (U^M)^\intercal = \mathrm{diag}(M_1, M_2, M_3)$. We write M_R as

$$M_R = \begin{pmatrix} M_{\mathrm{sol}}e^{i\eta} & 3M_{\mathrm{sol}}e^{i\eta} & M_{\mathrm{sol}}e^{i\eta} \\ 3M_{\mathrm{sol}}e^{i\eta} & M_{\mathrm{atm}} + 9M_{\mathrm{sol}}e^{i\eta} & M_{\mathrm{atm}} + 3M_{\mathrm{sol}}e^{i\eta} \\ M_{\mathrm{sol}}e^{i\eta} & M_{\mathrm{atm}} + 3M_{\mathrm{sol}}e^{i\eta} & M_{\mathrm{atm}} + M_{\mathrm{sol}}e^{i\eta} + M_{\mathrm{dec}} \end{pmatrix}. \tag{D.12}$$

Naïvely, the mixing angles can again be approximated by

$$\begin{aligned}
\theta_{12}^M &\approx \left|\frac{(M_R)_{12}}{(M_R)_{22}}\right| \approx \frac{3M_{\rm sol}}{\sqrt{M_{\rm atm}^2 + 18 M_{\rm atm} M_{\rm sol}\cos\eta + 81 M_{\rm sol}^2}}, \\
\theta_{13}^M &\approx \left|\frac{(M_R)_{13}}{(M_R)_{33}}\right| \approx \frac{M_{\rm sol}}{M_{\rm dec}}, \\
\theta_{23}^M &\approx \left|\frac{(M_R)_{23}}{(M_R)_{33}}\right| \approx \frac{M_{\rm atm} + 3M_{\rm sol}\cos\eta}{M_{\rm dec}}.
\end{aligned} \tag{D.13}$$

Given the expected mass hierarchy $M_{\rm atm,sol} \ll M_{\rm dec}$, we expect these approximations to work well for θ_{13}^M and θ_{23}^M, while the validity for θ_{12}^M depends on the hierarchy between $M_{\rm atm}$ and $M_{\rm sol}$ which is less firmly established and requires further study.

Ultimately this depends on the best fit values $\mu_{\rm atm,sol}$ and the ratio $y_{\rm atm}/y_{\rm sol}$ between coefficients of the Dirac neutrino matrix. To see this, we rearrange the seesaw relations to give $M_i = (v^u y_i)^2/\mu_i$, where $i = {\rm atm}, {\rm sol}$. Defining

$$\alpha \equiv \frac{y_{\rm atm}^2}{y_{\rm sol}^2} = \frac{\mu_{\rm atm}}{\mu_{\rm sol}}\frac{M_{\rm atm}}{M_{\rm sol}} \approx 10\frac{M_{\rm atm}}{M_{\rm sol}}, \tag{D.14}$$

we arrive at

$$\theta_{12}^M \approx \frac{3}{\sqrt{\dfrac{\mu_{\rm sol}^2}{\mu_{\rm atm}^2}\alpha^2 + \dfrac{18\mu_{\rm sol}\cos\eta}{\mu_{\rm atm}}\alpha + 81}} \approx \frac{1}{\sqrt{0.0011\alpha^2 - 0.10\alpha + 9}}. \tag{D.15}$$

The function $\theta_{12}^M(\alpha)$ is plotted in Figure D.1. The set blue points is obtained by numerical diagonalisation of M_R for a randomly generated set of inputs y_i. As anticipated, the result is insensitive to the third family. We find the the analytical approximation works well for a large range of α. If we assume $Y^\nu \approx Y^u$, we can compare $Y_{\rm atm,sol}$ to the corresponding quark best fit values $y_{1,2}^u$. This gives $\alpha \approx 0.028$, which is marked in the figure.

However, a small shift is present between the approximation in Eq. D.13, denoted by the solid yellow line, and the exact results. We note that the above result assumes mixing is small enough that $\sin\theta \approx \tan\theta \approx \theta$ and $\cos\theta \approx 1$, which breaks down for large θ. Small α implies that the upper-left block of Y^ν (or equivalently, M_R) is dominated by the rank-1 matrix proportional to $y_{\rm sol}$ ($M_{\rm sol}$). The mixing angle may then be read off as $\tan\theta_{12}^M \approx \theta_{12}^M \approx 1/3$. But $\arctan(1/3)/(1/3) = 3\,{\rm arccot}\,3 \approx 0.965$, a discrepancy of $3-4\%$. We multiply $\theta_{12}^M(\alpha)$ by this correction factor to give the dotted yellow line in Figure D.1, which is in excellent agreement. The peak at $\alpha \approx 45$ arises because $\cos\eta$, found in the denominator of θ_{12}^M, is negative; if $\eta \approx \pi$, $\theta_{12}^M(\alpha)$ blows up and is not a reliable approximation.

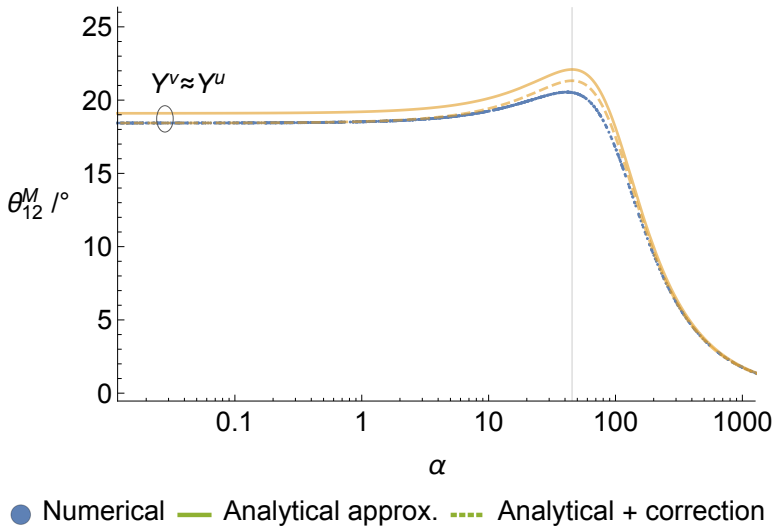

Figure D.1: Variation in θ_{12}^M with $\alpha \equiv (y_{\text{atm}}/y_{\text{sol}})^2$. Blue points are from numerical diagonalisation. Yellow lines plot the analytical result in Eq. D.13, with and without a correction factor $3 \operatorname{arccot} 3$.

We have also derived analytical expressions for the right-handed neutrino mass eigenvalues by doing a series expansion in the mass parameters. We need to consider two cases, depending on the relative sizes of M_{atm} and M_{sol}. In both cases $M_3 \approx M_{\text{dec}}$, while we have

- Case 1: $M_{\text{atm}} \lesssim 10 M_{\text{sol}}$.

$$M_1 \approx \frac{M_{\text{atm}}}{10}, \qquad M_2 \approx 10 M_{\text{sol}} + \frac{9 \cos\eta}{10} M_{\text{atm}}. \tag{D.16}$$

- Case 2: $M_{\text{atm}} \gg M_{\text{sol}}$.

$$M_1 \approx M_{\text{sol}}, \qquad M_2 \approx M_{\text{atm}} + 9 M_{\text{sol}} \cos\eta. \tag{D.17}$$

In both cases, M_1 is necessarily an order of magnitude smaller than M_2.

D.4 Neutrino Yukawa matrix in the flavour basis

With an understanding of mixing in Y^e and M_R, we can establish the neutrino Yukawa matrix Y^ν in the flavour basis. Recall that it is given by

$$Y^{\nu,\text{fb}} = U^e Y^\nu (U^M)^\intercal. \tag{D.18}$$

As a first attempt, let us ignore all phases in $U^{e,M}$ and assume all angles are small. We approximate the diagonalising matrices by

$$U^e \sim \begin{pmatrix} 1 & \theta^e_{12} & \theta^e_{13} \\ -\theta^e_{12} & 1 & \theta^e_{23} \\ -\theta^e_{13} & -\theta^e_{23} & 1 \end{pmatrix}, \qquad U^M \sim \begin{pmatrix} 1 & \theta^M_{12} & \theta^M_{13} \\ -\theta^M_{12} & 1 & \theta^M_{23} \\ -\theta^M_{13} & -\theta^M_{23} & 1 \end{pmatrix}. \tag{D.19}$$

Keeping only the largest contributions in the product, $Y^{\nu\prime}$ approximates to

$$Y^{\nu\prime} \sim Y^\nu - \theta^M_{12} e^{i\eta} \begin{pmatrix} 3y_{\rm sol} & 0 & 0 \\ 9y_{\rm sol} & 0 & 0 \\ y_{\rm atm} + 3y_{\rm sol} & 0 & 0 \end{pmatrix} - y_{\rm dec} \begin{pmatrix} 0 & 0 & \theta^e_{13} \\ 0 & 0 & \theta^e_{23} \\ \theta^M_{13} & \theta^M_{23} & 0 \end{pmatrix}. \tag{D.20}$$

The first correction term is proportional to θ^M_{12}. As discussed above, if $Y^\nu \approx Y^u$, $\theta^M_{12} \approx 0.33$. These corrections can therefore of the same size as the original elements, meaning particularly the (1,1) and (2,1) elements may be significantly suppressed, depending on relative phases.

The second correction comes from smearing of the large (3,3) element $y_{\rm dec}$ into the third row and column. While $\theta^e_{13,23}$ and $\theta^M_{13,23}$ are small, $y_{\rm dec}$ is sufficiently large that it may still give a significant contribution. Particularly, as $\theta^e_{23} \sim 0.065 \approx 4^\circ$, the (2,3) element gets a correction several times larger than the original value. The exact size of this correction is directly correlated with the value of $y_{\rm dec}$, which is unknown. However, the terms of the third column are not expected to be strongly contributing to leptogenesis, as the loop contributions from N_3 neutrinos are very suppressed compared to N_2 in the hierarchical assumption.

There are nevertheless indications that there are corrections of an equal order of magnitude. Whether this leads to enchancements or cancellations in the elements of Y^ν depends on the relative phases between terms. Let us keep only those contributions involving either θ^M_{12} or $y_{\rm dec}$, but keeping all phases $\delta^{e,M}_{e,\mu,\tau}$, $\varphi^{e,M}_{1,2}$. Then

$$\begin{aligned} Y^{\nu\prime} \approx\ & y_{\rm atm} \begin{pmatrix} 0 & 0 & 0 \\ -\theta^M_{12} e^{i\sigma_{21}} & e^{i\eta_{22}} & e^{i\eta_{23}} \\ -\theta^M_{12} e^{i\sigma_{31}} & e^{i\eta_{32}} & e^{i\eta_{33}} \end{pmatrix} \\ & + y_{\rm sol} e^{i\eta} \begin{pmatrix} e^{i\eta_{11}} - 3\theta^M_{12} e^{i\sigma_{11}} & 3e^{i\eta_{12}} + \theta^M_{12} e^{i\sigma_{12}} & e^{i\eta_{13}} \\ 3e^{i\eta_{21}} - 9\theta^M_{12} e^{i\sigma_{21}} & 9e^{i\eta_{22}} + 3\theta^M_{12} e^{i\sigma_{22}} & 3e^{i\eta_{23}} \\ e^{i\eta_{31}} - 3\theta^M_{12} e^{i\sigma_{31}} & 3e^{i\eta_{23}} + \theta^M_{12} e^{i\sigma_{23}} & e^{i\eta_{33}} \end{pmatrix} \\ & + y_{\rm dec} e^{i\eta} \begin{pmatrix} 0 & 0 & -\theta^e_{13} e^{i\sigma^c_{13}} \\ 0 & 0 & -\theta^e_{23} e^{i\sigma^c_{23}} \\ -\theta^M_{13} e^{i\sigma^c_{31}} & -\theta^M_{23} e^{i\sigma^c_{32}} & e^{i\eta_{33}} \end{pmatrix}, \end{aligned} \tag{D.21}$$

where

$$\begin{aligned}
\eta_{11} &= \delta_e^e + \delta_e^M - \varphi_1^e/2 - \varphi_1^M/2, & \sigma_{11} &= \delta_e^e + \delta_\mu^M - \varphi_1^e/2 - \varphi_1^M/2, \\
\eta_{12} &= \delta_e^e + \delta_\mu^M - \varphi_1^e/2 - \varphi_2^M/2, & \sigma_{12} &= \delta_e^e + \delta_e^M - \varphi_1^e/2 - \varphi_2^M/2, \\
\eta_{13} &= \delta_e^e + \delta_\tau^M - \varphi_1^e/2, & \sigma_{21} &= \delta_\mu^e + \delta_\mu^M - \varphi_1^M/2 - \varphi_2^e/2, \\
\eta_{21} &= \delta_\mu^e + \delta_e^M - \varphi_1^M/2 - \varphi_2^e/2, & \sigma_{22} &= \delta_\mu^e + \delta_e^M - \varphi_2^e/2 - \varphi_2^M/2, \\
\eta_{22} &= \delta_\mu^e + \delta_\mu^M - \varphi_2^e/2 - \varphi_2^M/2, & \sigma_{31} &= \delta_\tau^e + \delta_\mu^M - \varphi_1^M/2, \\
\eta_{23} &= \delta_\mu^e + \delta_\tau^M - \varphi_2^e/2, & \sigma_{32} &= \delta_\tau^e + \delta_e^M - \varphi_2^M/2, \\
\eta_{31} &= \delta_\tau^e + \delta_e^M - \varphi_1^M/2, & \sigma_{13}^c &= \delta_\tau^e + \delta_\tau^M - \varphi_1^e/2 + \delta^e, \\
\eta_{32} &= \delta_\tau^e + \delta_\mu^M - \varphi_2^M/2, & \sigma_{23}^c &= \delta_\tau^e + \delta_\tau^M - \varphi_2^e/2, \\
\eta_{33} &= \delta_\tau^e + \delta_\tau^M, & \sigma_{31}^c &= \delta_\tau^e + \delta_\tau^M - \varphi_1^M/2 + \delta^M, \\
& & \sigma_{32}^c &= \delta_\tau^e + \delta_\tau^M - \varphi_2^M/2.
\end{aligned} \tag{D.22}$$

Unfortunately there are no obvious simplifications that can be made to these phase relations.

References

[1] F. Björkeroth and S. F. King. Testing constrained sequential dominance models of neutrinos. *J. Phys.*, G42(12):125002, 2015. [arXiv:1412.6996].

[2] F. Björkeroth, F. J. de Anda, I. de Medeiros Varzielas and S. F. King. Towards a complete $A_4\times$ SU(5) SUSY GUT. *JHEP*, 06:141, 2015. [arXiv:1503.03306].

[3] F. Björkeroth, F. J. de Anda, I. de Medeiros Varzielas and S. F. King. Leptogenesis in minimal predictive seesaw models. *JHEP*, 10:104, 2015. [arXiv:1505.05504].

[4] F. Björkeroth, F. J. de Anda, I. de Medeiros Varzielas and S. F. King. Towards a complete $\Delta(27) \times SO(10)$ SUSY GUT. *Phys. Rev.*, D94(1):016006, 2016. [arXiv:1512.00850].

[5] F. Björkeroth, F. J. de Anda, I. de Medeiros Varzielas and S. F. King. Leptogenesis in a $\Delta(27) \times SO(10)$ SUSY GUT. *JHEP*, 01:077, 2017. [arXiv:1609.05837].

[6] F. Björkeroth, F. J. de Anda, S. F. King and E. Perdomo. A natural $S_4 \times SO(10)$ model of flavour. 2017. [arXiv:1705.01555].

[7] G. Aad et al. Observation of a new particle in the search for the Standard Model Higgs boson with the ATLAS detector at the LHC. *Phys. Lett.*, B716:1–29, 2012. [arXiv:1207.7214].

[8] S. Chatrchyan et al. Observation of a new boson at a mass of 125 GeV with the CMS experiment at the LHC. *Phys. Lett.*, B716:30–61, 2012. [arXiv:1207.7235].

[9] Y. Fukuda et al. Evidence for oscillation of atmospheric neutrinos. *Phys. Rev. Lett.*, 81:1562–1567, 1998. [arXiv:hep-ex/9807003].

[10] Q. R. Ahmad et al. Direct evidence for neutrino flavor transformation from neutral current interactions in the Sudbury Neutrino Observatory. *Phys. Rev. Lett.*, 89:011301, 2002. [arXiv:nucl-ex/0204008].

[11] H. Fritzsch, M. Gell-Mann and H. Leutwyler. Advantages of the Color Octet Gluon Picture. *Phys. Lett.*, 47B:365–368, 1973.

[12] H. D. Politzer. Reliable Perturbative Results for Strong Interactions? *Phys. Rev. Lett.*, 30:1346–1349, 1973.

[13] D. J. Gross and F. Wilczek. Ultraviolet Behavior of Nonabelian Gauge Theories. *Phys. Rev. Lett.*, 30:1343–1346, 1973.

[14] S. L. Glashow. Partial Symmetries of Weak Interactions. *Nucl. Phys.*, 22:579–588, 1961.

[15] A. Salam and J. C. Ward. Electromagnetic and weak interactions. *Phys. Lett.*, 13:168–171, 1964.

[16] S. Weinberg. A Model of Leptons. *Phys. Rev. Lett.*, 19:1264–1266, 1967.

[17] A. Salam. Weak and Electromagnetic Interactions. *Conf. Proc.*, C680519:367–377, 1968.

[18] F. Englert and R. Brout. Broken Symmetry and the Mass of Gauge Vector Mesons. *Phys. Rev. Lett.*, 13:321–323, 1964.

[19] P. W. Higgs. Broken symmetries, massless particles and gauge fields. *Phys. Lett.*, 12:132–133, 1964.

[20] P. W. Higgs. Broken Symmetries and the Masses of Gauge Bosons. *Phys. Rev. Lett.*, 13:508–509, 1964.

[21] G. S. Guralnik, C. R. Hagen and T. W. B. Kibble. Global Conservation Laws and Massless Particles. *Phys. Rev. Lett.*, 13:585–587, 1964.

[22] P. J. Mohr, D. B. Newell and B. N. Taylor. CODATA Recommended Values of the Fundamental Physical Constants: 2014. *Rev. Mod. Phys.*, 88(3):035009, 2016. [arXiv:1507.07956].

[23] C. Patrignani et al. Review of Particle Physics. *Chin. Phys.*, C40(10):100001, 2016.

[24] M. Bona et al. The 2004 UTfit collaboration report on the status of the unitarity triangle in the standard model. *JHEP*, 07:028, 2005. [arXiv:hep-ph/0501199].

[25] P. Minkowski. $\mu \to e\gamma$ at a Rate of One Out of 10^9 Muon Decays? *Phys. Lett.*, B67:421–428, 1977.

[26] T. Yanagida. Proceedings of the Workshop on Unified Theory and Baryon Number of the Universe, eds. O. Sawada and A. Sugamoto (KEK, 1979) p.95;.

[27] P. Ramond. The Family Group in Grand Unified Theories. In *International Symposium on Fundamentals of Quantum Theory and Quantum Field Theory Palm Coast, Florida, February 25-March 2, 1979*, pages 265–280. 1979. [arXiv:hep-ph/9809459].

[28] M. Gell-Mann, P. Ramond and R. Slansky. Complex Spinors and Unified Theories. *Conf. Proc.*, C790927:315–321, 1979. [arXiv:1306.4669].

[29] R. N. Mohapatra and G. Senjanovic. Neutrino Mass and Spontaneous Parity Violation. *Phys. Rev. Lett.*, 44:912, 1980.

[30] J. Schechter and J. W. F. Valle. Neutrino Masses in SU(2) x U(1) Theories. *Phys. Rev.*, D22:2227, 1980.

[31] M. Magg and C. Wetterich. Neutrino Mass Problem and Gauge Hierarchy. *Phys. Lett.*, 94B:61–64, 1980.

[32] G. Lazarides, Q. Shafi and C. Wetterich. Proton Lifetime and Fermion Masses in an SO(10) Model. *Nucl. Phys.*, B181:287–300, 1981.

[33] R. N. Mohapatra and G. Senjanovic. Neutrino Masses and Mixings in Gauge Models with Spontaneous Parity Violation. *Phys. Rev.*, D23:165, 1981.

[34] R. Foot, H. Lew, X. G. He and G. C. Joshi. Seesaw Neutrino Masses Induced by a Triplet of Leptons. *Z. Phys.*, C44:441, 1989.

[35] E. Ma. Pathways to naturally small neutrino masses. *Phys. Rev. Lett.*, 81:1171–1174, 1998. [arXiv:hep-ph/9805219].

[36] I. Esteban, M. C. Gonzalez-Garcia, M. Maltoni, I. Martinez-Soler and T. Schwetz. Updated fit to three neutrino mixing: exploring the accelerator-reactor complementarity. *JHEP*, 01:087, 2017. [arXiv:1611.01514].

[37] P. A. R. Ade et al. Planck 2015 results. XIII. Cosmological parameters. *Astron. Astrophys.*, 594:A13, 2016. [arXiv:1502.01589].

[38] M. Kobayashi and T. Maskawa. CP Violation in the Renormalizable Theory of Weak Interaction. *Prog. Theor. Phys.*, 49:652–657, 1973.

[39] P. Ramond. Dual Theory for Free Fermions. *Phys. Rev.*, D3:2415–2418, 1971.

[40] A. Neveu and J. H. Schwarz. Quark Model of Dual Pions. *Phys. Rev.*, D4:1109–1111, 1971.

[41] J.-L. Gervais and B. Sakita. Field Theory Interpretation of Supergauges in Dual Models. *Nucl. Phys.*, B34:632–639, 1971.

[42] Yu. A. Golfand and E. P. Likhtman. Extension of the Algebra of Poincare Group Generators and Violation of p Invariance. *JETP Lett.*, 13:323–326, 1971. [Pisma Zh. Eksp. Teor. Fiz.13,452(1971)].

[43] J. Wess and B. Zumino. Supergauge Transformations in Four-Dimensions. *Nucl. Phys.*, B70:39–50, 1974.

[44] S. P. Martin. A Supersymmetry primer. 1997. [Adv. Ser. Direct. High Energy Phys.18,1(1998)], [arXiv:hep-ph/9709356].

[45] M. T. Grisaru, W. Siegel and M. Rocek. Improved Methods for Supergraphs. *Nucl. Phys.*, B159:429, 1979.

[46] H. Georgi and S. L. Glashow. Unity of All Elementary Particle Forces. *Phys. Rev. Lett.*, 32:438–441, 1974.

[47] J. C. Pati and A. Salam. Lepton Number as the Fourth Color. *Phys. Rev.*, D10:275–289, 1974. [Erratum: Phys. Rev.D11,703(1975)].

[48] H. Georgi. The State of the Art—Gauge Theories. *AIP Conf. Proc.*, 23:575–582, 1975.

[49] H. Fritzsch and P. Minkowski. Unified Interactions of Leptons and Hadrons. *Annals Phys.*, 93:193–266, 1975.

[50] R. N. Mohapatra. Supersymmetric grand unification. In *Supersymmetry, supergravity and supercolliders. Proceedings, Theoretical Advanced Study Institute in elementary particle physics, TASI'97, Boulder, USA, June 2-27, 1997*, pages 601–657. 1997. [arXiv:hep-ph/9801235].

[51] S. F. King and G. G. Ross. Fermion masses and mixing angles from SU(3) family symmetry. *Phys. Lett.*, B520:243–253, 2001. [arXiv:hep-ph/0108112].

[52] S. F. King and G. G. Ross. Fermion masses and mixing angles from SU (3) family symmetry and unification. *Phys. Lett.*, B574:239–252, 2003. [arXiv:hep-ph/0307190].

[53] G. Altarelli and F. Feruglio. Discrete Flavor Symmetries and Models of Neutrino Mixing. *Rev. Mod. Phys.*, 82:2701–2729, 2010. [arXiv:1002.0211].

[54] H. Ishimori, T. Kobayashi, H. Ohki, Y. Shimizu, H. Okada and M. Tanimoto. Non-Abelian Discrete Symmetries in Particle Physics. *Prog. Theor. Phys. Suppl.*, 183:1–163, 2010. [arXiv:1003.3552].

[55] S. F. King and C. Luhn. Neutrino Mass and Mixing with Discrete Symmetry. *Rept. Prog. Phys.*, 76:056201, 2013. [arXiv:1301.1340].

[56] S. F. King, A. Merle, S. Morisi, Y. Shimizu and M. Tanimoto. Neutrino Mass and Mixing: from Theory to Experiment. *New J. Phys.*, 16:045018, 2014. [arXiv:1402.4271].

[57] R. Kallosh, A. D. Linde, D. A. Linde and L. Susskind. Gravity and global symmetries. *Phys. Rev.*, D52:912–935, 1995. [arXiv:hep-th/9502069].

[58] C. D. Froggatt and H. B. Nielsen. Hierarchy of Quark Masses, Cabibbo Angles and CP Violation. *Nucl. Phys.*, B147:277–298, 1979.

[59] P. F. Harrison, D. H. Perkins and W. G. Scott. Tri-bimaximal mixing and the neutrino oscillation data. *Phys. Lett.*, B530:167, 2002. [arXiv:hep-ph/0202074].

[60] P. F. Harrison and W. G. Scott. Permutation symmetry, tri - bimaximal neutrino mixing and the S3 group characters. *Phys. Lett.*, B557:76, 2003. [arXiv:hep-ph/0302025].

[61] M. Holthausen, K. S. Lim and M. Lindner. Lepton Mixing Patterns from a Scan of Finite Discrete Groups. *Phys. Lett.*, B721:61–67, 2013. [arXiv:1212.2411].

[62] S. F. King, T. Neder and A. J. Stuart. Lepton mixing predictions from $\Delta(6n^2)$ family Symmetry. *Phys. Lett.*, B726:312–315, 2013. [arXiv:1305.3200].

[63] S. F. King and T. Neder. Lepton mixing predictions including Majorana phases from $\Delta(6n^2)$ flavour symmetry and generalised CP. *Phys. Lett.*, B736:308–316, 2014. [arXiv:1403.1758].

[64] L. Lavoura and P. O. Ludl. Residual $\mathbb{Z}_2 \times \mathbb{Z}_2$ symmetries and lepton mixing. *Phys. Lett.*, B731:331–336, 2014. [arXiv:1401.5036].

[65] R. M. Fonseca and W. Grimus. Classification of lepton mixing matrices from finite residual symmetries. *JHEP*, 09:033, 2014. [arXiv:1405.3678].

[66] T. Araki, H. Ishida, H. Ishimori, T. Kobayashi and A. Ogasahara. CKM matrix and flavor symmetries. *Phys. Rev.*, D88:096002, 2013. [arXiv:1309.4217].

[67] H. Ishimori and S. F. King. A model of quarks with $\Delta(6N^2)$ family symmetry. *Phys. Lett.*, B735:33–39, 2014. [arXiv:1403.4395].

[68] H. Ishimori, S. F. King, H. Okada and M. Tanimoto. Quark mixing from $\Delta(6N^2)$ family symmetry. *Phys. Lett.*, B743:172–179, 2015. [arXiv:1411.5845].

[69] G. Lemaître. L'univers en expansion. In *Annales de la Société Scientifique de Bruxelles*, volume 53. 1933.

[70] A. G. Riess, A. V. Filippenko, P. Challis, A. Clocchiatti, A. Diercks, P. M. Garnavich, R. L. Gilliland, C. J. Hogan, S. Jha, R. P. Kirshner et al. Observational evidence from supernovae for an accelerating universe and a cosmological constant. *The Astronomical Journal*, 116(3):1009, 1998.

[71] A. H. Guth. The Inflationary Universe: A Possible Solution to the Horizon and Flatness Problems. *Phys. Rev.*, D23:347–356, 1981.

[72] A. D. Linde. The New Inflationary Universe Scenario. In *Nuffield Workshop on the Very Early Universe Cambridge, England, June 21-July 9, 1982*, pages 205–249. 1982.

[73] A. Albrecht and P. J. Steinhardt. Cosmology for Grand Unified Theories with Radiatively Induced Symmetry Breaking. *Phys. Rev. Lett.*, 48:1220–1223, 1982.

[74] P. Di Bari. An introduction to leptogenesis and neutrino properties. *Contemp. Phys.*, 53(4):315–338, 2012. [arXiv:1206.3168].

[75] S. Blanchet and P. Di Bari. The minimal scenario of leptogenesis. *New J. Phys.*, 14:125012, 2012. [arXiv:1211.0512].

[76] A. D. Sakharov. Violation of CP Invariance, c Asymmetry, and Baryon Asymmetry of the Universe. *Pisma Zh. Eksp. Teor. Fiz.*, 5:32–35, 1967. [Usp. Fiz. Nauk161,61(1991)].

[77] V. A. Kuzmin, V. A. Rubakov and M. E. Shaposhnikov. On the Anomalous Electroweak Baryon Number Nonconservation in the Early Universe. *Phys. Lett.*, B155:36, 1985.

[78] M. Fukugita and T. Yanagida. Baryogenesis Without Grand Unification. *Phys. Lett.*, B174:45–47, 1986.

[79] W. Buchmuller, P. Di Bari and M. Plumacher. Leptogenesis for pedestrians. *Annals Phys.*, 315:305–351, 2005. [arXiv:hep-ph/0401240].

[80] D. Binosi and L. Theussl. JaxoDraw: A Graphical user interface for drawing Feynman diagrams. *Comput. Phys. Commun.*, 161:76–86, 2004. [arXiv:hep-ph/0309015].

[81] S. F. King. Atmospheric and solar neutrinos with a heavy singlet. *Phys. Lett.*, B439:350–356, 1998. [arXiv:hep-ph/9806440].

[82] S. F. King. Atmospheric and solar neutrinos from single right-handed neutrino dominance and U(1) family symmetry. *Nucl. Phys.*, B562:57–77, 1999. [arXiv:hep-ph/9904210].

[83] S. F. King. Large mixing angle MSW and atmospheric neutrinos from single right-handed neutrino dominance and U(1) family symmetry. *Nucl. Phys.*, B576:85–105, 2000. [arXiv:hep-ph/9912492].

[84] S. F. King. Constructing the large mixing angle MNS matrix in seesaw models with right-handed neutrino dominance. *JHEP*, 09:011, 2002. [arXiv:hep-ph/0204360].

[85] F. P. An et al. Observation of electron-antineutrino disappearance at Daya Bay. *Phys. Rev. Lett.*, 108:171803, 2012. [arXiv:1203.1669].

[86] J. K. Ahn et al. Observation of Reactor Electron Antineutrino Disappearance in the RENO Experiment. *Phys. Rev. Lett.*, 108:191802, 2012. [arXiv:1204.0626].

[87] Y. Abe et al. Indication of Reactor $\bar{\nu}_e$ Disappearance in the Double Chooz Experiment. *Phys. Rev. Lett.*, 108:131801, 2012. [arXiv:1112.6353].

[88] S. F. King. Predicting neutrino parameters from SO(3) family symmetry and quark-lepton unification. *JHEP*, 08:105, 2005. [arXiv:hep-ph/0506297].

[89] S. Lavignac, I. Masina and C. A. Savoy. Large solar angle and seesaw mechanism: A Bottom up perspective. *Nucl. Phys.*, B633:139–170, 2002. [arXiv:hep-ph/0202086].

[90] M.-C. Chen and S. F. King. A4 See-Saw Models and Form Dominance. *JHEP*, 06:072, 2009. [arXiv:0903.0125].

[91] S. F. King. Vacuum misalignment corrections to tri-bimaximal mixing and form dominance. *JHEP*, 01:115, 2011. [arXiv:1011.6167].

[92] S. Antusch, S. F. King, C. Luhn and M. Spinrath. Trimaximal mixing with predicted θ_{13} from a new type of constrained sequential dominance. *Nucl. Phys.*, B856:328–341, 2012. [arXiv:1108.4278].

[93] S. F. King. Minimal predictive see-saw model with normal neutrino mass hierarchy. *JHEP*, 07:137, 2013. [arXiv:1304.6264].

[94] S. F. King. Minimal see-saw model predicting best fit lepton mixing angles. *Phys. Lett.*, B724:92–98, 2013. [arXiv:1305.4846].

[95] S. F. King. Littlest Seesaw. *JHEP*, 02:085, 2016. [arXiv:1512.07531].

[96] S. F. King and C. Luhn. Littlest Seesaw model from $S_4\times$ U(1). *JHEP*, 09:023, 2016. [arXiv:1607.05276].

[97] P. Ballett, S. F. King, S. Pascoli, N. W. Prouse and T. Wang. Precision neutrino experiments vs the Littlest Seesaw. *JHEP*, 03:110, 2017. [arXiv:1612.01999].

[98] S. F. King. A model of quark and lepton mixing. *JHEP*, 01:119, 2014. [arXiv:1311.3295].

[99] S. F. King. A to Z of Flavour with Pati-Salam. *JHEP*, 08:130, 2014. [arXiv:1406.7005].

[100] S. Antusch, S. F. King, M. Malinsky, L. Velasco-Sevilla and I. Zavala. Flavon Inflation. *Phys. Lett.*, B666:176–180, 2008. [arXiv:0805.0325].

[101] S. Antusch, J. Kersten, M. Lindner, M. Ratz and M. A. Schmidt. Running neutrino mass parameters in see-saw scenarios. *JHEP*, 03:024, 2005. [arXiv:hep-ph/0501272].

[102] F. Feruglio, K. M. Patel and D. Vicino. Order and Anarchy hand in hand in 5D SO(10). *JHEP*, 09:095, 2014. [arXiv:1407.2913].

[103] K. S. Babu, B. Bajc and S. Saad. New Class of SO(10) Models for Flavor. *Phys. Rev.*, D94(1):015030, 2016. [arXiv:1605.05116].

[104] K. S. Babu, B. Bajc and S. Saad. Yukawa Sector of Minimal SO(10) Unification. *JHEP*, 02:136, 2017. [arXiv:1612.04329].

[105] M. C. Gonzalez-Garcia, M. Maltoni and T. Schwetz. Updated fit to three neutrino mixing: status of leptonic CP violation. *JHEP*, 11:052, 2014. [arXiv:1409.5439].

[106] R. Andrae, T. Schulze-Hartung and P. Melchior. Dos and don'ts of reduced chi-squared, 2010. [arXiv:1012.3754].

[107] P. A. R. Ade et al. Planck 2013 results. XVI. Cosmological parameters. *Astron. Astrophys.*, 571:A16, 2014. [arXiv:1303.5076].

[108] S. Antusch, S. F. King and A. Riotto. Flavour-Dependent Leptogenesis with Sequential Dominance. *JCAP*, 0611:011, 2006. [arXiv:hep-ph/0609038].

[109] A. Abada, S. Davidson, F.-X. Josse-Michaux, M. Losada and A. Riotto. Flavor issues in leptogenesis. *JCAP*, 0604:004, 2006. [arXiv:hep-ph/0601083].

[110] E. Nardi, Y. Nir, E. Roulet and J. Racker. The Importance of flavor in leptogenesis. *JHEP*, 01:164, 2006. [arXiv:hep-ph/0601084].

[111] A. Abada, S. Davidson, A. Ibarra, F. X. Josse-Michaux, M. Losada and A. Riotto. Flavour Matters in Leptogenesis. *JHEP*, 09:010, 2006. [arXiv:hep-ph/0605281].

[112] S. F. King. Invariant see-saw models and sequential dominance. *Nucl. Phys.*, B786:52–83, 2007. [arXiv:hep-ph/0610239].

[113] E. E. Jenkins and A. V. Manohar. Tribimaximal Mixing, Leptogenesis, and theta(13). *Phys. Lett.*, B668:210–215, 2008. [arXiv:0807.4176].

[114] E. Bertuzzo, P. Di Bari, F. Feruglio and E. Nardi. Flavor symmetries, leptogenesis and the absolute neutrino mass scale. *JHEP*, 11:036, 2009. [arXiv:0908.0161].

[115] D. Aristizabal Sierra, F. Bazzocchi, I. de Medeiros Varzielas, L. Merlo and S. Morisi. Tri-Bimaximal Lepton Mixing and Leptogenesis. *Nucl. Phys.*, B827:34–58, 2010. [arXiv:0908.0907].

[116] S. Choubey, S. F. King and M. Mitra. On the Vanishing of the CP Asymmetry in Leptogenesis due to Form Dominance. *Phys. Rev.*, D82:033002, 2010. [arXiv:1004.3756].

[117] S. Antusch, P. Di Bari, D. A. Jones and S. F. King. Leptogenesis in the Two Right-Handed Neutrino Model Revisited. *Phys. Rev.*, D86:023516, 2012. [arXiv:1107.6002].

[118] P. Di Bari and S. F. King. Successful N_2 leptogenesis with flavour coupling effects in realistic unified models. *JCAP*, 1510(10):008, 2015. [arXiv:1507.06431].

[119] J. M. Cline, K. Kainulainen and K. A. Olive. Protecting the primordial baryon asymmetry from erasure by sphalerons. *Phys. Rev.*, D49:6394–6409, 1994. [arXiv:hep-ph/9401208].

[120] S. Antusch, S. F. King, C. Luhn and M. Spinrath. Right Unitarity Triangles and Tri-Bimaximal Mixing from Discrete Symmetries and Unification. *Nucl. Phys.*, B850:477–504, 2011. [arXiv:1103.5930].

[121] G. G. Ross, L. Velasco-Sevilla and O. Vives. Spontaneous CP violation and non-Abelian family symmetry in SUSY. *Nucl. Phys.*, B692:50–82, 2004. [arXiv:hep-ph/0401064].

[122] S. Antusch, S. F. King and M. Malinsky. Solving the SUSY Flavour and CP Problems with SU(3) Family Symmetry. *JHEP*, 06:068, 2008. [arXiv:0708.1282].

[123] H. M. Lee, S. Raby, M. Ratz, G. G. Ross, R. Schieren, K. Schmidt-Hoberg and P. K. S. Vaudrevange. Discrete R symmetries for the MSSM and its singlet extensions. *Nucl. Phys.*, B850:1–30, 2011. [arXiv:1102.3595].

[124] H. M. Lee, S. Raby, M. Ratz, G. G. Ross, R. Schieren, K. Schmidt-Hoberg and P. K. S. Vaudrevange. A unique $\mathbb{Z}_4^R$ symmetry for the MSSM. *Phys. Lett.*, B694:491–495, 2011. [arXiv:1009.0905].

[125] A. Masiero, D. V. Nanopoulos, K. Tamvakis and T. Yanagida. Naturally Massless Higgs Doublets in Supersymmetric SU(5). *Phys. Lett.*, B115:380–384, 1982.

[126] B. Grinstein. A Supersymmetric SU(5) Gauge Theory with No Gauge Hierarchy Problem. *Nucl. Phys.*, B206:387, 1982.

[127] S. Antusch, I. de Medeiros Varzielas, V. Maurer, C. Sluka and M. Spinrath. Towards predictive flavour models in SUSY SU(5) GUTs with doublet-triplet splitting. *JHEP*, 09:141, 2014. [arXiv:1405.6962].

[128] S. Antusch and M. Spinrath. New GUT predictions for quark and lepton mass ratios confronted with phenomenology. *Phys. Rev.*, D79:095004, 2009. [arXiv:0902.4644].

[129] S. Antusch, S. F. King and M. Spinrath. GUT predictions for quark-lepton Yukawa coupling ratios with messenger masses from non-singlets. *Phys. Rev.*, D89(5):055027, 2014. [arXiv:1311.0877].

[130] I. de Medeiros Varzielas, S. F. King and G. G. Ross. Tri-bimaximal neutrino mixing from discrete subgroups of SU(3) and SO(3) family symmetry. *Phys. Lett.*, B644:153–157, 2007. [arXiv:hep-ph/0512313].

[131] T. J. Burrows and S. F. King. A(4) Family Symmetry from SU(5) SUSY GUTs in 6d. *Nucl. Phys.*, B835:174–196, 2010. [arXiv:0909.1433].

[132] T. J. Burrows and S. F. King. A_4 x SU(5) SUSY GUT of Flavour in 8d. *Nucl. Phys.*, B842:107–121, 2011. [arXiv:1007.2310].

[133] I. K. Cooper, S. F. King and C. Luhn. SUSY SU(5) with singlet plus adjoint matter and A4 family symmetry. *Phys. Lett.*, B690:396–402, 2010. [arXiv:1004.3243].

[134] S. Antusch, S. F. King and M. Spinrath. Measurable Neutrino Mass Scale in $A_4\times$ SU(5). *Phys. Rev.*, D83:013005, 2011. [arXiv:1005.0708].

[135] S. Antusch, C. Gross, V. Maurer and C. Sluka. Inverse neutrino mass hierarchy in a flavour GUT model. *Nucl. Phys.*, B879:19–36, 2014. [arXiv:1306.3984].

[136] S. Antusch, C. Gross, V. Maurer and C. Sluka. A flavour GUT model with $\theta_{13}^{PMNS} \simeq \theta_C/\sqrt{2}$. *Nucl. Phys.*, B877:772–791, 2013. [arXiv:1305.6612].

[137] G. Altarelli, F. Feruglio and C. Hagedorn. A SUSY SU(5) Grand Unified Model of Tri-Bimaximal Mixing from A_4. *JHEP*, 03:052, 2008. [arXiv:0802.0090].

[138] P. Ciafaloni, M. Picariello, E. Torrente-Lujan and A. Urbano. Neutrino masses and tribimaximal mixing in Minimal renormalizable SUSY SU(5) Grand Unified Model with A(4) Flavor symmetry. *Phys. Rev.*, D79:116010, 2009. [arXiv:0901.2236].

[139] B. D. Callen and R. R. Volkas. Large lepton mixing angles from a 4+1-dimensional SU(5) x A(4) domain-wall braneworld model. *Phys. Rev.*, D86:056007, 2012. [arXiv:1205.3617].

[140] D. Meloni. Bimaximal mixing and large theta13 in a SUSY SU(5) model based on S4. *JHEP*, 10:010, 2011. [arXiv:1107.0221].

[141] S. F. King, C. Luhn and A. J. Stuart. A Grand Delta(96) x SU(5) Flavour Model. *Nucl. Phys.*, B867:203–235, 2013. [arXiv:1207.5741].

[142] A. Meroni, S. T. Petcov and M. Spinrath. A SUSY SU(5)xT' Unified Model of Flavour with large θ_{13}. *Phys. Rev.*, D86:113003, 2012. [arXiv:1205.5241].

[143] C. Hagedorn, S. F. King and C. Luhn. SUSY $S_4\times$ SU(5) revisited. *Phys. Lett.*, B717:207–213, 2012. [arXiv:1205.3114].

[144] Y. Chikashige, R. N. Mohapatra and R. D. Peccei. Are There Real Goldstone Bosons Associated with Broken Lepton Number? *Phys. Lett.*, 98B:265–268, 1981.

[145] S. Antusch and V. Maurer. Running quark and lepton parameters at various scales. *JHEP*, 11:115, 2013. [arXiv:1306.6879].

[146] B. R. Greene, K. H. Kirklin, P. J. Miron and G. G. Ross. A Three Generation Superstring Model. 2. Symmetry Breaking and the Low-Energy Theory. *Nucl. Phys.*, B292:606–652, 1987.

[147] I. de Medeiros Varzielas, S. F. King and G. G. Ross. Neutrino tri-bi-maximal mixing from a non-Abelian discrete family symmetry. *Phys. Lett.*, B648:201–206, 2007. [arXiv:hep-ph/0607045].

[148] S. F. King and M. Malinsky. A(4) family symmetry and quark-lepton unification. *Phys. Lett.*, B645:351–357, 2007. [arXiv:hep-ph/0610250].

[149] I. de Medeiros Varzielas and G. G. Ross. Family symmetries and the SUSY flavour problem, 2006. [arXiv:hep-ph/0612220].

[150] I. de Medeiros Varzielas. *Family symmetries and the origin of fermion masses and mixings*. Ph.D. thesis, Oxford U., 2007. [arXiv:0801.2775].

[151] R. Howl and S. F. King. Solving the Flavour Problem in Supersymmetric Standard Models with Three Higgs Families. *Phys. Lett.*, B687:355–362, 2010. [arXiv:0908.2067].

[152] A. E. Nelson. Naturally Weak CP Violation. *Phys. Lett.*, B136:387–391, 1984.

[153] A. E. Nelson. Calculation of θ Barr. *Phys. Lett.*, B143:165–170, 1984.

[154] S. M. Barr. Solving the Strong CP Problem Without the Peccei-Quinn Symmetry. *Phys. Rev. Lett.*, 53:329, 1984.

[155] S. M. Barr. A Natural Class of Nonpeccei-quinn Models. *Phys. Rev.*, D30:1805, 1984.

[156] J. M. Pendlebury et al. Revised experimental upper limit on the electric dipole moment of the neutron. *Phys. Rev.*, D92(9):092003, 2015. [arXiv:1509.04411].

[157] S. Aoki et al. Review of lattice results concerning low-energy particle physics. *Eur. Phys. J.*, C77(2):112, 2017. [arXiv:1607.00299].

[158] R. D. Peccei and H. R. Quinn. CP Conservation in the Presence of Instantons. *Phys. Rev. Lett.*, 38:1440–1443, 1977.

[159] R. D. Peccei and H. R. Quinn. Constraints Imposed by CP Conservation in the Presence of Instantons. *Phys. Rev.*, D16:1791–1797, 1977.

[160] S. Antusch, M. Holthausen, M. A. Schmidt and M. Spinrath. Solving the Strong CP Problem with Discrete Symmetries and the Right Unitarity Triangle. *Nucl. Phys.*, B877:752–771, 2013. [arXiv:1307.0710].

[161] S. Morisi, M. Picariello and E. Torrente-Lujan. Model for fermion masses and lepton mixing in SO(10) x A(4). *Phys. Rev.*, D75:075015, 2007. [arXiv:hep-ph/0702034].

[162] F. Bazzocchi, M. Frigerio and S. Morisi. Fermion masses and mixing in models with SO(10) x A(4) symmetry. *Phys. Rev.*, D78:116018, 2008. [arXiv:0809.3573].

[163] C. Hagedorn, M. A. Schmidt and A. Yu. Smirnov. Lepton Mixing and Cancellation of the Dirac Mass Hierarchy in SO(10) GUTs with Flavor Symmetries T(7) and Sigma(81). *Phys. Rev.*, D79:036002, 2009. [arXiv:0811.2955].

[164] F. Bazzocchi and I. de Medeiros Varzielas. Tri-bi-maximal mixing in viable family symmetry unified model with extended seesaw. *Phys. Rev.*, D79:093001, 2009. [arXiv:0902.3250].

[165] S. F. King and C. Luhn. A Supersymmetric Grand Unified Theory of Flavour with PSL(2)(7) x SO(10). *Nucl. Phys.*, B832:414–439, 2010. [arXiv:0912.1344].

[166] C. Hagedorn, M. Lindner and R. N. Mohapatra. S(4) flavor symmetry and fermion masses: Towards a grand unified theory of flavor. *JHEP*, 06:042, 2006. [arXiv:hep-ph/0602244].

[167] B. Dutta, Y. Mimura and R. N. Mohapatra. An SO(10) Grand Unified Theory of Flavor. *JHEP*, 05:034, 2010. [arXiv:0911.2242].

[168] P. S. Bhupal Dev, B. Dutta, R. N. Mohapatra and M. Severson. θ_{13} and Proton Decay in a Minimal $SO(10) \times S_4$ model of Flavor. *Phys. Rev.*, D86:035002, 2012. [arXiv:1202.4012].

[169] K. M. Patel. An SO(10)XS4 Model of Quark-Lepton Complementarity. *Phys. Lett.*, B695:225–230, 2011. [arXiv:1008.5061].

[170] D.-G. Lee and R. N. Mohapatra. An SO(10) x S(4) scenario for naturally degenerate neutrinos. *Phys. Lett.*, B329:463–468, 1994. [arXiv:hep-ph/9403201].

[171] Y. Cai and H.-B. Yu. A SO(10) GUT Model with S4 Flavor Symmetry. *Phys. Rev.*, D74:115005, 2006. [arXiv:hep-ph/0608022].

[172] P. S. Bhupal Dev, R. N. Mohapatra and M. Severson. Neutrino Mixings in SO(10) with Type II Seesaw and θ_{13}. *Phys. Rev.*, D84:053005, 2011. [arXiv:1107.2378].

[173] I. de Medeiros Varzielas and G. G. Ross. Discrete family symmetry, Higgs mediators and $theta_{13}$. *JHEP*, 12:041, 2012. [arXiv:1203.6636].

[174] A. Anandakrishnan, S. Raby and A. Wingerter. Yukawa Unification Predictions for the LHC. *Phys. Rev.*, D87(5):055005, 2013. [arXiv:1212.0542].

[175] G. C. Branco, J. M. Gerard and W. Grimus. Geometrical T Violation. *Phys. Lett.*, B136:383–386, 1984.

[176] I. de Medeiros Varzielas and D. Emmanuel-Costa. Geometrical CP Violation. *Phys. Rev.*, D84:117901, 2011. [arXiv:1106.5477].

[177] I. de Medeiros Varzielas, D. Emmanuel-Costa and P. Leser. Geometrical CP Violation from Non-Renormalisable Scalar Potentials. *Phys. Lett.*, B716:193–196, 2012. [arXiv:1204.3633].

[178] I. de Medeiros Varzielas. Geometrical CP violation in multi-Higgs models. *JHEP*, 08:055, 2012. [arXiv:1205.3780].

[179] G. Bhattacharyya, I. de Medeiros Varzielas and P. Leser. A common origin of fermion mixing and geometrical CP violation, and its test through Higgs physics at the LHC. *Phys. Rev. Lett.*, 109:241603, 2012. [arXiv:1210.0545].

[180] I. P. Ivanov and L. Lavoura. Geometrical CP violation in the N-Higgs-doublet model. *Eur. Phys. J.*, C73(4):2416, 2013. [arXiv:1302.3656].

[181] I. de Medeiros Varzielas and D. Pidt. Geometrical CP violation with a complete fermion sector. *JHEP*, 11:206, 2013. [arXiv:1307.6545].

[182] I. de Medeiros Varzielas and D. Pidt. Towards realistic models of quark masses with geometrical CP violation. *J. Phys.*, G41:025004, 2014. [arXiv:1307.0711].

[183] M. Fallbacher and A. Trautner. Symmetries of symmetries and geometrical CP violation. *Nucl. Phys.*, B894:136–160, 2015. [arXiv:1502.01829].

[184] S. Dimopoulos and F. Wilczek. Report. No. NSF-ITP-82-07, 1981. (unpublished).

[185] K. S. Babu and S. M. Barr. Natural suppression of Higgsino mediated proton decay in supersymmetric SO(10). *Phys. Rev.*, D48:5354–5364, 1993. [arXiv:hep-ph/9306242].

[186] S. M. Barr and S. Raby. Minimal SO(10) unification. *Phys. Rev. Lett.*, 79:4748–4751, 1997. [arXiv:hep-ph/9705366].

[187] I. de Medeiros Varzielas. Neutrino tri-bi-maximal mixing through sequential dominance. 2008. [arXiv:0804.0015].

[188] E. H. Moore. The fourteenth western meeting of the American Mathematical Society. *Bulletin of the American Mathematical Society*, 26(9):385–396, 1920. ISSN 0002-9904.

[189] P. Nath and P. Fileviez Perez. Proton stability in grand unified theories, in strings and in branes. *Phys. Rept.*, 441:191–317, 2007. [arXiv:hep-ph/0601023].

[190] A. Bueno, Z. Dai, Y. Ge, M. Laffranchi, A. J. Melgarejo, A. Meregaglia, S. Navas and A. Rubbia. Nucleon decay searches with large liquid argon TPC detectors at shallow depths: Atmospheric neutrinos and cosmogenic backgrounds. *JHEP*, 04:041, 2007. [arXiv:hep-ph/0701101].

[191] H. Murayama and D. B. Kaplan. Family symmetries and proton decay. *Phys. Lett.*, B336:221–228, 1994. [arXiv:hep-ph/9406423].

[192] S. Davidson and A. Ibarra. A Lower bound on the right-handed neutrino mass from leptogenesis. *Phys. Lett.*, B535:25–32, 2002. [arXiv:hep-ph/0202239].

[193] P. Di Bari. Seesaw geometry and leptogenesis. *Nucl. Phys.*, B727:318–354, 2005. [arXiv:hep-ph/0502082].

[194] S. Antusch, P. Di Bari, D. A. Jones and S. F. King. A fuller flavour treatment of N_2-dominated leptogenesis. *Nucl. Phys.*, B856:180–209, 2012. [arXiv:1003.5132].

[195] P. Di Bari and A. Riotto. Testing SO(10)-inspired leptogenesis with low energy neutrino experiments. *JCAP*, 1104:037, 2011. [arXiv:1012.2343].

[196] P. Di Bari and L. Marzola. SO(10)-inspired solution to the problem of the initial conditions in leptogenesis. *Nucl. Phys.*, B877:719–751, 2013. [arXiv:1308.1107].

[197] P. Di Bari, L. Marzola and M. Re Fiorentin. Decrypting $SO(10)$-inspired leptogenesis. *Nucl. Phys.*, B893:122–157, 2015. [arXiv:1411.5478].

[198] P. Di Bari and M. Re Fiorentin. Supersymmetric $SO(10)$-inspired leptogenesis and a new N_2-dominated scenario. *JCAP*, 1603(03):039, 2016. [arXiv:1512.06739].

[199] P. Di Bari and M. Re Fiorentin. Full analytic solution of $SO(10)$-inspired leptogenesis. 2017. [arXiv:1705.01935].

[200] A. Yu. Smirnov. Seesaw enhancement of lepton mixing. *Phys. Rev.*, D48:3264–3270, 1993. [arXiv:hep-ph/9304205].

[201] W. Buchmuller and M. Plumacher. Baryon asymmetry and neutrino mixing. *Phys. Lett.*, B389:73–77, 1996. [arXiv:hep-ph/9608308].

[202] E. Nezri and J. Orloff. Neutrino oscillations versus leptogenesis in SO(10) models. *JHEP*, 04:020, 2003. [arXiv:hep-ph/0004227].

[203] F. Buccella, D. Falcone and F. Tramontano. Baryogenesis via leptogenesis in SO(10) models. *Phys. Lett.*, B524:241–244, 2002. [arXiv:hep-ph/0108172].

[204] G. C. Branco, R. Gonzalez Felipe, F. R. Joaquim and M. N. Rebelo. Leptogenesis, CP violation and neutrino data: What can we learn? *Nucl. Phys.*, B640:202–232, 2002. [arXiv:hep-ph/0202030].

[205] E. K. Akhmedov, M. Frigerio and A. Yu. Smirnov. Probing the seesaw mechanism with neutrino data and leptogenesis. *JHEP*, 09:021, 2003. [arXiv:hep-ph/0305322].

[206] R. Gatto, G. Sartori and M. Tonin. Weak Selfmasses, Cabibbo Angle, and Broken SU(2) x SU(2). *Phys. Lett.*, 28B:128–130, 1968.

[207] I. P. Ivanov and L. Lavoura. SO(10) models with flavour symmetries: Classification and examples. *J. Phys.*, G43(10):105005, 2016. [arXiv:1511.02720].

[208] P. M. Ferreira, W. Grimus, D. Jurčiukonis and L. Lavoura. Flavour symmetries in a renormalizable SO(10) model. *Nucl. Phys.*, B906:289–320, 2016. [arXiv:1510.02641].

[209] G. G. Ross. Family symmetries. *J. Phys. Conf. Ser.*, 171:012006, 2009.

[210] N. Metropolis, A. W. Rosenbluth, M. N. Rosenbluth, A. H. Teller and E. Teller. Equation of state calculations by fast computing machines. *J. Chem. Phys.*, 21:1087–1092, 1953.

[211] F. Björkeroth, S. F. King, K. Schmitz and T. T. Yanagida. Leptogenesis after Chaotic Sneutrino Inflation and the Supersymmetry Breaking Scale. *Nucl. Phys.*, B916:688–708, 2017. [arXiv:1608.04911].

[212] S. F. King. Unified Models of Neutrinos, Flavour and CP Violation. *Prog. Part. Nucl. Phys.*, 94:217–256, 2017. [arXiv:1701.04413].

[213] E. Ma and G. Rajasekaran. Softly broken A(4) symmetry for nearly degenerate neutrino masses. *Phys. Rev.*, D64:113012, 2001. [arXiv:hep-ph/0106291].

[214] C. Luhn, S. Nasri and P. Ramond. The Flavor group Delta(3n**2). *J. Math. Phys.*, 48:073501, 2007. [arXiv:hep-th/0701188].

[215] L. E. Ibanez and G. G. Ross. SU(2)-L x U(1) Symmetry Breaking as a Radiative Effect of Supersymmetry Breaking in Guts. *Phys. Lett.*, B110:215–220, 1982.

[216] M. Fallbacher, M. Ratz and P. K. S. Vaudrevange. No-go theorems for R symmetries in four-dimensional GUTs. *Phys. Lett.*, B705:503–506, 2011. [arXiv:1109.4797].

[217] I. de Medeiros Varzielas. $\Delta(27)$ family symmetry and neutrino mixing. *JHEP*, 08:157, 2015. [arXiv:1507.00338].